1-1-2015

Impact Of Fault Current Limiters And Demand Response On Electric Utility Asset Management Programs

Shayan Behzadirafi

IMPACT OF FAULT CURRENT LIMITERS AND DEMAND RESPONSE ON ELECTRIC UTILITY ASSET MANAGEMENT PROGRAMS

by

Shayan Behzadirafi
Bachelor of Science, University of Tehran, 1997
Master of Science, Sharif University of Technology, 1999

A Dissertation
Submitted to the Graduate Faculty

of the

University of North Dakota

in partial fulfillment of the requirements

for the degree of

Doctor of Philosophy

Grand Forks, North Dakota
December
2015

This dissertation, submitted by Shayan Behzadirafi in partial fulfillment of the requirements for the Degree of Doctor of Philosophy from the University of North Dakota, has been read by the Faculty Advisory Committee under whom the work has been done and is hereby approved.

Name of Chairperson

Name of Committee Member

Name of Committee Member

Name of Committee Member

Name of Committee Member

This dissertation is being submitted by the appointed advisory committee as having met all of the requirements of the School of Graduate Studies at the University of North Dakota and is hereby approved.

Wayne Swisher
Dean of the School of Graduate Studies

December 11, 2015
Date

PERMISSION

Title Impact of Fault Current Limiters and Demand Response on Electric Utility Asset Management Programs

Department Electrical Engineering

Degree Doctor of Philosophy

In presenting this dissertation in partial fulfillment of the requirements for a graduate degree from the University of North Dakota, I agree that the library of this University shall make it freely available for inspection. I further agree that permission for extensive copying for scholarly purposes may be granted by the professor who supervised my dissertation work or, in his absence, by the Chairperson of the department or the dean of the School of Graduate Studies. It is understood that any copying or publication or other use of this dissertation or part thereof for financial gain shall not be allowed without my written permission. It is also understood that due recognition shall be given to me and to the University of North Dakota in any scholarly use which may be made of any material in my dissertation.

Shayan Behzadirafi
Dec 2015

TABLE OF CONTENTS

LIST OF FIGURES

LIST OF TABLES

Table Page

ACKNOWLEDGMENTS

First and foremost, I want to thank God, whose many blessings have made me who I am today. After that, this doctoral dissertation would not have been possible without help and support from many mentors, colleagues, friends and family members over this past few years and throughout my entire life. I would like to take this opportunity to express my gratitude to them to the extent which is possible through words.

First of all, I wish to express my sincere appreciation to my advisers Dr. Hossein Salehfar and Dr. Michael Mann for their support, patience and generosity. I would like to thank my committee members Dr. Arash Nejadpak, Dr. Prakash Ranganathan and Dr. Hassan Reza for their support and assistance. I appreciate their comments, suggestions and thoughtful reviews that helped improve the quality of this work and add to its value in every possible ways. I also wish to thank Professor emeritus Dr. Arthur Miles. Every time I walked into his office, I didn't get anything but his kind and welcoming words and tons of new knowledge, experience and insights. Also a big thank to Dave Poppke for his ideas and consistent help and also my friends that helped make my moments memorable and are my reasons to miss the University of North Dakota and city of Grand Forks.

Also my friends in other places in the US and back home have been a continuous source of support and encouragement. Special thanks go to my friends: late Kamyar Nikanjam, Jalal Jahanshah khani, Mohammad Reza Ghane, Mohammad Hadi Varahram, Amir Hossein Partovi,

Reza Navid, Hormoz Mogarei, Khosro Khosravani, Farshid Safavi, Siby Jose, Gashu Lemma, Rex Sorensen, and Farah Ramezanzadeh.

Last but not least, I would like to thank my parents, my brother and my sister. Without their encouragement, support and sacrifice, I would not have made it this far and could not have finished this dissertation. It was my mom that originally generated my love for science and learning more. I also want to thank my wife for her understanding, patience and support through all the ups and downs. Without their help, support and inspiration, I could not have completed this work. This work is dedicated to them.

To my mom and my dad,
The world's best parents! And my wife for her support and understanding

ABSTRACT

Over-currents are known to be the dominant cause of power system component failures or deterioration from full functionality. Some of these effects may remain unknown and could later result in catastrophic failures of the entire or large portions of the system. There are plenty of devices/methods available to limit the undesirable consequences of the over-current events. These devices/methods have great impact on system reliability by reducing stress on power system components and increasing their useful lifetime. Due to the importance of the subject, there is tremendous need to analyze and compare these devices/methods in terms of reliability. However, few researches have been reported on analyzing reliability impacts of these devices. Reported studies, in the meantime, appear to have investigated these effects qualitatively rather than quantitatively. This is mainly due to lack of a mathematical model to study the direct impacts of over-current values on system reliability. The main stream of reliability calculations are normally based on statistical measures of system outages rather than electrical parameters such as over-current values.

Over-currents usually appear in two common forms of fault currents and overload currents. Fault Current Limiters (FCL) and protection devices are commonly used to limit the impact of fault currents. FCL's limit the magnitude of fault currents and protection devices limit the exposure time of the component to the fault current and therefore have great impact on increasing the lifetime of the components. Overloads, on the other hand, have smaller magnitudes than those of fault currents but can still be destructive because of normally much longer exposure times. Overcoming overload problems usually requires control strategies such as generation rescheduling

and/or load shedding, and optimized usage of existing assets. Using Demand Response (DR) programs are one of the most effective ways of reducing overload burdens on the power system.

In this dissertation, simulation models are developed and used to determine the effect of FCL on reducing the magnitude of fault currents. Various case studies will be performed to calculate the effectiveness of FCL's in real power system applications. Then, security/dependability studies on the protection systems will be performed to analyze and calculate their effectiveness in reducing exposure times to fault currents. Based on the calculated indices, proper selection of protection schemes can be made based on the desired level of dependability/security.

In the next part of the work, a mathematical model is developed to calculate the effect of fault current magnitude and duration on the reliability and asset management. Using the developed model and results of the earlier sections of this research work, the impact of protection systems and FCL devices on reliability and asset management programs are quantitatively calculated and compared. The results from such studies will assist in maintenance planning and in proper selection of the fault current limiting devices with regards to desired reliability and asset management programs.

DR programs are introduced and modeled in this dissertation as an effective tool in reducing overload burdens on power system components. Using the developed mathematical model, DR programs are studied and compared in terms of reliability improvement that they provide by preventing unnecessary increase in the component failure rates.

CHAPTER I
INTRODUCTION

Power systems around the world are changing from the management and operating points of view and there is a strong tendency towards separating generation from the primary transmission grid. In this new deregulated and competitive environment, the power utility responsible for operating the primary grid loses control over the sitting and scheduling of generating units. This has the consequence that considerable attention would be devoted to the generation expansion in areas where previously generation deficiencies existed. Growth in the generation of electrical energy particularly in the form of connecting independent power producers (IPP's) to the grid and an increased interconnection of the power grids lead to higher fault currents which have not been included in the original long term planning forecasts. One of the consequences of this growth is that the network and the associated equipment reach or even exceed their limits with respect to the over- current withstand capabilities. At the same time, consumers request higher level of reliability which can be achieved by providing parallel transmission facilities. This will, however, raise the fault current level which in turn imposes a severe burden on circuit breakers and power system apparatuses. These problems are not avoidable due to the over-current events that may occur anywhere and anytime in the power network. The challenge of the future network designs will be to face these challenges by the application of new and effective technologies in the network [1] .

Over-currents mainly appear in two common forms of short circuit and overload. Short circuit currents (also called fault currents) are known to be the dominant cause of power

system component failures or deterioration from full functionality [2] . Some of these effects may remain unknown and could later lead to cascading failures of the entire or large portions of the system. It is a common practice to use Fault Current Limiters (FCL's) and protection devices to eliminate undesirable impacts of short circuit currents. They do so by reducing the magnitude and exposure time to fault currents.

While short circuit can cause catastrophes by posing huge amount of stress and mechanical forces in a very short amount of time, overloads can also raise serious issues due to much longer periods of exposure. Overcoming overloads problems usually requires control strategies such as generation rescheduling and/or load shedding, and optimized usage of existing assets. Smart grids have made it a priority to address customer interactions in forms of Demand Response (DR) as a powerful tool to provide load/generation balance throughout the peak/off-peak hours, in order to reduce the overload burdens in the power system. DR is defined as: "Changes in electric usage by end-use customers from their normal consumption patterns in response to changes in the price of electricity over time, or to incentive payments". There are several DR programs based on different price patterns/incentive payments designed to improve power system operation. These programs allow for better usage of existing assets, by reducing energy consumption during peak hours and increasing it in non-peak hours.

Over-current effects are not limited to the region of exposure as they could influence the performance of remote equipment as well. The effects of over-currents include mechanical

stress, undesirable overheating, deterioration of insulation, etc. Despite the importance of increased over current levels on power system operation and components, few investigations have been reported on the evaluation of the effects of over-current on reliability [2]. Reported studies, in the meantime, appear to have investigated these effects qualitatively rather than quantitatively and suggesting a method to model them. Due to lack of proper models that consider the direct effect of overcurrent on failure rates, destructive impacts of increased over-current levels on power system reliability and the potential damages and resulting risk of cascading failures have been ignored. Due to their destructive nature, however, the recognition of these effects on component failure rates and on system reliability cannot and should not be underestimated.

State of the Art of the Subject

Current literature on reliability analysis involving FCL and protection devices are majorly with regard to the role of these devices in reducing outages. This is due to the fact that current reliability evaluation techniques (such as failure modes and effects analysis) usually rely on number and duration of system outages to calculate system availability indices [3].

There are numerous studies that show the reliability improvements due to using FCL's [4-10]. Many studies have been carried out concerning different type of FCL's [4], their structural designs [5], [6], and their impact on static and dynamic behavior of faulted systems [7] , [8]. In [9] , no particular substation configurations are assumed, and the FCL's are located in distribution networks. [10] Has suggested a Markov model for operation of

fault current limiters and has calculated reliability indices based on system outages at each state of the Markov model. These works are all based on outage reductions that these devices offer. Chapter four of this dissertation shows some of the application studies and reliability calculations of FCL's using existing techniques.

There are also several works done to study reliability improvements due to protection systems [17-21]. [11] has studied the impact of protection system on power system reliability using a new method of finding cut-sets. These cut-sets are various paths that lead to the system partial/total outages. [12] and [13] have studied the effects of protection system failures on power system reliability. These failures are failure to operate when protection system is required to operate and malfunction when it is not required to operate. Again due to the nature of the existing reliability methods, these calculations are all based on the ability of protection system in preventing power system outages.

In case of overloads, reliability calculations become more complicated. Since there are usually no immediate outages following the overload events, there are no practical ways to capture the reliability impact of overload currents in existing reliability evaluation methods. As a result, overloads are being ignored in almost all standard reliability calculations.

Problem with the Existing Approach

While outage reduction is a very important benefit of using FCL's, and allows us to calculate improvements in reliability indices such as "Expected Energy Not Supplied"

(EENS), “Expected Load Not Supplied”, (ELNS), Capacity Outage Probability Table [14], etc.; it wouldn’t picture the entire story. In most cases, current limitation devices improve reliability without necessarily preventing outages. This becomes evident by looking at the works that use failure mode and effect analysis to calculate reliability indices, and seeing that in many cases using these devices eliminates just a few number of cases leading to major outages [15].

Using an outage-based approach, gives misleading results in case of protection devices as well. Protection devices are usually idle during the normal operation of power systems. Therefore in existing models, in order to assign a meaningful reliability improvement due to a protection system, it must be capable of preventing major outages [16]. However, a major part of the system reliability due to the protection system, is in it continuously eliminating stress on the power system equipment regardless of having/not having major outages [1]. On the other hand, speed of action and the relative timing incorporated in various protection schemes have a profound impact on power system reliability that can’t be fully evaluated using outage-based approaches [17]. Therefore, existing techniques underestimate the reliability enhancement caused by protection systems.

It is known that equipment that are more frequently exposed to short circuit conditions are more likely to fail later as a result of such stresses. In terms of reliability, the failure rate of these equipment will increase rapidly with time [17]. The increment in failure rate is obviously a function of frequency and severity of the faults. [18] has proposed an approach

that considers a coefficient for failure rate reduction caused by installing FCL's, without discussing the details and modeling how failure rate is actually decreased. These reliability impacts can not be captured using existing reliability evaluation techniques [1], [17].

As stated earlier, impact of overload currents on system reliability calculations are mostly ignored due to their less sever role in system outages. As a result, role of DR programs to alleviate overload conditions are not studied to their full potentials in reliability literatures. [19] is the only work that has addressed the impact of overloads on power system reliability. According to [19], overloads can combine with scheduled outages of other components leading to major power system outages. The truth is that the impact of overload currents, as suggested by [19], are less frequent compared to the actual continuous stresses that overloads pose on power system components on daily basis, causing a huge increase in their failure rates.

Contribution of this work

In this dissertation, the author proposes, develops, and presents an analytical method that models the direct impact of over currents magnitude and exposure times on the failure rate of power systems components. Unlike the existing reliability models that rely heavily on number/duration of system outages, the authors approach provides a mathematical model for calculating the impact of fault currents on system reliability. In case of fault currents, the new method enables us to directly quantify negative effects of different fault current values, rather than studying the system outages caused by those fault currents. Using the

proposed method, impacts of fault current limitation techniques on reliability improvement and increasing useful lifetime of power system components are calculated in this dissertation. Also guidelines are provided to show how to use the developed model to derive practical maintenance schedules for the affected components.

There are several DR programs based on different price patterns/incentive payments designed to improve power system operation. These programs allow for better usage of existing assets by reducing the energy consumption during peak hours and increasing it in non-peak hours. Using the developed mathematical model introduced in above, the reliability impact of DR programs in reducing overload current levels are calculated and compared.

Another major contribution of this dissertation is in modeling of the DR programs. Many models of DR programs have already been proposed by others, but they all have assumed a constant price elasticity [20]. This might be helpful in simplifying the problem and giving general results but is not acceptable for accurate studies. Another problem with constant elasticity models is that when the price approaches zero, it reaches a steady value while it should grow unlimitedly in a free market. Some other studies have modified the constant-elasticity assumption by considering an elasticity that is constant but also changes depending on the spot price being considered [21]. This approach needs elasticity values to be recalculated for every change in the price but still has the deficiency of considering a linear demand function in the first place. In the current research work a new model for DR

programs is introduced that allows for more accurate studies of DR impacts on asset management, and is more consistent with real behavior of electricity price versus demand.

Organization of this Dissertation

The organization of this dissertation is as follows: Chapter two studies techniques that are widely used to reduce fault currents. Effectiveness of protection systems in reducing exposure times to fault currents are studied in Chapter three where security and dependability analysis are performed to examine and compare their performance. Effectiveness of FCL's in reducing the magnitude of fault currents are studied and compared in Chapter four. Case studies of using FCL's are also illustrated in this chapter that show several real world applications of these devices. Chapter five presents and develops a new analytical model to analyze the direct impact of fault current magnitudes and exposure times in reliability calculations. Chapter six uses this model along with results of the previous chapters to study the impact of FCL's and protection systems on reliability/asset management. Chapter seven will study reliability improvements caused by using DR programs to reduce the overload burdens on power systems. Finally, conclusion and recommendations for future work are given in Chapter eight.

Figure 1 shows the flow chart of the work presented in this dissertation.

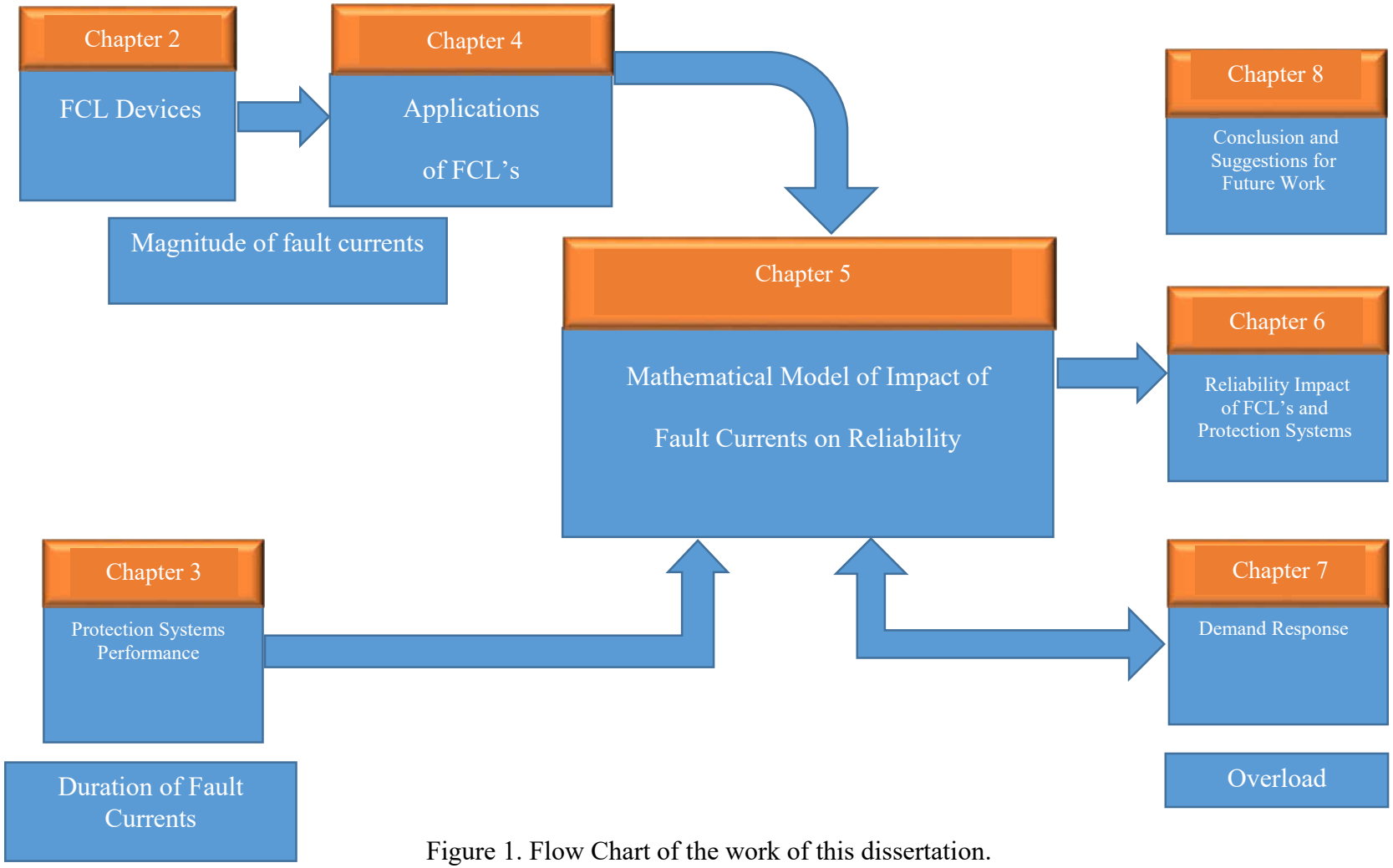

Figure 1. Flow Chart of the work of this dissertation.

CHAPTER II
FAULT CURRENT LIMITERS

Introduction

In later chapters of this work, we will model fault current limiting devices and study their impact on asset management. Therefore it is best to first have a basic understanding of these devices and their role in power system operation.

Growth in the generation of electrical energy, particularly in the form of connecting independent power producers (IPP's) to the grid, and an increased interconnection of the power grids would lead to higher fault currents which have not been included in the conventional long term planning forecasts [22]. One of the consequences of this system growth and the resulting high fault currents is that the network and the associated equipment reach or even exceed their limits with respect to the short circuit current withstand capabilities. At the same time, consumers request higher levels of reliability which can be achieved by providing parallel transmission facilities. This will, however, raise the fault current levels which in turn impose a severe burden on circuit breakers and power system apparatuses. The challenge of the future network designs will then be to face these challenges by utilizing new and effective technologies in the network.

The fault current over-duty problem can be alleviated by either replacing the existing equipment with ones with higher fault current ratings and tolerances, or limiting the fault current to values that could be safely interrupted by the existing equipment.

Replacement of equipment could be avoided for the sake of cost savings. Reducing fault levels is a more practical alternative and could have a positive impact on the life of electrical components. Electric power system planners and operators, therefore, need new techniques to limit short circuit currents at different voltage levels of the existing networks.

Fault Reduction Techniques

Conventional solutions for limiting fault current magnitudes to interruptible levels by the existing circuit breakers include [23]:

- Construction of new substations: Fault current over-duties coupled with other factors may result in a utility selecting this solution, which will correct the immediate problems, as well as providing for future growth. However, this is the most expensive and most time consuming of all the other solutions.

- Bus splitting and reconfiguring: This entails separation and isolation of fault sources that could possibly feed a fault by opening normally closed bus ties, or by splitting the existing busses. This effectively reduces the number of sources that can feed a fault, but also reduces the number of sources that supply load currents during normal or contingency operating conditions. This approach in turn can reduce the reliability and security of the power system [14]. Splitting the buses is not desirable due to the decreased flexibility and the cost associated with high voltage connections [24] and [25].

- Multiple circuit breaker upgrades: When a fault duty problem occurs, usually more than one circuit breaker will be affected. Replacing or upgrading circuit breakers with ones with

higher ratings, has the disadvantage of not reducing available high fault currents and their associated hazards. This approach is also associated with the often prohibitive expense of replacing the switchgears within a substation.

- Current limiting reactors and high impedance transformers: Fault current limiting reactors limit fault currents by the impedance across their terminals, which increases during faults. However, current limiting reactors also have a voltage drop under normal loading conditions and present a constant source of losses. They can also interact with other system components and cause potential instabilities.

- Sequential breaker tripping: A sequential tripping scheme prevents circuit breakers from interrupting excessive fault currents at once. If a fault is detected, a breaker upstream to the location of the fault current is tripped first. This reduces the fault current seen by the breaker within the zone of protection at the location of the fault and this breaker can then open safely. A disadvantage of the sequential tripping scheme is that it adds a delay of one breaker operation before the fault is finally cleared. Also, opening the breaker upstream to the fault location affects protection zones that were not originally impacted by that fault [24]. Moreover, sequential tripping requires complex strategies that are technically very difficult in some cases.

The above fault current reduction strategies, in spite of their benefits in lowering the stress on interrupting devices, have the main disadvantage of unnecessarily tripping other additional breakers and disconnects. This brings successive power outages that lower the

reliability of the network. It would also cause potential instabilities in the power system, which in some cases may contribute to major cascading failures.

-Fault Current Limiters (FCL's): There is a considerable interest in devices which are capable of limiting fault currents designated as Fault Current Limiters (FCL) [26], [27], [28], [29], and [30]. The FCL's reduce fault currents to low and safe levels so that the existing switchgears can still protect the grid [31]. The use of FCL's allows equipment to remain in service even if the fault current exceeds the peak and short-time withstand capabilities of the equipment. These capabilities would be the rated short-circuit and the breaking currents in the case of circuit breakers [25]. It follows that FCL's would prevent unnecessary outages and therefore improve system reliability.

There are many types of FCL's [25]. These devices are basically required to provide: (1) rapid respond to fault currents, (2) low impedance in normal operation, and (3) large impedance during fault conditions [32]. The unique property of superconductor materials to enter a highly resistive state once the transport current exceeds a critical limit, makes them an ideal choice for making FCL's [33]. Superconductive Fault Current Limiters (SFCL's) are therefore receiving considerable attentions as one of the key elements of the future smart grids [24], [34], [35], [36], [37], [38], [39], [40] and [41].

Comparison and Economic Considerations

Table 1 summarizes the conventional solutions -for limiting fault currents to levels tolerable by existing breakers-, and their respective pros, cons, and relative cost. The

expected cost of a Superconductive Fault Current Limiter (SFCL), as a representative of the category of FCL devices, is also shown. Table 1 primarily considers the initial capital installation cost in the comparison. In the cases of multiple circuit breaker upgrades, the cost of bus work reinforcement must also be considered, since the level of fault current is not being reduced. As shown in Table 1, the SFCL is expected to be also cost-competitive with all of the other solutions with the exception of current limiting reactors and sequential breaker tripping. In these cases, a consideration of life-cycle costs and negative impacts on system reliability may cause a utility consider the SFCL over other solutions.

Table 1. SFCL vs Conventional Solutions

Solution	**Advantage**	**Disadvantage**	**Relative Expense**	**Relative Expense to SFCL**
New Substation	Provides for future growth	Expensive and lengthy to install	The most expensive solution	More expensive than SFCL
Bus Splitting	Separate the sources of fault current	Separate the sources of load current from load centers and undermines reliability	High, if split bus not already installed	More expensive than SFCL
Multiple Circuit Breaker Upgrades	Most direct solution with no adverse side effects	Difficult to schedule outages; bus work reinforcement also required	High to medium, depending on number of replaced breakers	Most multiple breaker upgrades are more expensive than SFCL
Current Limiting Reactors	Easy to install	Voltage drop and power losses; Potentially causes instability	Medium to low	SFCL cost higher
Sequential breaker tripping	No major hardware installation involved	Expands impact of fault to wider range of the system	Low	SFCL cost higher

Classification of Fault Current limiters (FCL's)

Pyrotechnic fault current limiters (Is-limiter)

The Is-Limiter consists of an extremely fast switch, which is capable of carrying a high rated current but incapable of limiting the fault current, and a high rupturing capacity fuse arranged in parallel as shown in Figure 2 [42]. The switch is connected in series with the main conductor and an external trigger is required to open it when a fault occurs in the system. When the main conductor is opened, the current start flowing through the parallel fuse, where it is limited within 0.5 ms and then finally interrupted at the next voltage zero crossing [43].

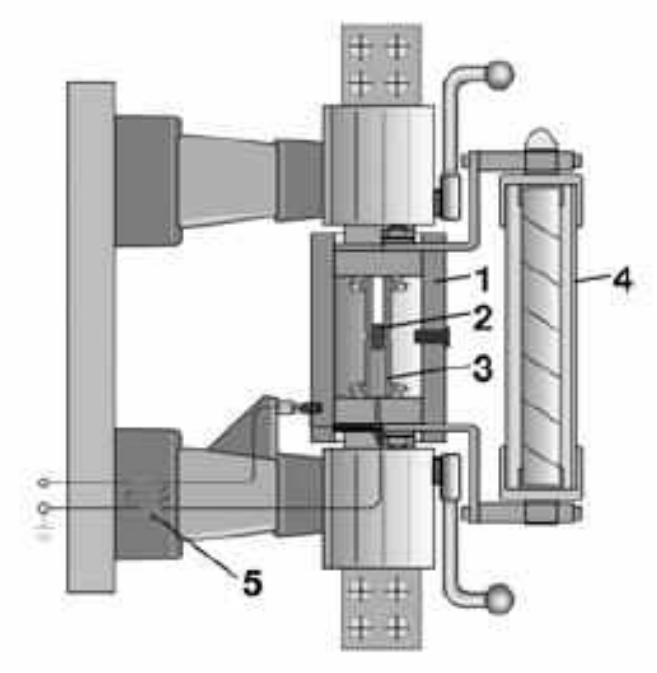

Figure 2. Is-Limiter: 1- Insulating Tube, 2- Charge, 3- Main Conductor, 4- Fuse, 5- Pulse Transformer [42].

The current flowing through the Is-Limiter is monitored by an electronic measuring and tripping device. At the very first rise of a fault current, this device decides whether tripping of the Is-Limiter is necessary. In order to reach this decision, the instantaneous current value and the rate of current rise through the Is-Limiter are constantly measured and evaluated.

When the set points are simultaneously reached or exceeded, the Is-Limiter trips in the faulty phases. After operation, the limiter has to be disconnected by a series connected circuit-breaker in order to get access for changing the tripped Is-Limiter. The invention of the Is- Limiter was in 1955 and large number of them have been successfully used in DC, AC and particularly in three phase systems since then. Is-Limiter is claimed to be capable of interrupting fault currents up to 5 kA, within 1 millisecond after occurrence of the fault. However, it is still limited to 40 kV rated voltage levels [44].

Current limiting reactor

Current Limiting reactors (CLR) are coils used to limit current during fault conditions. These devices are widely used for fault current limiting in medium and low voltage distribution systems, and is the most common and simplest type of fault current limiters. Such reactors have a large value of inductive reactance and low ohmic resistances.

CLR is generally of two types: air cored type and iron cored type. For a current limiting reactor, it is important that the magnetic saturation at high currents does not reduce the coil reactance necessary to limit the fault current. Because of this, iron cores are not generally

used in CLRs ([45] and [46]). Air cored reactor does not suffer from magnetic saturation and therefore their reactance is independent of the current. For this reason, air cored reactors are the one that show more desirable characteristics and are therefore most commonly used.

One of the main problems associated with this device, however, is the safety problem due to the magnetic flux distributed through the space around CLR. Therefore, CLRs require proper fencing due to the personnel safety considerations. Constant voltage drops that would degrade the voltage profile of the system, possible resonance with other circuit elements of the circuit causing potential stability problems, constant energy waste, and distributed magnetic flux are among other important issues in regards to using CLR. [45] has addressed the issue of selecting and placing CLR in various substation arrangements to get optimized results in terms of limiting the fault effects and minimizing avoidable side effects.

Solid State Fault Current Limiters

Solid-state fault current limiters consist of semiconductor devices which are able to interrupt a fault current during its rise times before the peak value is reached. It is an advanced current interruption technology which offers a viable solution against fault current occurrences in the transmission and distribution systems. Recent developments in power switching technology have made solid state limiters suitable for voltage and power levels necessary for distribution system applications. In particular the progress in

development of Silicon Carbide (SiC) semiconductors as well as advances in Silicon (Si) based devices has drawn increased attention within the FCL R&D community, to the utilization of these techniques/materials in making FCL devices. Solid state limiters use a combination of inductors, capacitors and thyristors or gate turn off thyristors (GTOs) to achieve fault limiting functionality.

[47] has done a comprehensive literature review on many different types of solid state FCL's. It suggests classifying the solid-state FCL topologies into three major groups: the series switch, the bridge, and the resonant types. Although work on solid state FCL indicates continuing progress in this field; however, a practical, efficient, reliable and economically feasible solid state device, suited to utility needs, till now, has remained elusive [47].

Electromagnetic Dynamic Fault Current Limiter (DFCL)

DFCL is an electromagnetic FCL which automatically & instantaneously adjusts its impedance depending on the magnitude of the fault current, thereby maintaining the let through current within a narrow range of values. A DFCL operates within half a cycle (8 milliseconds for 60Hz) to effectively protect downstream equipment and devices.

DFCL operates at ambient temperature and provides a variable impedance proportional to the short circuit current, such that the more current tries to increase the more limiting action will be provided by the device. DFCL has a very low power consumption and a low enough impedance for up to normal currents, so that it does not cause a poor voltage regulation at

normal operating conditions. DFCL's are self-triggered devices and automatically return back to their low impedance state after reduction of current to normal values. DFCL's are reliable and effective current limiting solutions for the smart grid. They are called "dynamic" FCL's because their impedance values vary with the current.

An DFCL essentially works on the principle of variation of inductive reactance of a coil wound on a core which has a magnetic permeability proportional to the magneto motive force (MMF) impressed upon the magnetic circuit. Such a variable permeability leads to a reactance proportional to the current passing through the coil. The permeability of the conventional magnetic materials for various flux densities is nearly constant in the operating range below magnetic saturation, thus leading to nearly constant inductance and inductive reactance values over a range of currents. The core material used in the DFCL's has radially pre-aligned magnetic domains in the inward and outward directions as compared to conventional cores with random domain alignment [48]. DFCL's have a power rating of 9.35 MVA and are operating at customer plants since 2008 [49].

Superconducting Fault Current Limiters (SFCL)

The unique property of a superconductor to passively enter a highly resistive state once the transport current exceeds a critical limit makes it an ideal choice for fault current limiters [33]. This is due to the properties that it inherits from its superconductive nature; i.e., rapid operation, having no resistance in the superconductivity mode but a large resistance in the normal mode. By using superconductor materials, Superconducting Fault Current Limiters

(SFCL's) need no auxiliary circuits to detect and limit fault currents and hence they have a high reliability. While other types of FCL's, such as current limiting reactors (CLR's), cause a large voltage drop and power losses during non-fault conditions, SFCL's produce a negligible loss during normal operation, due to their very small resistance in the superconductivity region. It is therefore expected that introduction of SFCL's in electric power systems can result in considerable improvements with respect to power quality, voltage quality, and network flexibility [50]. Reviewing the literature in the area of fault current limiters reveals that an absolute majority of published works on FCL's are related to superconductive FCL's [26]- [30]. Studies show that SFCL provides a cost-effective solution that besides a good performance in limiting the fault current at the very first cycle, it also offers the benefit of enhancing the system reliability [22]. A SFCL performs this function by reducing the stress on power equipment and preventing unnecessary outages.

Superconductors are materials that while in the super-conducting mode, have two main properties:

-They pass current without ohmic losses; i.e. zero resistance,

-They don't allow the magnetic field pass inside them; i.e. magnetic shield.

Superconductors lose the above properties when their critical current (or critical magnetic field) is surpassed and they quench into the normal state.

Based on the above two properties, in general there are two major types of SFCL's –each type using one of the above phenomenon, designated as resistive and shielded core [37]. Other main types of SFCLs include saturated iron-core type SFCL and Matrix Fault Current Limiter. These SFCL types are introduced below.

Resistive Type SFCL's

A resistive superconductor fault current limiter is directly connected in series with the current path to be protected. This fault current limiter relies on the rapid change of resistance with temperature. The principal schematic diagram of this type of FCL is shown in Figure 3.

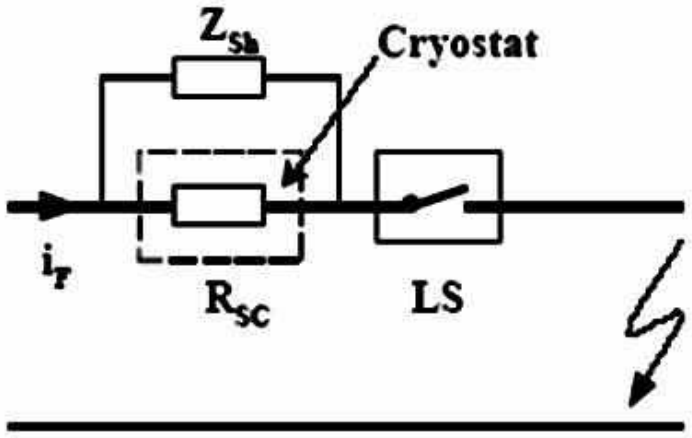

Figure 3. Resistive superconductive fault current limiters [22].

The resistive SFCL is designed such that under normal operating conditions the peak of the ac current flowing through the superconducting element is less than the critical current of the superconductor. In this situation SFCL is operating in the superconducting mode.

No major RI^2 losses or voltage drops are developed across the device in this mode. In other words the SFCL is basically "invisible" to the grid.

Under fault conditions, the current in the grid exceeds the critical current level of the superconductor. This surge current forces the superconductor to transit from its normal superconducting state to a resistive state; thereby introducing the necessary current limiting impedance into the grid. In order to protect the superconductor element from thermal damages and to decrease its recovery time, a resistive or inductive shunt Z_{sh} might be added to dissipate some part of the fault energy.

A cryostat holds the Superconductor resistor, R_{Sc} , which is connected straight to the power line by current leads. This is particularly designed for a minimal heat transfer. The load switch LS in series is necessary to save the resistor R_{Sc} from undue high power losses during fault conditions after tripping and allows for a sufficiently short recovery time (1-1.5 s).

Superconductive shielded core reactor (SSCR)

Another candidate for SFCL is the so-called superconductive shielded core reactor (SSCR) shown in Figure 4 [51]. This device uses a cylinder of bulk BSCCO-2212 or BSCCO-2223 superconductor to separate a normal copper coil from an iron core. In the normal operating mode, the field from the copper coil does not penetrate the iron core due to the shielding behavior of superconductor. In this case the impedance of the SFCL is limited to the small value of leakage inductance. Under fault conditions, however, the current induced in the

superconductor is sufficient to drive it to its non-superconductive state, and the magnetic field links the iron core. This greatly increases the impedance of the limiter, and hence would limit the current. In addition, installing a "control ring" in the system to absorb some of the energy deposited during a fault can reduce the recovery time of the shield following a faulted state. The main disadvantages of this type of SFCL are its size and weight.

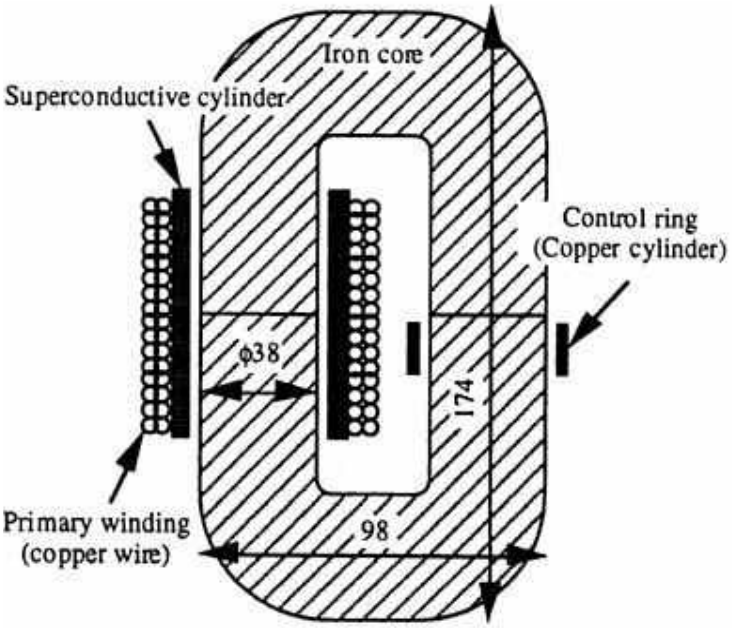

Figure 4. Inductive superconductive fault current limiter [51].

Saturated iron-core type SFCL

In the saturated-core SFCL's, two iron cores (one for each half of the cycle) are saturated by the dc magnetic field produced by a superconducting coil wrapped around each core. The main power line is wound around both cores and, when the current becomes high

enough (i.e. a fault) the cores are driven out of saturation and the impedance rises - limiting the current.

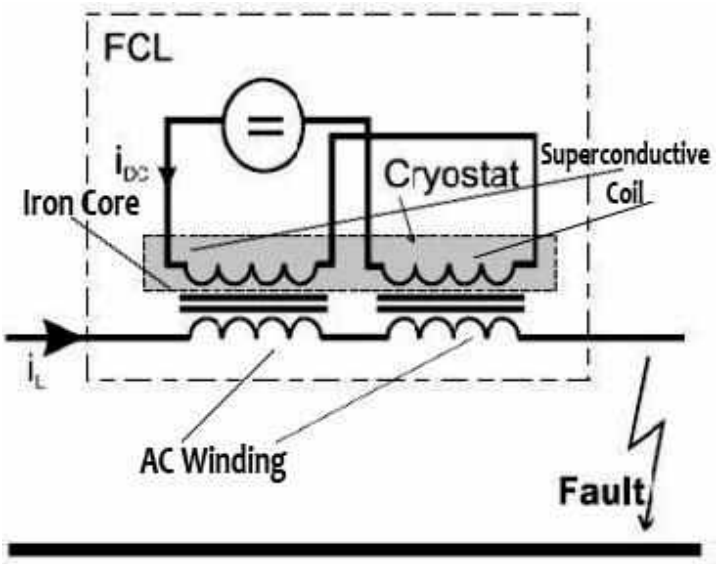

Figure 5. Saturated iron-core type SFCL [46].

Figure 5 above shows a structure diagram of single-phase magnetic saturated core type SFCL, which is composed of iron cores, AC windings, superconducting DC winding, DC power and the control circuit [46]. Under the normal operating conditions, DC superconducting coil generate a lot of magnetic flux which can make the iron core saturated. Therefore it offers very small impedance to the power system and thus has no adverse effects on normal transmission.

When a short circuit fault occurs, the current i_L surges, and the fault monitoring system will instantly cut off the DC exciting-current within a few milliseconds by means of a

power electronic switch, such as insulated gate bipolar transistor (IGBT) or integrated gate commutated thyristor (IGCT), in the DC control circuit. This will bring both of the two cores out of their deep saturation status. In this case, the large fault current in the two AC windings will produce a large inductive EMF which can limit the fault current. The advantage of this concept is that it does not require the superconductor to become normal to operate. However, it requires approximately twice as much iron (two cores). This system does not use the special properties a superconductive material has and theoretically it could be built without using superconductive conductors. In 2009, a saturated iron-core SFCL device was experimentally tested in small-scale distribution networks in California, United States [52]. In January 2010, the test field in California suffered a lightning-induced fault and the FCL device limited the fault current as designed. A field test in a 138 kV transmission network was also planned for the end of 2011 [52].

Matrix Fault Current Limiter

A particular type of SFCL, called Matrix Fault Current Limiter (MFCL), has been recently under development by “SuperPower” Inc. and Nexans Superconductors GmbH [23]. A MFCL uses the same current limiting strategy as a resistive type SFCL and its schematic diagram is shown in Figure 6 [53] and [54].

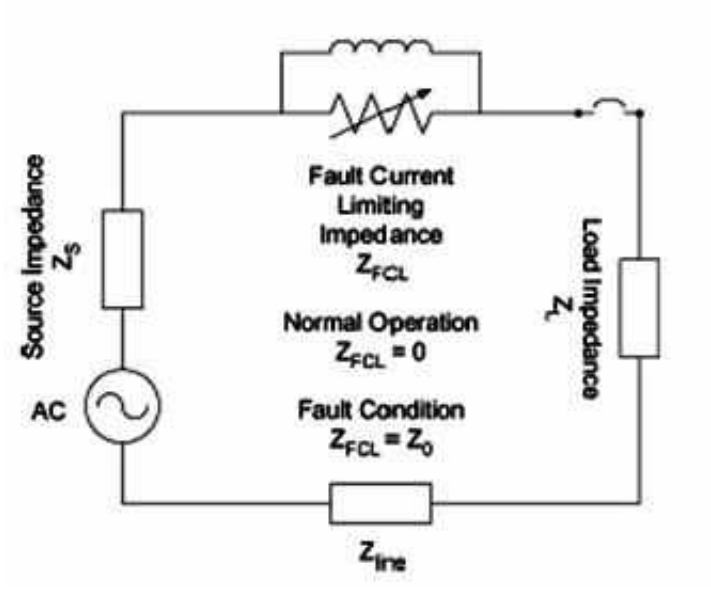

(a)

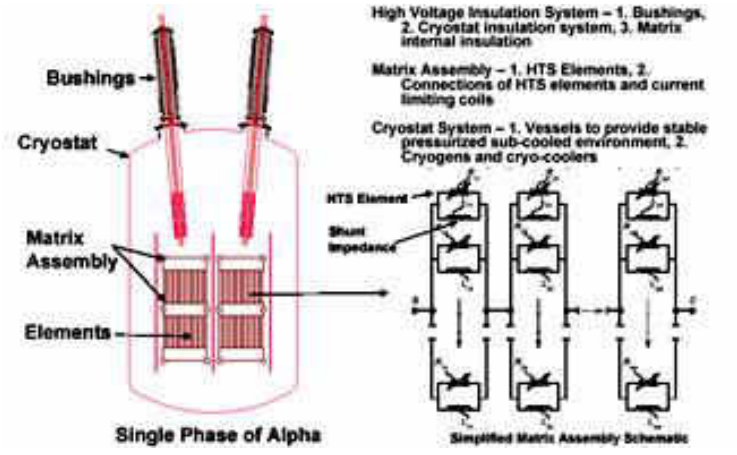

(b)

Figure 6. Matrix superconductive fault current limiter: (a) simplified model in an electric circuit (b) the matrix assembly [53].

Figure 6a shows a simplified equivalent representation of the MFCL in a power system. In this figure, the MFCL is shown as a variable resistor in parallel with a reactor. Under normal operating conditions, the peak of the AC current level of the power transmission network is always below the critical current level of the superconductor. Therefore, there is essentially no voltage drop and no ohmic losses caused by the device and the device is "invisible" to the grid. When a fault occurs, however, fault current level exceeds the critical current level of the superconductor, creating a quenching condition. The superconductor is forced to make a transition to high resistive state and most of the fault current is shunted into the parallel inductor to introduce a current limiting impedance of Z_0 into the grid to limit the fault current.

Figure 6.b shows a schematic diagram of the current-limiting matrix that includes "m" number of current-limiting modules electrically connected in series inside a MFCL. Each module further includes n number of current-limiting matrix elements electrically connected in parallel. The current-limiting matrix is, therefore, an $m \times n$ matrix. Each current-limiting matrix element includes a parallel electrical arrangement of a superconductor R and an inductor L.

The parallel-connected inductors in the current limiting matrices act as shunts. The partial divergence of the surge current to the inductors, serves to reduce the RI^2 heating of the superconductors during the current limiting phase of the MFCL operation. This allows for a fast recovery of the MFCL device to its superconducting state. Also, if a superconductor

element fails for any reason, the parallel connected inductor can continue to carry the load current, although a very small voltage drop will appear across the device [51].

Table 2 gives a comparison between current-limiting related features of various types of FCL's [46].

Table 2. Comparison of Various Types of Fault Current limiters [46]

Type	**Air Core Reactor**	**Is-Limiter**	**Resistive SFCL**	**Superco-nductive Shielded Core Reactor**	**Saturated Iron Core SFCL**	**Solid State SFCL**	**DFCL**	**Hybrid FCL**
Max Rating	36 kV 2500 A	40.5 kV 2500 A	138 kV 900 A	11 kV 2000 A	13.8 kV 1200 A	69 kV 3000 A	220 kV 200 A	12 kV 2000 A
Activation Time	-	<0.5 msec	<1/4 Cycle	Immediately	Immediately	µsec order	<10 msec	100 msec
Reset Time	-	Non Automatic Recovery	Tens of msec to 2 sec	<5 msec	Immediately	Controllable	20 msec	Controllable
Current Reduction	Depend on Reactor used	<70%	<80%	Low 20%	30% ~ 40%	Controllable	85%	Controllable
Need Cooling	Yes	No	Yes	Yes	Yes	Yes (Si) No (SiC)	No	Yes
Size/Weight	Bulky	Bulky	Small	Large and heavy	Large and Heavy	Small	Compact	Small but additional components

								may increase size
Status	Commercially available	Commercially available	Designed and Tested	R&D Stage	R&D Stage	Development Phase	Designed and Tested	Research Stage

It is shown in [55] and [56] that it is sufficient to limit fault currents with an activation time less than of a quarter cycle. So all of these FCL devices satisfy current limiting requirement in speed [57]. High limiting ratio of resistive SFCL's will make them attractive choices in areas with high fault duty problems. Immediate response of inductive type SFCL's, on the other hand, will minimize the exposure time to fault currents and hence will enhance many operational aspects of the power system including the transient stability and security.

Table 3 shows the recommended locations for some major type FCl's mentioned in Table 2 [57]. Based on Tables 2 and 3, it is concluded that SFCL's are the only suitable devices for application in the transmission/distribution level substations.

Table 3. Recommended locations of FCL devices in smart grids [57]

FCL Location in Smart Grid	Resistive SFCL	Saturated Iron Core SFCSL	Solid State Fault Current Limiters	DFCL
Micro-grid	No	No	Yes	No
Renewable Energy Resources	No	No	Yes	No
Distribution Substation	Yes	Yes	No	Yes
Transmission Substation	Yes	Yes	No	No

Comparing current limiting ratio of SFCL's

In later chapters of this dissertation, impact of fault current limiting devices on asset management are studied. Of specific importance is the performance of these devices in limiting fault currents, which is found to be the key element in determining how efficient they are in improving asset management and maintenance programs.

There are a number of literatures available that have performed quantitative and comparative analyses on current limiting behavior of the SFCL's. [58] has studied the

impact of design parameters, and in particular the turn's ratio, of the inductive type SFCL in limiting the fault currents and also reducing the power burden of the superconductive element. [58] has also shown that the performance of SFCL's can vary depending on the fault type on the power system. We will use some of the results presented in [58] in our quantitative analysis of the impacts of SFCL's. [59] has considered and compared various application locations of SFCL's and has shown that the performance of these devices in limiting fault currents can vary based on their installation locations in the power system. In [41], the effect of various fault types on limiting capability of SFCL's is studied and concludes that these devices can limit different fault types with different limiting ratios. It is shown that e.g. in case of a single line-to-ground fault, the fault current is effectively limited because the superconducting elements of the healthy phases and the reactors shared the burden of the fault. In case of a double line-to-ground fault, the burden of the superconducting elements was reduced because the power burden of the fault phases was shared by the remaining healthy phase, but the fault current limiting rate was lower than that of a single line-to-ground fault. The fault current limiting rate of the triple line-to-ground fault was similar to that of the double line-to-ground fault.

Studies in [60] and [61] show that better results in improving transient stability and security of the power system would be obtained by using resistive SFCL's compared to inductive SFCL's. [34] and [62] show that the resistive-SFCL displays greater resistance than inductive-SFCL. This greater resistance makes the resistive-SFCL more effective than inductive-SFCL for fault current limitation. Also the temperature of the superconductive

material of the resistive-SFCL is greater than that of the inductive-SFCL. This makes the operation of inductive-SFCL safer in comparison with the resistive-SFCL, and allow it to afford successive faults [34]. Finally, the optimal combination between SFCL design, type and location in power system would guarantee the best usage of this device in electric networks of the future.

Application of SFCL in Power Systems

Application of SFCL's is a viable approach to reduce the fault current. Under normal operating conditions, a SFCL retains low impedance values so that the power flow is unobstructed. In the event of a fault, however, the impedance of the SFCL rapidly increases. Figure 7 illustrates three major configurations appropriate for SFCL installation [63]. SFCL at the main position, A, can help reduce fault currents, prevent transformer damage, and alleviate voltage dips on the upstream high-voltage bus during faults on the medium-voltage bus. Thus, a larger, low impedance transformer can be used to maintain voltage regulation at higher power level and meet increased demand on a bus without circuit breaker upgrades. SFCL installed at bus tie position, B, in the event of a fault can help maintain the voltage level on the un-faulted bus. Smaller and less expensive SFCL's can be installed in the feeder position, C, to provide protection of old and/or overstressed equipment that are difficult to replace such as underground cables or transformers in vaults.

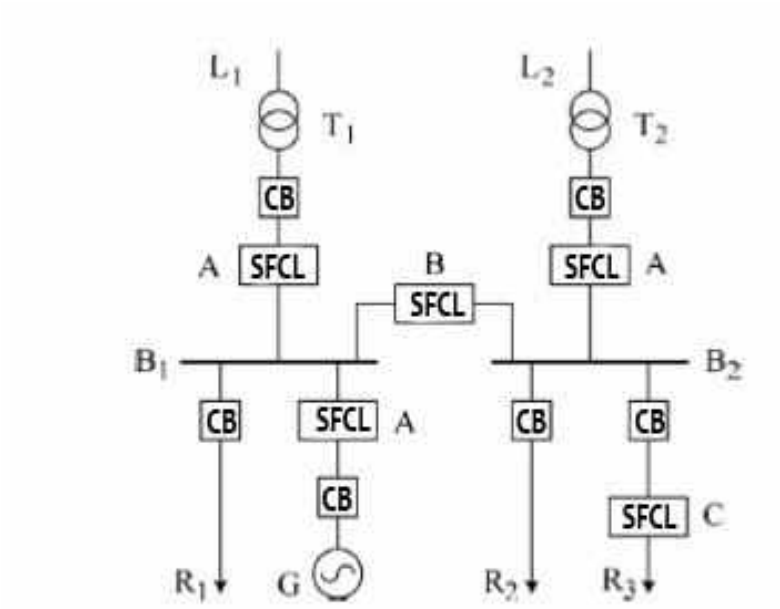

Figure 7. Main positions for SFCL in the power grid.

Diverse studies have been carried out on SFCL application in power systems to solve different issues due to fault current and other issues in the system. [64] and [24] introduce the various applications of the SFCL's in the transmission and distribution networks.

Using SFCL in Power Substations

As noted above, potential locations of SFCL's in the power system include interconnection of MV bus-bar, grid integration of distributed generation and power substations [64], [35] and [65]. The fast response of SFCL's and their higher voltage and current ratings would make them ideal choices for application in transmission and distribution level substations [57] , [46] and [36]. In next chapters of this document, application of SFCL's in transmission substations, including application of an SFCL in the electric transmission

network in the USA will be studied in more details and will show that using SFCL would improve the reliability and security measures of the load points and of the larger power system.. [66] proposes a smart sub-transmission level fault current mitigation solution using SFCL's and substation automation system for managing fault current issues in regions with high fault current levels. Application of SFCL's in substations has been studied in [36] and it is shown that SFCL's can effectively reduce the fault duty levels to those controllable by existing switchgears and protective devices. [22] studies application of SFCL's in a substation in North America and evaluates and compares the reliability indices with and without the SFCL, and concludes that SFCL plays an important role in improving the reliability and security indices of the substation and the entire power system.

A large number of possible substation configurations exist. The most commonly used ones are: single sectionalized bus arrangement, main and transfer bus system, breaker and a half and double bus systems [67]. These configurations are shown in Figure 8.

Single sectionalized bus arrangement.

All connections terminate on a common bus. This configuration is low in cost. However, all components connected to a single bus should be de-energized for the bus maintenance or if a fault occurs on a bus.

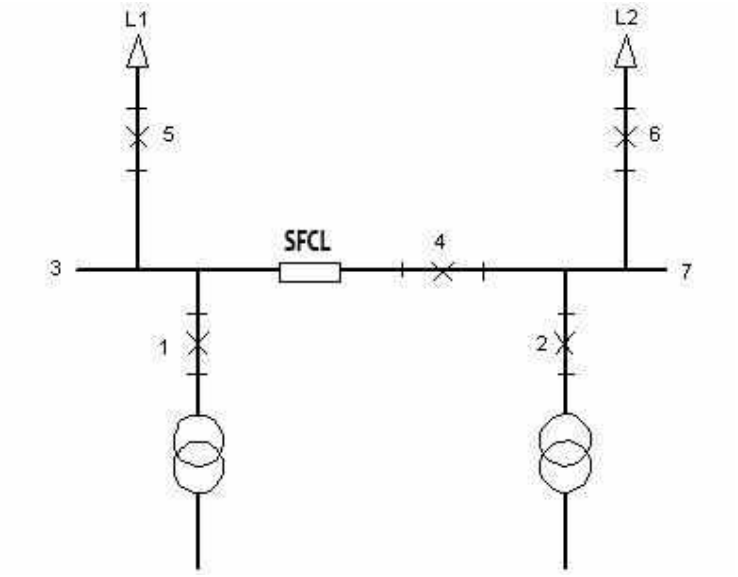

(a) Single sectionalized bus arrangement

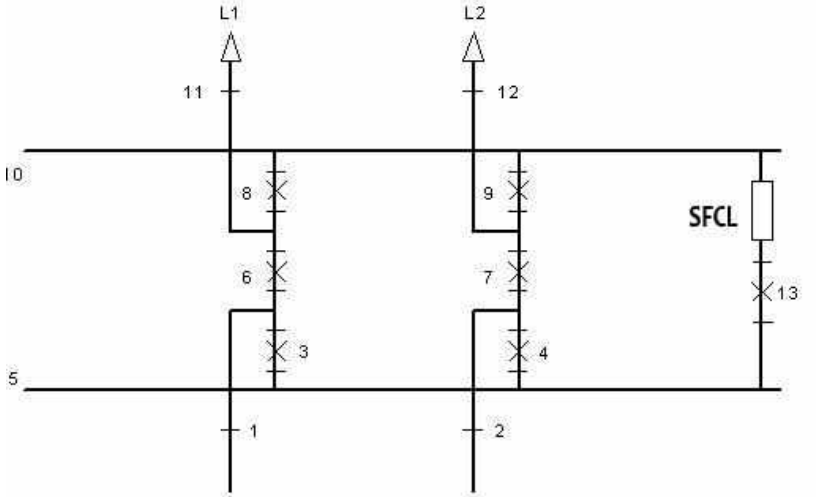

(b) Breaker and a half

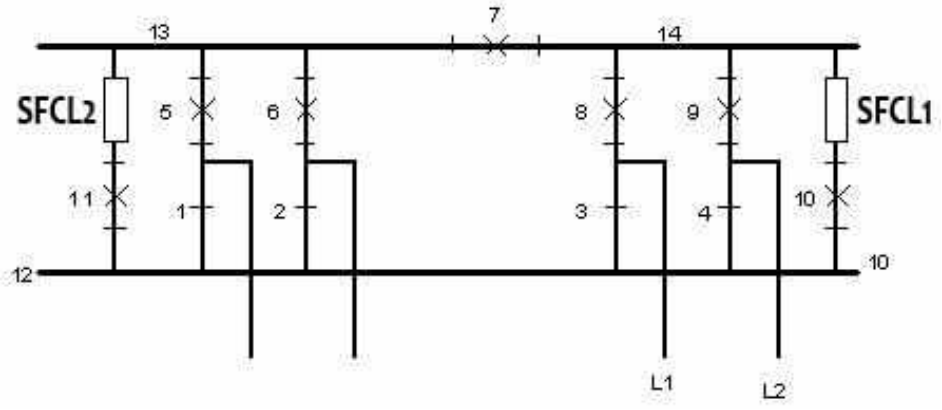

(c) Main and transfer bus system

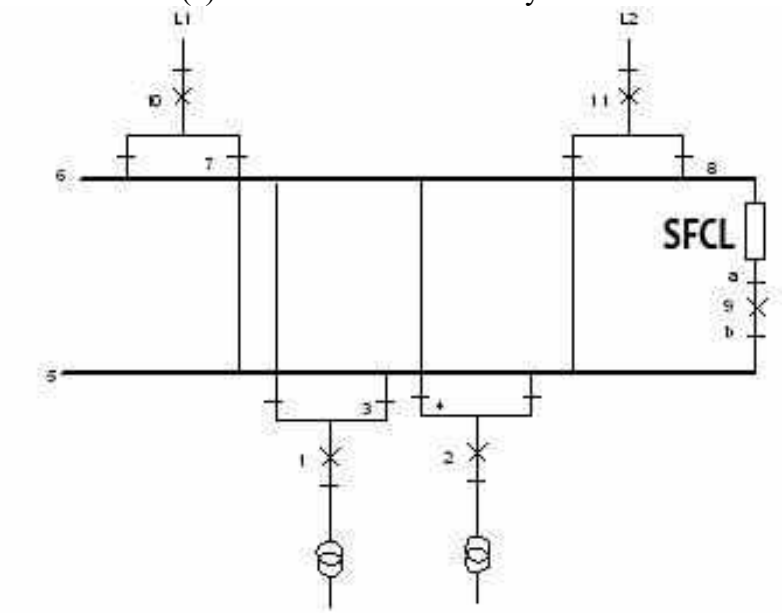

(d) Double bus system

Figure 8. Common configurations in switching substation.

Breaker and a half.

This configuration is made of legs consisting of three series breakers connected between two buses. Since two circuits are connected on each leg, 1.5 breakers are required for every

circuit. This configuration has a high degree of flexibility and reliability. Repair or maintenance could be performed on each breaker without disconnecting any circuit.

Main and transfer bus system.

A transfer bus is connected to a main bus through a tie breaker. All circuits are normally connected to the main bus, but they can be transferred to the other bus using sectionalizing switches. In this configuration, each breaker could be repaired without any circuit being interrupted. In this case the coupling switch between buses would temporarily replace the switch being repaired.

Double bus system.

In this system, a single breaker is used per circuit and that could be connected to either bus via disconnect switches. A tie breaker between buses allows circuits to be transferred without disconnecting them.

SFCL can be installed at three main locations in switching substations as shown in Figure 9. These locations include: feeder breaker position, main breaker position and bus-tie breaker position. In the feeder breaker position, SFCL protects the feeder and all downstream equipment. In this case, feeder equipment are either highly valuable or difficult and costly to replace. Underground cables are good examples of this type of equipment. Allocation of SFCL in the feeder breaker position has an advantage of requiring a smaller current rating and a disadvantage of requiring one device for each feeder [68].

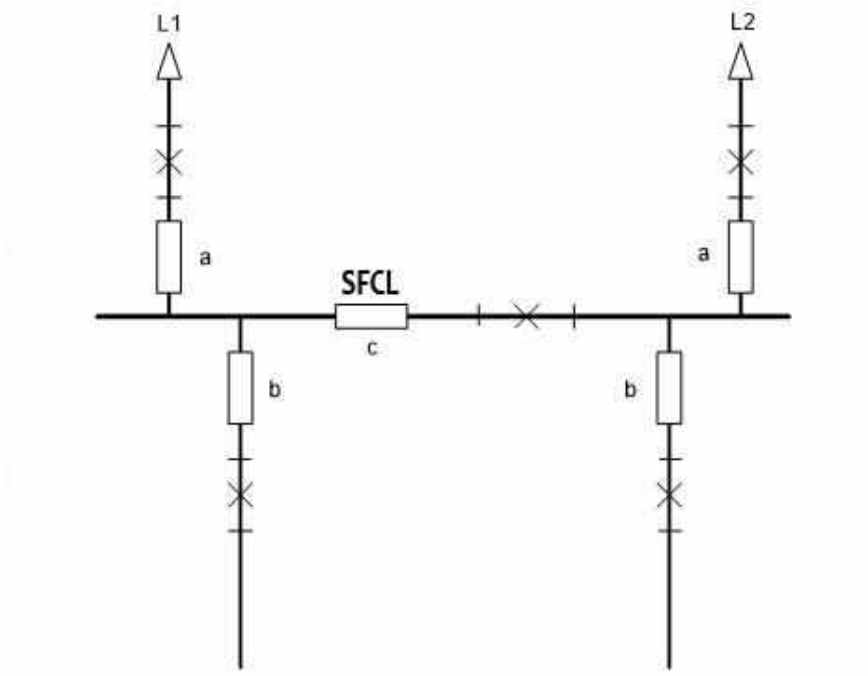

Figure 9.Three main locations for SFCL in a substation: (a) feeder breaker SFCL (b) main breaker SFCL (c) bus-tie breaker SFCL.

A SFCL in the main breaker position protects the main feeder and all bus-connected feeders. In this case, however, a separate SFCL is required for each individual incoming feeder.

A bus-tie SFCL allows two buses to be tied together without significantly raising fault current on either bus [38].

In the feeder breaker position, SFCL only limits the fault current passing through that feeder and therefore the worth of SFCL would only be equivalent to the cost of upgrading one feeder breaker. The worth of installing SFCL in the main breaker position is higher as the SFCL limits all fault currents coming from the main breaker and falling into outgoing

feeders. So the SFCL value in this location is limited to the avoided cost of upgrading the breakers connected to one bus. The bus-tie SFCL would eliminate the need to upgrade all the substation breakers. Given the limiting requirements of utilities and the avoided substation upgrading costs, installing SFCL in the bus-tie location represents an effective and cost saving application of SFCL [38] .

As it can be seen from Figure 9, SFCL has to continuously carry the full load current in the first two positions. Therefore, the bus-tie position SFCL appears to be the most economical option among other alternatives because it would have the lowest losses under normal operating conditions [68].

Coordination with Protection System

In order to provide sufficient current to the protective devices, SFCL should not limit the current to a level that would be below the operating current of the relays. This, however, does not apply when a SFCL is used at the bus-tie position [25]. In a bus-tie location, SFCL could reduce the fault current to the steady state level or even lower. Therefore, in the bus-tie location, the protective relaying is required to be able to detect the fault even though the fault current is reduced to the normal value or less. Below is an example of this situation.

Consider the circuit shown in Figure 10 (a) that shows a simple arrangement called “single sectionalized bus arrangement”. If an active failure (short circuit) occurs at breaker 4, fault currents will flow in the directions shown in Figure 10 (b). Current “I_2” is the actual short

circuit current while "I_1" has been limited by the SFCL. If the SFCL didn't exist, in case of a fault at breaker 4, the protective devices –which are usually differential relays- would detect the fault and open breakers 1 and 2 simultaneously. With SFCL in the circuit, although the current has been limited, it is still required to detect the fault and isolate it at the earliest possible. Therefore, breaker 2 opens as a result of large short circuit current. Breaker 1, however, doesn't open and continues to send the normal current to load L_1 until the fault is detected and the "load interruptible disconnector" (LID) no. 4a interrupts the fault current. Therefore, by installing the SFCL, load point L_1 is not curtailed.

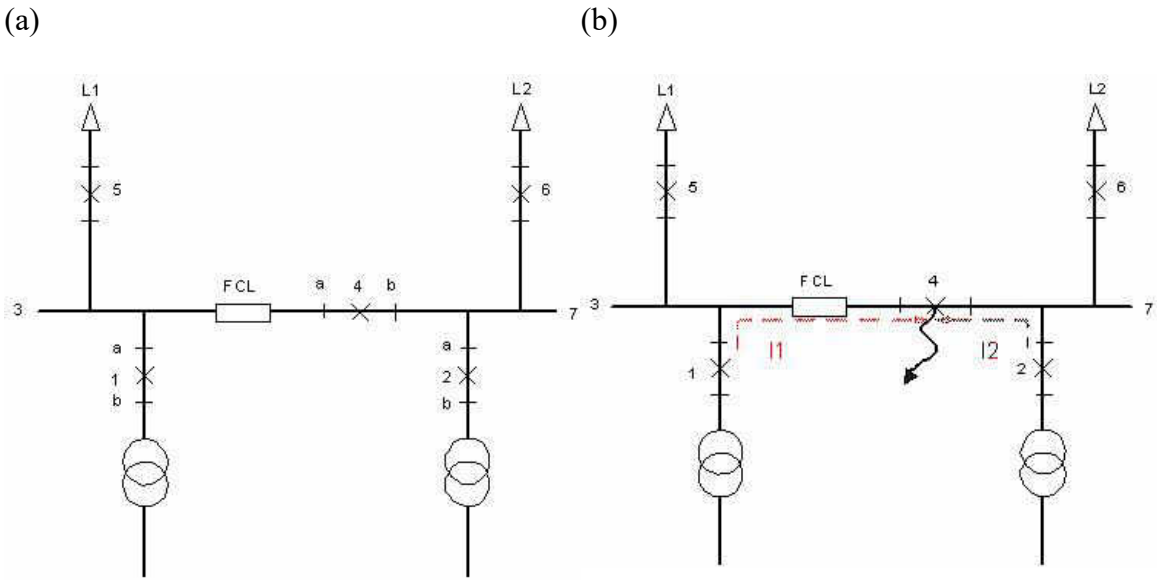

Figure 10. Single sectionalized bus arrangement: (a) before the fault (b) after the fault at "4".

Application of SFCL in these arrangements and locations and their impacts on asset management will be studied further later in this document, and results will be compared.

CHAPTER III
DEPENDABILITY/SECURITY ANALYSIS OF PROTECTION SYSTEMS

Another important class of devices that limit the impact of fault currents on power equipment and on the power system in general, are protection devices. Protection systems are inseparable parts of power systems and are responsible for protecting valuable assets and improving reliability and security of the power system. Protection systems perform this by acting on time in limiting the spread of fault current to the healthy parts of the system [69]. The degree of protection and assurance that these systems provide against fault currents, is therefore dependent on how much "on-time" or how fast they can act in detecting and clearing the faults in real time. This depends on factors such as design, relay structure, and the protection scheme that is in place.

In this chapter we perform security and dependability analysis of protection systems. We need the results of this analysis to be able to find the expected clearance time of various protection systems. We will then use the expected clearance time along with the theory developed in chapter five to determine impact of various protection systems on asset management.

Reliability of protection systems includes two major areas of security and dependability [70] and [71]. Security is the degree of certainty that protection systems will not operate incorrectly when they should not operate, while dependability is the degree of certainty that protection systems will operate correctly when they should operate [71].

In each moment of time, a protection system can reside in one of the following states:

S	Protection succeeds in clearing internal faults (instantaneous)
F	Protection fails in clearing internal faults (protection not healthy while needed to operate)
SB	Protection operated correctly to block over-tripping during external faults. (Does not operate when it is not required)
MF	Malfunction (protection operated incorrectly)
SN	Protection is healthy but not required to operate
FN	Protection is not healthy while not required to operate
SD	Protection succeeds in clearing fault but after a time delay (clearing is not instantaneous)

During an internal fault (fault in the zone of protection that should be cleared by the protection system), protection system can be in one of the states: S, F or SD. If T_S , T_F , and T_{SD} are clearing times associated with these states respectively, then the expected clearing time for the protection system would be:

$$\delta = P(S).T_S + P(F).T_F + P(SD).T_{SD} \quad (1)$$

Where $P(S)$, $P(F)$, and $P(SD)$ are probabilities of being in states S, F or SD, respectively. To find the value of these probabilities, performing security and dependability analysis is necessary.

To do this as a general practice, we focus our study on one of the most widely used types of protection systems known as the pilot distance protection scheme [72].

Distance Protection Schemes and Application of Pilot Protection

The distance protection method is the most used techniques for preventing damages that can be inflicted on transmission lines [72]. In recent decades, selectivity issues have raised the demand for introducing a means of communication and therefore the so called "pilot protection" into the regular distance protection schemes.

Selectivity in protection refers to the ability of protection system to isolate the faulty component without affecting non-faulty parts of the power system [73]. Usually each major component in power system is provided with its own protection system and their timing is set in a way that selectivity is ensured. If the protection system responsible for the isolation of the faulty component does not operate, a so called "back up" system will operate and will usually isolate a bigger part of the system. Therefore, tripping time of the backup system must be longer than that of the main system so that it can wait, and interferes only after the main system failed to operate in the designated time.

In transmission networks, selectivity issue is much more complicated due to the large number of equipment involved and their dispersed locations. In such systems, security calls

for employing a relatively large number of protection devices and arranging them so that sufficient time grading is allowed between tripping characteristics. As a result of this time grading, considerable time delays would be allotted to the remote end devices. In many applications such as EHV systems where lines carry large power transfers, delayed tripping of faults may cause drastic network stability problems.

To avoid the unnecessary time delays when instantaneous fault clearance is intended, pilot protection systems have been proposed. There are a number of pilot protection schemes available [69]. The most important ones are discussed in the following parts of the paper. These schemes differ widely in the degree of reliability they offer. A quantitative analysis should therefore be performed to determine the security and dependability of each scheme and to shed light on the subject of selecting the appropriate design with respect to the required level of the reliability.

In this chapter, first pilot protection systems are introduced and various types of these systems are discussed. Pilot protection systems generally include: DUTT[1], PUTT[2], POTT[3], DCB[4] and DCUB[5].

[1] Direct Under-reach Transfer Trip
[2] Permissive Under-reach Transfer Trip
[3] Permissive Over-reach Transfer Trip
[4] Directional Comparison Blocking Scheme
[5] Directional Comparison Unblocking Scheme

Distance protection is an accredited form of protection for transmission systems particularly when the line terminals are relatively far apart. In a typical power transmission line, such as the one shown in Figure 11, this is usually done by using the distance relays "*R*" and "*S*" at the two ends of the line.

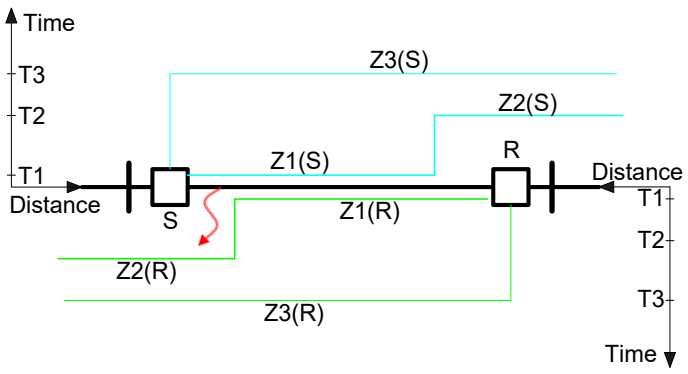

Figure 11. Typical transmission line protected by distance relays.

Assume that a fault occurs at the left end of the line close to relay "*S*". Relay "*S*" recognizes the fault as a zone 1 fault and trips the circuit breaker instantaneously. The relay at the other end of the line detects the fault as a zone 2 fault. It is, however, not able to determine if the fault near the left side bus is on one side or the other side of that bus. This will cause a timer at relay "*R*" to be started, which will result in delayed tripping. In many applications, this time delay is not acceptable. Adding a pilot channel from the left end to the right end of the line could be considered as a means of eliminating the time delay. The

pilot signal generated at relay "*S''* informs the right-end relay "*R*" that the fault is on the protected line, thereby tripping should be initiated without delay.

There are several advantages in high-speed simultaneous tripping of all line terminals for all internal faults [2]. Some of these advantages are as follows:

- Reduced possibility of line damage
- Improved power system transient stability
- Allowance for high speed tripping, which if successful, improves transient stability, minimizes the outage time, and improves voltage conditions.

Unit protection schemes compare the conditions at the two ends of the protected feeder simultaneously. These schemes can positively identify whether the fault is internal or external and are capable of providing high-speed protection for the whole feeder length. However, unit protection schemes don't provide backup protection to adjacent feeders as given by distance protection schemes. The most desirable scheme is the one that combines the features associated with both arrangements, i.e. instantaneous tripping for the whole feeder length plus back up protection to adjacent feeders. This can be achieved by interconnecting the distance protections at each end of the protected line by a signaling channel as shown in Figure 12.

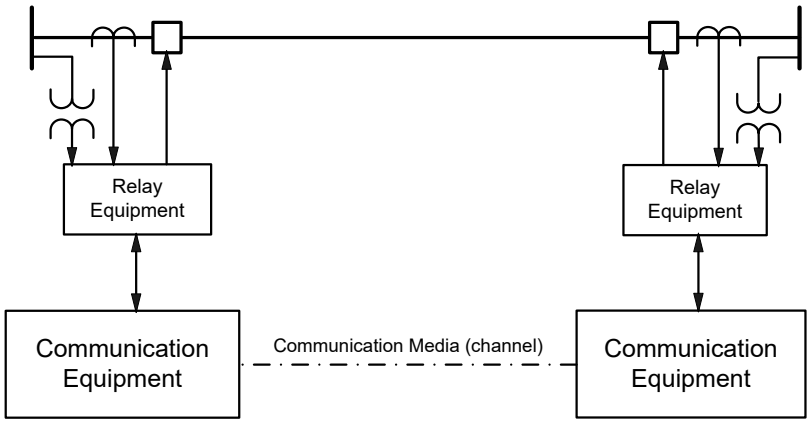

Figure 12. General view of a pilot protection system [69].

Traditional communication channels used for pilot protection include pilot wires, power line carrier (PLC), and microwaves. The latter two channels are still widely used by utilities.

Fiber optics emerged in the early 1980s as a new type of communication means for pilot protection [74]. Fiber optic channels have broad bandwidths and eliminate electrical induction, noise, and electrical insulation problems of pilot wire channels.

The voltages and currents at each end of the transmission line are monitored by the local relay equipment where trip signals maybe generated and sent to the local circuit breakers. In addition, the local relay sends a signal (either a logic information or phase or current information depending on the scheme of protection) to the relay equipment at the remote end of the line through the communication equipment and channel. This provides each relay location with important new information regarding the need for tripping [69].

Classification of Pilot Protection Systems

Pilot protection systems can be classified according to the transmission media or the channel usage [69].

By Transmission Media Used

The media used for the transmission of protection signals are: power line carrier (PLC), microwave, fiber optics, and telephone leased lines.

The choice of utilizing the pilot signals depends on several factors, such as the availability of fiber optic or microwave paths, cost, reliability, and type of the relay scheme.

In power system protection communications, the signaling applications have traditionally been analog transmission in any of these media, although digital systems are predominating as they are becoming available with reasonable costs.

By Channel Use:

In terms of channel use, pilot systems can be either transfer trip or blocking systems.

Transfer trip systems.

In the transfer trip systems, a channel signal must be transmitted and received before tripping occurs at internal faults. No channel signal is required for external faults. Transfer trip systems differ in the principle they use for sending the trip signals. The most important transfer trip systems are as follows:

Direct under-reach transfer trip scheme (DUTT) [75].

The DUTT scheme uses an instantaneous zone 1 element to trip the local circuit breaker and initiate a transfer trip to the remote end. Once the transfer trip signal is received, the remote end trips immediately without any additional verification. The basic logic circuit is shown in Figures 13.b and c. This scheme is extremely simple but is susceptible to undesired tripping if channel noise keys the direct trip signal. This is why it is rarely used. This risk can be minimized by using a dual-channel transfer trip, which requires the receipt of two signals from the remote ends to affect a trip.

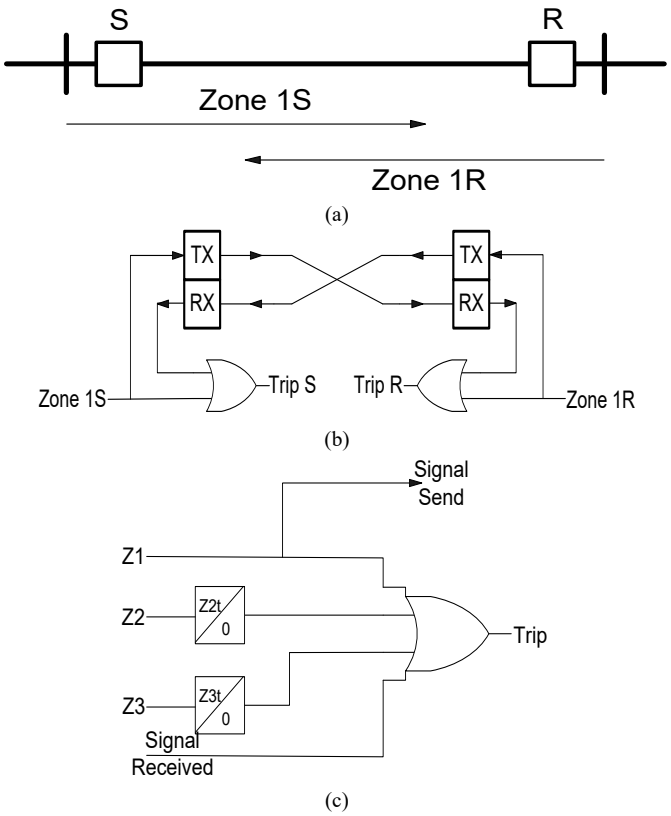

Figure 13. Direct under-reach transfer trip protection. (a) Zones of protection (b) Pilot protection logic.

Permissive under-reach transfer trip scheme (PUTT) [75].

The DUTT scheme can be modified to be more secure by supervising the received signal with the instantaneous zone 2 operations before permitting a trip, as shown in Figure 14.

This modified scheme; i.e. PUTT, uses zone 1 to trip the local breaker and sends a permissive trip signal to the remote end. The remote end breaker trips when it receives the permissive signal, if its zone 2 element detects a fault. As it uses the zone 2 element to supervise tripping on receipt of the permissive signal, unlike DUTT, this scheme is less susceptible to mal-operation under noisy channel conditions. Because the scheme uses an under-reaching element to send permission, PUTT doesn't send a permissive signal for out-of-section faults.

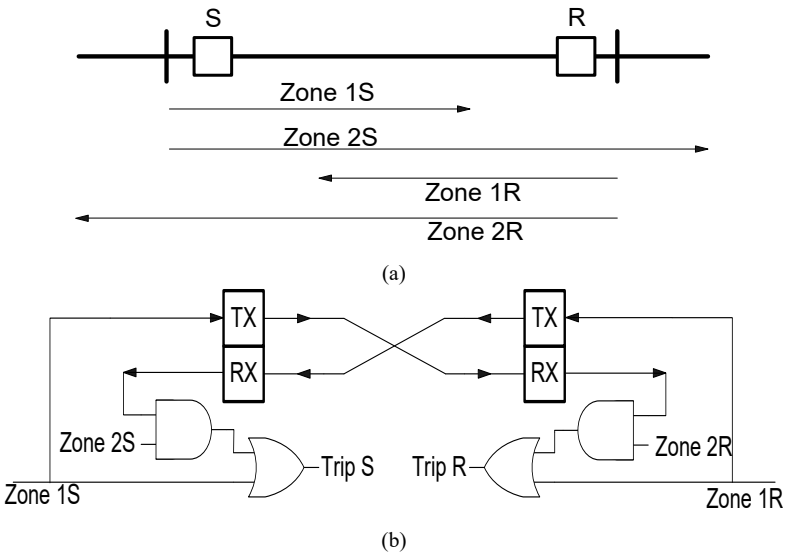

Figure 14. Permissive under-reach transfer trip protection. (a) Zones of protection (b) Protection Logic.

Permissive Over-reach Transfer Trip Scheme (POTT) [75] :

POTT schemes use an over-reaching zone 2 element to send a permissive trip signal to the remote end. The remote end breaker trips when it receives the permissive signal, if its zone 2 element is detecting a fault as well. Figure 15 illustrates the POTT scheme.

If distance relays with mho characteristics are used, the scheme is better suited than the PUTT for protecting short lines. The reason for this is that the resistive coverage of the zone 2 unit is greater than that of zone 1.

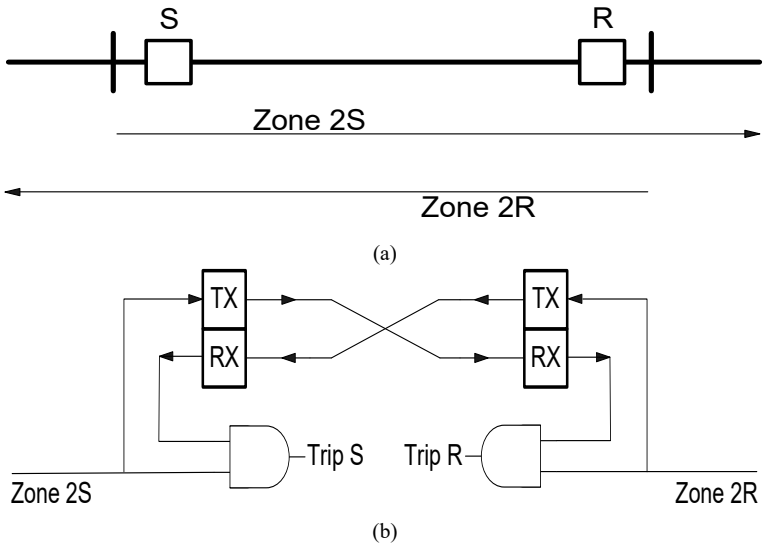

Figure 15. Permissive over-reach transfer trip protection. (a) Zones of protection (b) Pilot protection logic [75].

Blocking systems.

In the blocking systems, the channel is only used to prevent tripping of the remote circuit breakers on external faults. The channel signal is not required for internal faults; i.e. tripping occurs in the absence of a channel signal.

Directional comparison blocking scheme (DCB) [75].

Unlike the above schemes, in which a signal is sent when a fault is detected in the forward direction, DCB scheme sends a signal (block trip) when a fault is detected in the reverse direction. If the local relay detects a reverse fault (using zone 3), it sends a block trip signal to the remote end. At the remote end, the over-reaching zone 2 elements are allowed to trip, following a short coordinating time delay (shown in Figure 16 as T), if they are not blocked by the arrival of the block trip signal. In practice, zone 3 units are set with a forward offset characteristic to provide back-up protection for bus-bar faults after zone 3 time delay. This makes it necessary to stop the blocking signal being sent for internal faults. This is achieved by making the signal sending circuit conditional upon non-operation of the forward looking zone 2 unit, as shown in Figure 16.

The on-off power line carrier is the channel which is almost always used with DCB scheme. Since the communication channel is not required for tripping, internal faults that might short and interrupt the channel (in case of PLC) are not a problem. Over-tripping will occurs, however, if the channel or local relay equipment fail to operate for external faults

within the reach of the trip fault detectors. Since the carrier transmitter is normally off (non-transmitting state), channel failure can't be detected until the system is tested or an external fault occurs. This limitation has led to the development of a number of check-back schemes.

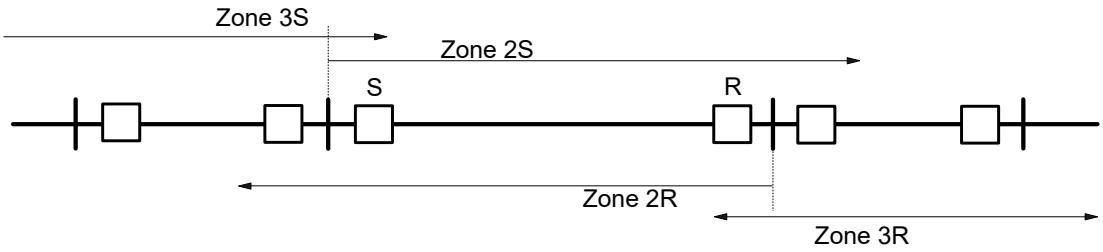

(a)

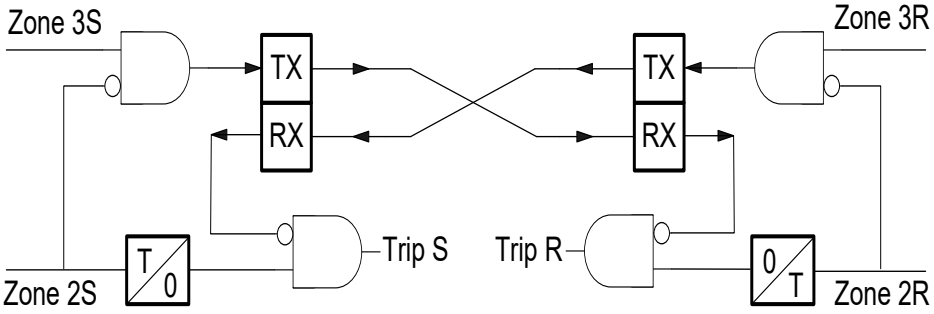

(b)

Figure 16. Directional comparison blocking protection. (a) Zones of protection (b) Pilot protection logic [75].

Directional comparison unblocking scheme (DCUB) [75].

The solid-state logic diagram for this type of system is shown in Figure 17(b).

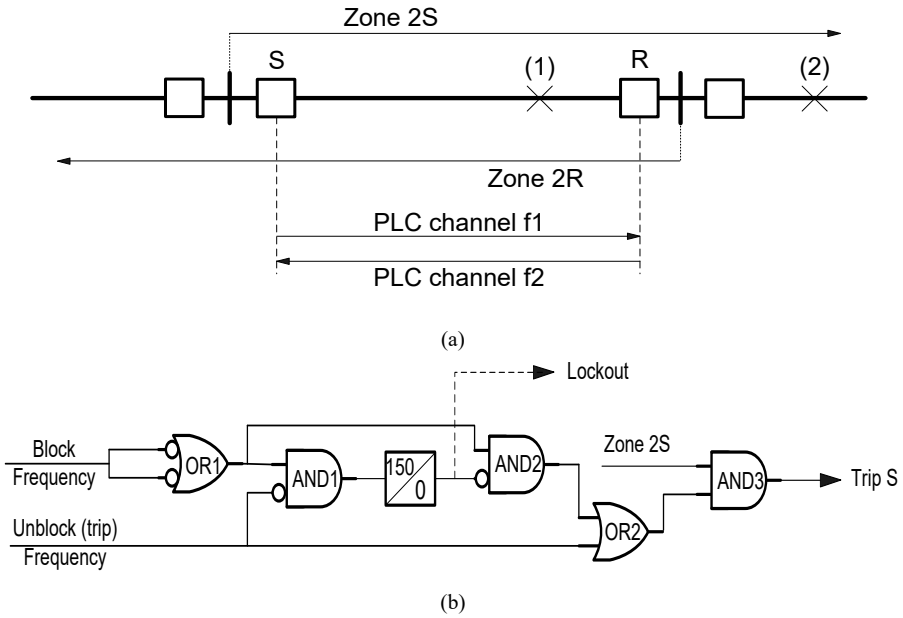

Figure 17. Directional comparison unblocking protection. (a) Zones of protection (b) logic circuit.

Normally, a block frequency is transmitted and OR-1 has no output. Therefore, both AND-1 and AND-2 are unsatisfied, which means that OR-2 has no output. The block frequency is removed for an internal fault, which means that OR-2 will be satisfied whether the unblock signal is operable or not. This is important as it is possible that the unblock signal is shorted out by the fault. When this occurs, OR-1 gives an input to AND-2 which satisfies this gate for 150ms. Then AND-2 picks up OR-2 to provide an input to AND-3. Without this unblock signal, 150ms is provided for tripping. After 150ms, lockout is initiated since one of the inputs to AND-2 is removed. This removes the input to AND-3.

If the unblock signal is received, this results in an input to OR-2 to directly provide input to AND-3, which results in a trip. The unblock signal also removes an input to AND-1 to

stop the timer. Table 4 describes the operation of the DCUB, associated with faults (1) and (2) shown in Figure 17(a).

Table 4. Summary of Operation of the Directional Comparison Unblocking

Type of fault	**Events at station S**	**Events at station R**
(1) Internal	Zone 2S operates. f1 channel shifts to unblock. Loss of block and/ or receipt of unblock (f2) inputs to AND-3. Trip.	Zone 2R operates. f2 channel shifts to unblock. Loss of block and/or receipt of unblock (f1) inputs to AND-3. Trip.
(2) External	Zone 2S operates. f1 channel shifts from block to unblock. F2 channel continues to block. No trip.	Zone 2R does not see fault. Loss of block and/or receipt of unblock (f1) inputs to AND-3. No trip.

In this work in order to compare the impact of adding redundancy to specific parts of the pilot protection system as well as using different media for communication, the following configurations have been considered and studied for each pilot scheme

- Single relay/ Single Microwave (MW) channel
- Single relay/ Redundant channel (MW+ relay to relay on phone line)
- Single relay/ Single channel (dedicated fiber optic)
- Single relay/ Single channel (multiplexed fiber optic)
- Redundant relay/ Single channel (MW)
- Redundant Relay/ Independent channels (MW+ relay to relay on phone line)

Event Tree Analysis

The event tree development process determines the boundaries of the particular analysis by defining the initiating event and the possible outcomes for each sequence of events. The event tree analysis defines possible scenarios including success, and partial and/or complete system/subsystem failure. Because of this, event tree analysis is a preferred method in studying complex systems and those whose response and consequences are not quite obvious and need a more in-depth cause and effect analysis. Other similar techniques such as fault trees are often used to quantify system events that are part of event tree sequences [3].

An event tree is a pictorial representation of all events which can occur in a system. It is defined as a tree because the pictorial representation gradually fans out like the branches of a tree as an increasing number of events are considered. Beginning with an initiating event; the event tree details a sequence of pivotal events that lead to specific end states (e.g. OK, Partial Failure or Failure).

In a protection system, event tree is typically started with a particular event – e.g. occurrence of a fault- and continues in each step by considering the operation or failure of the elements in that stage. This procedure is continued until it reaches the system success, failure, or any other modes of interest. In this way, a pictorial diagram of the system behavior is built up.

Here, the term “protection system success” is defined as “the ability of protection system to clear the fault in a prescribed time”; any deviation from this definition is not regarded as a system success. A list of abbreviations used in the event tree diagrams and a short definition of each term are given in the beginning of this chapter.

It should be noted that in order to calculate reliability indices from the event tree diagrams, failure rate and unavailability of various elements of the system should be known. In this chapter, after drawing the event tree diagrams, failure mechanisms of the protection system are studied.

Internal and External Faults

It is useful to note that, from the protection viewpoint, not all internal faults are the same within the zone of the protected line. There are two major areas to be considered throughout the line as shown in Figure 18. These areas include the two end zones of the line and the overlapping zone. The overlapping zone area is within the zone 1 reach of both relays. However, the end zones are detected as zone 1 by the nearby relay and as zone 2 by the remote relay. Different reaction is expected from the protection scheme in clearing the fault in these areas and consequently different event trees should be constructed for each case.

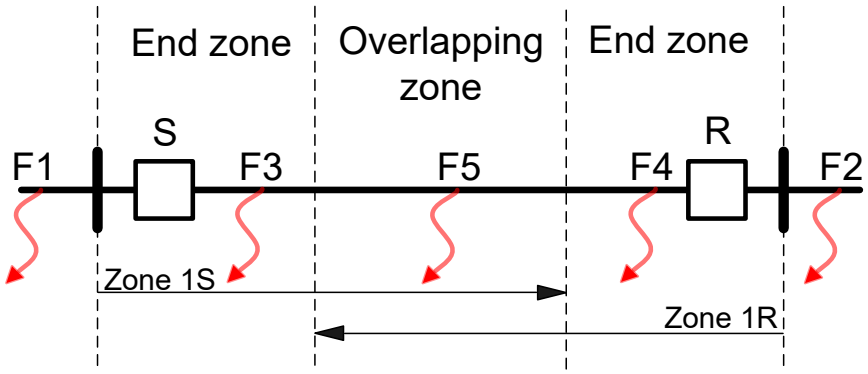

Figure 18. Classification of faults: F1&F2-External faults, F3&F4-internal end-zone faults, F5-internal overlapping-zone fault.

However, the above bordering rule is not completely rigid. The reason is that the accurate impedance of the line may not be available in each zone reach. In practice, faults near the borders of these areas could result in malfunction of the protection system. More accurate analysis is required in order to take these errors into account.

Building Event Trees

The inherent advantage of the event tree is its capability to investigate the attitude of the protection scheme when a fault occurs in the system. Since the philosophy of protection is different in case of internal and external faults, it is necessary to distinguish these two faults when building the event trees.

With respect to the above points, an event tree analysis has been performed for each pilot scheme discussed earlier and results are shown in Figures 18 to 20 as referring to the list provided in the following table.

Table 5. List of Event Tree Illustrations for Pilot Protection Schemes

Pilot Scheme	Type of fault	Configuration of pilot protection (see below)					
		Config. 1	**Config. 2**	**Config. 3**	**Config. 4**	**Config. 5**	**Config. 6**
DUTT	External fault	Fig.19.a	Fig.19.c	Fig.19.e	Fig.19.g	Fig.20.a	Fig.20.c
	Internal fault	Fig.19.b	Fig.19.d	Fig.19.f	Fig.19.h	Fig.20.b	Fig.20.d
DCB	External fault	Fig.21.a	Fig.21.c	Fig.21.e	Fig.21.g	Fig.21.i	Fig.21.k
	Internal fault	Fig.21.b	Fig.21.d	Fig.21.f	Fig.21.h	Fig.21.j	Fig.21.l
DCUB	External fault	Fig.22	Fig.24	Fig.26	Fig.28	Fig.30	Fig.32
	Internal fault	Fig.23	Fig.25	Fig.27	Fig.29	Fig.31	Fig.33

The referred configurations in above table are as follows:

config. 1: Single relay/ Single Microwave (MW) channel

config. 2: Redundant relay/ Single channel (MW)

config. 3: Single relay/ Redundant channel (MW+ relay to relay on phone line)

config. 4: Single relay/ Single channel (dedicated fiber optic)

config. 5: Single relay/ Single channel (multiplexed fiber optic)

config. 6: Redundant Relay/ Independent channels (MW+ relay to relay on phone line)

Event Trees for Direct Under-reach Transfer Trip (DUTT)

The event tree for this scheme is shown in Figures 19 a to h and 20 a to d.

The diagrams consist of individual events representing the failure or success of each component in the system. Failure rates and probabilities associated with these events will be introduced in the next part of the chapter.

It can be seen from these figures that for external faults failure of any component within the protection system would result in mode "FN" in case of an external fault. If all elements are healthy, though, the protection is healthy but yet not required to operate (SN). Please refer to beginning of this chapter for a complete list of protection system modes used in the figures.

In Figure 19.e, DUTT single relay/ redundant channels (MW+ relay to relay phone line), if any component of the MW channel- say tone equipment at "S" side- is faulty, the fault tree reaches to the point "A" in the fault tree diagram, where checks the second media channel (phone line here) for health and again results in "FN" if the auxiliary channel is faulty as well.

Figure 19.b1 illustrates the concept of redundancy in protective relays and can be described as follows: If the primary protection at “S” fails due to the hardware failure or relay being misapplied, the event tree reaches to point “B”. At this point, the backup protection is examined for health. If the protection at “S” (primary or backup) is neither hardware-faulty nor misapplied, the event tree continues to point “D” indicating that protection at “S” is healthy. The same scenario is repeated for the protection at “R”.

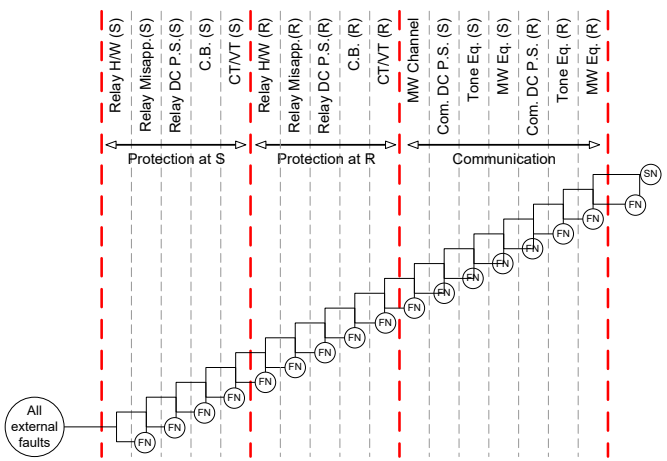
Relay H/W (S)
Relay Misapp.(S)
Relay DC P.S.(S)
C.B. (S)
CT/VT (S)
Relay H/W (R)
Relay Misapp.(R)
Relay DC P.S.(R)
C.B. (R)
CT/VT (R)
MW Channel
Com. DC P.S. (S)
Tone Eq. (S)
MW Eq. (S)
Com. DC P.S. (R)
Tone Eq. (R)
MW Eq. (R)
Protection at S
Protection at R
Communication
All external faults
FN
SN

(a)

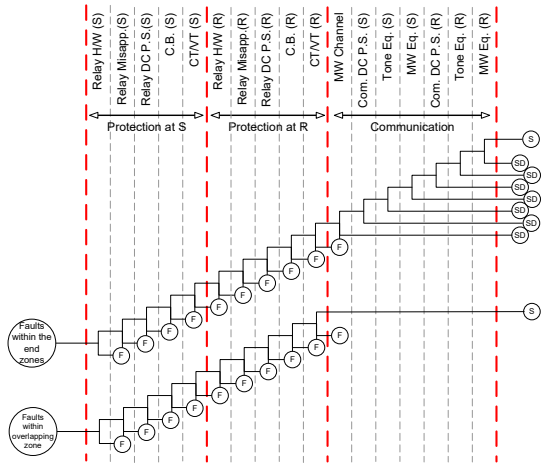
Relay H/W (S)
Relay Misapp.(S)
Relay DC P.S.(S)
C.B. (S)
CT/VT (S)
Relay H/W (R)
Relay Misapp.(R)
Relay DC P.S.(R)
C.B. (R)
CT/VT (R)
MW Channel
Com. DC P.S. (S)
Tone Eq. (S)
MW Eq. (S)
Com. DC P.S. (R)
Tone Eq. (R)
MW Eq. (R)
Protection at S
Protection at R
Communication
Faults within the end zones
Faults within overlapping zone
F
S
SD

(b)

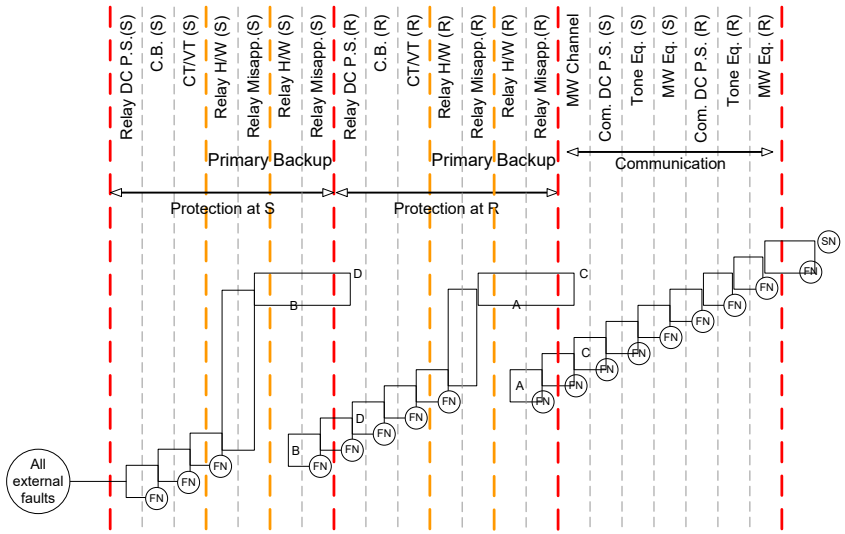
Relay DC P.S.(S)
C.B. (S)
CT/VT (S)
Relay H/W (S)
Relay Misapp.(S)
Relay H/W (S)
Relay Misapp.(S)
Relay DC P.S.(R)
C.B. (R)
CT/VT (R)
Relay H/W (R)
Relay Misapp.(R)
Relay H/W (R)
Relay Misapp.(R)
MW Channel
Com. DC P.S. (S)
Tone Eq. (S)
MW Eq. (S)
Com. DC P.S. (R)
Tone Eq. (R)
MW Eq. (R)
Primary Backup
Primary Backup
Communication
Protection at S
Protection at R
All external faults
A
B
C
D
FN
SN

(c)

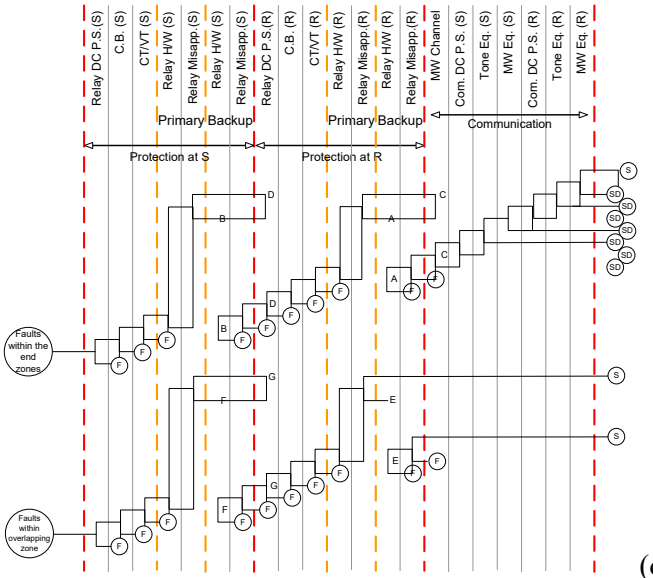
Relay DC P.S.(S)
C.B. (S)
CT/VT (S)
Relay H/W (S)
Relay Misapp.(S)
Relay H/W (S)
Relay Misapp.(S)
Relay DC P.S.(R)
C.B. (R)
CT/VT (R)
Relay H/W (R)
Relay Misapp.(R)
Relay H/W (R)
Relay Misapp.(R)
MW Channel
Com. DC P.S. (S)
Tone Eq. (S)
MW Eq. (S)
Com. DC P.S. (R)
Tone Eq. (R)
MW Eq. (R)
Primary Backup
Primary Backup
Communication
Protection at S
Protection at R
Faults within the end zones
Faults within overlapping zone
A
B
C
D
E
F
G
S
SD

(d)

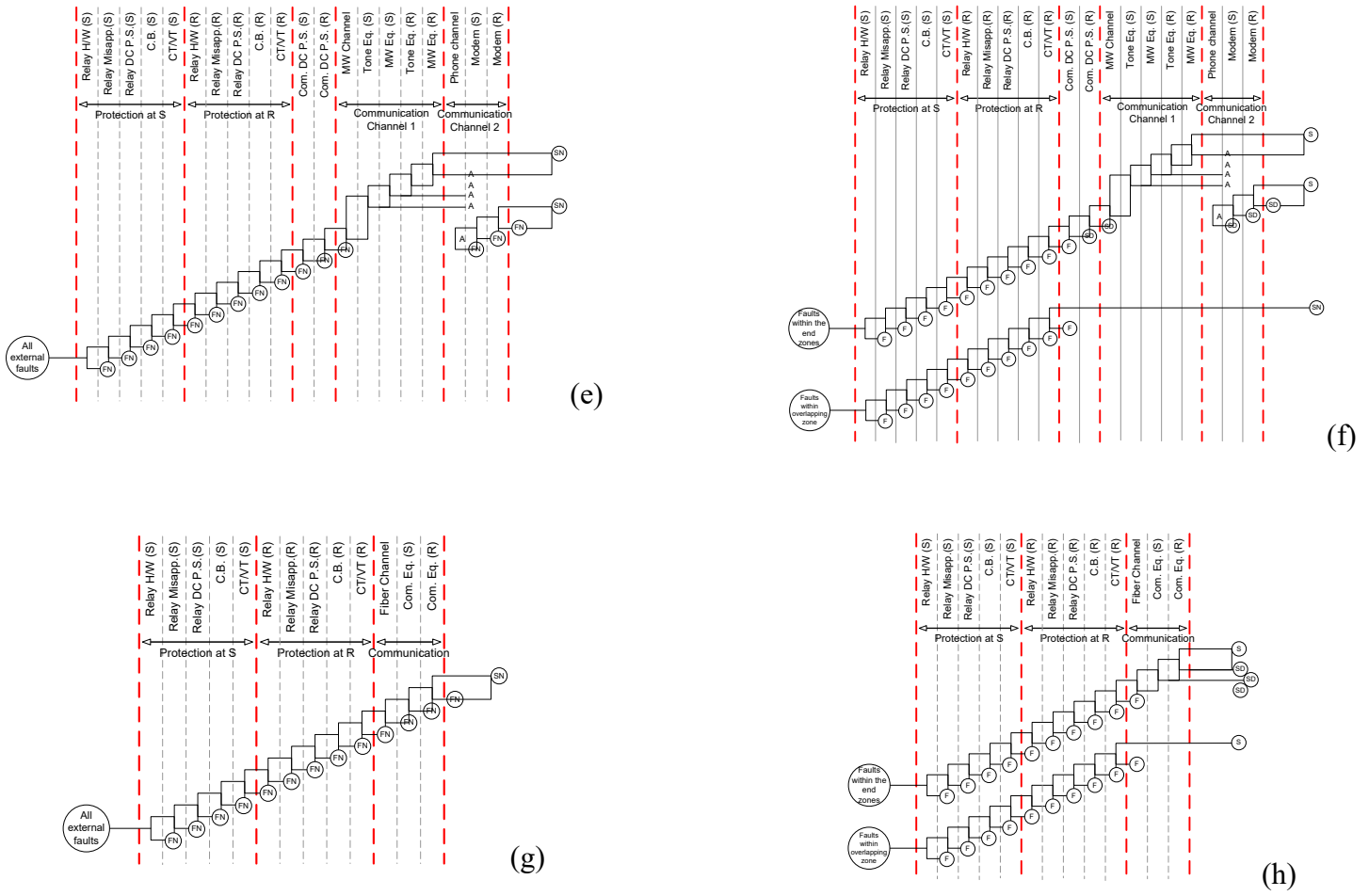

Figure 19. Event tree for DUTT. *S*: Protection successful, *F*: Protection fails, *SB*: successfully blocked over-tripping, *MF*: Malfunction, *SN*: Protection healthy but not required, *FN*: Protection not healthy and not required, *SD*: Protection succeeds after a time delay

Figure 20.c illustrates the situation where redundant relays and independent channels (MW+ relay to relay phone line) are applied. In this case, if the relay on channel 1 is faulty at “S”, the event tree reaches point “A” where the second channel relay is examined for being healthy. Should the channel 2 relay work, the event tree continues in the bottom branch or else the system stops in “FN” mode. In the bottom path, only channel 2 relay is healthy and hence the event tree continues regardless of status of channel 1 relay in station “R”. If in channel 2 of station “R”, both relay and communication are healthy, the entire system is healthy while not required to operate (SN); otherwise, it results in “FN”. Point “B” is where the channel 1 relay is healthy and channel 2 relay fails and continues on the middle branch with examining only channel 1 at station “R”.

The top path continues when both channel 1 and channel 2 relays at “S” station are healthy. In this case, if channel 1 relay at “R” fails, only channel 2 remains healthy and the event tree reaches point “C” to examine channel 2 media, i.e. microwave. Similarly, event tree reaches “D” when channel 2 relay at “R” fails leaving only channel 1 healthy. Moreover, if both channel relays at “R” are healthy, the system could work through either channel, i.e., if one media fails it goes straight to the other one. This concept is represented by point “E” in the event tree.

Figure 19.b states that any error in the protection system at “R” or “S” would result in “F” mode. Defects in the communication, however, stop the permissive protection and the fault is cleared with time delay of zone “2” that is denoted with “SD”. If the internal fault is in the overlapping zone as defined in Figure 19, instantaneous zone 1 elements of both relays directly clear the fault and the pilot media is bypassed (Figure 19.b second diagram).

In the next configurations, redundancy is added in terms of extra relays and/or channels and the same ideas are applied as above.

Note that in all cases, successful clearing of internal faults within the end zones requires proper pilot signaling while this is not the case in the overlapping area.

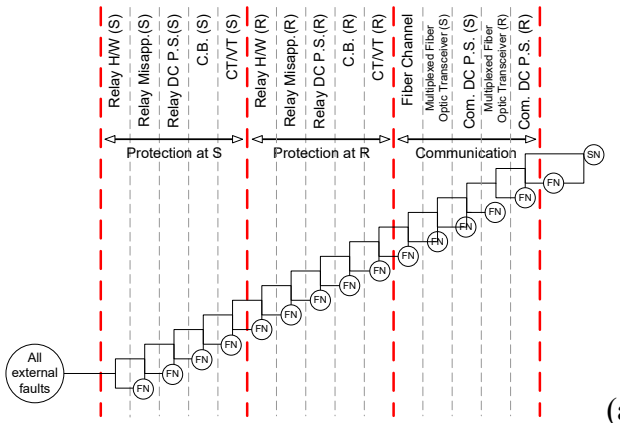
Relay H/W (S)
Relay Misapp.(S)
Relay DC P.S.(S)
C.B. (S)
CT/VT (S)
Relay H/W (R)
Relay Misapp.(R)
Relay DC P.S.(R)
C.B. (R)
CT/VT (R)
Fiber Channel
Multiplexed Fiber Optic Transceiver (S)
Com. DC P.S. (S)
Multiplexed Fiber Optic Transceiver (R)
Com. DC P.S. (R)
Protection at S
Protection at R
Communication
All external faults
FN
SN

(a)

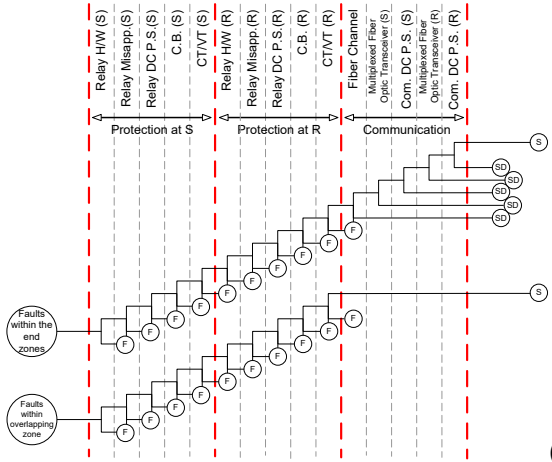
Relay H/W (S)
Relay Misapp.(S)
Relay DC P.S.(S)
C.B. (S)
CT/VT (S)
Relay H/W (R)
Relay Misapp.(R)
Relay DC P.S.(R)
C.B. (R)
CT/VT (R)
Fiber Channel
Multiplexed Fiber Optic Transceiver (S)
Com. DC P.S. (S)
Multiplexed Fiber Optic Transceiver (R)
Com. DC P.S. (R)
Protection at S
Protection at R
Communication
Faults within the end zones
Faults within overlapping zone
F
S
SD

(b)

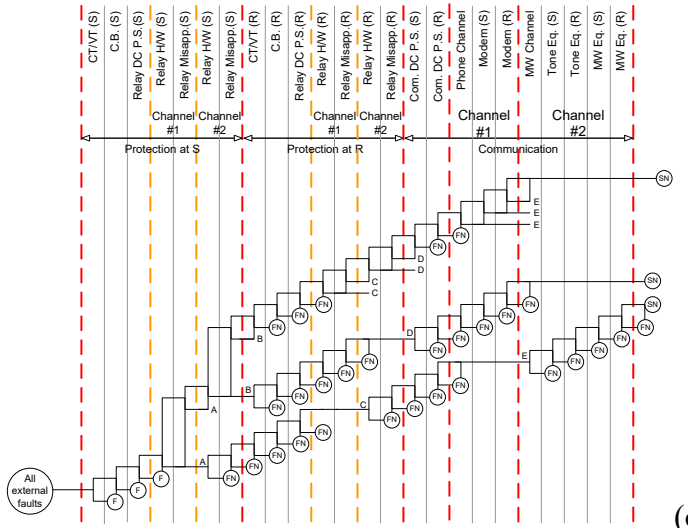
CT/VT (S)
C.B. (S)
Relay DC P.S.(S)
Relay H/W (S)
Relay Misapp.(S)
Relay H/W (S)
Relay Misapp.(S)
CT/VT (R)
C.B. (R)
Relay DC P.S.(R)
Relay H/W (R)
Relay Misapp.(R)
Relay H/W (R)
Relay Misapp.(R)
Com. DC P.S. (S)
Com. DC P.S. (R)
Phone Channel
Modem (S)
Modem (R)
MW Channel
Tone Eq. (S)
Tone Eq. (R)
MW Eq. (S)
MW Eq. (R)
Channel #1
Channel #2
Protection at S
Protection at R
Communication
All external faults
FN
SN
A
B
C
D
E
F

(c)

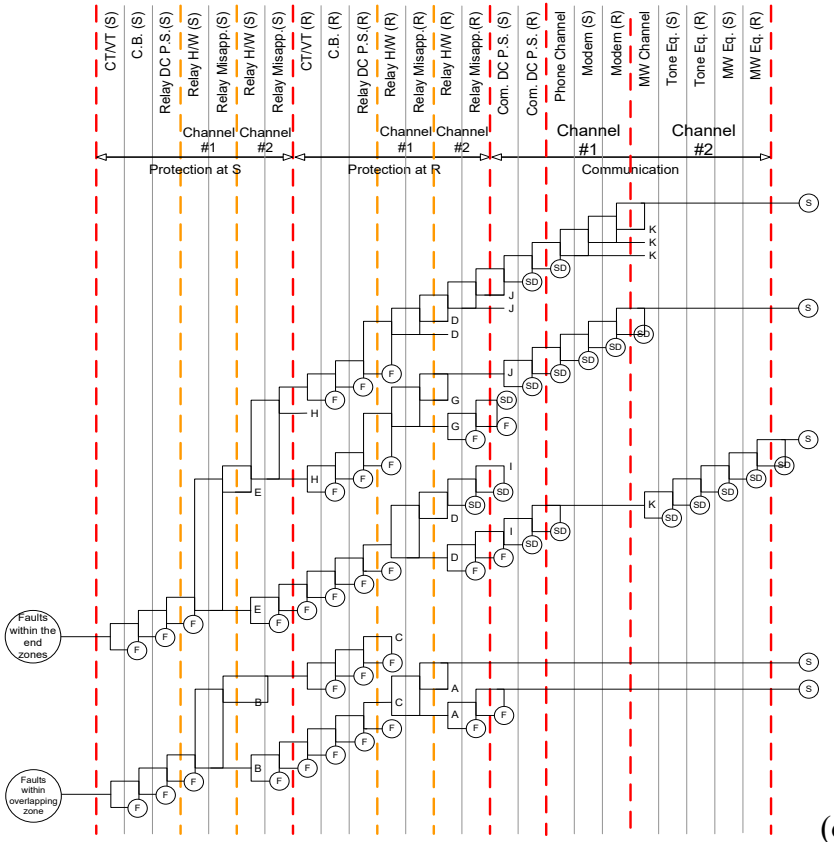

Figure 20. Event tree for DUTT. *S*: Protection successful, *F*: Protection fails, *SB*: successfully blocked over-tripping, *MF*: Malfunction, *SN*: Protection healthy but not required, *FN*: Protection not healthy and not required, *SD*: Protection succeeds after a time delay

Inclusion of Noisy Channels

In above calculations the impact of noisy channels was not considered. More accurate investigation could be performed by adding noise to the channel. Communication path is usually long and may be vulnerable to erroneous excitation by storms, mutual induction, or other means.

The impact of noise can be considered only on microwave channel due to its exposure to outdoor conditions. Moreover, it is often sufficient to study the effects of noise on the DUTT scheme since the other pilot schemes are made robust to the noisy channels by using the supervisory system that checks the validity of the received signal.

The overall reliability index of a protection scheme can be calculated using the concept of expectations as bellow:

$$\begin{aligned} Overal\ Reliability\ Index &= P(noisy channel)."index-with-noise" \\ &+ (1-P(noisy channel))."index-without-noise" \end{aligned} \quad (2)$$

Where $P(noisy channel)$ is the probability that the communication channel is noisy.

Event Tree for Permissive Under-reach Transfer Trip Scheme (PUTT)

As noted earlier the principle of protection is the same for DUTT and PUTT schemes in terms of using communication channels for various areas of protection. The main difference is that PUTT has been made secure to the channel noises using a supervising function. Therefore, the event tree diagrams for PUTT are the same as those of DUTT shown in Figures 19.a to 19.f. However, with an exception that in case of DUTT channel noises should be taken into account using Equation (1). This difference between DUTT and PUTT schemes are shown in Table 6.

Table 6. Performance of DUTT and PUTT against Noisy Channels

	Type of fault	Internal faults		External faults
		Overlapping zone	End zones	within zone 2 reach
DUTT	Communication channel required?	No	Yes	No
	Malfunction if channel noisy?	Yes	Yes	Yes
PUTT	Communication channel required?	No	Yes	No
	Malfunction if channel noisy?	No	No	No

Event Tree for Directional Comparison Blocking (DCB)

Figures 21.a to 21.l show the event trees for DCB scheme. Similar to the previous schemes, diagrams start with the case of a single relay - single channel and continue with adding appropriate redundancies in the scheme. Since the zone 1 element, in this scheme, does not play any role in clearing in-section faults, there is no difference between faults occurring in overlapping area and end zones. External faults are, however, treated based on their location against zone 2; e.g. external faults within the zone 2 reach of either relays are suspicious to mal-operation if the corresponding blocking signal is not received. This is shown in Figure 21.a by reaching the “MF” (mal-function) mode if the communication device or local relay fails in sending the block signal to the remote station. It is useful to note that status of the C.B. in the local station doesn’t have any effect on sending the block

signal, and therefore it is bypassed in the event tree. If the system is sound, however, over-trip is avoided and “SB” (success in blocking over-trip) is reached.

In case an internal fault happens (Figure 21.b), no block signal is transferred and both relays are allowed to clear the fault immediately or after a prescribed delay. In this situation, every failure of the protection system would lead to the “F” mode irrespective of the channel status.

Figures 21.c and 21.d describe the condition of dual redundant relays and a single channel. When an external fault occurs, the local relay should block tripping and if the primary relay fails the backup would perform this task. If neither primary nor backup relay manages and/or signaling fails, the relay will over-trip (MF).

Internal faults, however, are successfully cleared only when all protective devices at both sides act normally regardless of the communication.

In Figure 21.e if the first channel fails, the second one is examined at point “y” and if both channels fail the system would over-trip. If either channel manages to transmit the blocking signal, “SB” would result. Figure 21.f is the same as Figure 21.b, because the channel status is not important in internal faults.

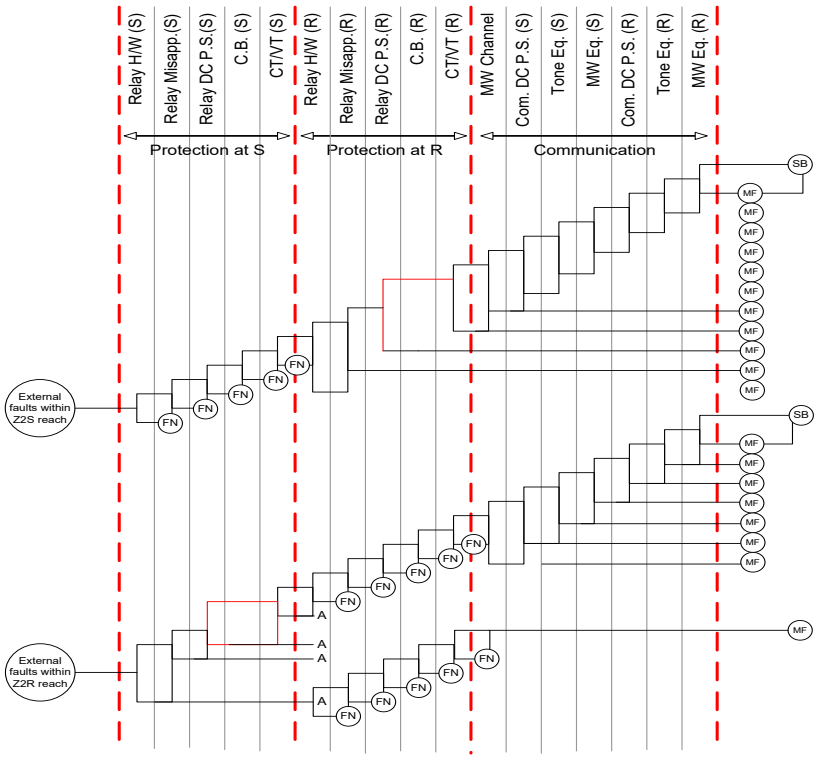
Relay H/W (S)
Relay Misapp.(S)
Relay DC P.S.(S)
C.B. (S)
CT/VT (S)
Relay H/W (R)
Relay Misapp.(R)
Relay DC P.S.(R)
C.B. (R)
CT/VT (R)
MW Channel
Com. DC P.S. (S)
Tone Eq. (S)
MW Eq. (S)
Com. DC P.S. (R)
Tone Eq. (R)
MW Eq. (R)
Protection at S
Protection at R
Communication
External faults within Z2S reach
External faults within Z2R reach
FN
A
SB
MF

(a)

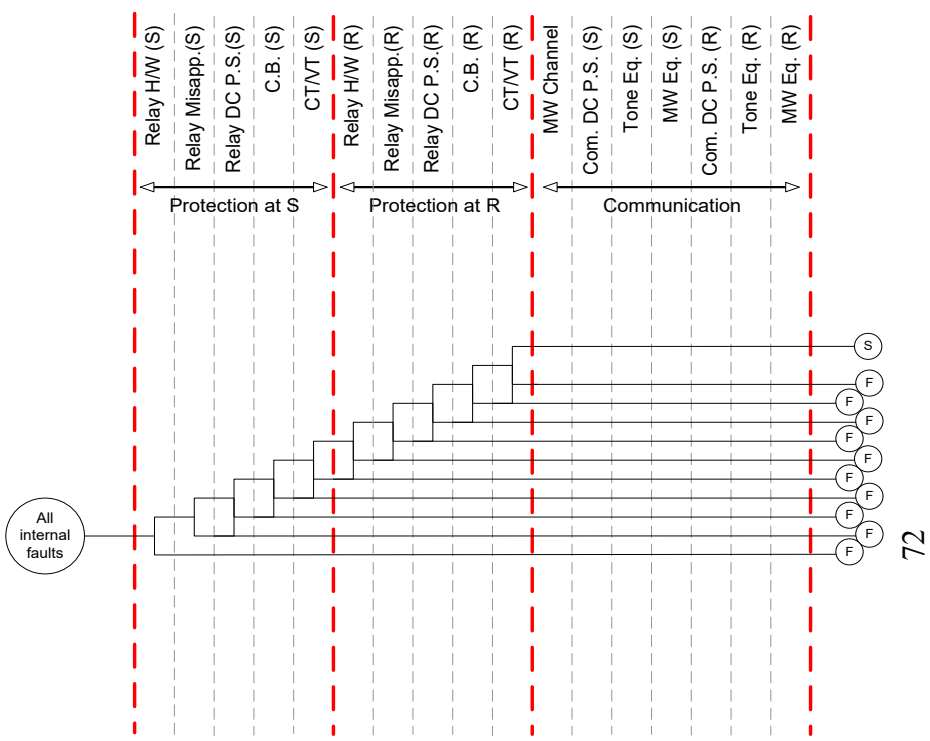
Relay H/W (S)
Relay Misapp.(S)
Relay DC P.S.(S)
C.B. (S)
CT/VT (S)
Relay H/W (R)
Relay Misapp.(R)
Relay DC P.S.(R)
C.B. (R)
CT/VT (R)
MW Channel
Com. DC P.S. (S)
Tone Eq. (S)
MW Eq. (S)
Com. DC P.S. (R)
Tone Eq. (R)
MW Eq. (R)
Protection at S
Protection at R
Communication
All internal faults
S
F

(b)

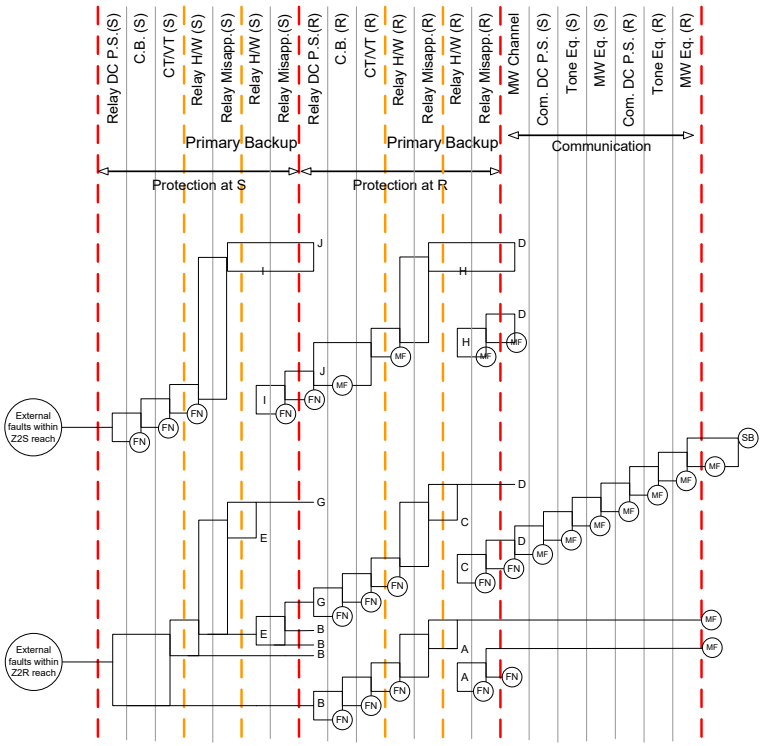
Relay DC P.S.(S)
C.B. (S)
CT/VT (S)
Relay H/W (S)
Relay Misapp.(S)
Relay H/W (S)
Relay Misapp.(S)
Relay DC P.S.(R)
C.B. (R)
CT/VT (R)
Relay H/W (R)
Relay Misapp.(R)
Relay H/W (R)
Relay Misapp.(R)
MW Channel
Com. DC P.S. (S)
Tone Eq. (S)
MW Eq. (S)
Com. DC P.S. (R)
Tone Eq. (R)
MW Eq. (R)
Primary Backup
Primary Backup
Communication
Protection at S
Protection at R
External faults within Z2S reach
External faults within Z2R reach
FN
MF
SB

(c)

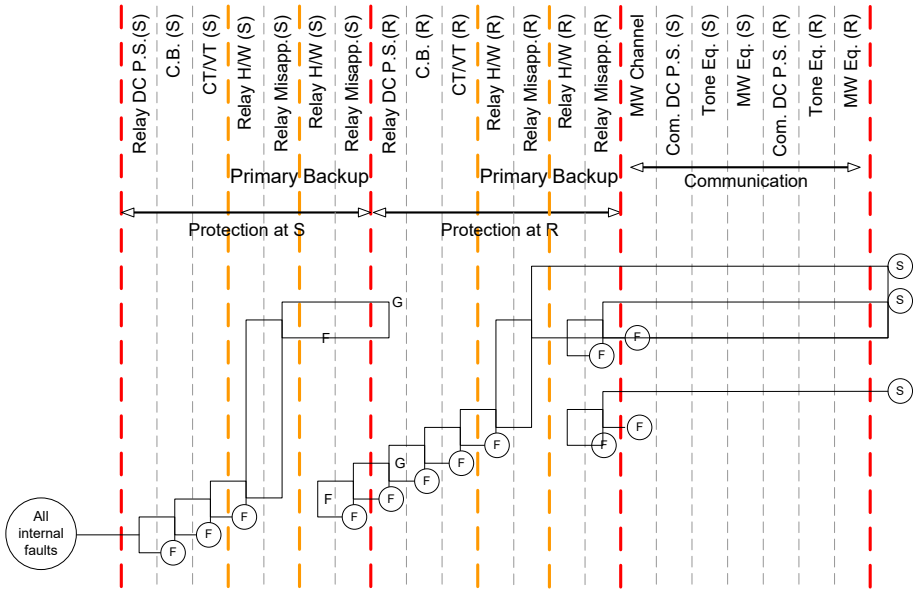
Relay DC P.S.(S)
C.B. (S)
CT/VT (S)
Relay H/W (S)
Relay Misapp.(S)
Relay H/W (S)
Relay Misapp.(S)
Relay DC P.S.(R)
C.B. (R)
CT/VT (R)
Relay H/W (R)
Relay Misapp.(R)
Relay H/W (R)
Relay Misapp.(R)
MW Channel
Com. DC P.S. (S)
Tone Eq. (S)
MW Eq. (S)
Com. DC P.S. (R)
Tone Eq. (R)
MW Eq. (R)
Primary Backup
Primary Backup
Communication
Protection at S
Protection at R
All internal faults
F
S

(d)

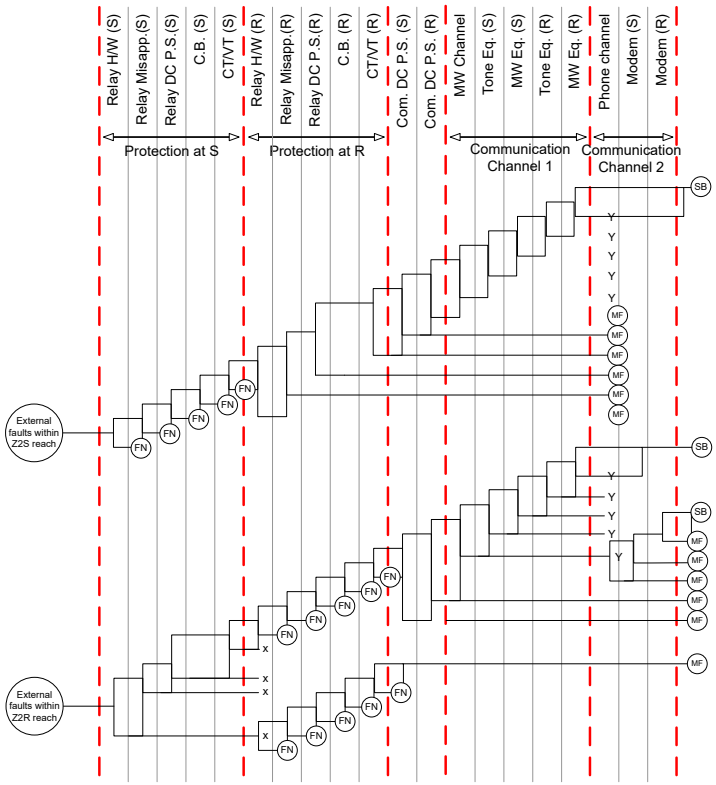
Relay H/W (S)
Relay Misapp.(S)
Relay DC P.S.(S)
C.B. (S)
CT/VT (S)
Relay H/W (R)
Relay Misapp.(R)
Relay DC P.S.(R)
C.B. (R)
CT/VT (R)
Com. DC P.S. (S)
Com. DC P.S. (R)
MW Channel
Tone Eq. (S)
MW Eq. (S)
Tone Eq. (R)
MW Eq. (R)
Phone channel
Modem (S)
Modem (R)
Protection at S
Protection at R
Communication Channel 1
Communication Channel 2
External faults within Z2S reach
External faults within Z2R reach
FN
MF
SB
Y
x

(e)

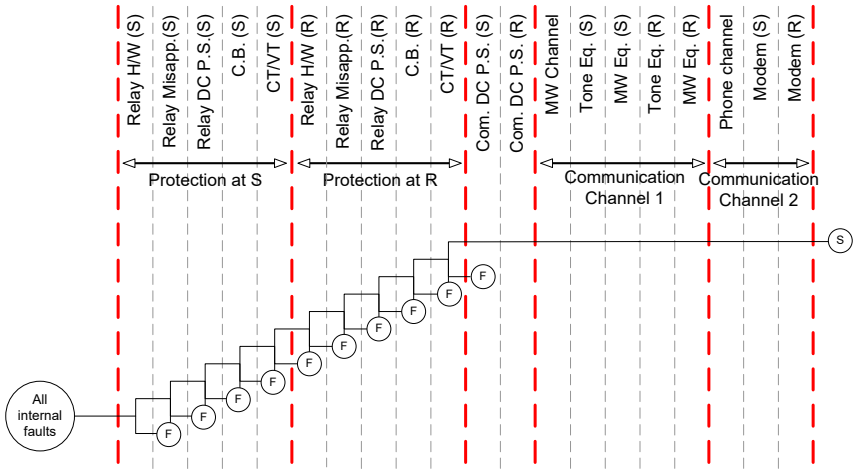
Relay H/W (S)
Relay Misapp.(S)
Relay DC P.S.(S)
C.B. (S)
CT/VT (S)
Relay H/W (R)
Relay Misapp.(R)
Relay DC P.S.(R)
C.B. (R)
CT/VT (R)
Com. DC P.S. (S)
Com. DC P.S. (R)
MW Channel
Tone Eq. (S)
MW Eq. (S)
Tone Eq. (R)
MW Eq. (R)
Phone channel
Modem (S)
Modem (R)
Protection at S
Protection at R
Communication Channel 1
Communication Channel 2
All internal faults
F
S

(f)

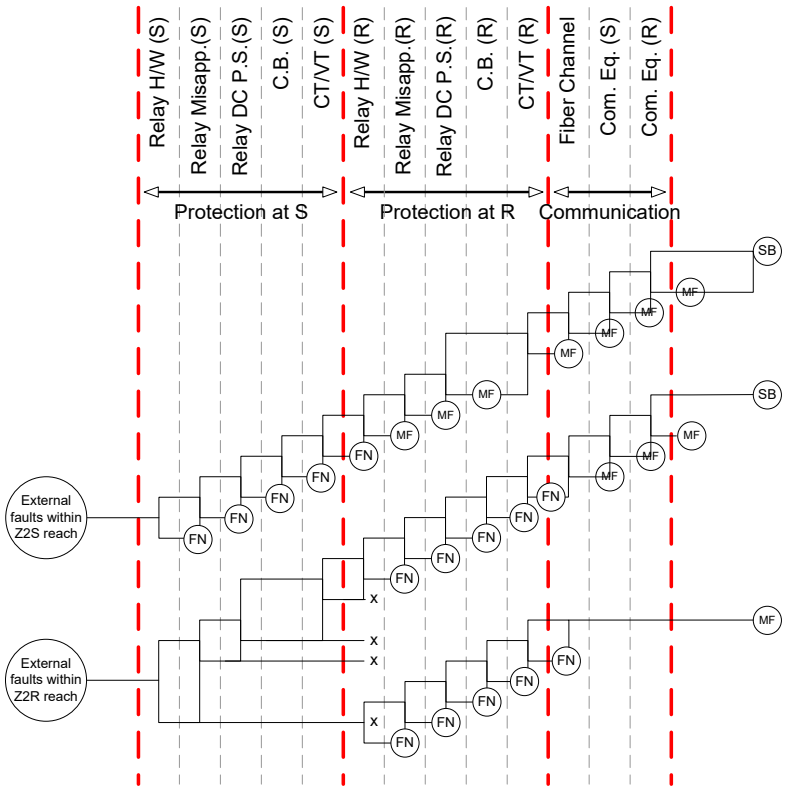
Relay H/W (S)
Relay Misapp.(S)
Relay DC P.S.(S)
C.B. (S)
CT/VT (S)
Relay H/W (R)
Relay Misapp.(R)
Relay DC P.S.(R)
C.B. (R)
CT/VT (R)
Fiber Channel
Com. Eq. (S)
Com. Eq. (R)
Protection at S
Protection at R
Communication
External faults within Z2S reach
External faults within Z2R reach
FN
MF
SB
x

(g)

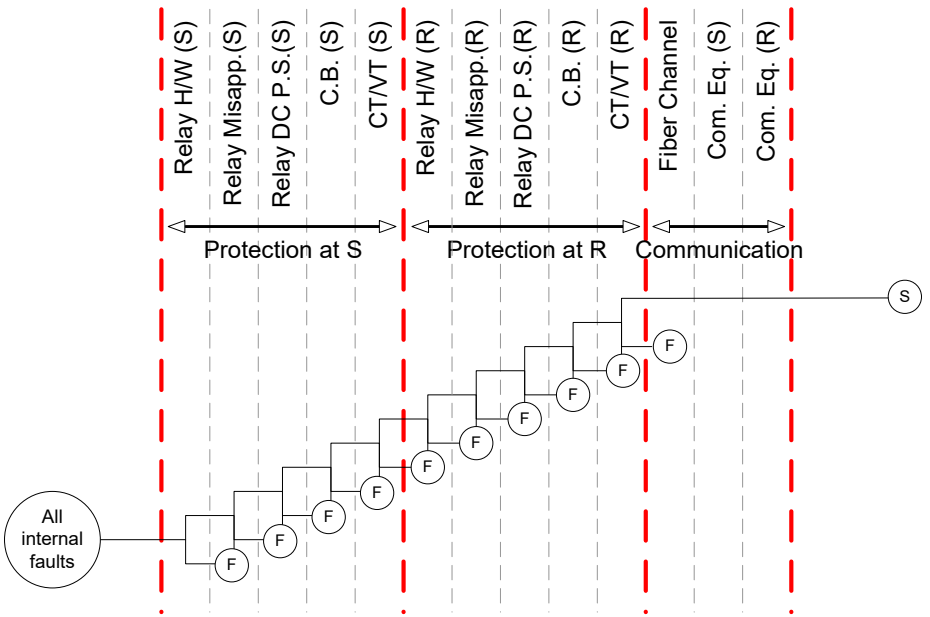
Relay H/W (S)
Relay Misapp.(S)
Relay DC P.S.(S)
C.B. (S)
CT/VT (S)
Relay H/W (R)
Relay Misapp.(R)
Relay DC P.S.(R)
C.B. (R)
CT/VT (R)
Fiber Channel
Com. Eq. (S)
Com. Eq. (R)
Protection at S
Protection at R
Communication
All internal faults
F
S

(h)

(i)

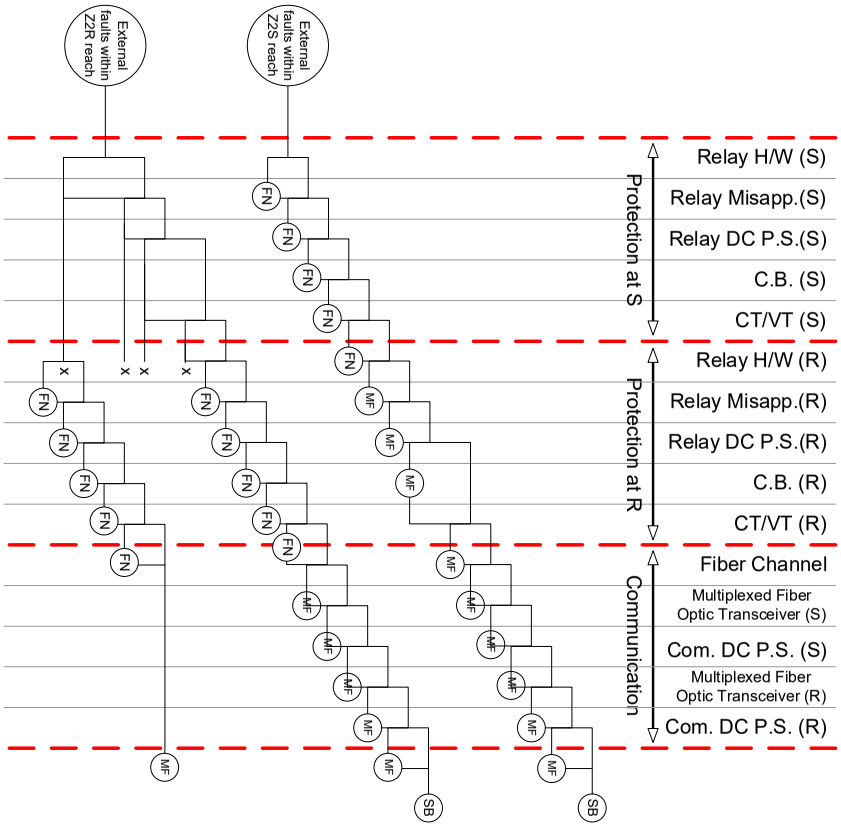
External faults within Z2R reach
External faults within Z2S reach
FN
MF
SB
Protection at S
Relay H/W (S)
Relay Misapp.(S)
Relay DC P.S.(S)
C.B. (S)
CT/VT (S)
Protection at R
Relay H/W (R)
Relay Misapp.(R)
Relay DC P.S.(R)
C.B. (R)
CT/VT (R)
Communication
Fiber Channel
Multiplexed Fiber Optic Transceiver (S)
Com. DC P.S. (S)
Multiplexed Fiber Optic Transceiver (R)
Com. DC P.S. (R)

(j)

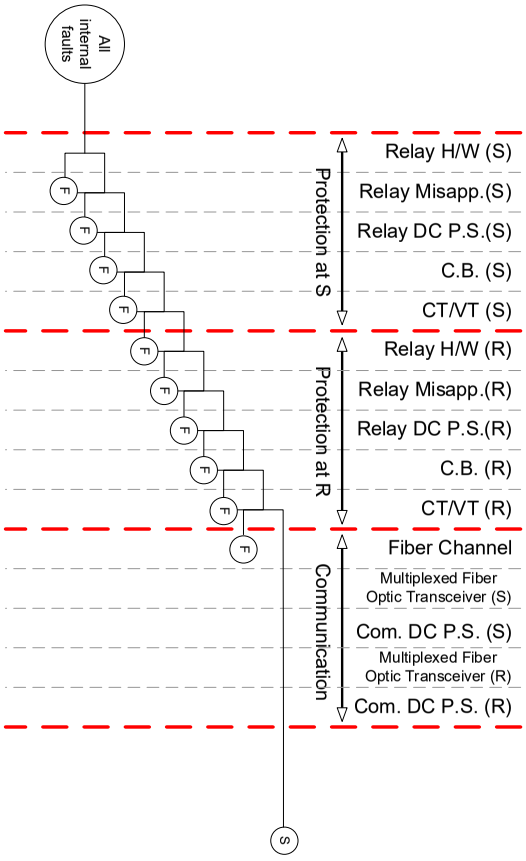
All internal faults
F
S
Protection at S
Relay H/W (S)
Relay Misapp.(S)
Relay DC P.S.(S)
C.B. (S)
CT/VT (S)
Protection at R
Relay H/W (R)
Relay Misapp.(R)
Relay DC P.S.(R)
C.B. (R)
CT/VT (R)
Communication
Fiber Channel
Multiplexed Fiber Optic Transceiver (S)
Com. DC P.S. (S)
Multiplexed Fiber Optic Transceiver (R)
Com. DC P.S. (R)

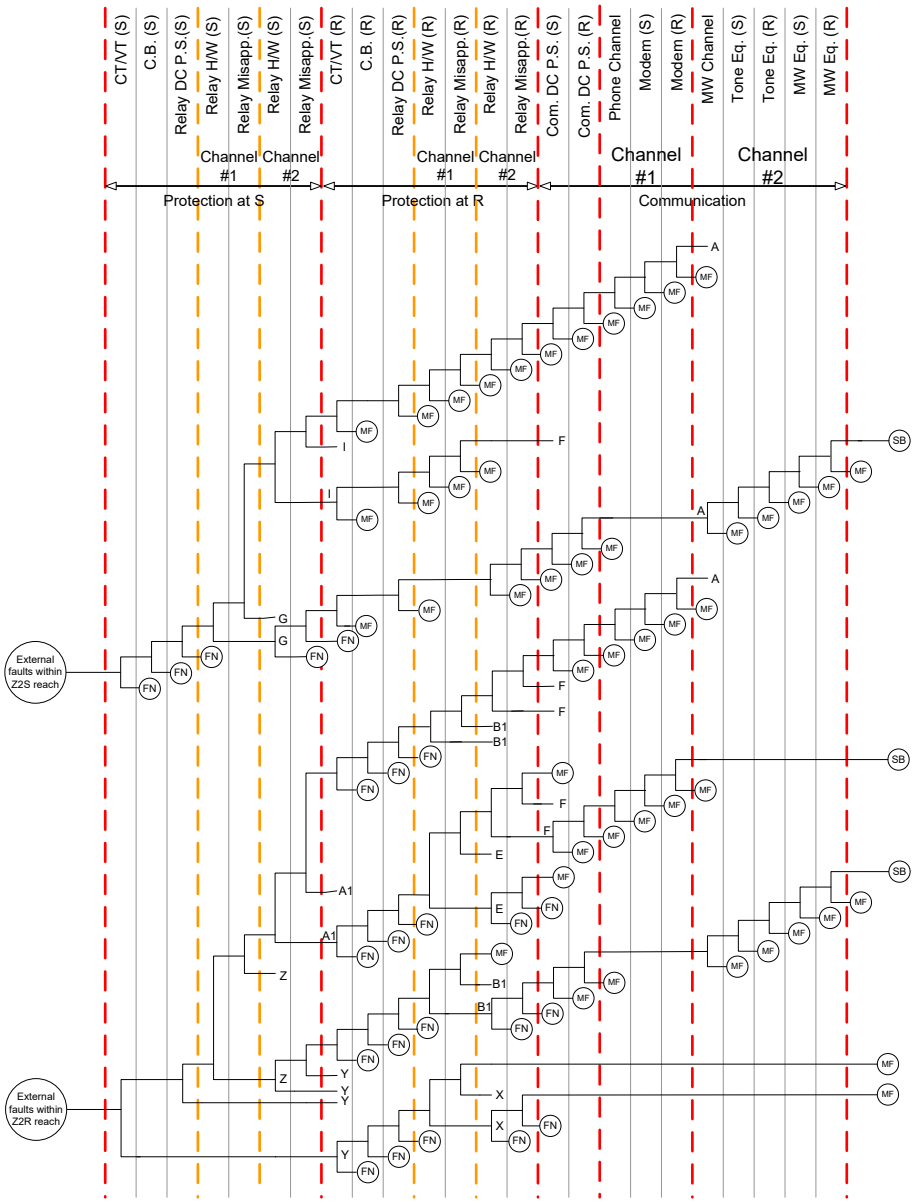
CT/VT (S)
C.B. (S)
Relay DC P.S.(S)
Relay H/W (S)
Relay Misapp.(S)
Relay H/W (S)
Relay Misapp.(S)
CT/VT (R)
C.B. (R)
Relay DC P.S.(R)
Relay H/W (R)
Relay Misapp.(R)
Relay H/W (R)
Relay Misapp.(R)
Com. DC P.S. (S)
Com. DC P.S. (R)
Phone Channel
Modem (S)
Modem (R)
MW Channel
Tone Eq. (S)
Tone Eq. (R)
MW Eq. (S)
MW Eq. (R)
Channel #1
Channel #2
Channel #1
Channel #2
Channel #1
Channel #2
Protection at S
Protection at R
Communication
External faults within Z2S reach
External faults within Z2R reach
MF
FN
A
SB
I
F
G
B1
E
A1
Z
Y
X

(k)

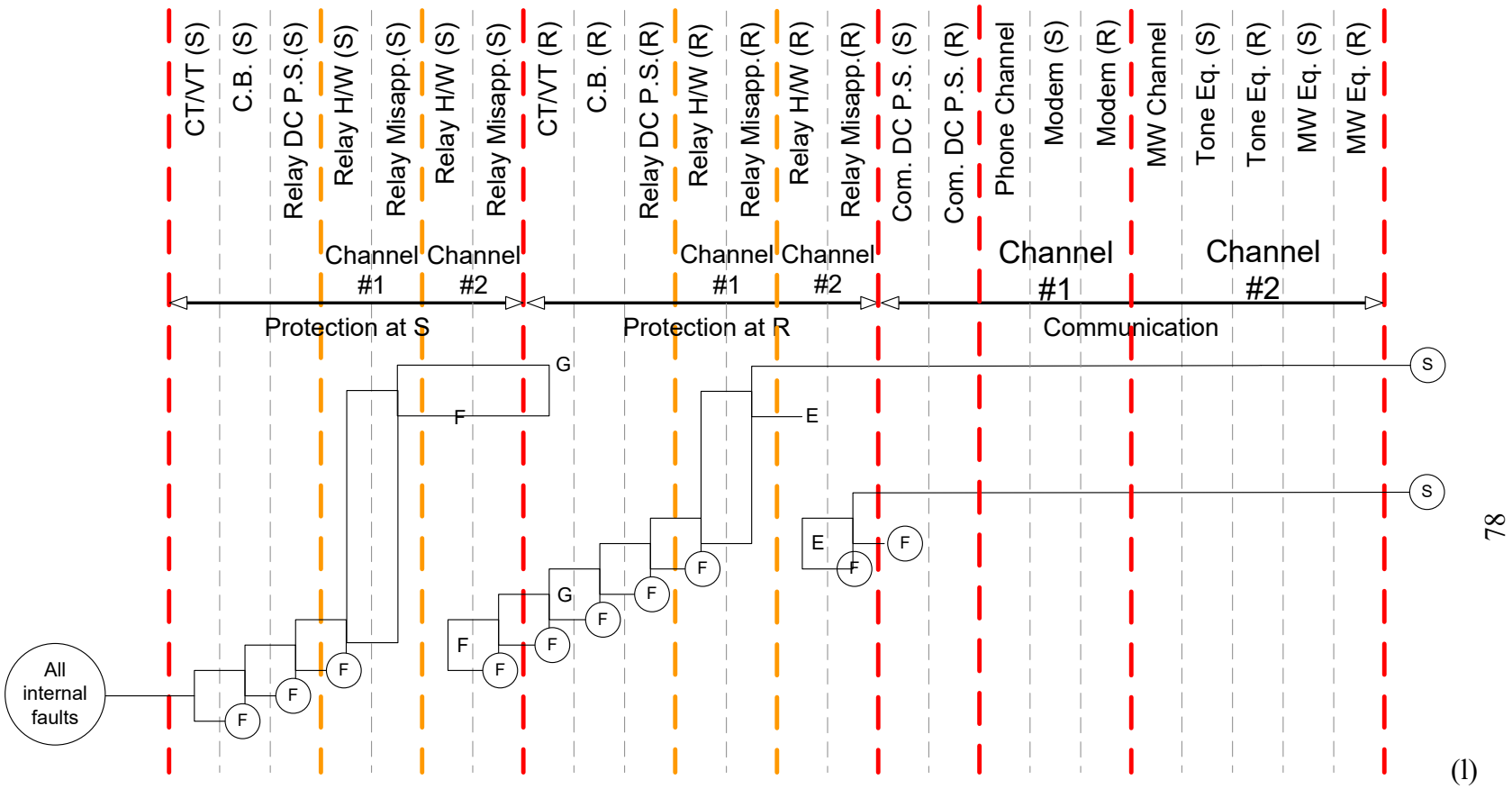

Figure 21. Event Tree for DCB. *S*: Protection successful, *F*: Protection fails, *SB*: successfully blocked over-tripping, *MF*: Malfunction, *SN*: Protection healthy but not required, *FN*: Protection not healthy and not required, *SD*: Protection succeeds after a time delay

Event Tree for Directional Comparison Unblocking Scheme (DCUB)

The event tree diagrams are shown in Figures 22 to 33. In drawing these diagrams. It is assumed that failure of the relay will not affect sending the blocking signal; i.e. blocking signal will continue when it should, regardless of the relay status.

Figure 22 illustrates the behavior of the scheme when an external fault occurs. If the fault happens to be in the zone two of relay S, this relay would stop sending block signal to relay "R", but since relay "R" doesn't see anything in its zone 2 reach it will never operate. Therefore, health or failure of relay "R" will not affect the whole performance. Relay "R", however, continues to block relay "S".

The scheme could malfunction if the communication fails after the fault inception. This is because if the communication fails, block signal is not received at "S" causing AND-2 in Figure 17.b to feed an input to OR-2 during a 150ms window. Since relay "S" sees the fault in its zone 2, P(R) =1 and thus will operate AND-3 during the time period. If this 150ms is sufficient for the protection at "S" to trip, mal-operation will occur. If not, a lockout signal will be generated after 150ms indicating that the channel is faulty and the conventional distance protection would stop mal-operation (SB).

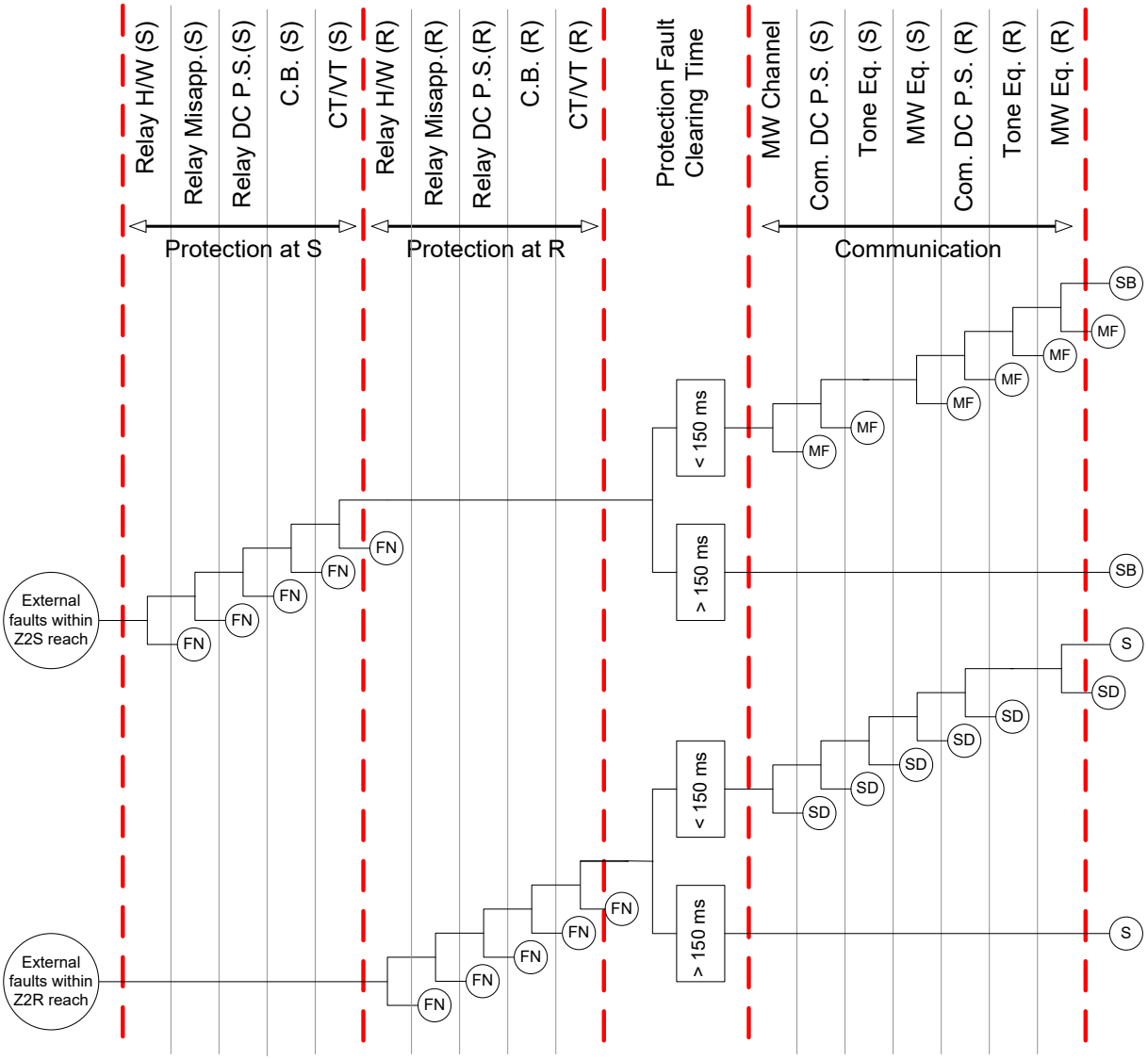

Figure 22. Event tree for DCUB single relay/ single channel (MW), external fault. *S*: Protection successful, *F*: Protection fails, *SB*: successfully blocked over-tripping, *MF*: Malfunction, *SN*: Protection healthy but not required, *FN*: Protection not healthy and not required, *SD*: Protection succeeds after a time delay

Internal faults are examined in Figure 23. If the fault occurs in the overlapping area, it is cleared by the instantaneous zone 1 elements of both relays, regardless of the communication media.

Fault in the end-zones, say R, is recognized by the instantaneous zone 1 element of relay "R" at local station and by zone 2 element of relay "S" at the remote station. Relay "R" clears the fault directly and stops the blocking signal to station "S". At station "S", loss of block signal along with the zone 2 detection signal allows a permissive trip in a 150ms window. If relay "S" manages to trip in the 150ms interval, fault is successfully cleared. Otherwise, a trip (unblock) signal is required for tripping. In the latter case, if the communication is healthy, the trip signal is received at "S" and fault is successfully cleared. If communication fails, however, a loss of block and unblock signals at "S" is reported via the lockout signal and fault is cleared with the zone 2 time delay of relay "S" (SD).

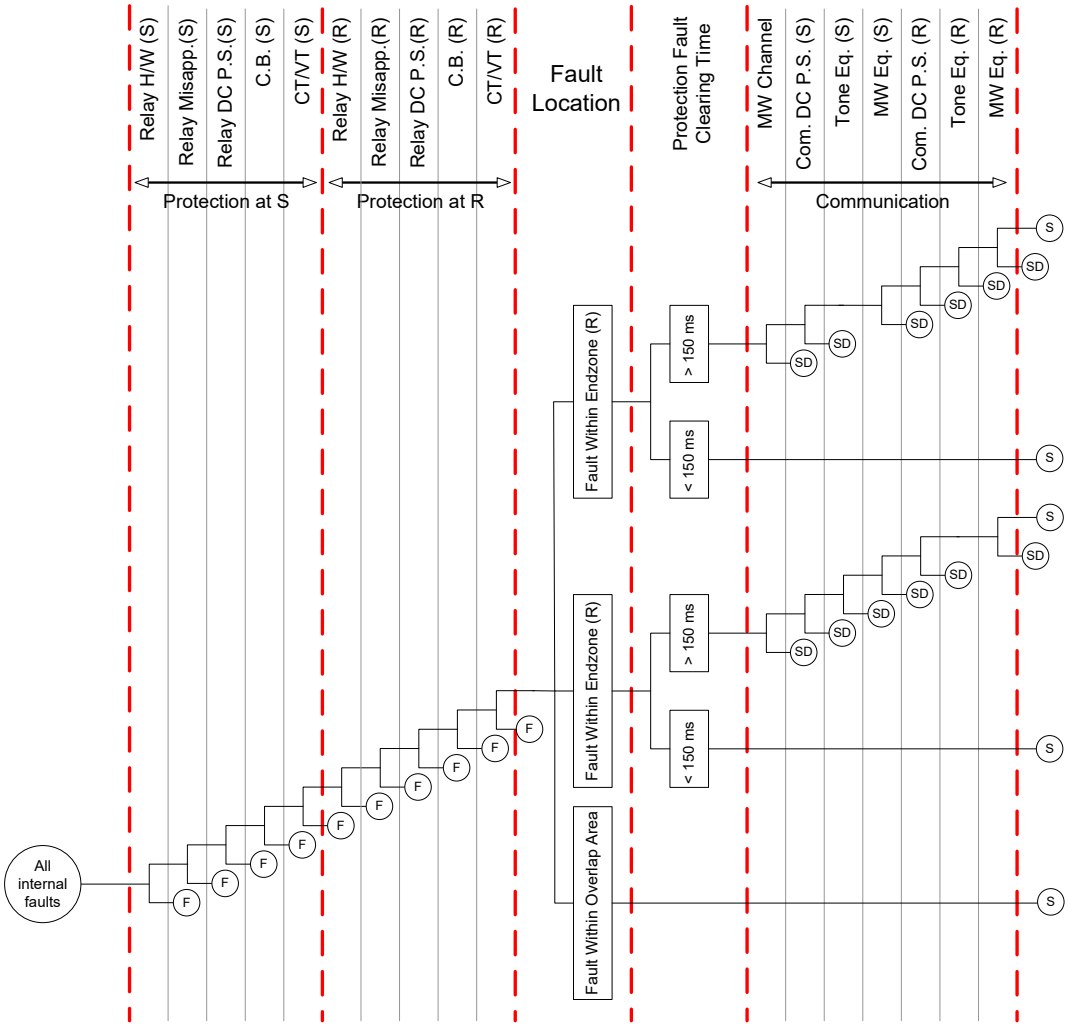

Figure 23. Event tree for DCUB single relay/ single channel (MW), internal fault.

S: Protection successful, *F*: Protection fails, *SB*: successfully blocked over-tripping, *MF*: Malfunction, *SN*: Protection healthy but not required, *FN*: Protection not healthy and not required, *SD*: Protection succeeds after a time delay

Figures 24 through 27 suggest the same idea as Figures 22 and 23 except for the relay or channel redundancy. The communication media is changed in Figures 28 and 29 to fiber optic but the basic principle remains the same.

Figure 32 illustrates the event tree diagram for redundant relays on independent channels when an external fault occurs. Similar to Figure 24, relay "R" doesn't play any role for the fault in zone two reach of relay "S". In this case, if both relays at station "S" work properly,

health in any of the channels would successfully block the over-tripping, SB (top path of tree). If both channels fail at this stage, loss of the blocking signal and zone 2 detection of relay “S” would allow for a 150ms trip window as before. If one of the relays on station “S” is faulty, the same scenario repeats with the communication media corresponding to the healthy relay.

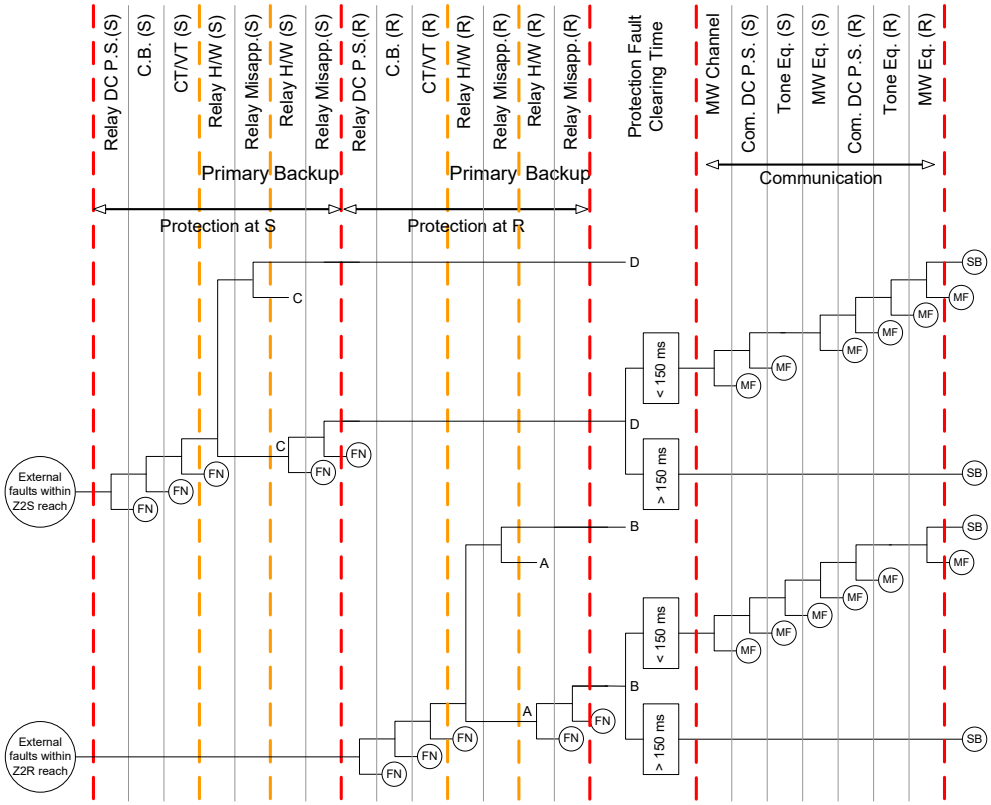

Figure 24. Event tree for DCUB redundant relay/ single channel (MW), external fault. *S*: Protection successful, *F*: Protection fails, *SB*: successfully blocked over-tripping, *MF*: Malfunction, *SN*: Protection healthy but not required, *FN*: Protection not healthy and not required, *SD*: Protection succeeds after a time delay

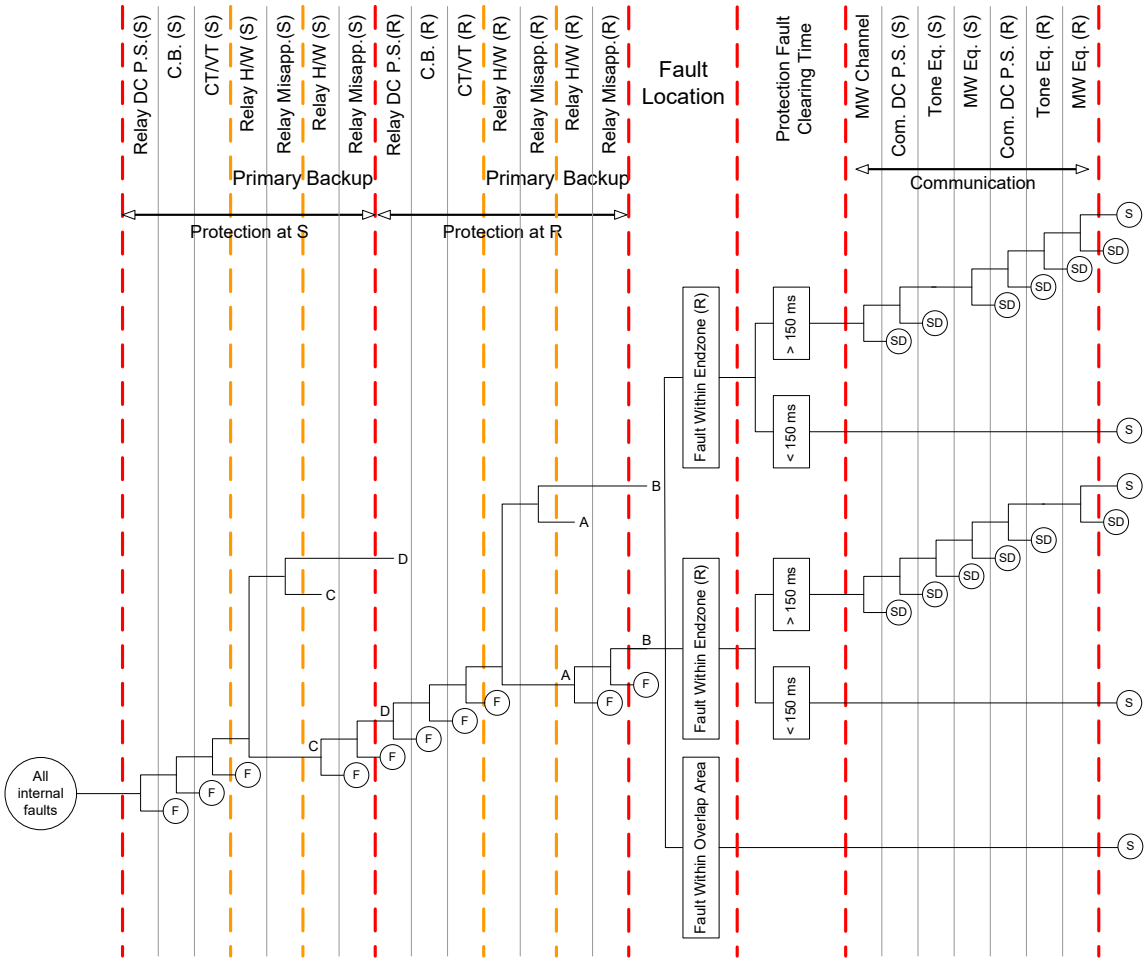

Figure 25. Event tree for DCUB redundant relay/ single channel (MW), internal fault.

S: Protection successful, *F*: Protection fails, *SB*: successfully blocked over-tripping, *MF*: Malfunction, *SN*: Protection healthy but not required, *FN*: Protection not healthy and not required, *SD*: Protection succeeds after a time delay

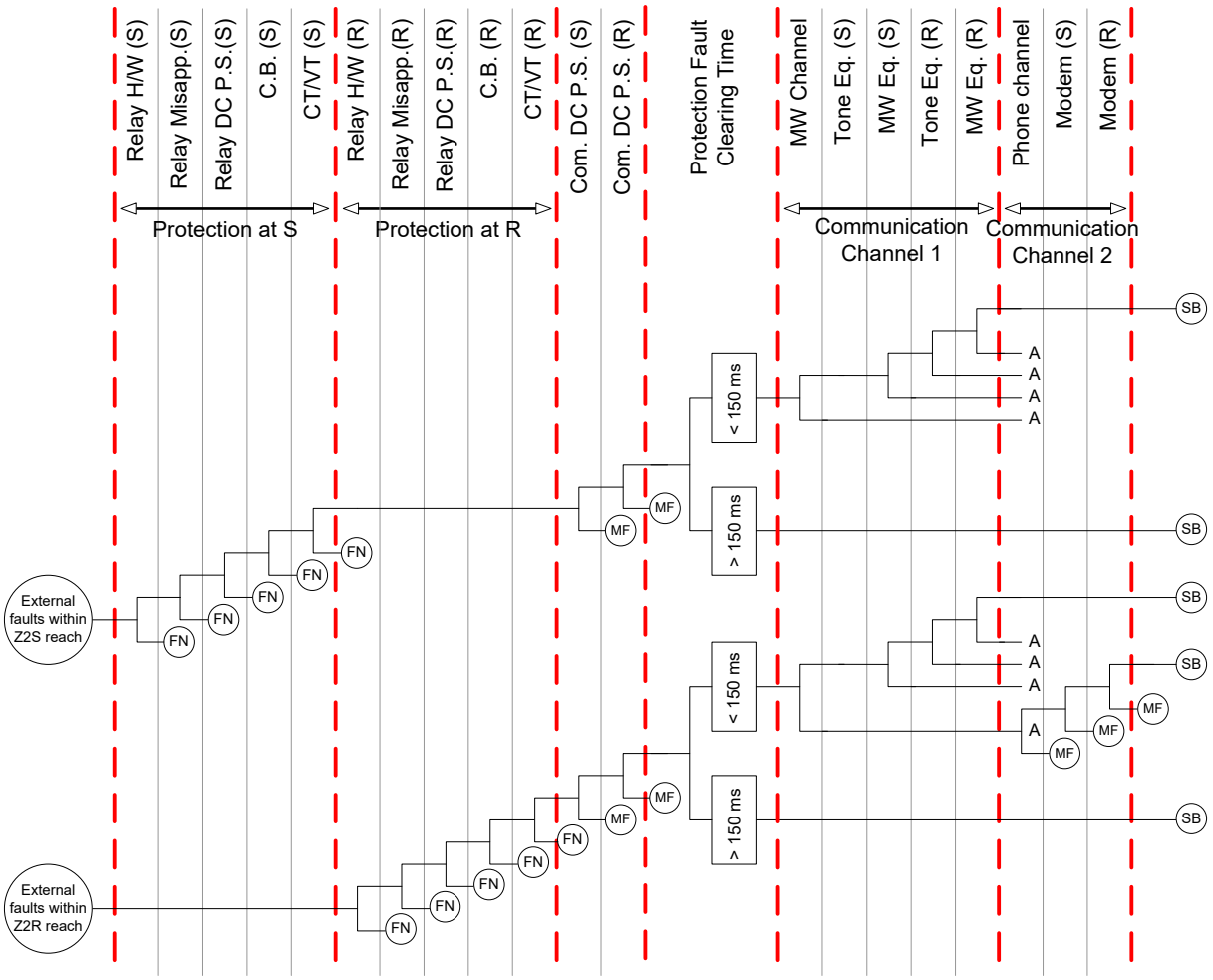

Figure 26. Event tree for DCUB single relay/ redundant channel (MW+ relay to relay phone line), external fault. *S*: Protection successful, *F*: Protection fails, *SB*: successfully blocked over-tripping, *MF*: Malfunction, *SN*: Protection healthy but not required, *FN*: Protection not healthy and not required, *SD*: Protection succeeds after a time delay

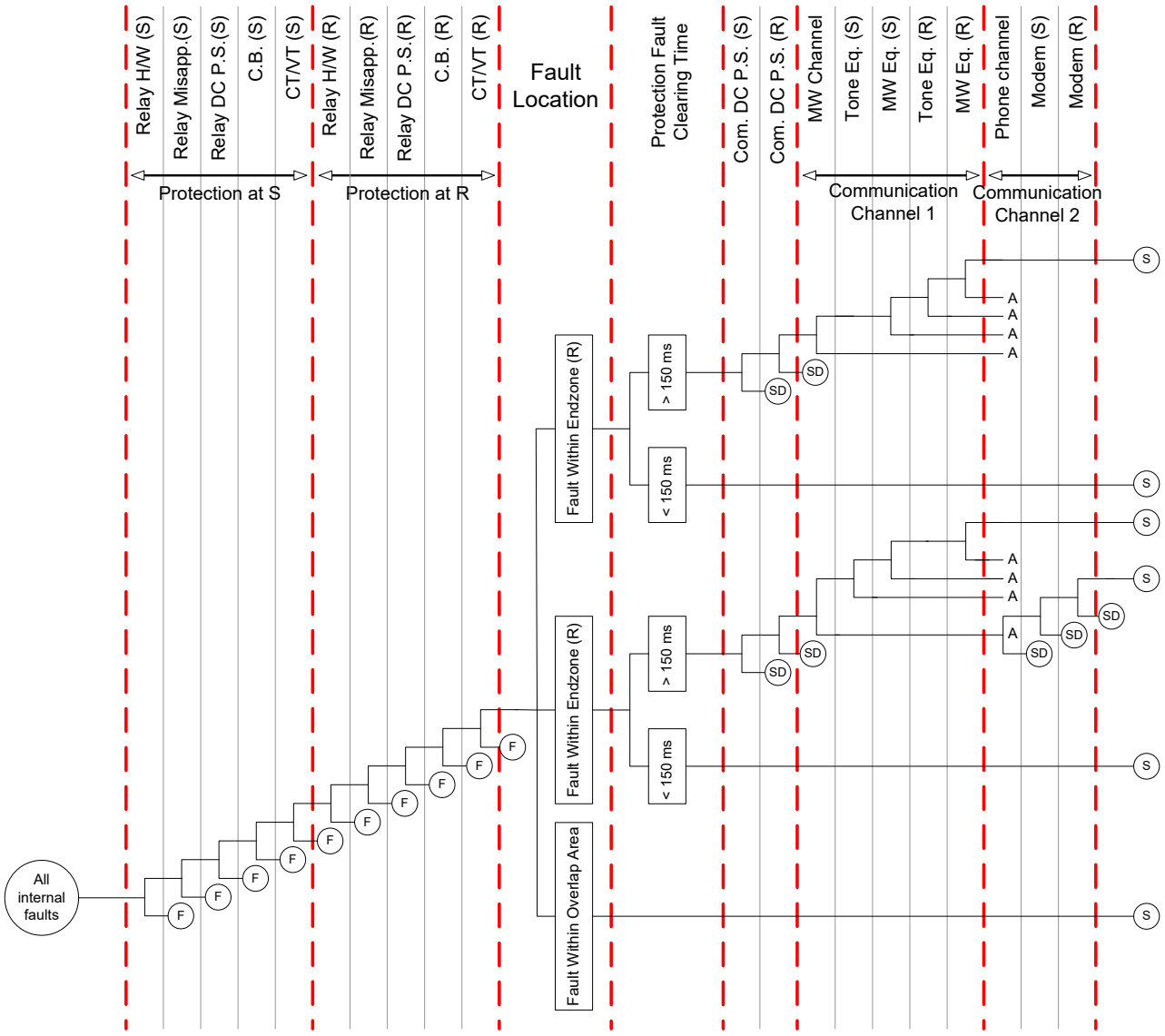

Figure 27. Event tree for DCUB single relay/ redundant channel (MW+ relay to relay phone line), internal fault. *S*: Protection successful, *F*: Protection fails, *SB*: successfully blocked over-tripping, *MF*: Malfunction, *SN*: Protection healthy but not required, *FN*: Protection not healthy and not required, *SD*: Protection succeeds after a time delay

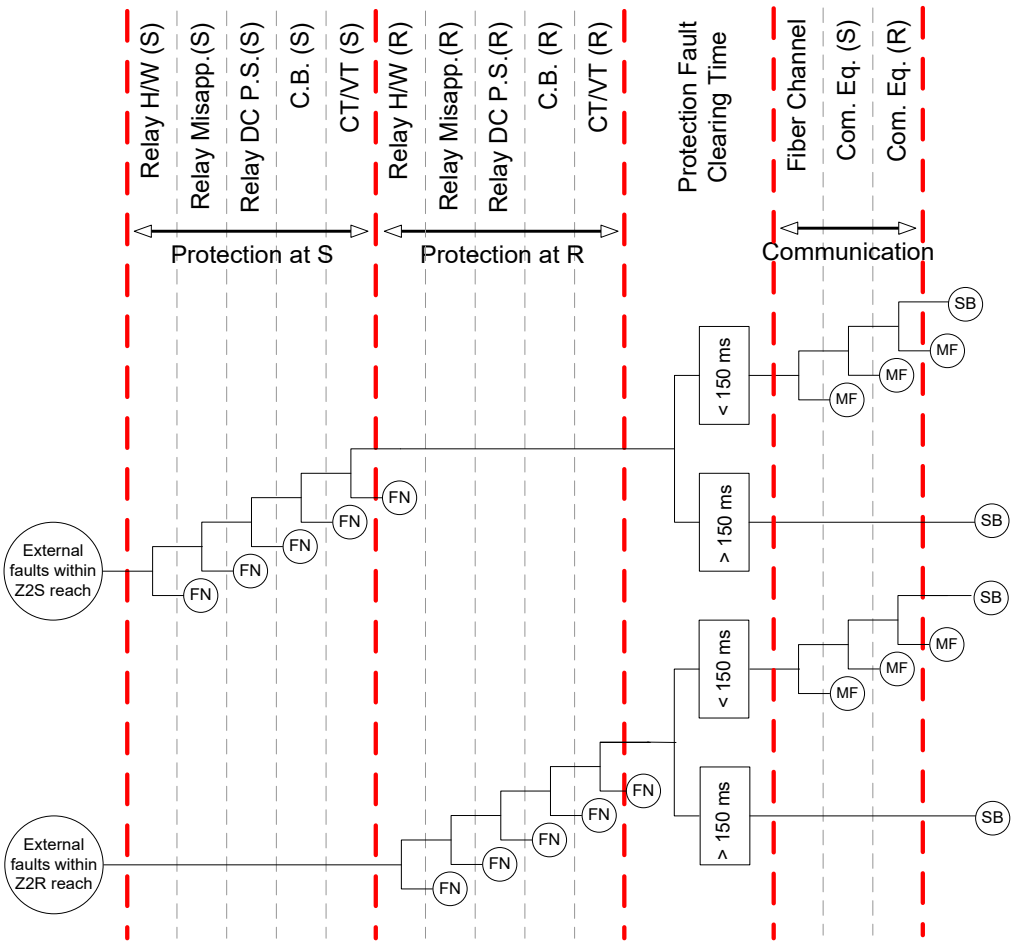

Figure 28. Event tree for DCUB single relay/ single channel (dedicated fiber), external fault. *S*: Protection successful, *F*: Protection fails, *SB*: successfully blocked over-tripping, *MF*: Malfunction, *SN*: Protection healthy but not required, *FN*: Protection not healthy and not required, *SD*: Protection succeeds after a time delay

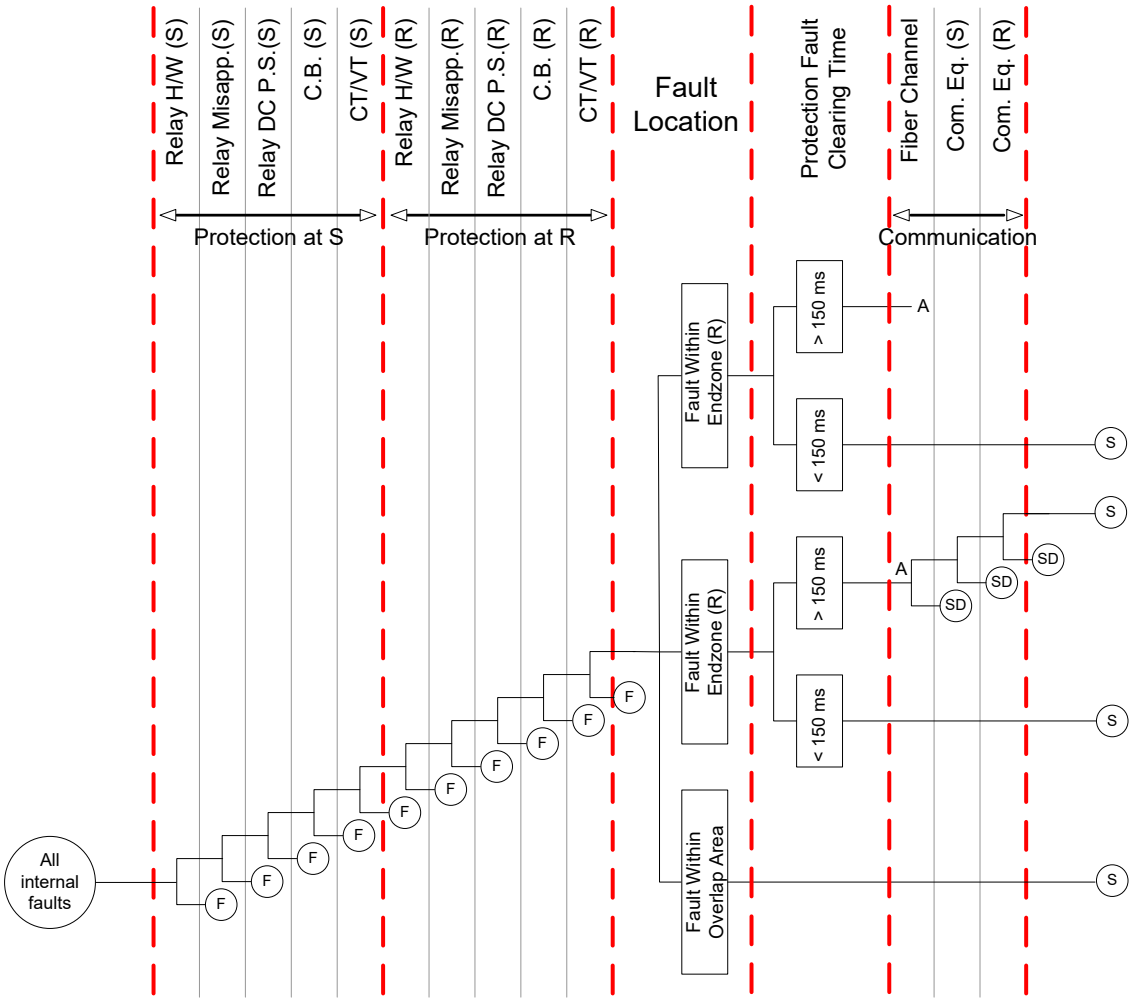

Figure 29. Event tree for DCUB single relay/ single channel (dedicated fiber), internal fault. *S*: Protection successful, *F*: Protection fails, *SB*: successfully blocked over-tripping, *MF*: Malfunction, *SN*: Protection healthy but not required, *FN*: Protection not healthy and not required, *SD*: Protection succeeds after a time delay

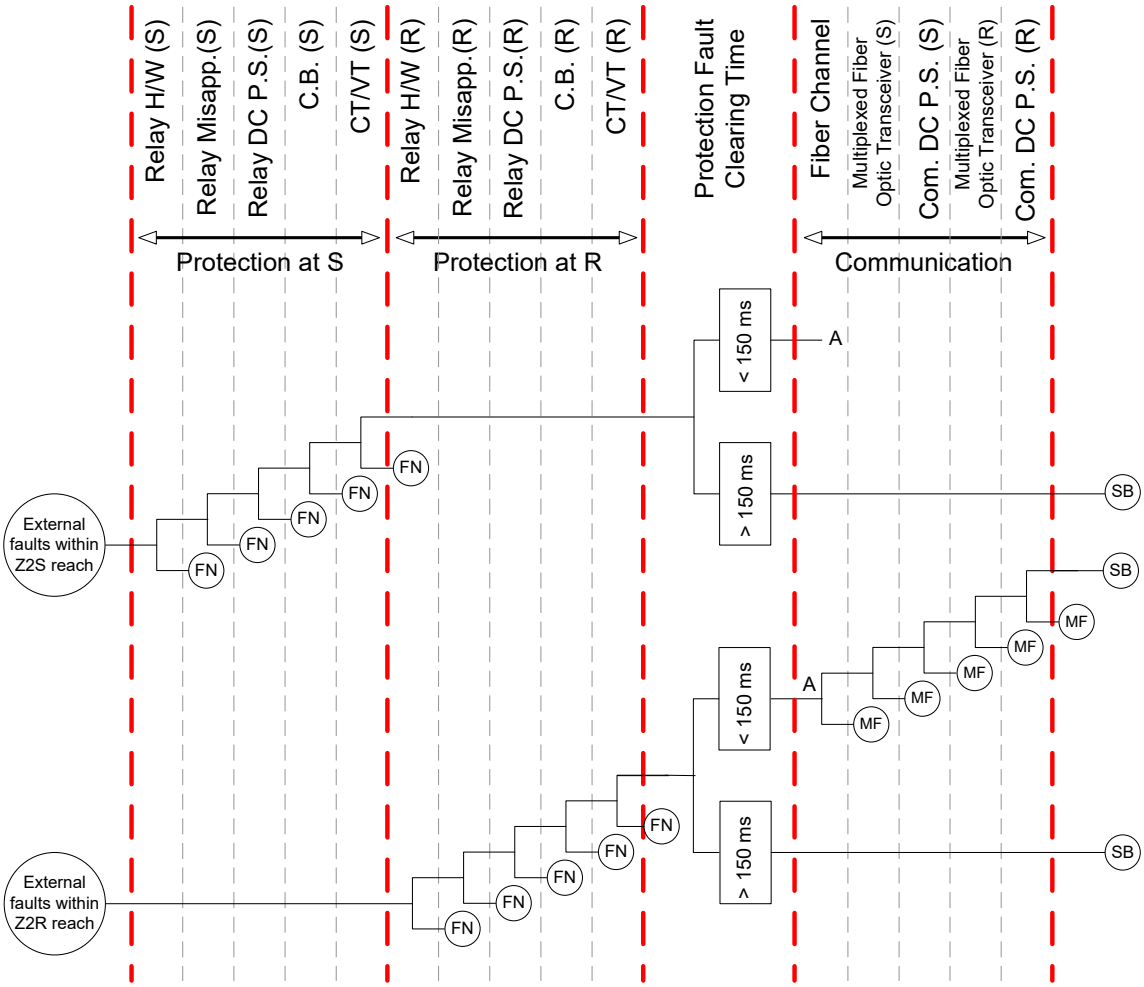

Figure 30. Event tree for DCUB single relay/ single channel (multiplexed fiber), external fault. *S*: Protection successful, *F*: Protection fails, *SB*: successfully blocked over-tripping, *MF*: Malfunction, *SN*: Protection healthy but not required, *FN*: Protection not healthy and not required, *SD*: Protection succeeds after a time delay

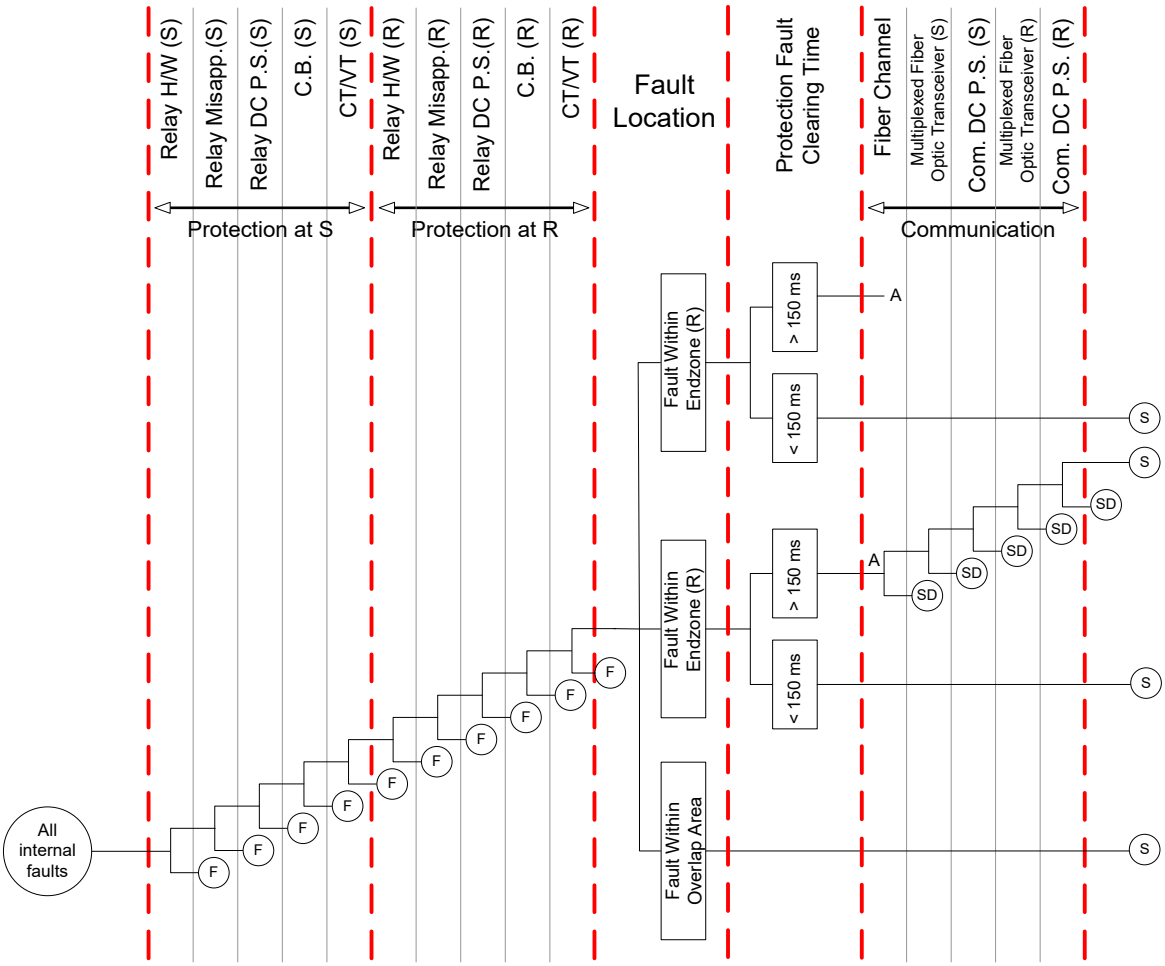

Figure 31. Event tree for DCUB single relay/ single channel (multiplexed fiber), internal fault. *S*: Protection successful, *F*: Protection fails, *SB*: successfully blocked over-tripping, *MF*: Malfunction, *SN*: Protection healthy but not required, *FN*: Protection not healthy and not required, *SD*: Protection succeeds after a time delay

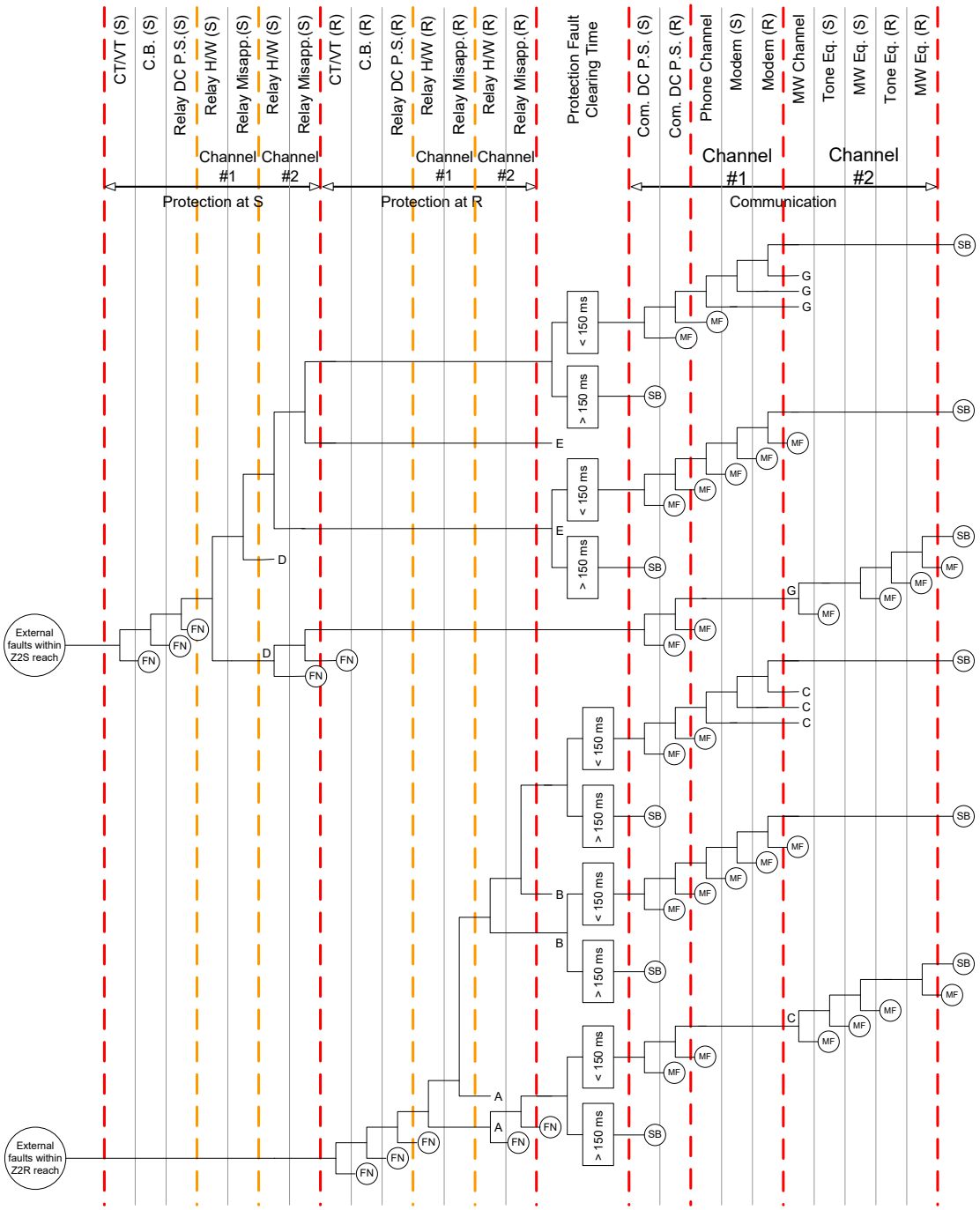

Figure 32. Event tree for DCUB redundant relay/ independent channels (MW+ relay to relay phone line), external fault. *S*: Protection successful, *F*: Protection fails, *SB*: successfully blocked over-tripping, *MF*: Malfunction, *SN*: Protection healthy but not required, *FN*: Protection not healthy and not required, *SD*: Protection succeeds after a time delay

Figure 33 shows the case of internal faults. The top branch of the tree diagram represents the situation where the relays on both channels are sound. In this case, the health of either channel could result in the protection system success.

If only one relay on either channel is healthy, tree reaches point “B” wherein signaling cannot be performed although each substation has a healthy relay. In this case, faults within the overlapping area could still be successfully cleared by zone 1 elements of healthy relays. Faults on end-zones can also be cleared successfully if the tripping takes place in the 150ms time interval. Otherwise, loss of both block and trip signals –due to healthy-faulty status of relays on either channel– results in a delayed tripping.

On the other hand, if both relays on either channel 1 or channel 2 are healthy, tree reaches points “I” or “C”, depending on the healthy relays being on channel 1 or channel 2, respectively. In this case, the tree diagram is continued as before with examining only the corresponding communication media.

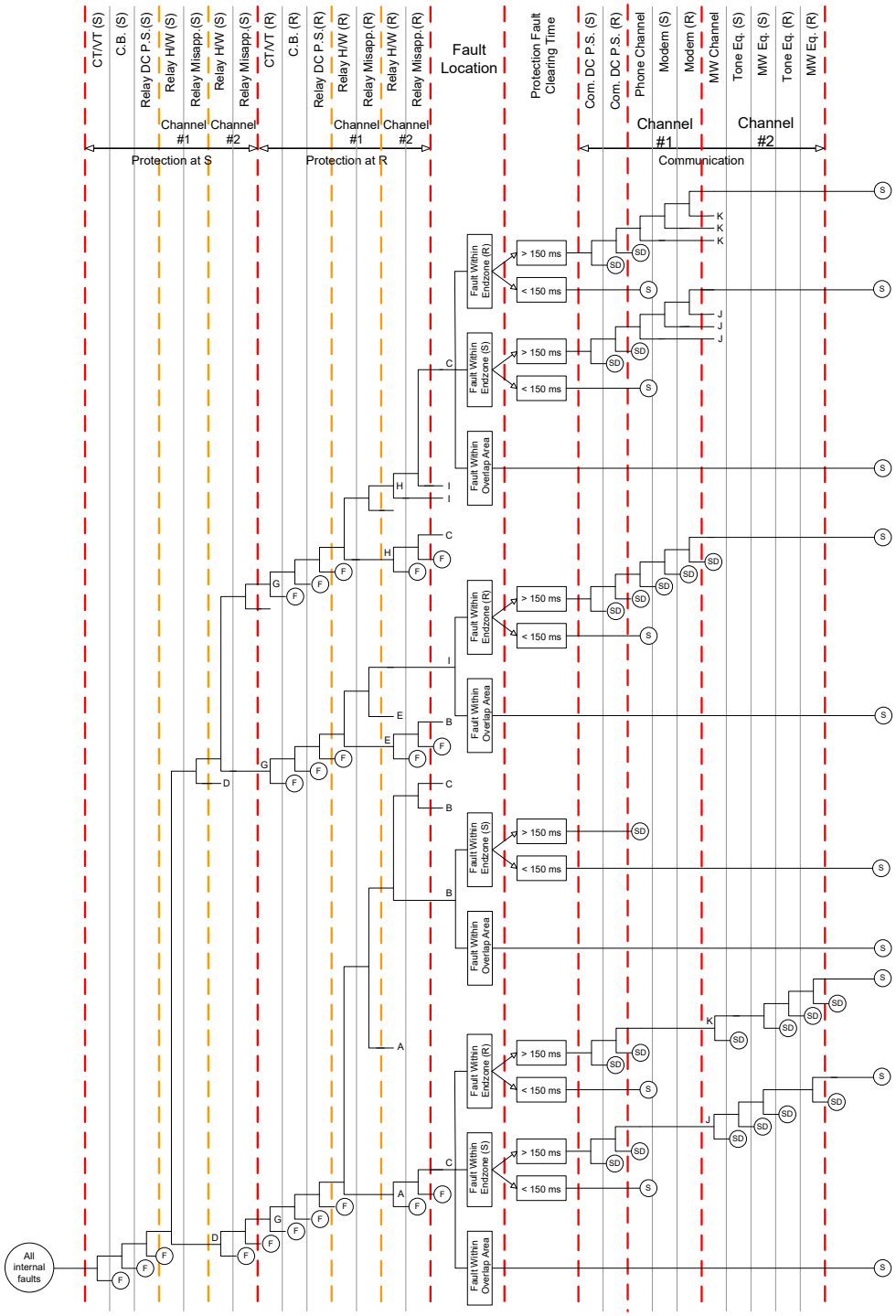

Figure 33. Event tree for DUCB redundant relay/ independent channels (MW+ relay to relay phone line), internal fault. *S*: Protection successful, *F*: Protection fails, *SB*: successfully blocked over-tripping, *MF*: Malfunction, *SN*: Protection healthy but not required, *FN*: Protection not healthy and not required, *SD*: Protection succeeds after a time delay

Device Failure Rates and Unavailability

To perform calculations based on the above event trees, it is required to have the reliability data associated with the protection system components. A device failure rate represents the average number of failures per unit time. A constant failure rate is normally assumed during the useful lifetime period of device. Failure rates can be obtained from theoretical calculations or from field experience [76].

Failure rates are very useful in predicting reliability characteristics, but do not tell the whole story about whether a device will be available when called upon to perform. Thus, it is required to consider unavailability. Unavailability is the fraction of time a device cannot perform its required task.

Available literature in reliability describes how to calculate unavailability from a failure rate [3].

$$q = \frac{T}{MTBF} \cong \frac{T}{MTTF} = \lambda T$$

where:

q : Unavailability

λ : Constant failure rate

T Average down-time per failure

$MTTF = \frac{1}{\lambda}$ is the Mean Time to Failure

$MTBF$ is the Mean Time Between Failures

Each failure causes downtime T. Therefore the system is unavailable for time T out of total time MTBF. The fraction of time the system is not available is therefore $\frac{T}{MTBF}$ [76] .

Table 7 shows the reliability data used in this dissertation to perform the analysis [76] .

Table 7. Reliability Data for Protection Schemes

Component	Unavailability x 10^6
Relay hardware	100
Relay applied properly	100
Current transformer (per phase)	10
Voltage transformer (per phase)	10
Circuit breaker	300
DC power supply	50
Leased telephone line	1000
Analog microwave equipment	200
Tone equipment	100
Microwave transmission channel	100
Fiber optic channel	100
Multiplexing fiber optic transceiver	100
Modem	30
Simple fiber optic transceiver	10

Impact of Protection System Structure and/or redundancies on Dependability/Security

The impact of the pilot protection scheme structures, as well as redundancy in various parts of the system, on the protection system reliability is quantified in this section.

To this end, probability of various paths in event tree diagrams are calculated. A path can occur, if all the events in that path occur. Considering that all the paths are mutually exclusive, the probability of a particular system outcome is calculated by summating the probability associated with each path leading to that outcome. The specific outcome could be system failure, success, mal-function or any other protection system mode. Clearly, the probability of each outcome depends on the paths leading to that outcome and the probability associated with events constituting each path.

Permissive Under-reach Transfer Trip (PUTT)

The first scheme to be considered is the PUTT scheme introduced in the previous sections. The reliability results for this scheme are illustrated in Figure 34.

Several observations can be made from the results:

- For a given configuration, the probability of the failure state is greatly affected by those events that, when occur, take the system to the failure state, regardless of the other events. The larger the number of such events (denoted as failing events), the higher the probability of a failure state. It can be observed that the number of failing events in the “single relay and single channel” is more than the other five configurations and so this configuration has the highest probability of failure, both in case of internal and external faults.

- Redundancy decreases the number of failing events and as such, configurations (b), (c) and (f) are less likely to fail. The number of failing events in (b) are slightly more than (c) in external faults resulting in a higher likelihood of failure.
- In the case of internal faults, the failing events are protection failures not the channel failures. Therefore, configurations that are made more robust to the protection failures; i.e. (b) and (f), have the lowest failure probability.
- The probability of state "SD"; i.e. delayed clearance of the internal fault, on the other hand, depends on the channel health. If the channel fails, the clearance of internal fault would be delayed. Therefore, configurations (c) and (f) with redundancy in channel, have less probability for reaching the "SD" mode.
- Fiber optic channels (d) and (e) have less complexity than microwave channels and therefore have better performance in channel-related modes such as "SD". Configuration (d) is even simpler than (e) and has a lower "SD" probability.
- The results indicate that this is a highly secure scheme as no malfunction occurs in case of internal faults.

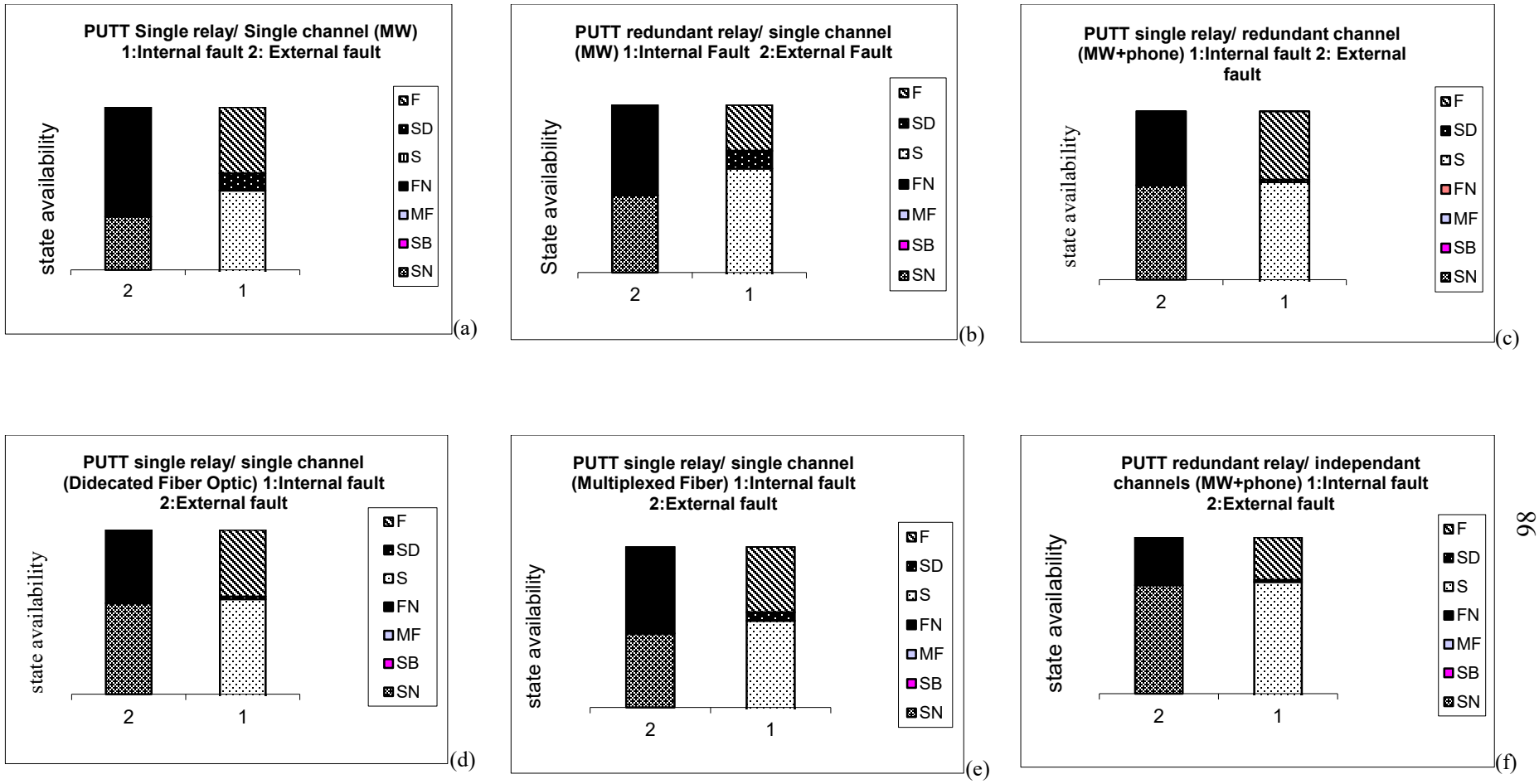

Figure 34. Dependability/Security results for PUTT scheme.

Directional Comparison Blocking Scheme (DCB)

Reliability diagrams for this scheme are shown in Figure 35. The following points are highlighted about this figure:

- Unlike PUTT, DCB scheme is subject to mal-function (MF) if the channel fails.
- Schemes with more reliable channels like (c), (d), and (e) are less susceptible to malfunction.
- Configuration (f) has the worst status in terms of mal-function. The reason for this is that, any failure of either channel could stop the block signal and result in mal-function. It should be noted that operation of each relay could open the breaker (relay contacts are tied to perform "or" function). It might be favorable to "and" the relay contacts to ensure more security in case of external faults, however, it would decrease dependability, resulting in more "F" states.

Directional Comparison Unblocking Scheme (DCUB)

Figure 36 illustrates the reliability indices for DCUB.

- In this scheme, "SD" is expected as activation of "lock out" signal will change the scheme to a conventional distance framework with associated zone 2 time delay.
- Mal-function depends on the channel status and configuration with more reliable channels like (c), (d), and (e) show a higher tendency towards malfunction.
- The malfunction is avoided if the fault clearance takes more than 150ms to be completed and therefore the scheme has better general performance than DCB in terms of mal-function.
- Unlike the PUTT that always has a delayed response (SD) when the channel fails; DCUB has delayed tripping when channel is faulty, only if the protection fails to

clear the fault within 150ms window. Hence, DCUB has a better performance against delayed tripping.

- Protection failure in clearing internal faults (F) is related to the protection availability. Configurations (b) and (f) with redundant relays are therefore less likely to fall into “F” mode.

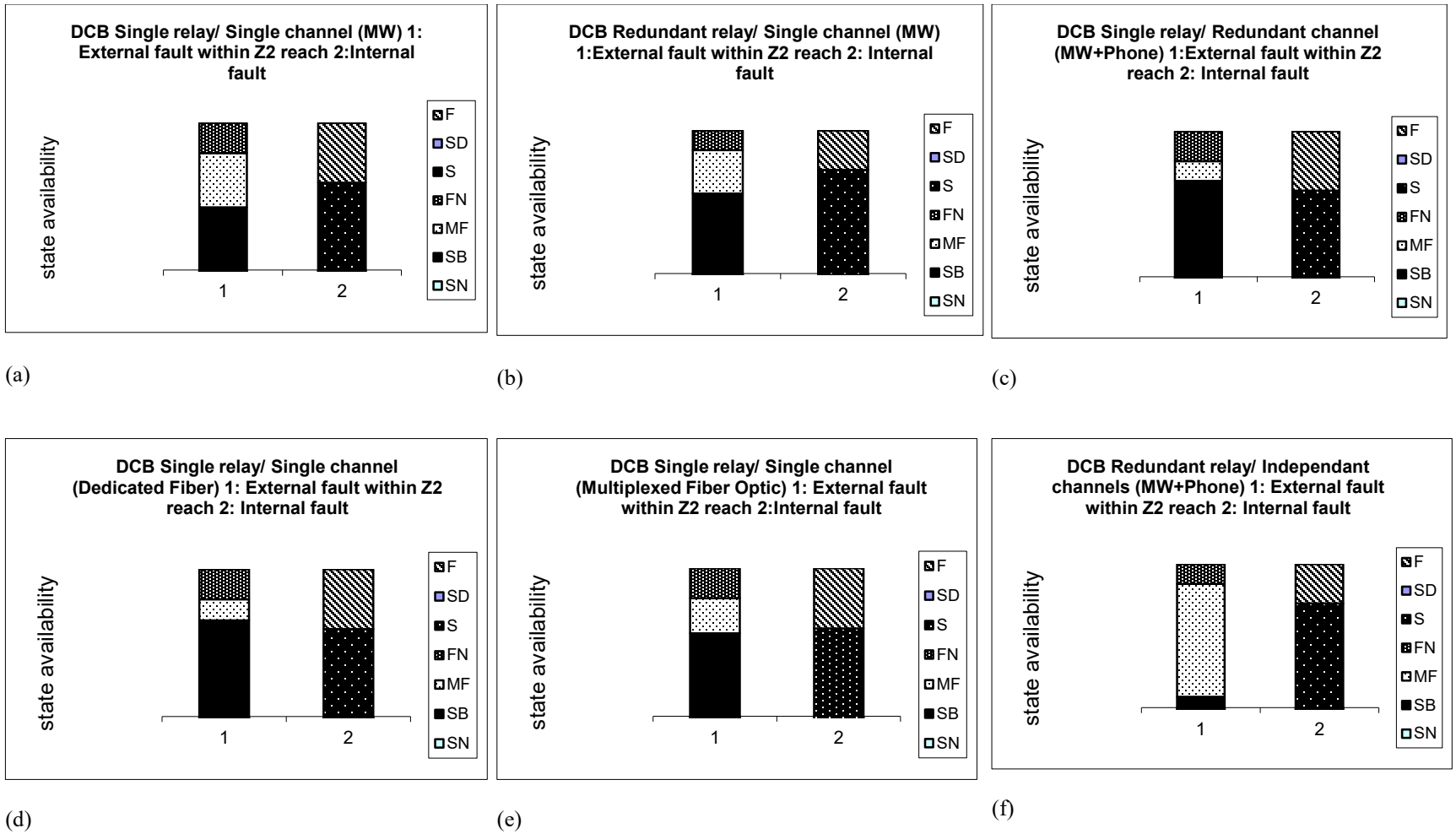

Figure 35. Dependability/Security results for DCB scheme

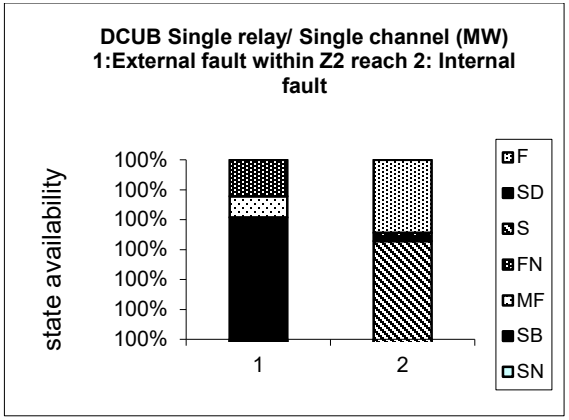

(a)

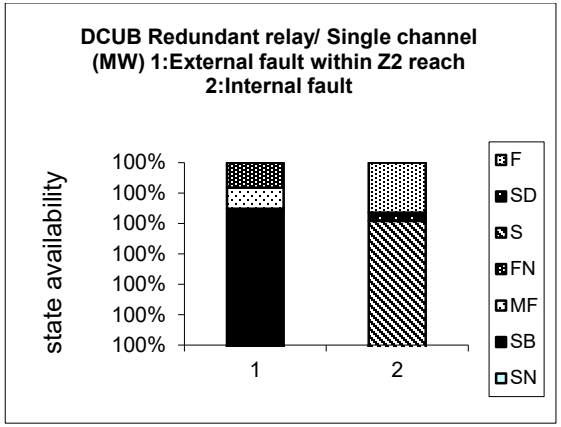

(b)

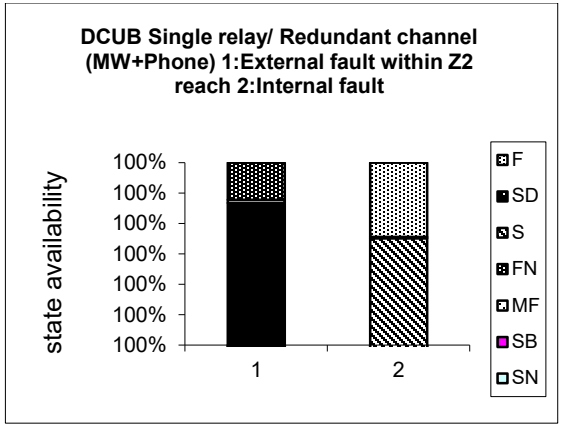

(c)

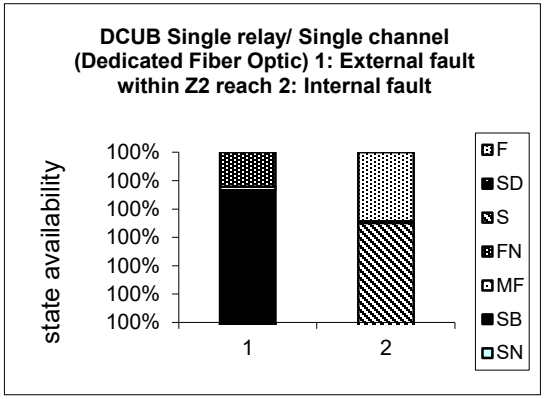

(d)

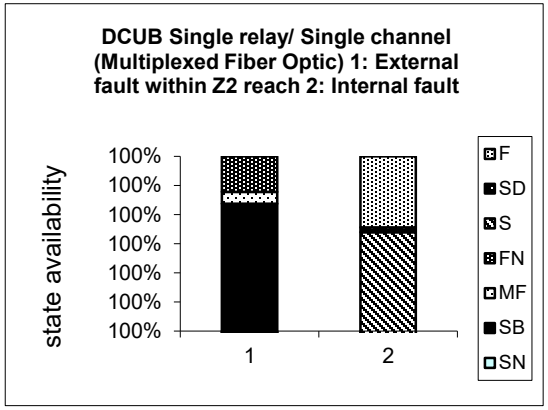

(e)

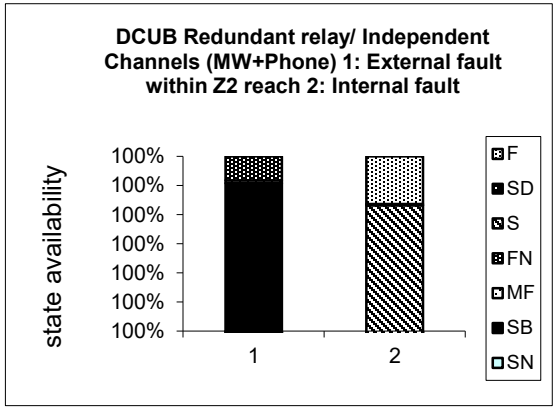

(f)

Figure 36. Dependability/Security results for DCUB scheme.

Summary

Pilot schemes differ widely in the communication media, and in the logic used for the fault detection as well as authentication of the received signal.

In this chapter, event trees were used to give a quantitative analysis and comparison of pilot protection schemes. Even though the unavailability of individual components are approximate values, event tree analysis gives useful "order of magnitude" results. These results, especially when used in comparison with each other and with a graphical interface, illuminate how various system structures and redundancies would affect the performance of protection. Some of the results are as follows:

- Blocking systems tend to be more dependable, while transfer-trip systems are more secure.
- The unblocking system combines the dependability of blocking systems with the security of the transfer-trip systems, providing a highly reliable directional pilot relaying system for transmission lines.
- The unblocking scheme shows less tendency to delayed tripping in case of channel failures.
- A large number of components in series results in poor reliability. It can be seen that in every scheme, fiber optic channels, and especially dedicated fibers have better performance than the others in channel-related failures. This is due to the

simplicity of the fiber optics media, due to less series components required for the channel success.

The results and conclusions can assist both utilities and manufacturers in making educated and substantiated decisions regarding system design and implementation. Results of study carried out in this chapter will be used in chapter 6 in determining the impact of protection schemes on asset management.

CHAPTER IV
CASE STUDIES: APPLICATION OF FAULT CURRENT LIMITERS

Application of FCL in Sporn Substation, West Virginia

This section is mainly focused on the application of a SFCL based on High Temperature Superconductor (HTS) in the American Electric Power (AEP) 138kV transmission grid [23]. The particular type of SFCL considered for this application is "Matrix Fault Current Limiter" (MFCL) and is presently under development by SuperPower Inc. and Nexans Superconductors GmbH [23].

Superpower Inc. and Nexans SuperConductors GmbH partnered to develop and demonstrate a High Temperature Superconducting (HTS) Fault Current Limiter (FCL) for utility transmission voltage level applications. This device employs technology that offers modular features that enable the scale-up to transmission voltage levels of 138 kV. In conjunction with Nexans' Melt-Cast Processed (MCP) BSCCO-2212 HTS elements, the MFCL provides a solution which is more economical than many conventional solutions to breaker over-duty problems [77].

Figure 37 shows a substation of the American Electric Power (AEP) grid in West Virginia.

The high current problem is originated by the auto-transformer T_3, which ties the 345 kV portion of the switchyard to the 138 kV portion. This tie is beneficial to the operation of the system during normal operation, but the transformer contributes an additional 13 kA at

the 138 kV bus during fault conditions. This puts 9 breakers of the substation, as indicted in the figure, in an over-duty situation.

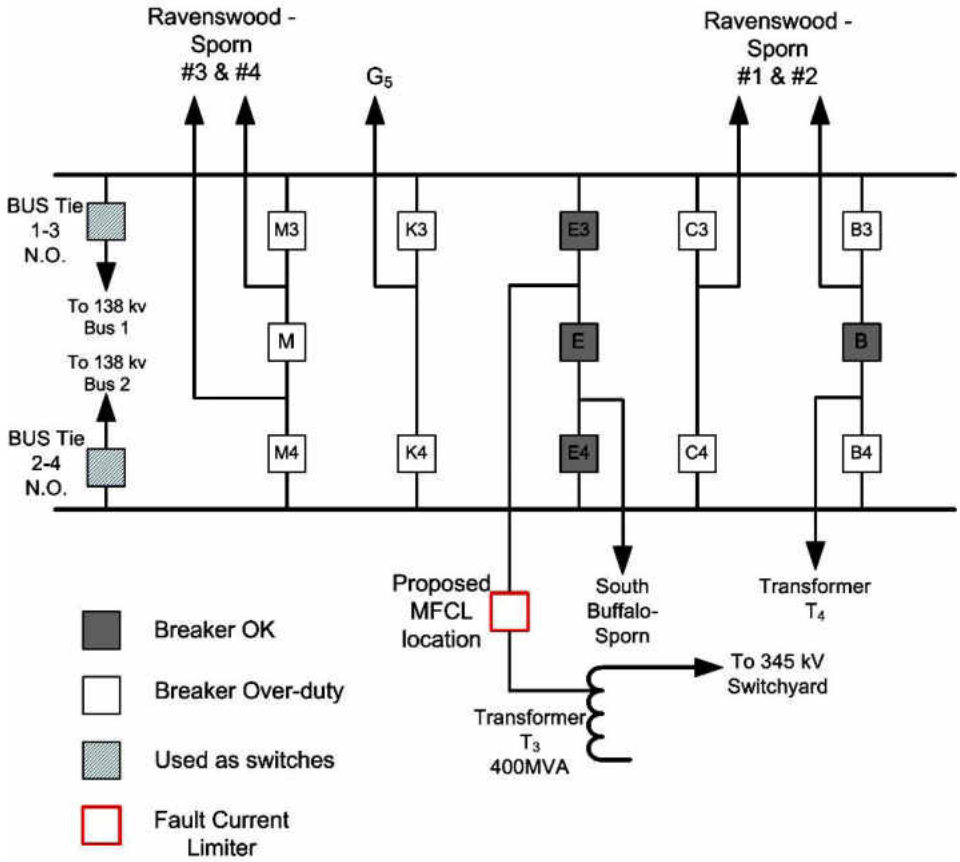

Figure 37. Potential MFCL application [23].

Chapter two gave a good review and comparison of current reduction techniques and devices used in different areas and situations based on the operating conditions, and desired levels of reliability and security. An effective economical and technical comparison between the above alternatives to solve the fault current over-duty problem at transmission level is reported in [24]. The comparison shows that SFCL is a cost-effective solution that besides a good performance in limiting the fault current at the very first cycle, it also offers

the benefit of enhancing the system reliability. A SFCL performs this function by reducing the stress on power equipment and preventing unnecessary outages.

Among solutions given in [24], the substation in Figure 37 currently employs a sequential tripping scheme to cope with high fault currents. In order to do this, breakers E_3 and E, which have sufficient rating, are tripped first if a fault is detected on Lines #1 to #4. This removes transformer T_3's contribution to the fault so that the affected over-duty breaker can safely open and isolate the fault. This sequential breaker scheme solves the problem, but has the disadvantage of delaying the fault clearing by adding E_3 and E breakers in the trip sequence. It also results in unnecessarily removing the normal T_3 load current to portions of the system that were not affected by the fault.

An alternative solution is to keep T_3 connected during the fault, but limit its current with a FCL [78]. American Electric Power (AEP; Columbus, Ohio, U.S.) and a team consisting of SuperPower Inc. (Schenectady, New York, U.S.), Nexans SuperConductors GmbH (Hürth, Germany) and Oak Ridge National Laboratory (ORNL; Oak Ridge, Tennessee, U.S.) have made it a priority to address fault current over-duty problems at the transmission voltage levels of 138-kV and higher [79].

Figure 37 shows how the addition of a MFCL in series with transformer T_3 could resolve the problem without resorting to the sequential breaker trip scheme. This location is also in agreement with the results published in [45] that reviews all possible locations for using fault current limiter in a substations and recommends that in a 1.5 breaker arrangement,

installing FCL's in series with critical lines would have the highest positive impact on fault level reduction.

Here the MFCL is transparent to the system, and transformer T_3 supplies load current from the 345 kV system to the 138 kV system. Under fault conditions, the MFCL transits to the high impedance state to limit the contribution of T_3 to the fault, allowing the existing breakers to clear the fault without having to open breakers E_3 or E first.

In following sections we deal with this application and, in quantitative terms, address the reliability of the above scheme and compare the two cases of using the sequential breaker trip scheme and using a FCL.

Failure Modes and Effects Analysis

Due to switching nature of power substations, we should use special methods that can take into account these switching actions and their effects on the system. Because of this reason, reliability assessment of substations is usually done using failure modes and effects analysis [80]. The basis of this method is to identify whether the failure of a component or combination of components causes the failure of the load point of interest. If it does, the event is counted as a load point failure event. Otherwise, it is disregarded at least as far as the load point of interest is concerned. The consequence of a given failure event is then identified according to the severity of the failure.

In this method, all events that contribute to unavailability of any given load point are recognized and recorded for that load point. Then for the event i, occurrence rate λ_i, outage time r_i , and unavailability U_i due to that event are calculated.

Each event *i* can be either a fault in one component or overlapping outage of two or more components. For instance the event where a short circuit happens in breaker 1 and transformer 3 is open (due to maintenance).

Equations 3 to 5 are, respectively, used to calculate the expected failure rate, average outage duration and average annual outage time associated with the overlapping outage of two components 1 and 2.

$$\lambda_{pp} = \frac{\lambda_1\lambda_2(r_1 + r_2)}{1 + \lambda_1 r_1 + \lambda_2 r_2} \cong \lambda_1\lambda_2(r_1 + r_2) \quad \text{when} \quad \lambda_i r_i << 1 \tag{3}$$

$$r_{pp} = \frac{r_1 r_2}{r_1 + r_2} \tag{4}$$

$$U_{pp} = \lambda_{pp} . r_{pp} = \lambda_1\lambda_2 r_1 r_2 \tag{5}$$

Where λ_1, r_1, λ_2, and r_2 are failure rates and outage times of components 1 and 2, respectively.

As all the events are assumed to be mutually exclusive, they are effectively in series from a reliability point of view, meaning that occurrence of one of them would result in unavailability of the load. The indices for the studied load point can therefore be evaluated

using Equations for series events- equations 6 to 8- in which λ_i and r_i are, respectively, the average failure rate and average outage time associated with the *i*th event.

$$\lambda_s = \sum_i \lambda_i \quad (6)$$

$$U_s = \sum_i \lambda_i \,.\, r_i \quad (7)$$

$$r_s = \frac{U_s}{\lambda_s} = \frac{\sum_i \lambda_i \,.\, r_i}{\sum_i \lambda_i} \quad (8)$$

Where λ_s, U_s, and r_s are the load point (or system) average failure rate, average unavailability and average outage time, respectively.

Study Results

Following are the assumptions that were made in this study. These assumptions are the most possible realistic ones, as to the best knowledge of the author. They are not, however, restrictive and similar results are obtained when they are altered.

1- In the absence of two transformers T_3 and T_4, generator G_5 in Figure 37 may not be able to supply the full load. In such circumstances (only unit G_5 in service), unit G_5 could become unstable depending on conditions such as the unit readiness to supply the loads, generating capacity status at the moment, speed of the generator response to the change in the load value, protection clearing time, etc. This event is, therefore, designated as "potential instability" which implies that it could potentially lead to system instability. Whether or not instability occurs, is determined by the probability P_{Instab} defined as follows:

$$P_{Instab} = \frac{\text{No. of instabilities when "only } G_5 \text{ in service"}}{\text{Total No. of exposure to "only } G_5 \text{ in service" in the period of study}} \quad (9)$$

The above probability could easily be obtained using the historical data recorded in event/fault recorders in the substation.

If we define event "A" as "G_5 becomes instable when only G5 remains in the circuit" and event "B" as the event that "only G_5 remains in the circuit", possible outcomes of event "B" are "A" and "$\bar{A}$ " ("$\bar{A}$ " being the case that G_5 doesn't becomes instable when only G5 remains in the circuit) , therefore the rate of event "A" is:

$$\lambda(A) = \lambda(B) \cdot P_{instab} \quad (10)$$

2- In the conventional sequential scheme, if breakers E or E_3 fail to open to disconnect T_3, some breakers maybe subject to over-duty. These cases are designated as "potential C.B. blast" as they may or may not result in a real breaker blast. P_{Blast} defines this probability as:

$$P_{Blast} = \frac{\text{No. of a specific breaker blast while E or E}_3 \text{ fails to open when they should}}{\text{Total No. of times that E or E}_3 \text{ fails to open when they should}} \quad (11)$$

Frequency of the event "C" defined as "A specific breaker blasts when E or E_3 fails to open when they should" is then:

$$\lambda(C) = \lambda(D) \cdot P_{Blast} \tag{12}$$

Where "D" is the event that E or E_3 fail to open when they should.

3- Transformer T_4 cannot carry the full load current. Therefore in case that only T_4 remains in the circuit, all loads are curtailed due to the overload of this transformer.

4- Transformer T_3 can carry the full load current for the duration of the switching time. Switching time is the time required to perform the switching action in substation to isolate the affected component or to transfer load to the healthy feeders. This time is typically selected to be one hour.

5- Combination "G5+One transformer" can carry the full load current without overload limitations.

6- Transformers T_3 and T_4 are capable of carrying the full load current without overload limitations.

Based on the above assumptions, comparative studies were conducted using the above method to examine the reliability impact of incorporating the MFCL in the transmission

substation. Figure 38 and 39 show the effect of MFCL on the failure rate and unavailability of individual load points. In these figures L1 to L4 are lines #1 to #4 and customer plant is unit G_5 in Figure 37 [22].

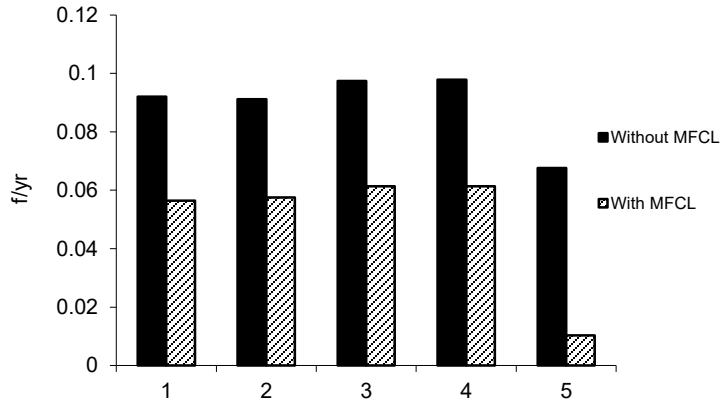

Figure 38. Load point failure rates without and with MFCL for 1:L1 2:L2 3:L3 4:L4 5: Customer Plant.

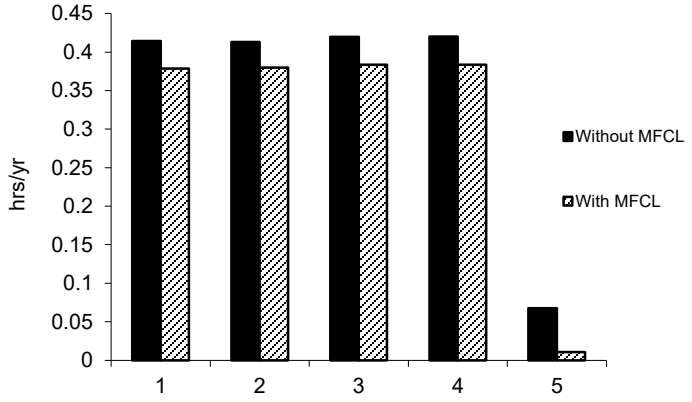

Figure 39. Load point unavailability without and with MFCL for 1:L1 2:L2 3:L3 4:L4 5: Customer Plant.

As expected, it is seen from these figures that using MFCL would decrease the failure rates and unavailability. It can be seen from the results that the maximum unavailability improvement is achieved for the customer plant with 0.0572 hrs/yr. This is due to the adverse effect that sequential trip has on the continuity of service to the customer plant and that MFCL prevents the unnecessary outages in this regard.

Potential instability of the substation without and with MFCL is illustrated in Figure 40. In these figures, "O/yr" is short for "occurrence per year" and indicates the rate of the events. In this case, MFCL reduces the potential instability from 0.0288 to 4.4466e-7. This is a considerable improvement with respect to stability and is mainly because the existing sequential scheme jeopardizes system stability by disconnecting the transformer T_4 and as such G_5 would have a lesser chance to remain stable.

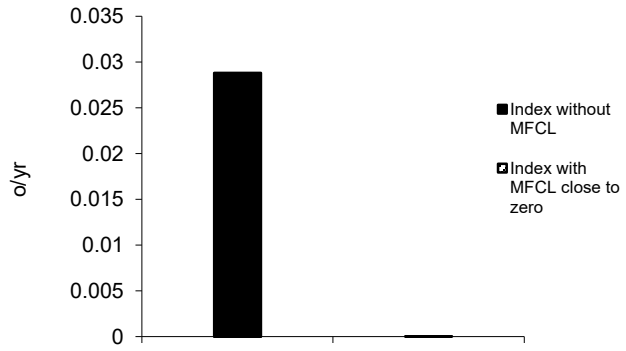

Figure 40. Potential instability without and with MFCL.

Figure 41 compares the bus isolation probability for the two cases of without and with MFCL.

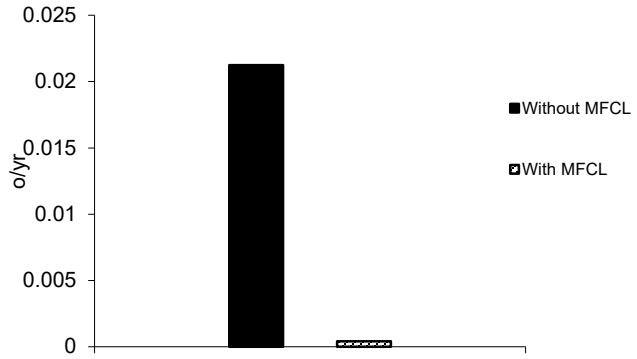

Figure 41. Bus isolation without and with MFCL.

In some cases, such as when breaker E_3 is faulty, transformer T_3 continues to send current to the fault. In these cases if the back-up protection of T_3 does not operate in time to disconnect the transformer, the transformer may become damaged. Therefore, these cases are designated as "potential T_3 damage". It is obvious that when MFCL is used, T_3 is prevented from getting damaged because of the limited current and so there is no "potential T_3 damage" in case of MFCL. Figure 42 shows the frequency of these cases without and with MFCL.

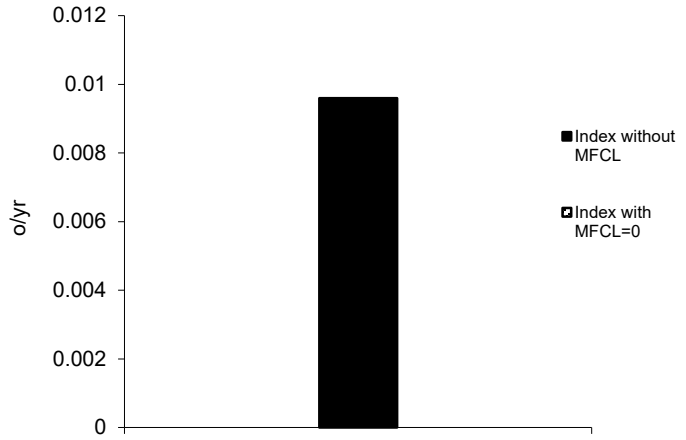

Figure 42. Potential T3 damage without and with MFCL.

Figure 43 shows the frequency of "Potential Circuit Breaker blast". It should be noted that this event, although not so common, once it occurs it impose a tremendous amount of extra cost and outage time on the system.

Figure 43. Potential CB Blast without and with MFCL.

Another interesting study that can be conducted is to examine the variation in expected failure rate due to changes in P_{Instab} for different load points with and without MFCL. This comparison is shown in Figures 44 through 48. As expected, failure rate increases as the P_{Instab} increases. The results also indicate that sensitivity of λ with respect to P_{Instab} is less when using MFCL compared to that of without MFCL. This indicates that when MFCL is used, station reliability is not much affected by operating condition of the substation.

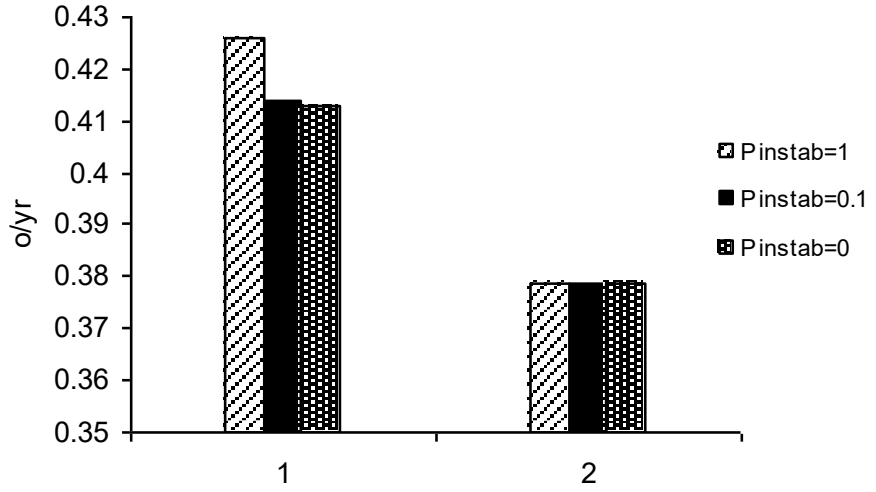

Figure 44. L1 Unavailability for different values of Pstab; 1: without MFCL 2: with MFCL

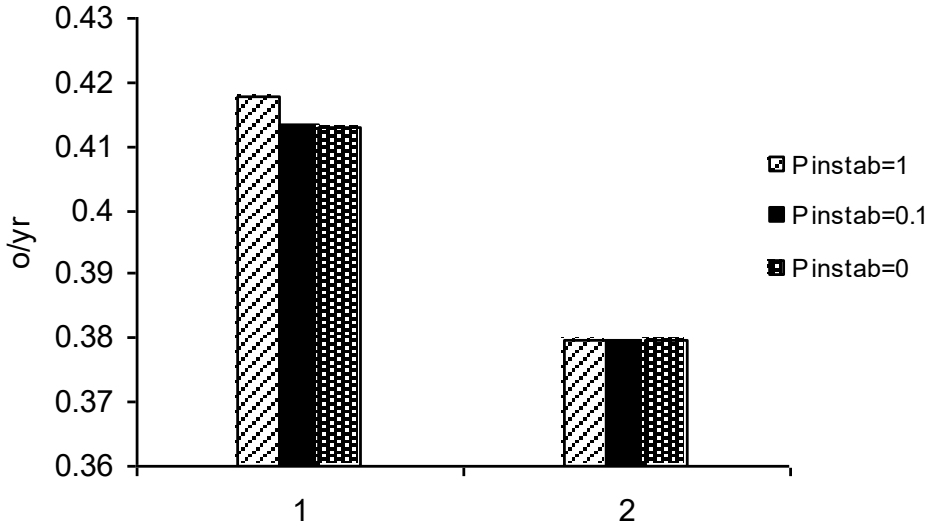

Figure 45.L2 Unavailability for different values of Pstab; 1: without MFCL 2: with MFCL.

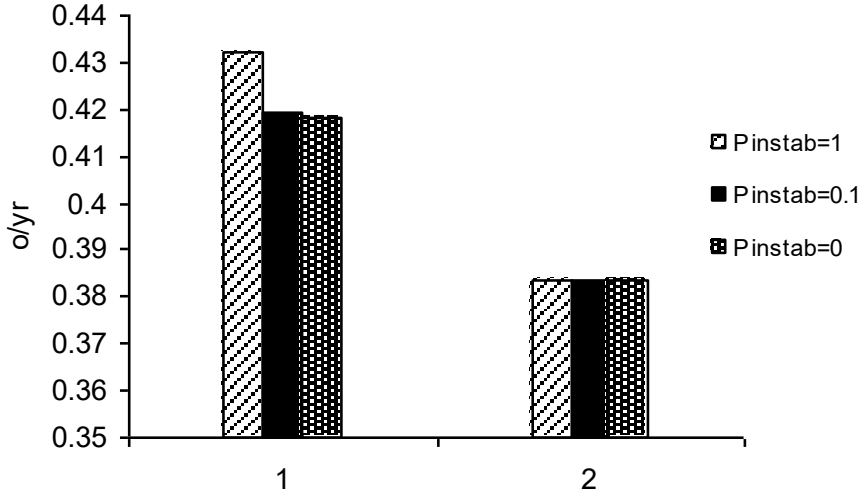

Figure 46. L3 Unavailability for different values of Pstab; 1: without MFCL 2: with MFCL.

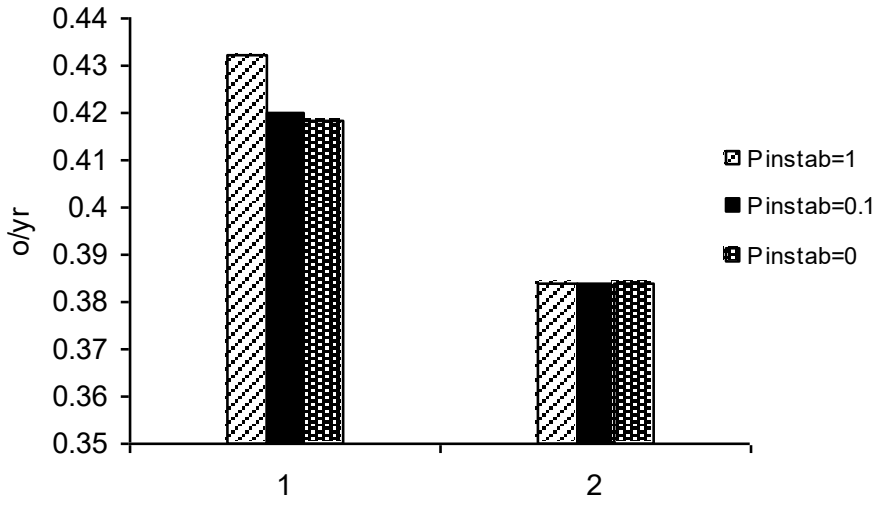

Figure 47. L4 Unavailability for different values of Pstab; 1: without MFCL 2: with MFCL.

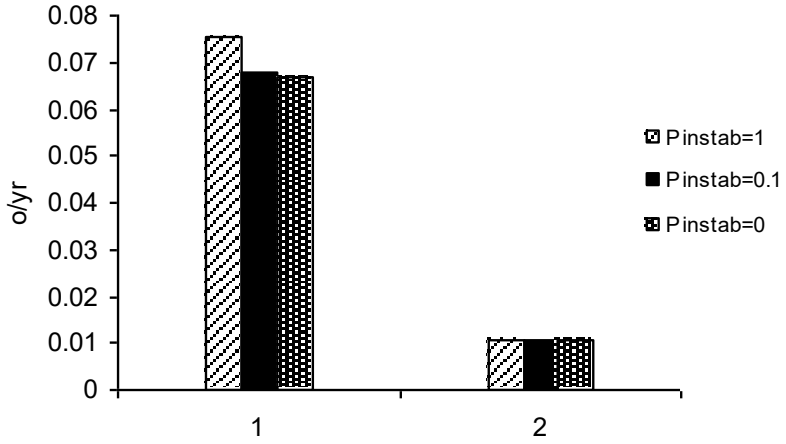

Figure 48. L5 Unavailability for different values of Pstab; 1: without MFCL 2: with MFCL.

Application of FCL in Wind Power Plants

In the coming years there will be more and more wind power plants connected to the electric grid. The integration of wind turbine generators, and large number of induction generators in wind power plants dramatically increases the fault current level beyond the capacity of existing protection devices [39]. The system stability and voltage quality may be corrupted. So the power system switchgear and power system protection should be carefully designed to obtain a secure operation of the system. Fault Current Limiters (FCL's) regulate the amount of current moving through the transmission and distribution systems under abnormal conditions. In [81], [82], and [83] it is shown that Fault Current Limiters (FCL's) suppress this negative influence of DG on distribution systems. The use of superconducting fault current limiter (SFCL) reduces fault current level at the stator side and improve the fault ride through capability of the system [40]. In this section, application of a type of FCL called Superconductive Shielded Core Reactor (SSCR[6]) is studied in a wind power plant. Computer simulation examines the effectiveness of SSCR in reducing the fault current level as well as provision for transient stability without affecting the normal operation of the system.

In following sections of this chapter, we will model a SSCR in Simulink. Since most generators used in wind power plants are induction generators, we will then develop a

[6] Described in Chapter two

model for simulation of induction generator in the Simulink. Using these two models we can simulate the performance of SSCR in a given wind power plant.

Simulation of SSCR

In [51] a SSCR is developed and tested in the circuit shown in Figure 49. The same circuit is used in this paper to simulate the operation of SSCR using a new model and compare it with experimental results presented in [51] .

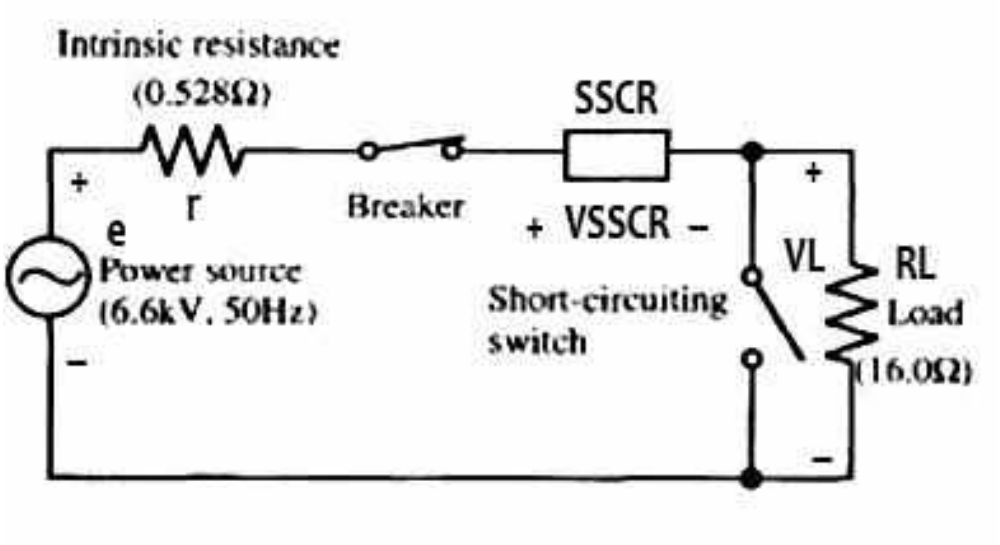

Figure 49. Circuit used in simulation of SSCR [51].

From the circuit shown in Figure 49:

$$i = \frac{e - (V_L + V_{SSCR})}{r} \tag{13}$$

$$V_L = R_L . i \tag{14}$$

Where e is Voltage of the power source, V_L is Voltage across the load R_L, V_{SSCR} is the voltage across the SSCR, r is the internal resistance of the source, and i is the current in the circuit.

Equation (13) could be simulated in SIMULINK using the block diagram of Figure 50 [84]. The block "SSCR" in the figure represents the superconductive limiter. Figure 51 shows details of the SSCR block. This figure simply denotes the relationship between I_{SSCR} and V_{SSCR}; i.e. current through the SSCR and voltage e across it, respectively. Despite the simplicity of the proposed model, it has sufficient accuracy to predict the behavior of a SSCR in limiting short circuit currents. The accuracy of the proposed model is then examined using the experimental data published in [51].

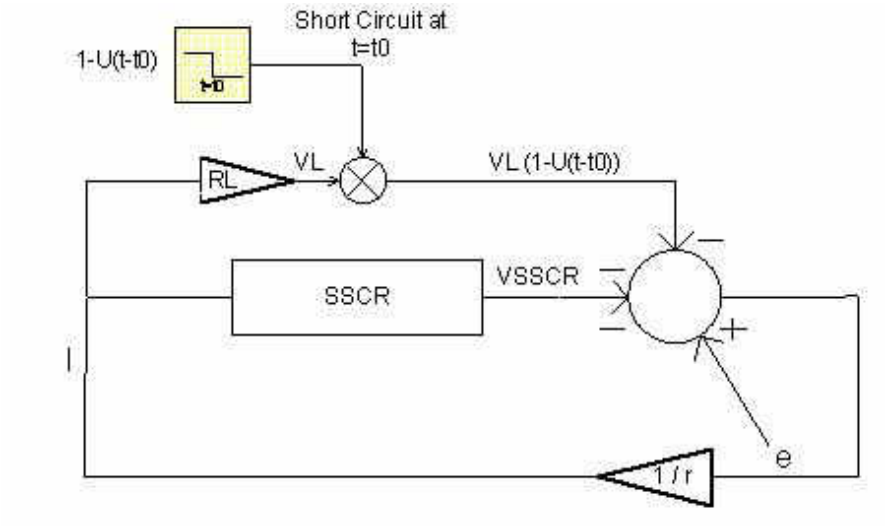

Figure 50. Block diagram used in simulation.

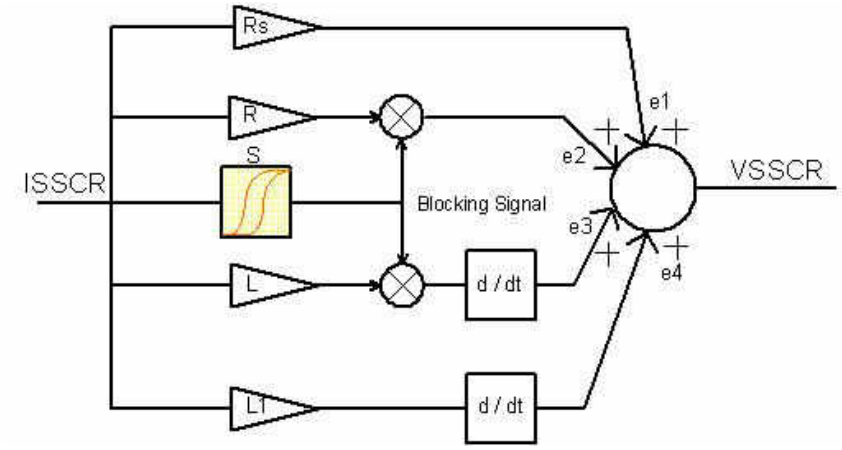

Figure 51. Inside the SSCR block.

It can be seen from Figure 51 that VSSCR consists of four parameters *e*1, *e*2, *e*3 and *e*4. *e*1 and *e*4 are voltage drops due to the resistance and leakage reactance of the copper coil of SSCR, respectively. These two terms always exist regardless of the mode of operation of SSCR. In other words, whether or not the SSCR works in superconductive region, it has

the resistive voltage drop and leakage voltage drop associated with the copper coil. Therefore $e1$ and $e4$ are directly added to give the final voltage drop. The other two voltage drops, i.e., $e2$ and $e3$ do not exist during the normal operation of SSCR. They appear only when the SSCR loses its shielding behavior as the result of a fault condition. $e2$ denotes the voltage drop corresponding to the resistance of the superconductor and $e3$ is the voltage drop across the reactance of the unshielded copper coil. As a matter of fact, the main function of SSCR is to expose the inductance of the copper coil when a fault occurs. Therefore, $e3$ is the main component in limiting the fault current. Since $e2$ and $e3$ do appear only during fault conditions, they are multiplied by a blocking signal prior to summation to give the final voltage drop. The blocking signal is multiplied by $e2$ and $e3$ and blocks them by outputting a zero when the current in the circuit is below the critical level. When the current passes this level, i.e. when the fault occurs, the output of this block jumps to "1", hence allowing $e2$ and $e3$ to contribute to the final VSSCR. Block "s" in Figure 51 generates this signal.

Figure 52 shows the output of block "s". It is clear that "s" is a simple switch with "0" output for currents below the critical current of superconductor and jumps to "1" when the current passes the threshold. The reason for using a hysteresis behavior for "s" is that when the current passing through the SSCR increases and makes the device to quench, it remains quenched and doesn't return to its superconducting state even if the current falls below the critical value. Therefore, once the output of "s" jumps to "1" it must remain at this level

and not return to “0” at any time. This irreversible behavior of SSCR is well simulated using the hysteresis path shown in Figure 52.

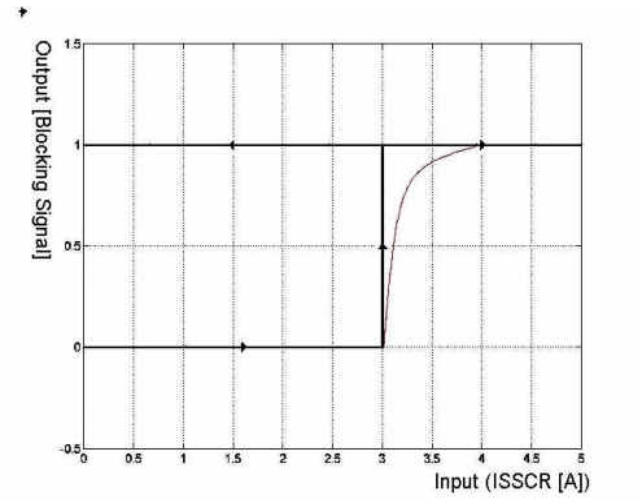

Figure 52. Output of block "s" in Figure 51.

Actually, in reality, at some time after the fault is detected and cleared, the SSCR returns to its superconductive state. Inclusion of this "reset time" is beyond the scope of this study. The model of this section simulates the macroscopic behavior of the SSCR for Grid study only. It should be noted that in order to simulate the exact behavior of the SSCR during quench the step function in the output of the block "s" should be replaced by an exponential function to take into account the effects of penetration depth, magnetic and thermal diffusion, and a possible transition into the flux flow state during quench.

Figure 53 shows the experimental and simulation results for the circuit. It can clearly be seen that the simulation results are in good agreement with those obtained from experiment in [51].

It should be noted that the new model receives the current passing through SSCR as input and gives the voltage across it as output. This is demonstrated in Figure 54.

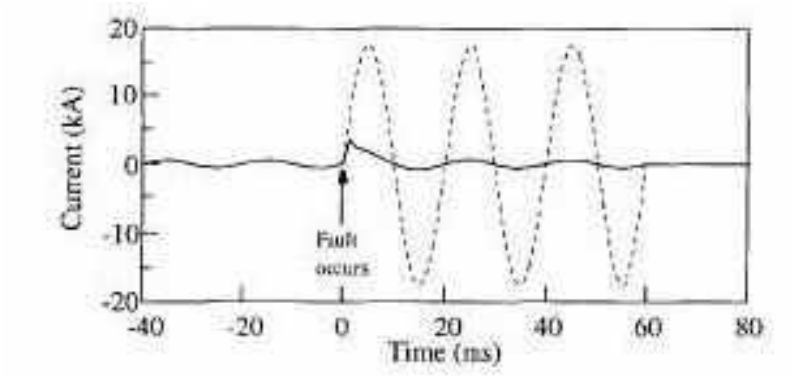

(a)

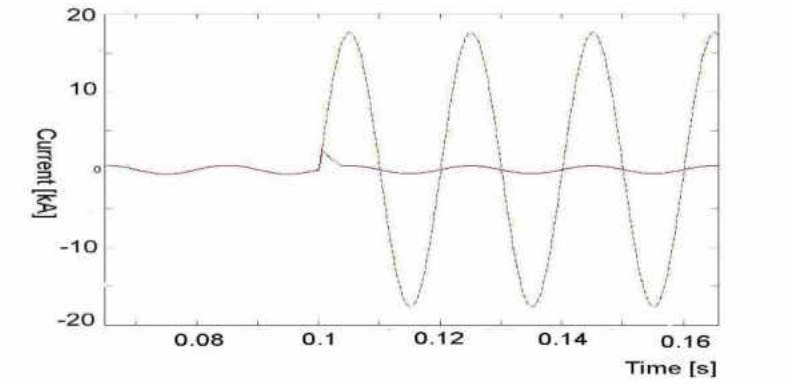

(b)

Figure 53. Limiting characteristics of SSCR: (a) experimental [51] (b) simulation .

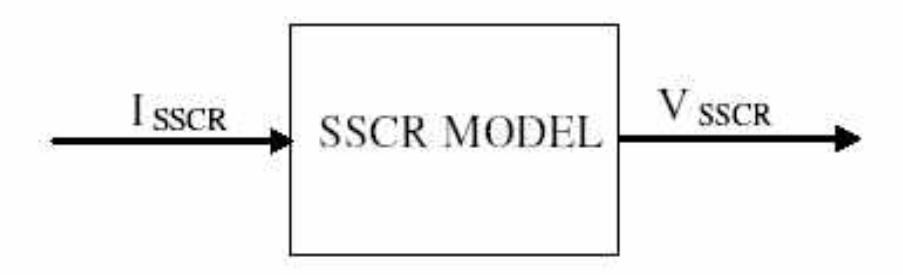

Figure 54. Input-output status of the proposed model for SSCR.

Simulation of Induction Generator

Equations of an induction machine in time domain are as below [85] :

Stator voltage equations.

$$v_{as} = i_{as}r_s + \frac{d\lambda_{as}}{dt} \tag{15}$$

$$v_{bs} = i_{bs}r_s + \frac{d\lambda_{bs}}{dt} \tag{16}$$

$$v_{cs} = i_{cs}r_s + \frac{d\lambda_{cs}}{dt} \tag{17}$$

Rotor voltage equations.

$$v_{ar} = i_{ar}r_r + \frac{d\lambda_{ar}}{dt} \tag{18}$$

$$v_{br} = i_{br}r_r + \frac{d\lambda_{br}}{dt} \tag{19}$$

$$v_{cr} = i_{cr}r_r + \frac{d\lambda_{cr}}{dt} \tag{20}$$

Flux linkage equations.

Flux linkage equations of the stator and rotor windings in matrix form are as below:

$$\begin{bmatrix}\lambda_s^{abc}\\ \lambda_r^{abc}\end{bmatrix}=\begin{bmatrix}L_{ss}^{abc} & L_{sr}^{abc}\\ L_{rs}^{abc} & L_{rr}^{abc}\end{bmatrix}\begin{bmatrix}i_s^{abc}\\ i_r^{abc}\end{bmatrix} \tag{21}$$

Where

$$\lambda_s^{abc}=[\lambda_{as}\quad \lambda_{bs}\quad \lambda_{cs}]^T \tag{22}$$

$$\lambda_r^{abc}=[\lambda_{ar}\quad \lambda_{br}\quad \lambda_{cr}]^T \tag{23}$$

$$i_s^{abc}=[i_{as}\quad i_{bs}\quad i_{cs}]^T \tag{24}$$

$$i_r^{abc}=[i_{ar}\quad i_{br}\quad i_{cr}]^T \tag{25}$$

The submatrices of stator and rotor winding inductances are :

$$L_{ss}^{abc}=\begin{bmatrix}L_{ls}+L_{ss} & L_{sm} & L_{sm}\\ L_{sm} & L_{ls}+L_{ss} & L_{sm}\\ L_{sm} & L_{sm} & L_{ls}+L_{ss}\end{bmatrix} \tag{26}$$

$$L_{rr}^{abc}=\begin{bmatrix}L_{lr}+L_{rr} & L_{rm} & L_{rm}\\ L_{rm} & L_{lr}+L_{rr} & L_{rm}\\ L_{rm} & L_{rm} & L_{lr}+L_{rr}\end{bmatrix} \tag{27}$$

$$L_{sr}^{abc}=[L_{rs}^{abc}]^T=L_{sr}\begin{bmatrix}Cos(\theta) & Cos(\theta+\frac{2\pi}{3}) & Cos(\theta-\frac{2\pi}{3})\\ Cos(\theta-\frac{2\pi}{3}) & Cos(\theta) & Cos(\theta+\frac{2\pi}{3})\\ Cos(\theta+\frac{2\pi}{3}) & Cos(\theta-\frac{2\pi}{3}) & Cos(\theta)\end{bmatrix} \tag{28}$$

Where θ is angle of the rotor. Applying park transformation in stationary reference frame to the voltage and flux linkage equations will time remove time dependency of the equations and result in equations (29) to (35) [85]. Figure 55 schematically shows this reference frame with respect to the stator and rotor windings.

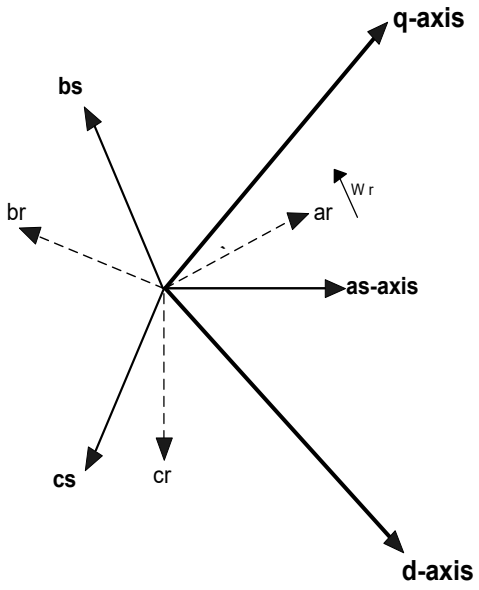

Figure 55. Stationary reference frame spatial diagram

$$v_{qs} = \frac{1}{\omega_b}\frac{d}{dt}\Psi_{qs} + r_s i_{qs} \tag{29}$$

$$v_{ds} = \frac{1}{\omega_b}\frac{d}{dt}\Psi_{ds} + r_s i_{ds} \tag{30}$$

$$v_{os} = \frac{1}{\omega_b}\frac{d}{dt}\Psi_{os} + r_s i_{os} \tag{31}$$

$$v'_{qr} = \frac{1}{\omega_b}\frac{d}{dt}\Psi'_{qr} - \frac{\omega_r}{\omega_b}\Psi'_{dr} + r'_r i'_{qr} \tag{32}$$

$$v'_{dr} = \frac{1}{\omega_b}\frac{d}{dt}\Psi'_{dr} + \frac{\omega_r}{\omega_b}\Psi'_{qr} + r'_r i'_{dr} \tag{33}$$

$$v'_{or} = \frac{1}{\omega_b}\frac{d}{dt}\Psi'_{or} + r'_r i'_{or} \tag{34}$$

$$\begin{bmatrix} \Psi_{qs} \\ \Psi_{ds} \\ \Psi_{os} \\ \Psi'_{qr} \\ \Psi'_{dr} \\ \Psi'_{or} \end{bmatrix} = \begin{bmatrix} x_{ls}+x_m & 0 & 0 & x_m & 0 & 0 \\ 0 & x_{ls}+x_m & 0 & 0 & x_m & 0 \\ 0 & 0 & x_{ls} & 0 & 0 & 0 \\ x_m & 0 & 0 & x'_{lr}+x_m & 0 & 0 \\ 0 & x_m & 0 & 0 & x'_{lr}+x_m & 0 \\ 0 & 0 & 0 & 0 & 0 & x'_{lr} \end{bmatrix} \begin{bmatrix} i_{qs} \\ i_{ds} \\ i_{os} \\ i'_{qr} \\ i'_{dr} \\ i'_{or} \end{bmatrix} \tag{35}$$

Where the primed rotor quantities are their referred values to the stator side, and

$\Psi_{(\,)} = \omega_b \lambda_{(\,)}$ in all equations.

By defining mutual flux linkages as:

$$\psi_{mq} = X_m(i_{qs} + i'_{qr}) \tag{36}$$

and

$$\psi_{md} = X_m(i_{ds} + i'_{dr}) \tag{37}$$

the mutual flux linkages of the machine can be expressed as:

$$\psi_{qs} = X_{ls} \cdot i_{qs} + \psi_{mq} \tag{38}$$

$$\psi_{ds} = X_{ls} \cdot i_{ds} + \psi_{md} \tag{39}$$

$$\psi'_{qr} = X'_{lr} \cdot i'_{qr} + \psi_{mq} \tag{40}$$

$$\psi'_{dr} = X'_{lr} \cdot i'_{dr} + \psi_{md} \tag{41}$$

Solving the above equations for currents yields:

$$i_{qs} = \frac{\psi_{qs} - \psi_{mq}}{X_{ls}} \tag{42}$$

$$i_{ds} = \frac{\psi_{ds} - \psi_{mq}}{X_{ls}} \tag{43}$$

$$i'_{qr} = \frac{\psi'_{qr} - \psi_{mq}}{X'_{lr}} \tag{44}$$

$$i'_{dr} = \frac{\psi'_{dr} - \psi_{mq}}{X'_{ls}} \tag{45}$$

Substituting (42) to (45) into (36) and (37) and rearranging terms would result in:

$$\psi_{mq} = X_M \cdot (\frac{\psi_{qs}}{X_{ls}} + \frac{\psi'_{qr}}{X'_{lr}}) \tag{46}$$

and

$$\psi_{md} = X_M \cdot (\frac{\psi_{ds}}{X_{ls}} + \frac{\psi'_{dr}}{X'_{lr}}) \tag{47}$$

Where

$$\frac{1}{X_M} = \frac{1}{X_m} + \frac{1}{X_{ls}} + \frac{1}{X'_{lr}} \tag{48}$$

It is now possible to rearrange the equations of the induction machine into a suitable form for simulation. Substituting Equations (42)-(45) into voltage equations (29) to (34) and rearranging the terms would result in:

$$\psi_{qs} = \omega_b \cdot \int \left\{ v_{qs} + \frac{r_s}{X_{ls}} (\psi_{mq} - \psi_{qs}) \right\} dt \tag{49}$$

$$\psi_{ds} = \omega_b \cdot \int \left\{ v_{ds} + \frac{r_s}{X_{ls}} (\psi_{md} - \psi_{ds}) \right\} dt \tag{50}$$

$$i_{os} = \frac{\omega_b}{X_{ls}} \cdot \int \{v_{os} + i_{os} \cdot r_s\} dt \tag{51}$$

$$\psi'_{qr} = \omega_b \cdot \int \left\{ v'_{qr} + \frac{\omega_s}{\omega_b} \psi'_{dr} + \frac{r'_r}{X'_{lr}} (\psi_{mq} - \psi_{qr}) \right\} dt \tag{52}$$

$$\psi'_{dr} = \omega_b \cdot \int \left\{ v'_{dr} + \frac{\omega_r}{\omega_b} \psi'_{qr} + \frac{r'_r}{X'_{lr}} (\psi_{md} - \psi_{dr}) \right\} dt \tag{53}$$

$$i'_{or} = \frac{\omega_b}{X'_{lr}} \cdot \int \{v'_{or} + i'_{or} \cdot r'_r\} dt \tag{54}$$

The torque equation is (considering P poles in the machine):

$$T_{em} = \frac{3}{2} \quad \frac{P}{2\omega_b} (\psi_{ds} \cdot i_{qs} - \psi_{qs} . i_{ds}) \tag{55}$$

The equation of the motion of the rotor is:

$$J \frac{d\omega_{rm}}{dt} = T_{em} - T_{mech} - T_{damp} \tag{56}$$

In Equation (56), T_{mech} is the externally applied mechanical torque and T_{damp} is the damping torque in the direction opposite to rotation. The value of T_{mech} is negative for the motoring condition, as in the case of a load torque and is positive for the generating

condition, as in the case of an applied shaft torque from a prime mover. Equations (49) to (56) give a proper simulation model that can be easily implemented in simulation programs such as SIMULINK. Block diagrams of simulation of the above equations in SIMULINK are given in Figures 56.

Based on the above discussion, the overall simulation of the induction generator presented here receives the terminal voltage of the machine as input and calculates the generator current as output. This input output status of the presented model is shown in Figure 57 (compare it with Figure 54 for SSCR).

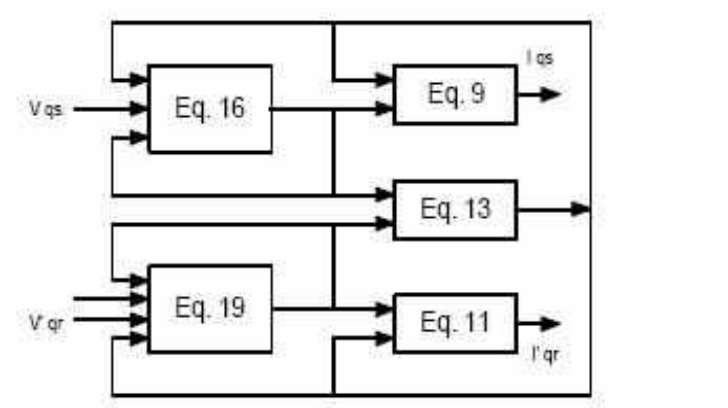

(a) q-axis circuit

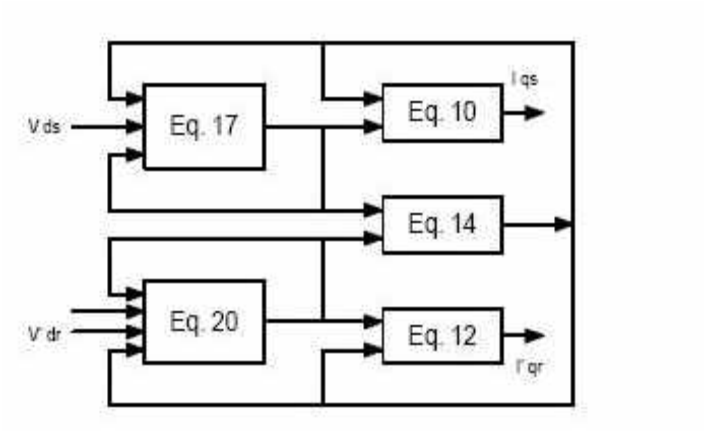

(b) d-axis circuit

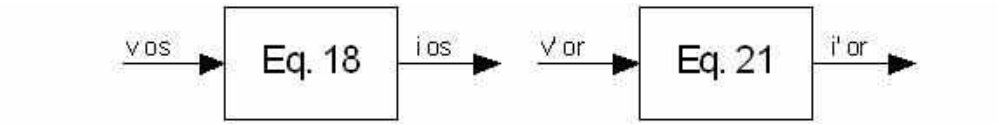

(c) o-axis circuit

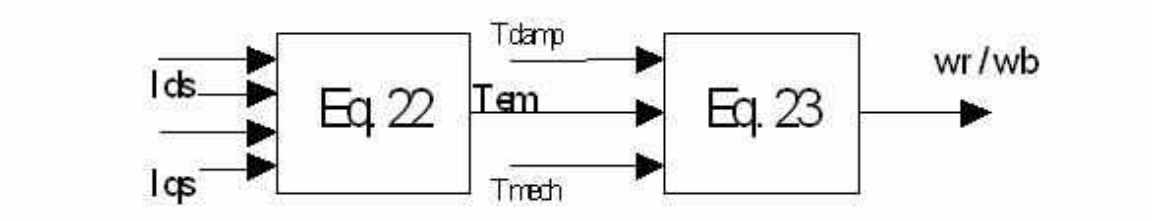

(d) Developed torque and speed

Figure 56. Block diagram used in the simulation of induction generator.

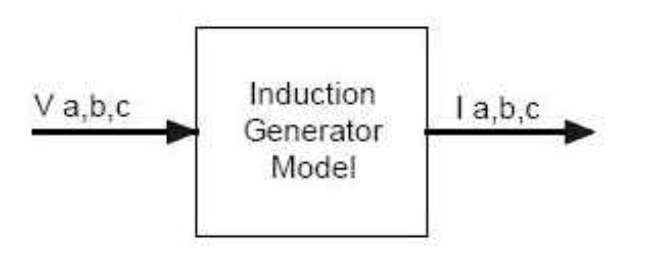

Figure 57. Input- output status of the presented induction generator model.

Inclusion of SSCR in Wind Power Plants

Figure 58 shows a typical wind power plant where an induction generator is used along with a SSCR. In this figure, "C" represents the capacitor bank and "L" represents the transmission line.

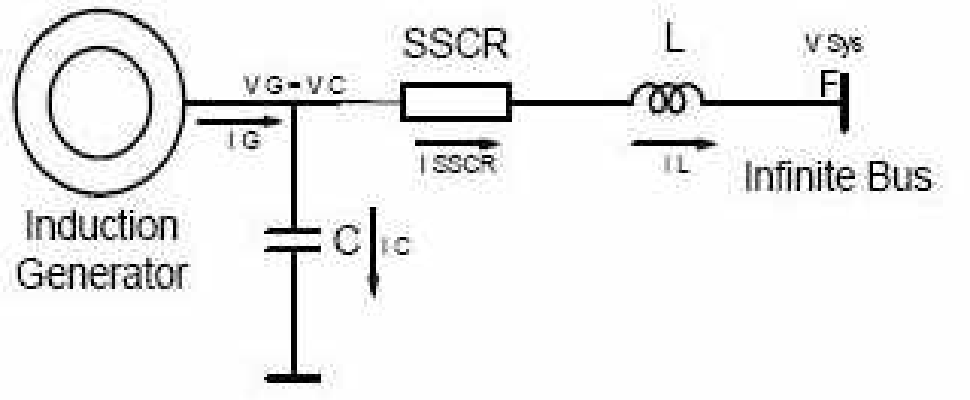

Figure 58. Test system used in the simulation.

In order to simulate this system, the network equations should be derived first and used with the two models presented above for the SSCR and the generator. Network equations for the circuit shown in Figure 58 are presented by Equations (57) and (58).

$$v_G = \int \frac{1}{C} \cdot (i_G - i_{SSCR}) dt \tag{57}$$

$$i_L = \int \frac{1}{L} \cdot (v_c - v_{SSCR} - v_{sys}) dt \tag{58}$$

The block diagram in Figure 59 illustrates the computer simulation flow graph for the circuit in Figure 58. In this block diagram the two previously discussed models for SSCR and generator are used in addition to the network model Equations (57) and (58).

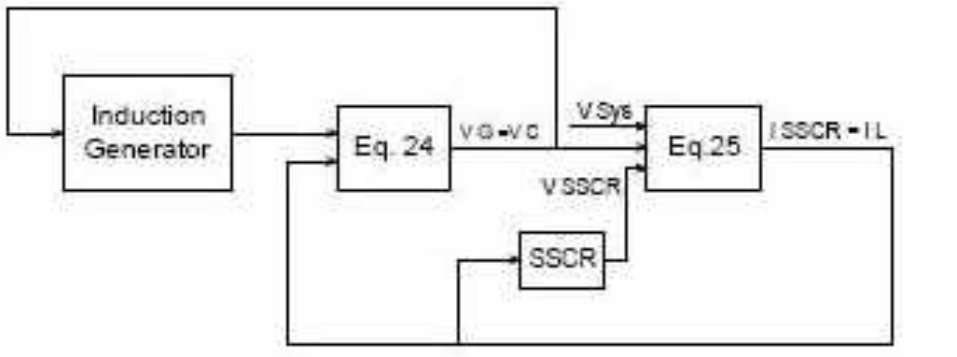

Figure 59. Computer simulation flow graph for the circuit of Figure 58.

Using the SSCR and induction generator model in the block diagram of Figure 59, the test system was simulated using SIMULINK. Point “F” in Figure 58 was subject to a single-line-to-ground fault as well as a three phase-to-ground fault and current responses were examined in each case. In both cases the faults occur at t=4 sec. Figures 60 (a) and (b) show the results for three-phases fault and Figures 60 (c) to (d) and 61 (a) to (d) illustrate the results for single-line-to-ground fault. Since the generator is supplied via the infinite bus, in the case of the three-phases-to-ground fault at “F”, the main supply to the generator is short circuited by the fault and hence removed. In this case, the short circuit current appears to decline automatically even without existence of SSCR, however, SSCR serves as a limiting device that efficiently reduces the fault current at its peak level.

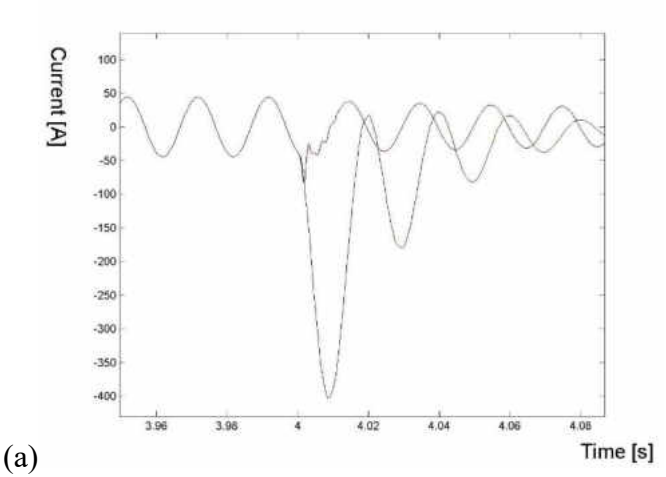

(a)

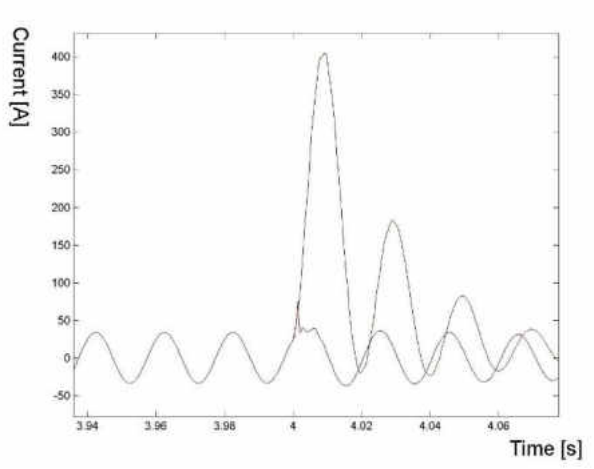

(b)

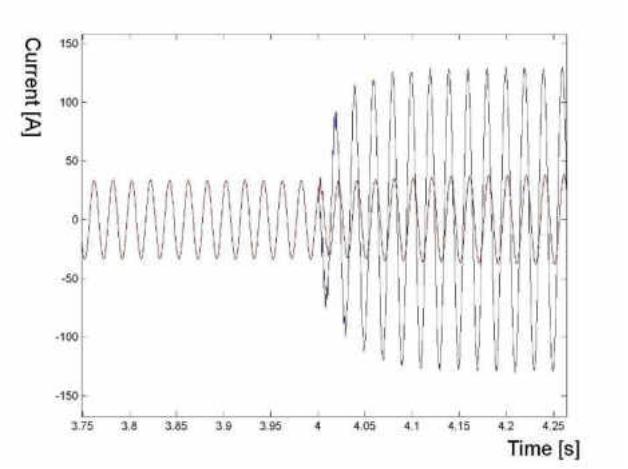

(c)

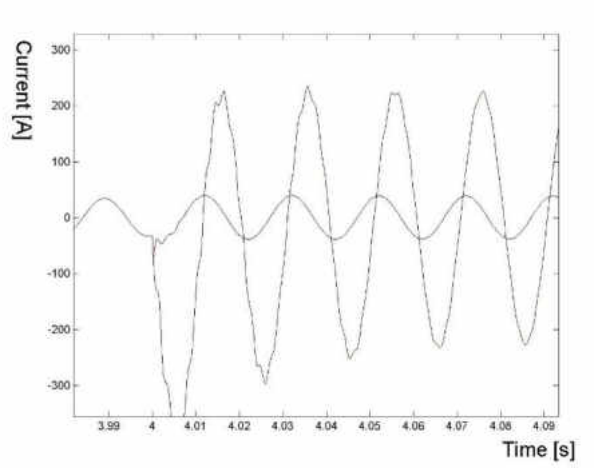

(d)

Figure 60. Three-phase fault at point F (a) iG phase a (b) iL phase a -- One Phase-to-ground fault (LG) at point F (c) iL phase a (d) iL phase b

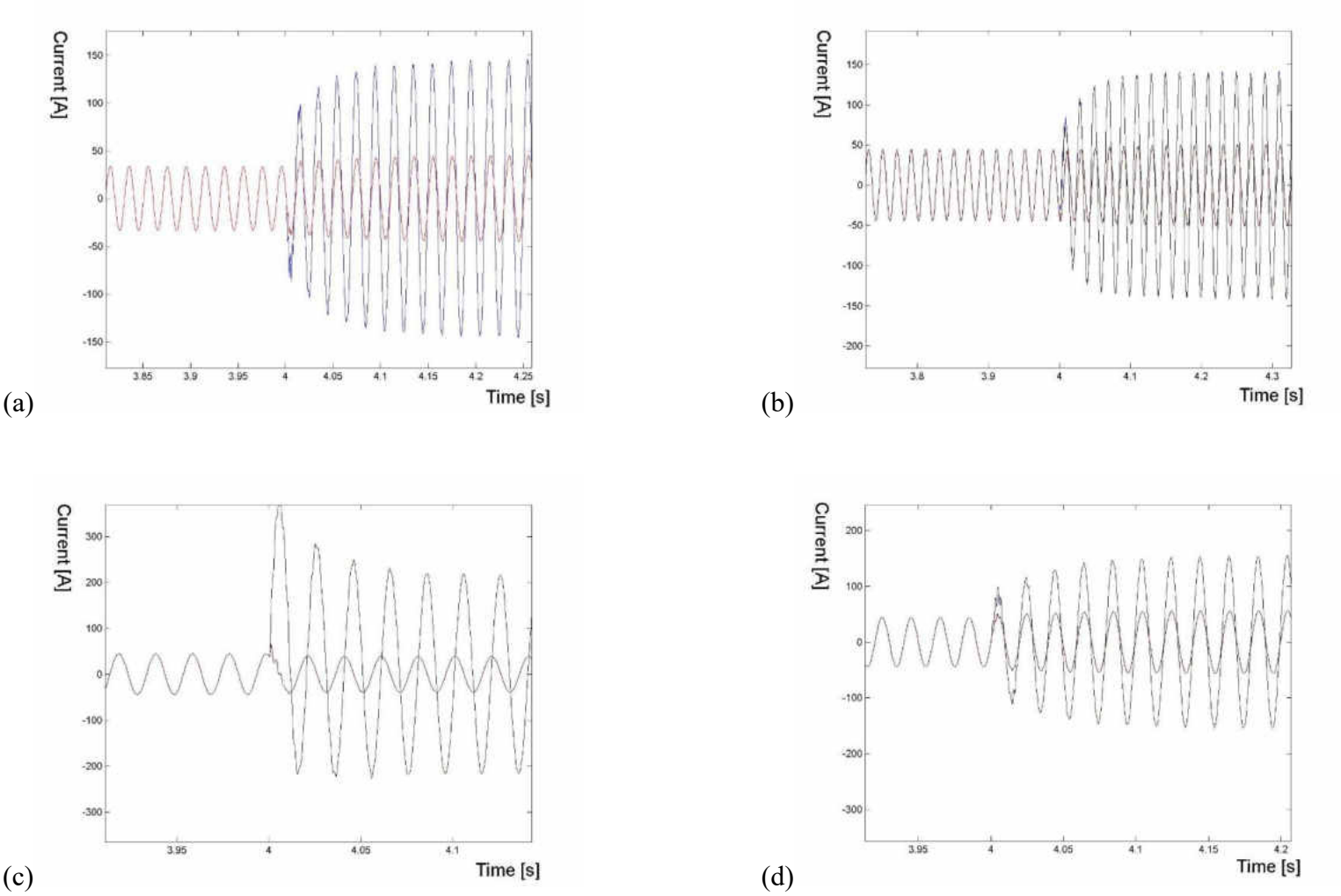

Figure 61. Single-line-to-ground fault (LG) at point F (a) iL, phase c (b) iG, phase a (c) iG, phase b (d) iG, phase c .

Application of SFCL in Power Substations to Enhance Reliability

In order to examine the impact of employing SFCL on station reliability, all the configuration shown in Figure 8 chapter 2 are used for this analysis. These arrangements are repeated here in Figure 62 for easy reference. As noted earlier, SFCL would prevent loads from being curtailed in case of a short circuit in the system. This implies that some of the failure modes of substations which cause interruption of Load points in the absence of SFCL, are eliminated when the SFCL is employed.

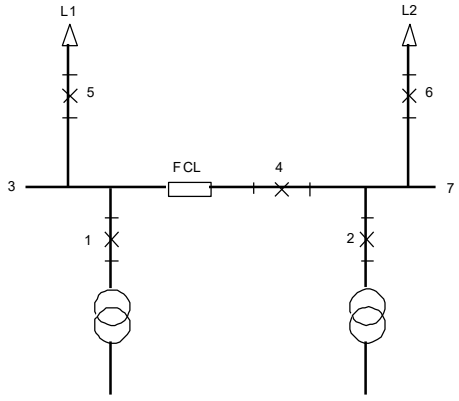

(a) single sectionalized bus arrangement

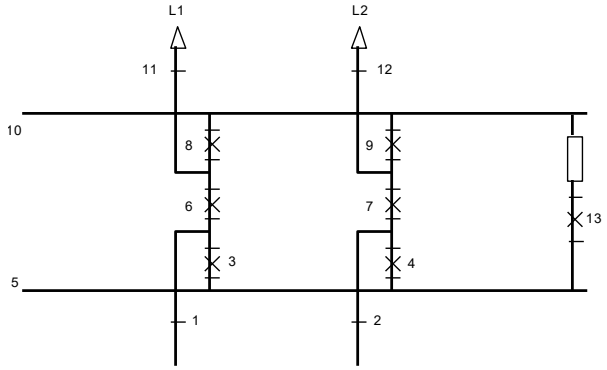

(b) breaker and a half

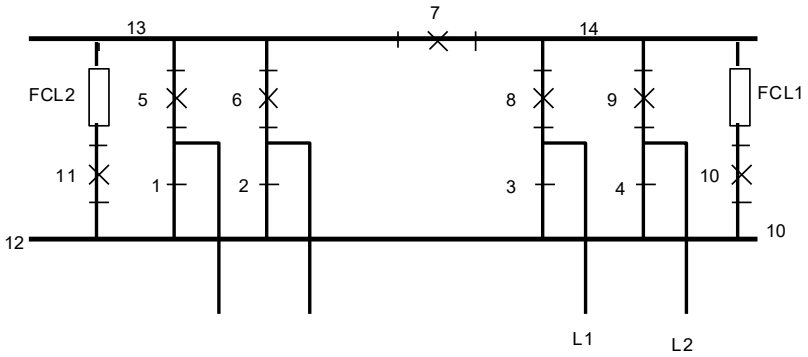

(c) main and transfer bus system

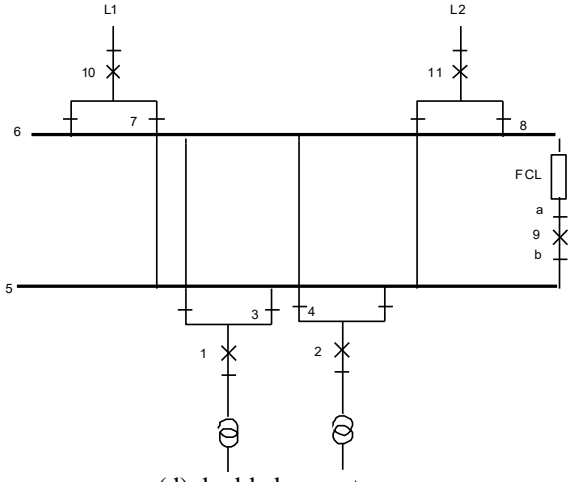

(d) double bus system

Figure 62. Common configurations in switching substation.

Failure modes and effects has been used to study impact of using SFCL in various substation arrangements and locations [14]. Table 1 in Appendix shows that SFCL eliminates a large number of failure modes. Since the reliability indices of the entire substation are determined through these failure modes, using SFCL improves the reliability indices of substations, as it was expected [14].

The worth of employing SFCL is examined by comparing the reliability indices for two cases. In the first case, the reliability indices associated with each station configuration are

calculated without installing SFCL. In the second case, the reliability indices are calculated in the presence of SFCL. The reliability data used in these calculations are shown in Table 8 [22] .

Table 8. Station Reliability Data [22]

element	Failure Rate (f/yr)			repair time (hrs)	switching time (hrs)
	open circuit	short circuit	total		
CB	0.005	0.005	0.01	12	1
Disconnector Switch	0.005	0.005	0.01	4	1
Bus	0.005	0.005	0.01	4	1

Table 2 in Appendix shows the study results associated with the station configurations "main and transfer bus" shown in Figures 49.c. All the failure events affecting Load point L1 are shown in the tables. Similar calculations could be conducted for “L2” due to the symmetry of the circuits. Some of the failure events which were previously affecting Load point L1 are eliminated by installing the SFCL. These failure modes have been highlighted in the Appendix of this document and summarized in Table 9. The associated events are therefore disregarded for the load point of interest.

In the results presented in this dissertation, overlapping forced outages up to second-order, first order active failures and first-order active failures overlapping a stuck breaker are

considered [14] . The probability that a breaker fails to open when required (stuck-breaker probability) is assumed to be 0.1 for all cases. Moreover, the SFCL is assumed to be fully reliable, i.e. failure rate of the SFCL is assumed to be zero.

Table 9. Events Eliminated due to Employing SFCL(s) in main and transfer bus system

Events	**Events Deleted Due to**		
	SFCL 1	**SFCL 2**	**SFCL 1&2**
9A	**X**	**X**	**X**
10A	**X**		**X**
11A		**X**	**X**
1A+11S		**X**	**X**
4A+11S		**X**	**X**
4A+10S	**X**		**X**

Table 10. Reliability indices for bus arrangements without SFCL.

Bus Arrangement	λ (f/yr)	r (hours)	U (hours/yr)
Single Sectionalized Bus	0.031000622	5.516126591	0.171003356
Breaker and a half	0.024001495	2.249994085	0.054003221
Main and Transfer	0.06750085	1.888926615	0.127504153
Double bus	0.042500845	3.588247776	0.152503562

Table 11. Reliability indices for bus arrangements with SFCL.

Bus Arrangement	λ (f/yr)	r (hours)	U (hours/yr)
Single Sectionalized Bus	0.020000622	7.999918952	0.160003356
Breaker and a half	0.022501356	2.33333045	0.052503098
Main and Transfer			
SFCL1	0.058000925	2.034521926	0.118004153
SFCL2	0.05750085	2.043520262	0.117504153
SFCL1 & SFCL2	0.05150085	2.16509343	0.111504153
Double bus	0.025000845	5.399960001	0.135003562

Tables 10 and 11 summarize the results of these calculations. It can be seen from the results shown in these two tables that the most reliability improvement is achieved in case of a "double bus system" with a "0.0175 f/yr" decrease in the average failure rate. This, however, reaches its minimum variation in "breaker and a half" with a "0.0015 f/yr" decrease.

It can be seen from the results of calculation that using SFCL in each case improves the reliability indices. The impacts on the reliability indices vary for different configurations. For the single sectionalized bus arrangement, the expected failure rate and the annual outage time decreases from 0.3 to 0.20 f/yr and 0.171 to 0.16 hrs/yr, respectively, when

SFCL is used. This improvement, however, is different for the case of breaker and a half station configuration. The reliability improvement in this case is less compared with the case of the single sectionalized bus arrangement. The decrease in the average failure rates for these two configurations is in the order of 35.5% and 6.25%, respectively. The reason for this is that one and a half station configuration is inherently more reliable than the single sectionalized bus arrangement.

Comparing the reliability indices for different substation arrangements also shows that "breaker and a half" is the most reliable one with a "0.054 hrs/yr" unavailability, while "single sectionalized bus arrangement" is the least reliable with a "0.171 hrs/yr" unavailability. This information is useful when selecting the substation arrangements among available alternatives.

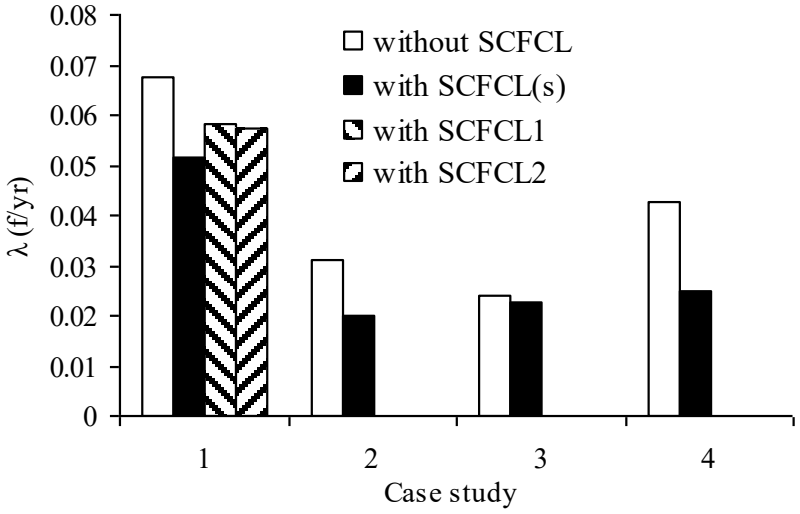

Figure 63. Comparison of failure rates for various arrangements with and without SFCL: (1) Main and transfer (2) Single sectionalized bus (3) Breaker and a half (4) Double bus..

Figure 63 shows failure rate of load point L1 for the four configurations with and without SFCL. Another interesting study that can be conducted is to examine the variation in expected failure rate due to changes in stuck-breaker probability for different station configurations with and without SFCL. This comparison is shown in Figure 64. Stuck breaker is a situation in which a circuit breaker fails to operate even after receiving a tripping signal from a relay or a switch. Stuck breaker can undermine the protection scheme and can cause damage to machinery and is a danger to personnel. Common reasons for a circuit breaker not opening are a disconnection in the trip circuit or a mechanical problem with the circuit breaker.

As expected, failure rate increases as the stuck breaker probability increases. The results also indicate that sensitivity of failure rate λ with respect to stuck breaker probability is less when using SFCL compared to that without SFCL. This can clearly be seen as the slope of the lines associated with the case with SFCL is less than that of the case without SFCL. This is much more significant for single sectionalized bus arrangement and double bus system shown with the horizontal lines. This indicates that when SFCL is used, station reliability is not much affected by high stuck breaker probability.

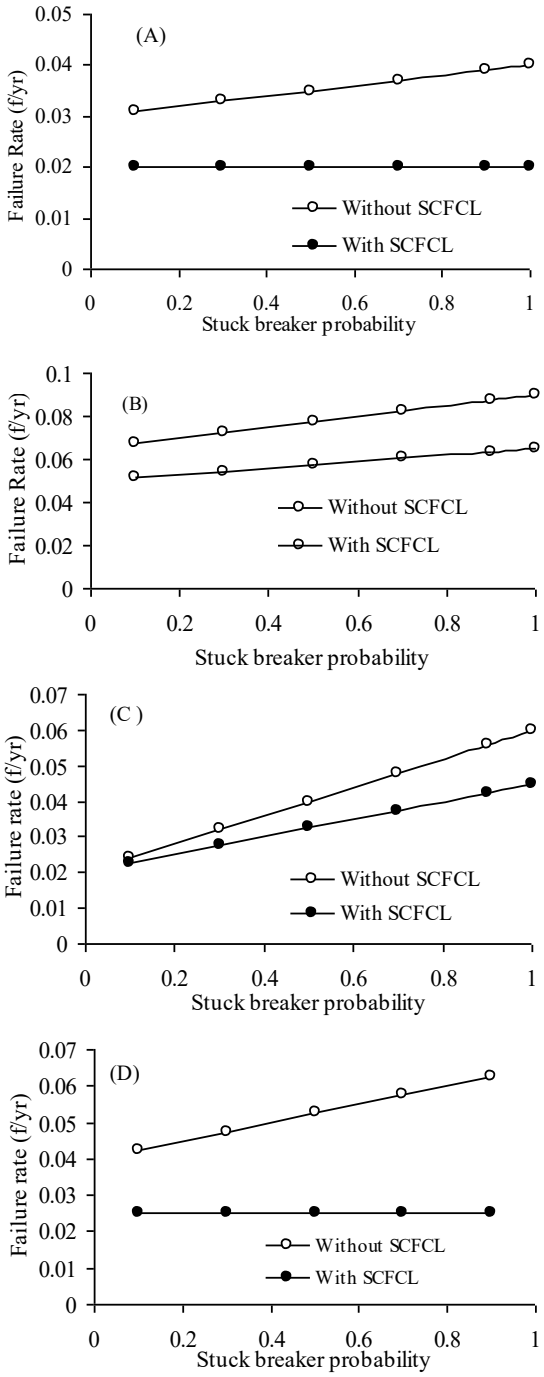

Figure 64. Variation of λ with respect to stuck breaker probability : (a) Single sectionalized bus arrangement (b) Main and transfer bus system (c) Breaker and a half system (d) Double bus system.

Other Studies on Reliability Improvements by Using Fault Current Limiters

Literatures on reliability impacts of FCL's can be divided into two main categories: those focusing on proposing models for the FCL as a new element in the power system, and those working on modeling the impacts/behaviors of FCl's in the power grid. Studies in the first category are helpful in providing models for the system incorporating the new element, but their values are limited by how accessible it is to build up the proposed model in the reality. It is especially important to be able to find/calculate the recommended model parameters using in-field data and non-destructive tests.

[86] proposes a Markov model for operation of SFCL shown in Figure 65. This model is then used to calculate the reliability indices of a three bus system with the SFCL installed, and comperes it with the non-FCL case. [87] and [88] use this model to asses reliability of a distribution system with the SFCL installed.

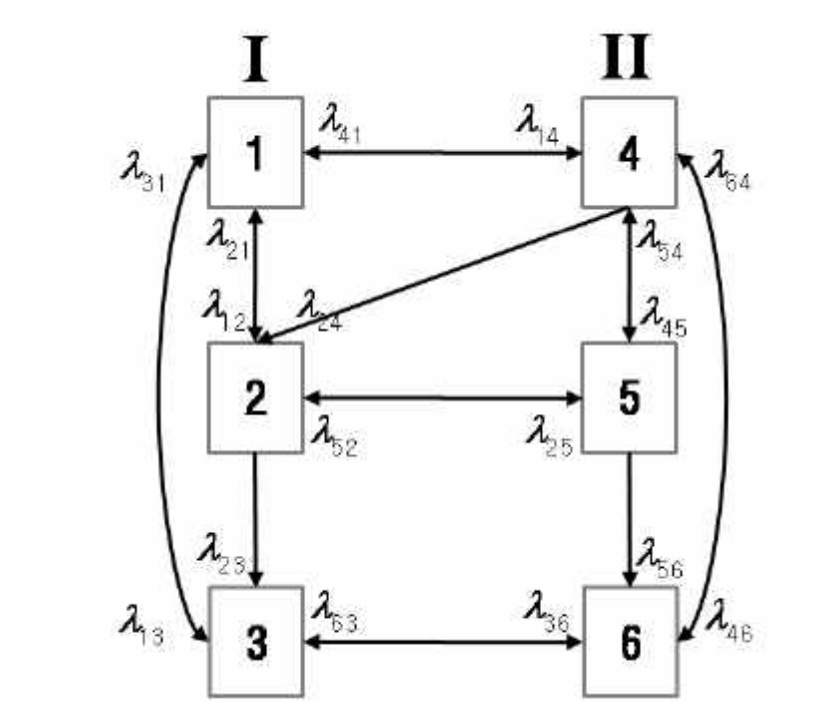

Figure 65. Six-state model of SFCL recommended in [86].

Parameters of this model are as below:

λ_{12}: Failure rate at which resistance zero state can be changed into the quench state in normal condition

λ_{21}: Repair rate at which the extra resistance by quench can be changed into zero resistance in normal condition

λ_{13}: Failure rate at which SFCL with zero resistance can be separated from network in normal condition

λ_{31}: Repair rate at which SFCL with zero resistance can be reconnected to network in normal condition

λ_{23}: Failure rate at which SFCL with extra resistance can be separated from network in normal condition

λ_{45}: Failure rate at which perfect operation is interrupted as SFCL partly limits fault current in abnormal condition

λ_{54}: Repair rate at which perfect operation is recovered from partial fault current limit in abnormal condition

λ_{46}: Failure rate at which perfect operation is interrupted as SFCL is separated from network in abnormal condition

λ_{64}: Repair rate at which perfect operation is recovered from disconnection in abnormal network

λ_{56}: Failure rate at which SFCL with extra resistance can be separated from network in abnormal condition

λ_{42}: Failure rate at which SFCL can't recover superconductivity in normal after perfect operation in abnormal

$\lambda_{14}, \lambda_{25}, \lambda_{36}$: Transition rates from normal condition (I) to abnormal condition (II)
$\lambda_{41}, \lambda_{52}, \lambda_{63}$: Transition rates from abnormal condition (II) to normal condition (I)

The illustrated model in Figure 65 is a very detailed model and could be used to give accurate results and indices, but it encounters a large number of transition rates and parameters that aren't normally available. Such data would need very detailed information and historical data regarding the system under study.

[10] uses the Markov model of Figure 66 to model the operation of a SFCL. States 1 and 3 indicate that the SFCL operates perfectly under normal and abnormal conditions, respectively, where abnormal conditions mean that a fault has occurred in the network. State 2 is determined as the operation of the SFCL that fails under normal conditions. The main source of this problem is the cooling devices. State 4 results from the fault of the superconductor or module when a fault occurs in the network. The value of λ_{13} is the success rate where the SFCL operates perfectly after detecting a fault. The value of λ_{14} is the failure rate where the SFCL fails to limit fault current in a network, and λ_{41} is the repair rate from State 4 to State 1. The value of λ_{31} is the repair rate of the network. After a fault in the network is cleared, the SFCL in State 3 can be restored to normal State 1. The transition rates of λ_{12} and λ_{21} are the failure rate caused by the SFCL itself and the repair rate of the SFCL itself without any fault in a network, respectively.

Although this model uses less parameters than the model of Figure 65, it still needs some data that are not easy to find/calculate in real system operations. There are also confusions regarding definitions of some of the rates; e.g. λ_{31} is the rate in which SFCL goes from state 3 to sate 1; i.e. from limiting state back to the normal state; in other words the recovery

rate of the superconductor. System repair can start during this transition or after, however λ_{31} is the SFCL recovery rate and not the system repair rate as shown in [10] .

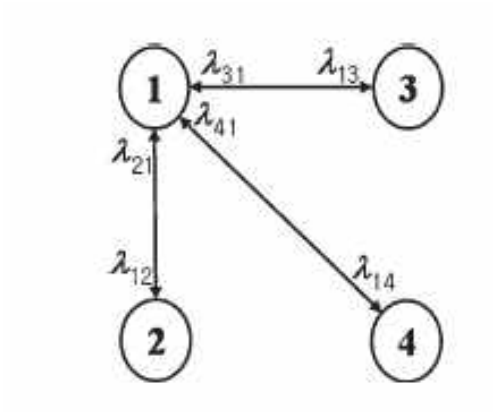

Figure 66. Four-state reliability model for SFCL.

Since FCL's and specially SFCL's are still in R&D phases and with limited practical applications and data available, usage of such detailed models will be less realistic and most likely delayed until more data becomes industrially available on operation and application of these devices in the future decades .

As stated earlier, second category of works have tried to address the reliability impact of SFCL by modeling the behavior of the device in the system without focusing on the model of the SFCL itself. Many studies have been carried out concerning different type of FCL's [4] ; their structural designs [5] , [6]; and their impact on static and dynamic behavior of faulted systems [7] and [8] . In [9], no particular substation configuration is assumed, and the FCL is located in a distribution network.

A big portion of this group of research works have used cut set techniques such as failure modes and effects analysis to address the reliability impacts of the FCL devices [36] , [89] , [22] and [15].

Failure modes and effects has a huge advantage in saving the calculation time by just inspecting a certain cut-sets/events of the system leading to the desired outcomes, instead of looking at all of the events/cases as in other methods such as Markov or event tree/fault tree [3]. Also, the input parameters to this method are mostly failure rates and switching/repair times that can be readily calculated or estimated with good degree of accuracy through practical data available from day to day operation or from devices such as event or fault recorders. However, using this technique in finding reliability of FCL devices, only gives us that part of reliability improvements caused by FCL in preventing the loads from being curtailed. While this is a good advantage and allows us to calculate improvements in indices such as "Expected Energy Not Supplied" (EENS), "Expected Load Not Supplied", (ELNS), Capacity Outage Probability Table [14] , etc., this doesn't give us the whole reliability improvement caused by using FCL's. Main reliability improvement comes from the main responsibility of FCL which is limiting the fault current, and that doesn't necessarily lead to prevention of load outage. This becomes evident by looking at the works that use failure modes and effects analysis to address reliability enhancements due to FCL's, and seeing that using FCL eliminates just a few number of cases leading to the load outage [15]. Therefore using failure modes and effects analysis would underestimate the reliability enhancement caused by using FCL. In order

to fully compute the effects of FCL in improving reliability, there should be a method to calculate the effects of fault current levels in the power system reliability. FCL's limit the fault current in the power system and reduce the stress on circuit breakers, protection system and all other elements of the system. In order to capture all these effects, there should be a model that addresses the direct effects of fault current levels on the system/component reliability levels.

There is a second group of these categories that tries to address the fault limiting behavior of FCL's in the reliability calculations. In [10] Monte Carlo simulation method has been used along with the Markov model of [86] to find the reduction in stress caused by using FCL's. [10] first uses Monte Carlo method to apply faults in various locations of the system and calculates the fault currents in various components and protection systems. Then calculates the failure probability of protection system in clearing the fault, based on an assumed failure density function for the protection system. [10] uses the following formula to calculate failure probability of the protection system in clearing the faults:

$$P(F_j) = \sum_i P(I_j^i).P(F_j|I_j^i) \tag{59}$$

Where $P(I_j^i)$ is the probability that i_{th} level of fault current passes through protection device j, and $P(F_j|I_j^i)$ is the conditional probability that the protection device j fails, given that that i_{th} level of fault current passes through it [10]. $P(F_j|I_j^i)$ is the conditional failure probability density function of the protection system and is very hard to find in practice,

and not easy to generalize given the huge variety of protection system types and their characteristics. This approach also has the disadvantage of using the Markov model of [86] and the associated problems mentioned earlier.

[90] uses a similar method to calculate stress on circuit breakers and appreciate the role of FCL in mitigating these stresses in power system. It uses the function given in Figure 67 as failure probability of circuit breaker in interrupting a fault current. Again, finding this probability density function is not easy in practice and needs lots of on-field/historical data resulting from tests or operations that aren't normally available.

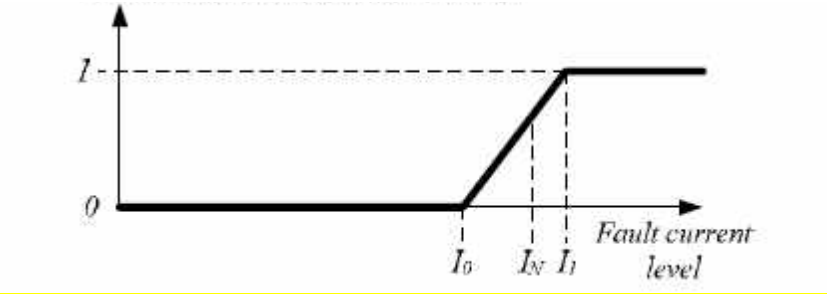

Figure 67. Failure probability of circuit breaker vs. fault current magnitude.

Another big disadvantage associated with all these methods is that Monte Carlo method (or any other simulation method) need extremely large amount of calculation time that usually increases exponentially as the size of the system under study increases.

In the next chapter, we develop an analytical model that considers the impact of fault current levels in the reliability evaluation of power systems, and therefore allows to take into consideration the benefits of FCL in reducing fault current levels and hence mitigating

the stress on power system components. This way larger benefit of FCL in enhancing the reliability will be revealed and calculated: not just its minor role of keeping the loads connected, but also its major role of reducing stress and fault-caused damages to the power system components and elements and the entire system in general.

This developed model will be available using normal operational/historical data relating to the usual power equipment, and unlike Monte Carlo or other simulation methods it does not employ huge amounts of computational time.

CHAPTER V
MODELING THE IMPACT OF OVERCURRENT ON RELIABILITY AND ASSET MANAGEMENT

In this chapter we develop a theory that will help analyze impacts of fault currents on reliability and asset management. As noted earlier there are few works done on impacts of over-currents on reliability. However, these studies have not gone beyond the conceptual phase and no studies have developed the topic to analyze the direct impact of fault currents on system reliability. The main focus of the current reliability calculations are solely based on statistical values and not electrical parameters. In this context, reliability of an electrical power system is evaluated in the same exact way as the reliability of an urban logistics system. Reliability indices calculated in such a framework will only reflect the general ability of the system to deliver its defined tasks, and will not allow to model the direct impact of electrical variables on the system reliability indices. Author sincerely believes the work that is reported in this dissertation would be the first that brings the "relationship between electrical variables such as current and the reliability indices to a new level.

Modeling the Effects of Overcurrent on Component Failure Rates

A huge short circuit current can cause a component to fail by exceeding its strength value in a short period of time. A long duration overload condition can also cause the component to fail by eventually exceeding the strength of the component as shown later in Figure 71. Although short circuits and overloads are two distinct physical phenomena, having different causes and effects, their deteriorating effects can both be described using the model proposed later in this chapter. As such, henceforth in this document both events are

referred to as abnormal or overcurrent. However, when a short circuit is mentioned, a higher current in a shorter period of time is meant as opposed to an overload that would be a lower current over a longer period of time.

Overconsumption of electricity by users, especially during peak hours can be another reason for having larger than intended currents through conductors that would shorten the useful lives of electrical components, by having continuous exposure to higher than designed electrical and mechanical stresses. In order to avoid these consequences, utilities advise demand response programs for their customers that will incentivize customers for reducing their consumption in certain times or through certain patterns. Chapter seven of this document will study the impact of these demand response programs on asset management, useful lifetime and maintenance planning of electrical components.

In a power system, over-currents occur at intermittent intervals and the likelihood that an exposed component fails increases during the exposure time. In order to model the effect of these occurrences, a model similar to the one used for adverse weather conditions can be used [14].

Data on overcurrent (short circuits or overloads) collected from event recorders over a period of time would produce a chronological variation as shown in Figure 68.

If the failure rate of an arbitrary component during normal conditions is λ, then during abnormal conditions, its failure rate changes to λ' which is clearly greater than λ. The average failure rate of this component, $\hat{\lambda}$, can then be derived as follows:

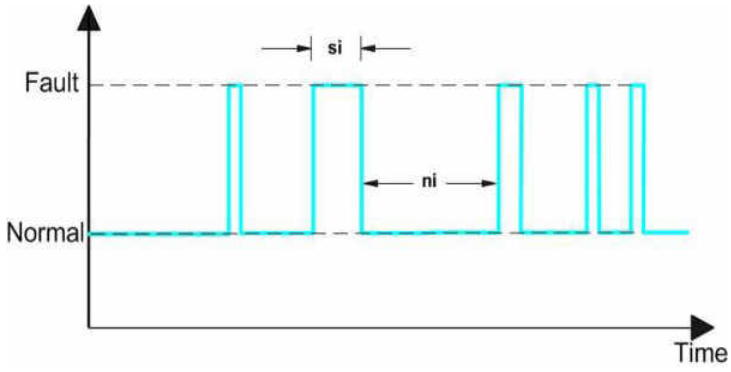

Figure 68. Chronological diagram of normal and faulty conditions.

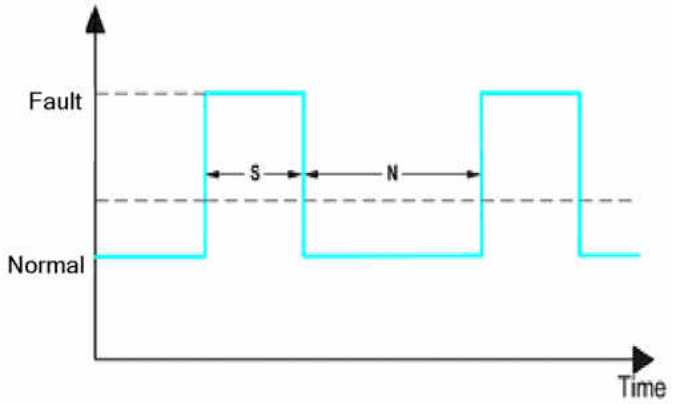

Figure 69. Average profile for normal-faulty conditions

$$\hat{\lambda} = \frac{N}{S+N}\lambda + \frac{S}{S+N}\lambda' \tag{60}$$

Where $N = \sum_i n_i / T$ is the expected duration of normal conditions and $S = \sum_i s_i / T$ is the expected duration of abnormal conditions. n_i and s_i are as shown in Figure 68. In this way, the average profile could be as shown in Figure 69.

Derivation of the model

It is clear that as the current through a component increases during the abnormal time intervals S, the failure rate of the component, λ, would also increase, λ', and the component will be more likely to fail. In order to model the behavior of a component under abnormal conditions, it is helpful to study the strength pattern of the component. Suppose J is the maximum tolerable current that can pass through the component. This J represents the strength of the component against over-currents and is therefore designated as the "strength current". If I is the actual flowing overcurrent, the component endures as long as $J \geq I$. The strength current J depends on various factors and it changes over time due to aging. Therefore, it is reasonable to consider J as a random variable and that its average value and variance change over time to account for component deterioration.

There are a number of statistical distribution functions that can be used to model the behavior of J [91]. In this document, a Rayleigh distribution is used to model the strength current J (maximum tolerable current) of the component as shown in Figure 70. This current could be broken into its active and reactive elements, each following a normal distribution as considered in standard stress and strength literature [91]. As a result, the absolute value of J, i.e., the magnitude of the current strength, would follow a Rayleigh distribution [91], [3] and [92]. This distribution function has been used in many relevant documented studies in the literature and has the advantage of not sliding over into the negative side of the strength region [91] and [3].

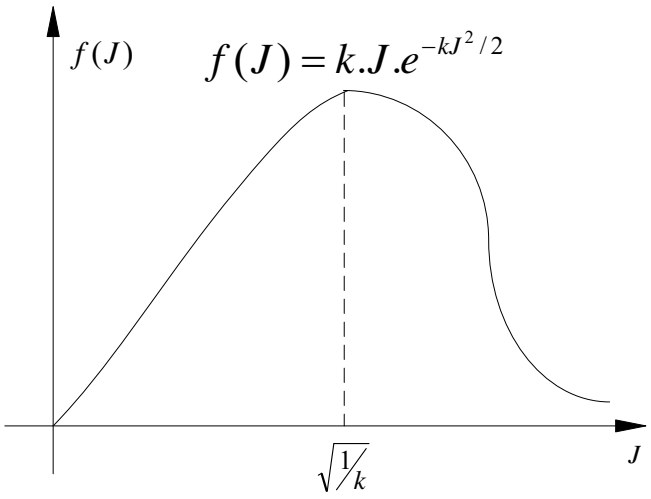

Figure 70. Rayleigh model of strength current.

Let us assume that an overcurrent with a given magnitude of I occurs at $t_0 = 0$ and it lasts for a duration of t. Component reliability at time t is the probability that the component endures at time t:

$$R(t) = p(J > I)(t) = \int_I^\infty f(J,t)dJ = \int_I^\infty k(t).J.\exp\{-\frac{k(t).J^2}{2}\}dJ = \exp\{-\frac{k(t).I^2}{2}\} \quad (61)$$

In (61) k is the inverse of variance of the strength current and is assumed to be an increasing function of time in order to model the deterioration of strength with time. Specifically, k is allowed to vary exponentially with time as in (62) and shown in Figure 71.

$$k(t) = k_1.e^{k_2 t} \quad (62)$$

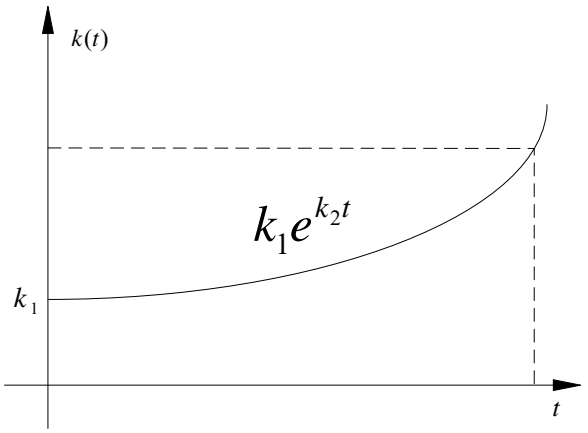

Figure 71. Growth of *k* with time

Substituting (62) in (61) yields:

$$R(t) = \exp(-\frac{k_1 e^{k_2 t} I^2}{2}).u(t) \qquad (63)$$

where $u(t)$ in (63) is the unit step function and is used simply because there are no faults when $t < 0$.

In a more general case, consider a component with a constant failure rate λ is exposed to an abnormal current at $t = t_0$ and the event lasts for at least t. $R(t)$ in (63) then implies two probabilities: the probability that the component is healthy for $t < t_0$, and the probability that it remains healthy during the abnormal condition. The first probability is

$e^{-\lambda.t}$ and the second one is the time-shift of (63) by t_0. These two probabilities are independent and hence:

$$R(t) = e^{-\lambda t}.\exp\{(-\frac{k_1 e^{k_2(t-t_0)} I^2}{2}).u(t-t_0)\} \tag{64}$$

Or:

$$R(t) = \exp\{-\lambda t - (\frac{k_1 e^{k_2(t-t_0)} I^2}{2}).u(t-t_0)\} \tag{65}$$

Since $R(t) = e^{-\int_0^t \lambda(\tau)d\tau}$, we can rewrite (65) as:

$$R(t) = \exp(-\int_0^t d/d\tau \{\lambda\tau + (\frac{k_1 e^{k_2(\tau-t_0)} I^2}{2}).u(\tau-t_0)\}d\tau \tag{66}$$

Therefore, in terms of failure rate $\lambda(t)$:

$$\lambda\ (t) = \lambda + (\frac{k_1 e^{k_2(t-t_0)} I^2}{2}).\delta(t-t_0) + (\frac{k_1 k_2 e^{k_2(t-t_0)} I^2}{2}).u(t-t_0) \tag{67}$$

Where $\delta(t-t_0)$ is an impulse function starting at t_0.

Since in general $f(t).\delta(t-t_0) = f(t_0).\delta(t-t_0)$, (67) can then be rewritten as:

$$\lambda\ (t) = \lambda + (\frac{k_1 I^2}{2}).\delta(t - t_0) + (\frac{k_1 k_2 e^{k_2 (t - t_0)} I^2}{2}).u(t - t_0) \qquad (68)$$

In (68) the time varying part of failure rate which is caused by the abnormal current is λ' as denoted in Figure 68 and Equation (60).

Equation (68) shows that the effect of abnormal current I is twofold: a rapid impact in the form of the impulse function at the beginning of the fault; and an exponentially increasing impact as to the third term of (9). The impulse function simulates the component failure at the very beginning of the abnormal current and could be neglected if we discard the initial failures.

Figure 72 shows a conceptual pictorial representation of (68). As seen in this figure, this behavior is similar to the simple model of Figure 68 or Figure 69.

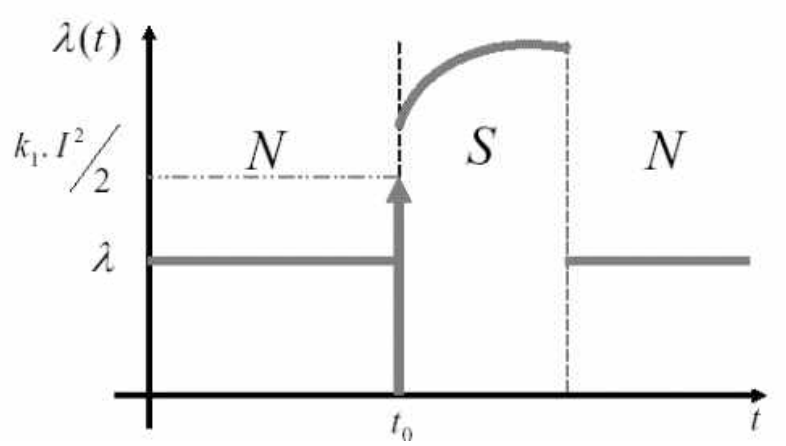

Figure 72. Plot of $\lambda(t)$ versus time for an abnormal current situation starting at t_0

Equation (68) shows that failure rate during the abnormal current condition S is proportional to the square of the abnormal current I . Therefore in Equation (60), although S is generally of a very short duration compared to N , severe fault currents would highly increase the failure rate during fault conditions. This indicates that the contribution of the second term in Equation (60) can be considerable.

Markov Model Considering Overcurrent States

Here we develop a Markov Model to find various reliability indices of the component considering over-currents in the system.

Figure 73 shows a proposed Markov model for calculating preventive maintenance cycles. In this figure F is the component failure state and f is the state where there is an overcurrent condition in the system. States D_0 through D_F are the component normal state and the various deterioration levels, respectively. D_F is when the component stops functioning as a result of continues deterioration, and it should be brought to maintenance. PM, the minimal preventive maintenance state, is assumed to bring the component back to the previous deteriorated condition.

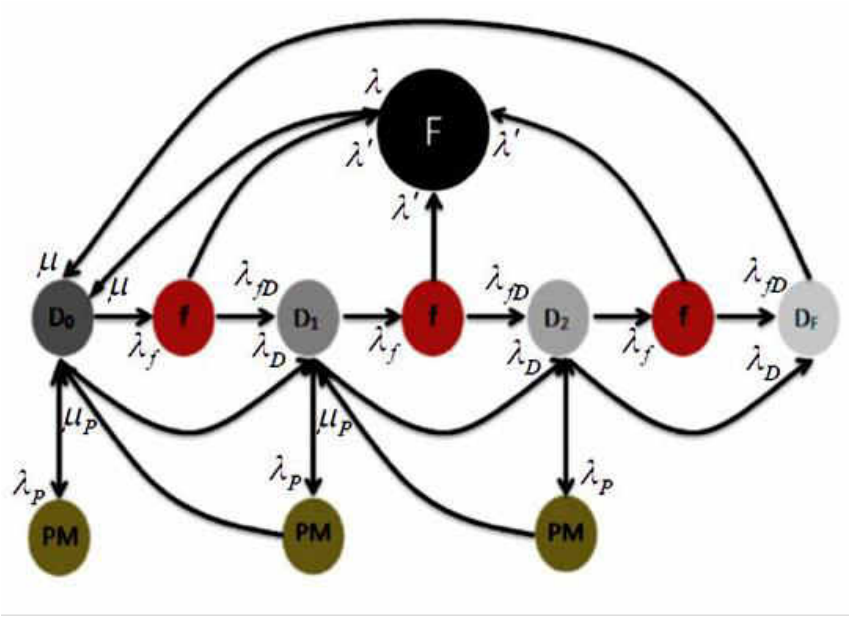

Figure 73. Markov Model for preventive maintenance considering system faults.

At state f, the component is exposed to an extra stress resulting from the overcurrent condition that has occurred in the system and the failure rate of the component in this period is λ'. Once in state f, the component can either fail and enter the failure state F, or its health condition further deteriorates and goes down one more level into the next deteriorating state (Figure 73). These events are shown with transition rates λ' and λ_{fD}, respectively. According to [3], transition rates λ' and λ_{fD} can be defined as follows:

$$\lambda' = \frac{Number\ of\ transitions\ to\ F\ from\ f}{Time\ spent\ in\ f}$$

And

$$\lambda_{fd} = \frac{Number\ of\ transitions\ to\ Deterioration\ state\ from\ f}{Time\ spent\ in\ f}$$

Therefore, the probability that the component fails (as opposed to being deteriorated) as the result of a system overcurrent is:

$$P_{fail} = \frac{\lambda'}{\lambda' + \lambda_{fD}} \qquad (69)$$

The value of probability P_{fail} can be obtained from the operation history of the component as:

$$\mathrm{P}_{fail} = \frac{\text{Number of component failures as a result of system overcurrent}}{\text{Number of overcurrents in the sytem under study}}$$

P_{fail} can then be plugged into (69) to get the value of λ_{fD}.

The following points should be noted in calculating λ' for the Markov model:

1- Instantaneous failure of components as a result of abnormal currents are disregarded in this analysis. This is mainly because we are interested in the non-instantaneous impacts of abnormal currents that develop with time. Instantaneous failures are the results of an imperfect design, or are due to an improper testing procedure, etc. Thus, the impulse term in (68) is omitted here.

2- The time dependent portion of Equation (68), λ', is considered in two ways: using an approximate model and an average model.

In the approximate model, the value of λ' during an abnormal current is assumed to be constant. This constant value is obtained from (68) by setting $t = t_0$ in the third term as follows:

$$\lambda' = \frac{k_1 k_2}{2} I^2 \tag{70}$$

In the average model, however, the average value of λ' during a fault is calculated by integrating the third term in (68) over the abnormal current interval:

$$\lambda'_{ave} = \frac{1}{\epsilon} \int_{t_i}^{t_i+\epsilon} \frac{k_1 k_2}{2} e^{k_2 (t-t_i)} . I^2 dt = k_1 \frac{e^{k_2 \epsilon} - 1}{2\epsilon} . I^2 \tag{71}$$

where

t_i is the instant when abnormal current occurs

ϵ is the duration of the abnormal current

k_1 , k_2 are the strength current constants

The average value of the failure rate given in (71), is believed to be a reasonable choice because the relation $R(t) = e^{-\int \lambda(t) dt}$ shows that two systems with the same value of $\int \lambda(t) dt$ will have the same reliability values.

The difference between the approximate and the average models (i.e., λ_i' and $\lambda_{ave,i}'$) increases with length of interval ϵ_i of the abnormal current as shown later in the current document.

The average outage duration r for the Markov model shown in Figure 73 is calculated using (72). In (72), the numerator is the cumulative probability of failure and the denominator is the cumulative frequency of failure [3] :

$$r = \frac{\sum_{i=1}^{3} PM_i + P_F + P_{DF}}{\sum_{i=1}^{3} PM_i.\mu_P + (P_F + P_{DF}).\mu} \qquad (72)$$

In this equation, variables used are as below:

PM_i: Probability of residing in the i_{th} preventive maintenance state

P_F: Probability of the component failure state

P_{DF}: Probability of state D_F

μ_P: Repair rate from preventive maintenance states

μ: Repair rate from state D_F

Study Results Using the Markov Model

In what follows, various simulation case studies are conducted using the proposed Markov model to examine the variation of component outage duration r with respect to various

abnormal current parameters. First, the overload impacts are studied followed by that of short circuits.

As an example, assume that the average failure rate of a component is $\lambda = 0.01$ f/yr and its repair lasts for 12.5 hours. Furthermore, assume that accelerated lifetime tests have shown that $k_1 = 0.4$ in the strength current model of the component. The value of k_2 and other parameters are specified for each of the simulation case studies as discussed below.

Variation of outage time with overloads.

In this and the next simulation study, state f of the Markov model is considered to be an overload condition. In addition to the above parameter values, other parameter values used in this study are:

$k_2 = 0.08$

$\lambda_f = 1$ (occ/yr) ,

$\mu = 200$ (occ/yr)

Varying the overload duration from 100 msec to 20 days, the average outage duration r is calculated and the results are shown in Figure 74. In this study, the approximate value of failure rate λ' during the overload condition is calculated using Equation (70). The study is repeated for three different values of the overload current *I*; i.e., 1.5, 1.7, and 2 p.u. It can be seen from the results in Figure 74 that the average outage duration r increases as

the duration of overload increases. The curve starts from an outage duration of 12.514 hours when no overload occurs. It can be seen from the results that both magnitude and duration of the overload current have considerable effects on the component outage time.

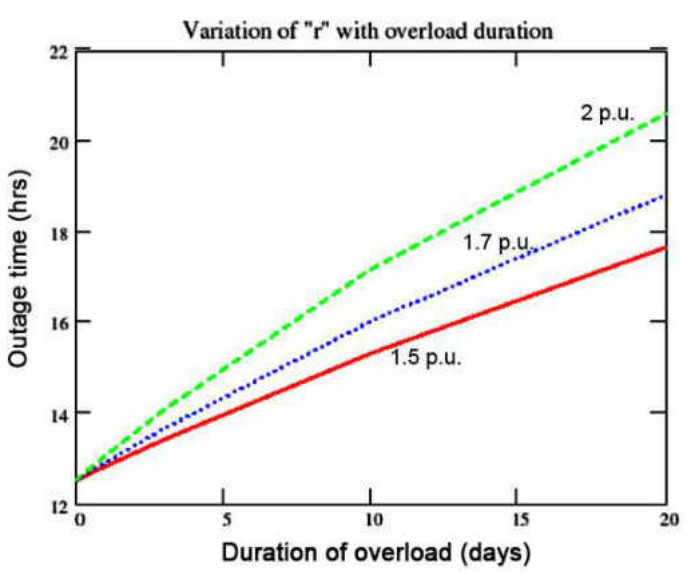

Figure 74. Variation of outage duration with duration of the overload current values of Case1: 1.5 p.u., Case2: 1.7 p.u., and Case3: 2 p.u..

Variation of outage time with strength deterioration.

As shown in Figure 71, k_2 is a parameter of the strength current model that defines the time constant of the component strength deterioration. A large value of k_2 indicates that the component strength deteriorates rapidly and the component is more likely to fail due to over-currents. Simulation studies were conducted with both average and approximate models of λ' given by (70) and (71). The results are presented in Figure 75 for different

values of k_2. In these studies, the overload current is set at 1.5 p.u. Other parameters have similar values as those in the previous study.

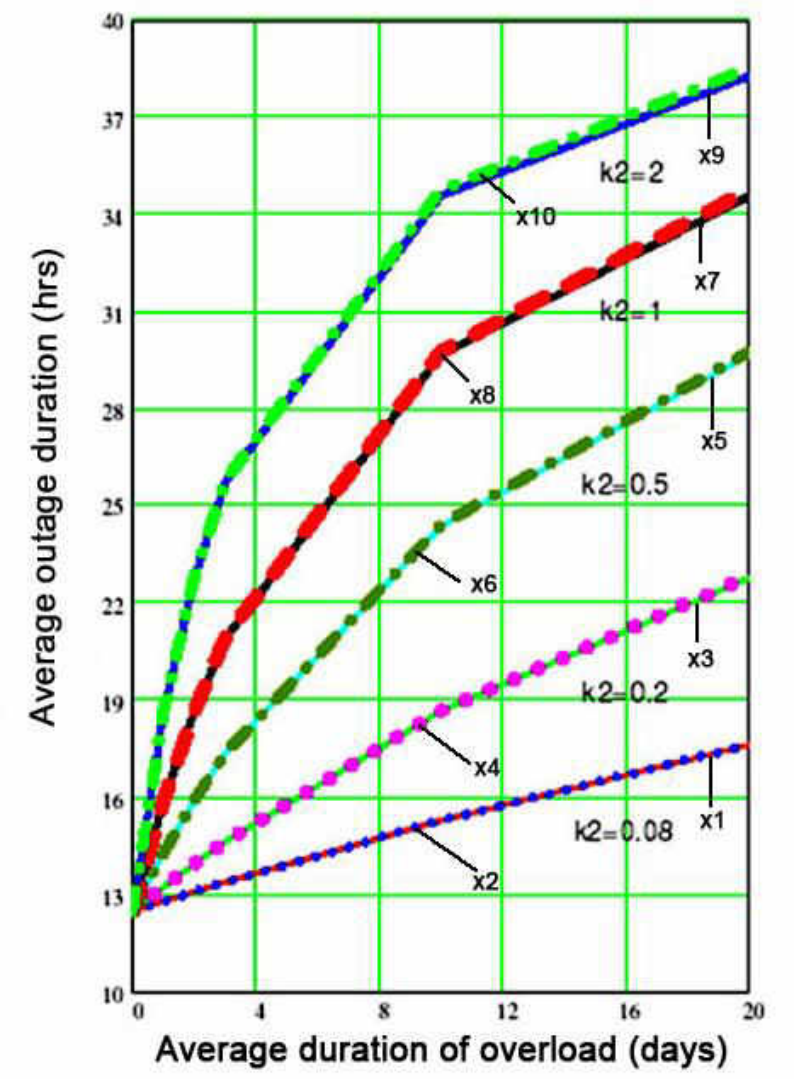

Figure 75. Variation of outage duration versus duration of the overload current for the approximate model (x1, x3, x5, x7, x9) and the average model (x2, x4, x6, x8, x10).

It can be seen from Figure 75 that for a given value of k_2, the difference between the two models increases with the overload duration. This is clearly shown in Figure 76 where the plots of differences of the two models versus the overload duration are shown.

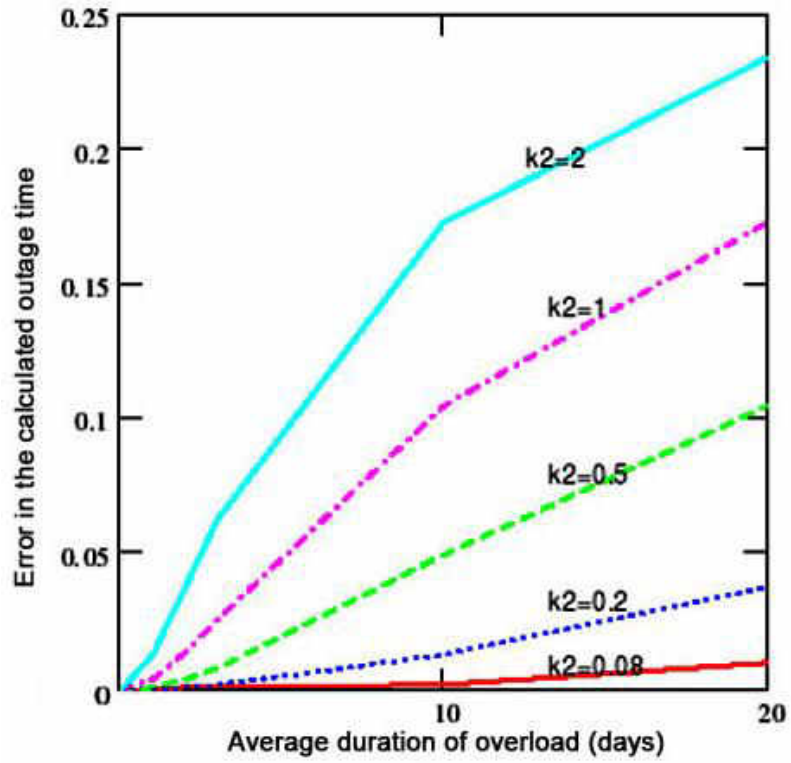

Figure 76. : Differences between two models of Figure 75 versus the overload duration.

These results make sense because when the overload duration is long, the increase in λ' over time would be considerable (Figure 72). This means that it is not justified to consider λ' as a constant during the whole duration of the overload condition. It is also seen that the difference between the two models increases when k_2 increases. This is because larger values of k_2 indicate that the system is strongly time dependent and hence assuming a

constant value for λ' is actually inaccurate. Furthermore, it could easily be shown that if k_2 or ϵ (duration of the overload) in (71) is sufficiently small, then using a Taylor series expansion and neglecting the higher order terms would yield:

$$k_1 \frac{e^{k_2\epsilon}-1}{2\epsilon}.I^2 \approx k_1 \left\{ \frac{\left(1+k_2\epsilon+\frac{k_2^2\epsilon^2}{2!}+\cdots\right)-1}{2\epsilon}.I^2 \right\} \approx \frac{k_1 k_2}{2}.I^2 \qquad (73)$$

This shows that the approximate and the average models of λ' are almost identical.

The differences, however, are negligible in practice and therefore the approximate model serves well, particularly in case of over-currents that have short durations. If a high accuracy is required, on the other hand, an accurate time model should be used for long overload durations.

Variation of outage duration with short circuit rate.

In this study and the next one, state f of the Markov model is now considered to be the short circuit state instead of the overload state as in the above studies and that it lasts for 100 msec. Other parameters used in this study are as follows:

$k_2 = 2$

$I_f = 2$ p.u.

$\mu = 200$ (occ/yr)

The rate of the short circuit state f, λ_f, is varied from 1 to 7 "occ/yr" and the impact on outage duration r is studied. The results are shown in Figure 77. For this study, the approximate model of λ' in (70) is used for simplicity. It can be seen from Figure 77 that rate of the short circuit has little effect on the outage duration.

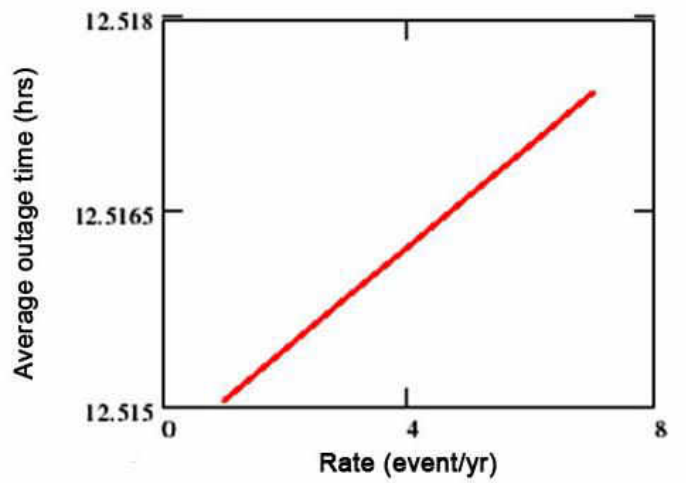

Figure 77. Variation of outage time versus short circuit rate.

Figure 78 shows the component outage time versus the component maintenance rate for various short circuit levels. It can be seen from Figure 78 that if repair is performed more frequently, then the outage time will be reduced. This reduction is mainly affected by the

maintenance frequency and the short circuit level doesn't play a significant role at the beginning. But as the short circuit level increases higher than a critical value, the maintenance program should be updated to adjust for the short circuit effects. For high short circuit levels, a scheduled maintenance would result in lower-than-expected outage reductions and thus the schedule must be updated accordingly.

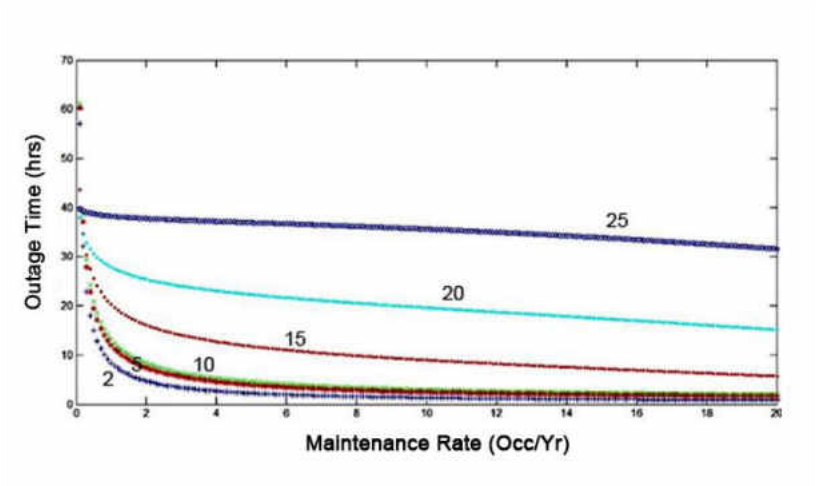

Figure 78. Variation of outage time with maintenance rate for short circuit levels of 2,5,10,15,20,25 (from bottom to top).

Preventive maintenance scheduling

Existing methods of maintenance scheduling can be classified into several categories. First group includes those based on heuristic methods, which provide the most primitive solution

using trial-and-error principles [93] [94] [95]. Second category is based on artificial intelligence (AI) methods [96] [97] [98] which include expert systems, simulated annealing, fuzzy theory, genetic algorithms, and various other combinations of AI methods. AI techniques have the capability of dealing with multi-objective requirements. However, the expert systems approach is difficult to generalize since an inference engine must be designed according to the particular characteristics of a designated problem. None of these methods can be generalized to give an applicable general practice, due to large number of parameters and variables required, and the fact that large portion of the techniques are configured according to the specific requirements of the specific designated power system [99]. Another major problem with all of these techniques is that they deal with maintenance of electrical components as a general engineering challenge and none of them treat it in the context of electrical parameters such as overcurrent levels. Although there is a general agreement that mathematical models provide more reliable and versatile solutions to maintenance scheduling, to the best of authors' knowledge there is no analytical methods that address the impact of overcurrent on reliability functions and therefore on maintenance scheduling [100].

Equation (68) gives an expression for the failure rate and Figure 72 shows the failure rate versus time, which is repeated here again in Figure 79 for easy reference.

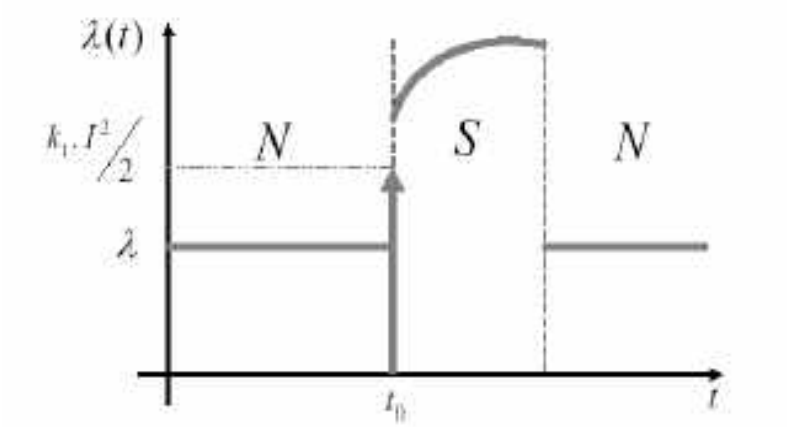

Figure 79. Plot of $\lambda(t)$ versus time for an abnormal current situation starting at t_0

The average failure rate can be calculated by integrating this curve over a time period as follows (ϵ is duration of overcurrent, t_0 is when the fault occurs, and assume T=1 year for simplicity):

$$\lambda_{ave} = \frac{1}{\mathrm{T}}\int_0^{\mathrm{T}}[\lambda + \left(\frac{k_1 I^2}{2}\right).\delta(t-t_0) + \frac{k_1 k_2 e^{k_2(t-t_0)I^2}}{2}u(t-t_0)]\,dt \tag{74}$$

Since the second term exists only around t_0 and the third term exists within the fault period; i.e. $t_0 < t < t_0 + \epsilon$ (Consider $\mathrm{T} = 1$)

$$\lambda_{ave} = \lambda + \frac{1}{\mathrm{T}}\left(\frac{k_1 I^2}{2}\right)\int_{t_{0-}}^{t_{0+}}\delta\,(t-t_0)dt + \frac{1}{\mathrm{T}}\int_{t_0}^{t_0+\epsilon}\frac{k_1 k_2 e^{k_2(t-t_0)I^2}}{2}dt = \lambda + \left(\frac{k_1 I^2}{2}\right) +$$

$$\left[\frac{k_1 e^{k_2(t-t_0)I^2}}{2}\right]_{t_0}^{t_0+\epsilon} = \lambda + \left(\frac{k_1 e^{k_2 \epsilon I^2}}{2}\right) \tag{75}$$

Therefore:

$$\lambda_{ave} = \lambda + \left(\frac{k_1 e^{k_2 \epsilon I^2}}{2}\right) \tag{76}$$

(76) shows that impact of a single overcurrent is an increase in the average value of the failure rate by $\left(\frac{k_1 e^{k_2 \epsilon I^2}}{2}\right)$.

For several overcurrent faults with values of I_1, I_2, …, I_n occurring at times t_{01}, t_{02}, …t_{0n} with durations of ϵ_1, ϵ_2, …., ϵ_n, respectively, the average failure rate will be:

$$\lambda_{ave} = \begin{cases} \lambda\,, & t < t_{01} \\ \lambda + \left(\frac{k_1 e^{k_2 \epsilon I^2}}{2}\right)\,, & t_{01} < t < t_{02} \\ \lambda + \left(\frac{k_1 e^{k_2 \epsilon_1 I^2}}{2}\right) + \left(\frac{k_1 e^{k_2 \epsilon_2 I^2}}{2}\right), & t_{02} < t < t_{03} \\ \cdots & \\ \lambda + \sum_{i=1}^{n} \frac{k_1 e^{k_2 \epsilon_n I^2}}{2}, & t_{0n} < t \end{cases} \tag{77}$$

Figure 80 shows the average failure rate in the presence of several overcurrent events occurring in the system based on (77).

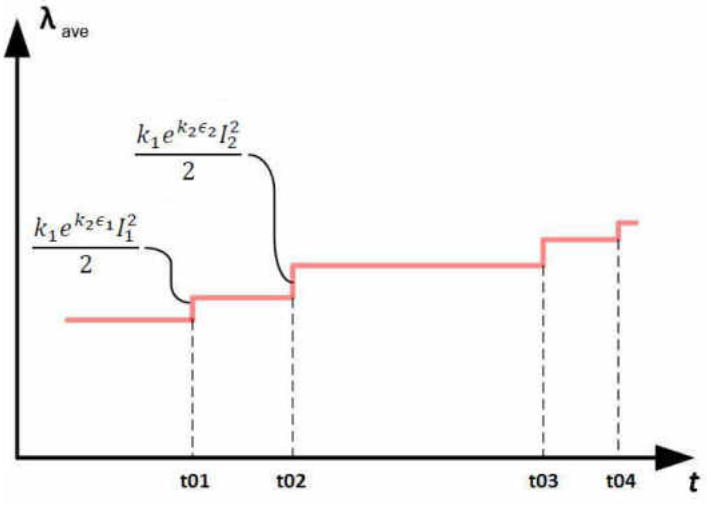

Figure 80. Average failure rate versus overcurrent events.

With the average failure rate as shown in Figure 80, we can calculate the reliability function for different time sections of the curve as follows.

For $t_0 < t < t_0 + \epsilon$ (during fault), using $R(t) = e^{-\int_0^t \lambda(t)dt}$ and Equation (68) for $\lambda(t)$, we can write:

$$R(t) = e^{-\int_0^t \lambda(t)dt} = Exp\{-\int_0^t \left[\lambda + \left(\frac{k_1 I^2}{2}\right).\delta(t-t_0) + \frac{k_1 k_2 e^{k_2(t-t_0)} I^2}{2} u(t-t_0)\right] dt\} \quad (78)$$

Since the second term exists only around t_0 and the third term exists between t_0 and t:

$$R(t) = Exp(-\lambda t - \left(\frac{k_1 I^2}{2}\right) \int_{t_{0-}}^{t_{0+}} \delta\,(t-t_0) - \int_{t_0}^{t} \frac{k_1 k_2 e^{k_2(t-t_0)} I^2}{2} = Exp\left[-\lambda t - \left(\frac{k_1 I^2}{2}\right) - \int_{t_0}^{t}\left[\frac{k_1 e^{k_2(t-t_0)} I^2}{2}\right]\right] =$$

$$Exp\left[-\lambda t - \frac{k_1 e^{k_2(t-t_0)}}{2} I^2 u(t-t_0)\right]$$

(79)

Which is the same as Equation (65).

For the period after fault; i.e. $t_0 + \epsilon < t$ using $R(t) = e^{-\int_0^t \lambda(t)dt}$ and Equation (68) for $\lambda(t)$, we have:

$$R(t) = e^{-\int_0^t \lambda(t)dt} = Exp\{-\int_0^t \left[\lambda + \left(\frac{k_1 I^2}{2}\right).\delta(t-t_0) + \frac{k_1 k_2 e^{k_2(t-t_0)} I^2}{2} u(t-t_0)\right] dt\} \quad (79)$$

Since the second term exists only around t_0 and the third term exists between t_0 and $t_0 + \epsilon$ (as seen in Figure 79)

$$R(t) = Exp\left\{-\lambda t - \left(\frac{k_1 I^2}{2}\right)\int_{t_{0-}}^{t_{0+}} \delta\,(t - t_0) - \int_{t_0}^{t_0+\epsilon} \frac{k_1 k_2 e^{k_2(t-t_0)} I^2}{2}\right\} =$$

$$= Exp\left\{-\lambda t - \left(\frac{k_1 I^2}{2}\right) - \int_{t_0}^{t_0+\epsilon}\left[\frac{k_1 e^{k_2(t-t_0)} I^2}{2}\right]\right\} = Exp\{-\lambda t - \frac{k_1 e^{k_2 \epsilon}}{2} I^2\} \quad (80)$$

In summary, reliability function can be illustrated as below:

$$R(t) = \begin{cases} e^{-\lambda t} & t < t_0 \\ e^{-\lambda t - \frac{k_1 e^{k_2(t-t_0)}}{2} I^2 u(t-t_0)} & t_0 < t < t_0 + \epsilon \\ e^{-\lambda t - \frac{k_1 e^{k_2 \epsilon}}{2} I^2} & t_0 + \epsilon < t \end{cases} \quad (81)$$

Figure 81 shows the reliability $R(t)$ of a component with two overcurrent events at t=1 and t=2 based on equation (81). Both Figures 80 and 81 illustrate how failure rate and system reliability are influenced by occurrences of faults and can be used to develop schedules for preventive maintenance.

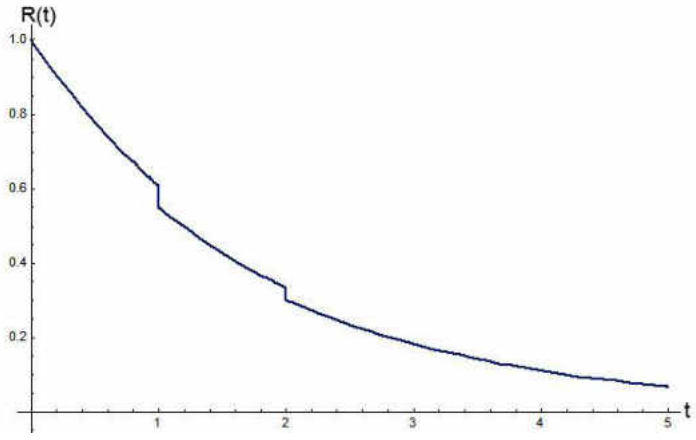

Figure 81. Reliability in the presence of two overcurrent events.

Figure 82 assumes that preventive maintenance is done at interval T on the component shown in Figure 80. As seen from Figure 82, preventive maintenance is assumed to bring the component back to the as-good-as new state. Maintenance interval T can be determined based on the maximum allowable value of the failure rate or the desired targeted value of reliability [101]. Knowing the average values and the number of overcurrent events in a system throughout the year, one can point out the approximate curve for λ_{ave} using (77) and then preventive maintenance can be scheduled based on the targeted value of reliability or failure rate to bring the components back to their as-good-as new states in intervals T [102] and [103].

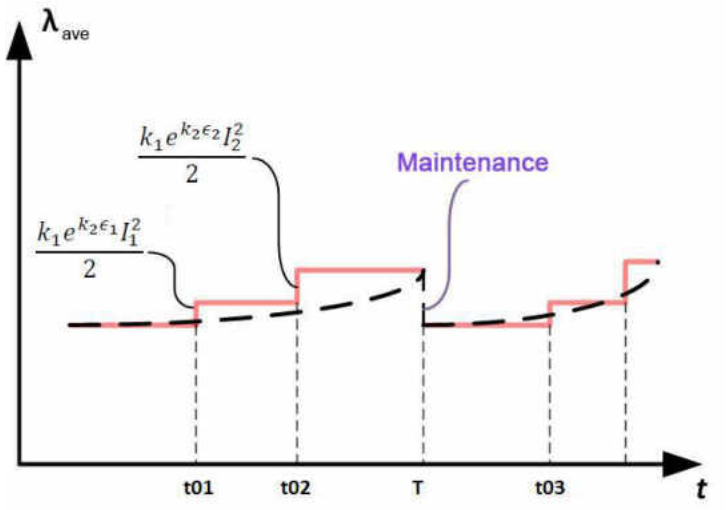

Figure 82. Impact of short circuits/overloads on failure rate and preventive maintenance scheduling.

CHAPTER VI: IMPACT OF PROTECTION SYSTEMS AND FAULT CURRENT LIMITERS ON ASSET MANAGEMENT

In this chapter, we study the impact of protection devices and fault current limiters (FCL's) on asset management in a substation in the North American electric network that has installed a superconducting fault current limiter (SFCL). The SFCL installed in this substation is a matrix fault current limiter (MFCL) type, described in Chapter 2. This application was studied in detail in Chapter 4 where impacts of installed MFCL in preventing load point outages were calculated and analyzed. As noted earlier, positive impacts of FCL devices is not limited to outage prevention. In this chapter we use our developed model to address the more important role of FCL's in limiting the fault current, and quantifying their impact on valuable assets in electric networks. For the sake of comparison, we study the impact of the installed MFCL on asset management in the presence of several different protection schemes, and compare it with the case without MFCL and other types of superconducting/non-superconducting FCL's.

Figure 83 shows a on-line diagram of a real substation in the US with SFCL installed. As noted in Chapter 4, the installation of SFCL is intended to minimize the contribution of transformer T_3 to the fault current. This was due to the fact that the extra fault duty from transformer T_3 would put some of the breakers in a situation of not being able to break the current safely. Installment of the MFCL in series with transformer T_3, as shown numerically prevents a portion of load point outages, and reduces the potential of unstable system operations. Fault current limitation, on the other hand, will reduce the stress on the

power system elements in fault instances, therefore preventing their exposure to future faults which would manifest themselves in their failure rates being inhibited from increasing. We will here deal with this aspect of the FCL, and quantify the impact of this device on failure rates of the substation elements.

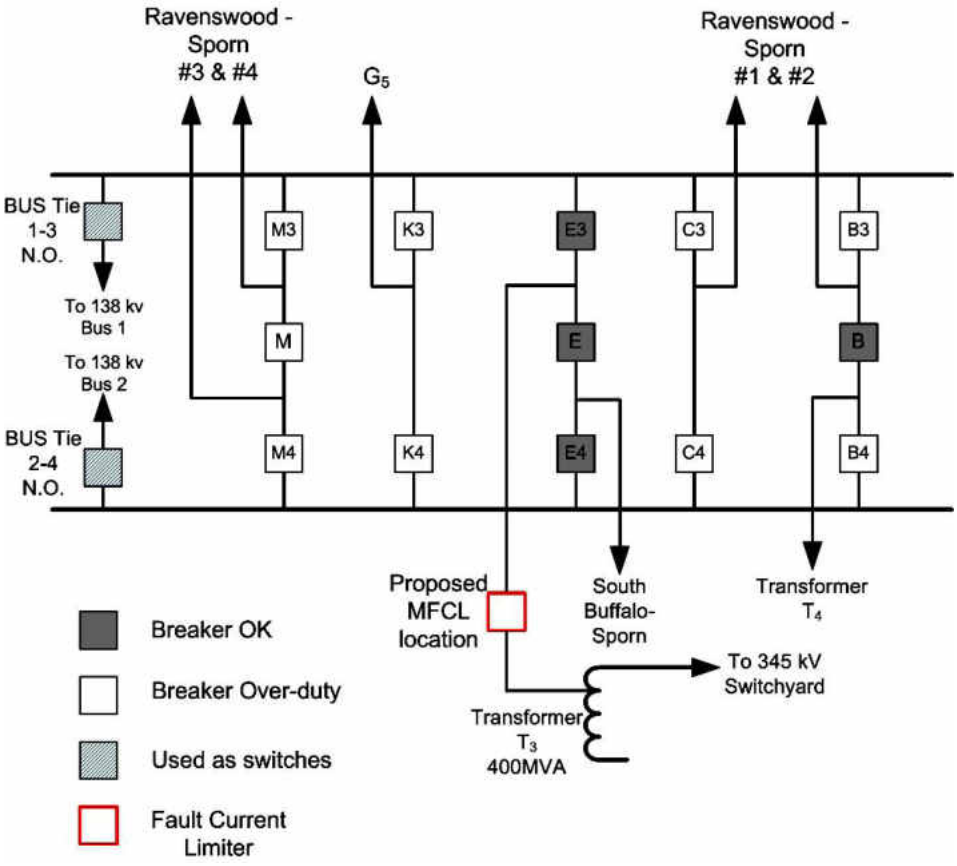

Figure 83. Electric Substation in the USA with SFCL installed [24].

Calculating the Impact of Protection Devices and FCL on Failure Rates

In order to perform the calculations, two possibilities have been considered for the fault in the substation:

F1 : short circuit in the secondary side of the transformer T_3. This could be anywhere in the bus bar, circuit breakers, or outgoing lines. The main current passing through transformer T_3 in this case is the transformer short circuit current which is determined from the transformer per-unit linkage impedance [104].

F2: This shows a fault in the primary circuit of transformer T_3. In case of a short circuit in primary side of transformerT_3 , the transformer does not have a major contribution to the fault. The major contributions to the fault current come from other sources such as transformer T_4 , other substations, and the generating unit G_5 . Calculating the short circuit current for this type of faults, is harder than previous case due to lack of exact data about specifications of transformer T_4 and unit G_5. However, the probability of this type of fault is much smaller than the first type since substations are normally considered as protected areas and are much less likely to be faulty compared to case F1 that can present any fault on any of the transmission lines. To calculate the fault current in this case, typical per unit values were assumed for transformer T_4 and unit G_5. Considering that similar machines usually have parameters with same typical per-unit values, this assumption will generate reasonably accurate results especially given the low probability of these types of faults [104].

In general, if a fault occurs at locations A_i in the system, and the fault current that passes through device j in this case is I_i^j, the average increase in failure rate of device j is as below:

$$\Delta\lambda_i^j = k_1 e^{k_2 \in_i} \frac{(I_i^j)^2}{2} \tag{82}$$

$\in_i$ is the duration of the fault current I_i^j, and can be calculated from the fault clearance time of the protection system. k_1 and k_2 are strength parameters of the component j in the power system.

If the rate of fault in zone A_i can be shown with λ_{A_i}, the average increase in failure rate of the component j over time interval T, $\Delta\lambda_T^j$ can be calculated as follows:

$$\Delta\lambda_T^j = \sum_i \lambda_{A_i}.T.\Delta\lambda_i^j = \sum_i \lambda_{A_i}.T.k_1 e^{k_2 \in_i} \frac{(I_i^j)^2}{2} \tag{83}$$

There are various elements and causes resulting in a fault in a given zone; for example for the fault F1 in above the reasons could be faults in any of the circuit breakers, faults in any of the lines, a fault in the secondary winding of transformer T_3 etc. If we assume these faults are independent of each other, the failure rate λ_{A_i} can be expressed as follows:

$$\lambda_{A_i} = \sum_k \lambda_{A_{i,k}} \tag{84}$$

Where $\lambda_{A_{i,k}}$ is the rate of the kth event that causes a fault in zone A_i. Substituting (84) into (83) yields:

$$\Delta\lambda_T^j = T \sum_i \sum_k \lambda_{A_{i,k}} k_1 e^{k_2 \in_i} \frac{(I_i^j)^2}{2} \quad (85)$$

With the FCL installed in the system, fault current form the fault in zone A_i will change to $I_{i,FCL}^j$. Therefore the average increase in the failure rate of component j in the presence of FCL (over time interval T) will be:

$$\Delta\lambda_{T,FCL}^j = T \sum_i \sum_k \lambda_{A_{i,k}} k_1 e^{k_2 \in_i} \frac{(I_{i,FCL}^j)^2}{2} \quad (86)$$

In order to calculate $\in_i$ or the fault duration in zone A_i , we need to use results from security analysis of protection systems in the previous chapters. It is assumed that a protection system will be in one of the following modes at any given time [69]:

S	Protection succeeds to clear the internal fault (instantaneous)
F	Protection fails to clear the internal fault (protection not healthy while needed to operate)
SB	Protection operates correctly to block the over-tripping during an external fault. (Does not work when it is not required)
MF	Protection malfunctions (protection operated incorrectly)
SN	Protection is healthy but not required to operate
FN	Protection is not healthy while not required to operate

SD Protection succeeds to clear the fault but after a time delay (clearing is not instantaneous)

If a fault occurs within zones of protection, protection system can only be in one of the states: S, F or SD. T_S , T_F , and T_{SD} are the clearing times associated with these states, respectively. T_S is the clearance time when the protection system can successfully clear the fault with no delay. T_F is the clearance time when protection system completely fails to clear the fault in the determined time frame, and therefore encounter the much bigger delay of the back-up protection system Finally. Finally, T_{SD} is the clearance time of the protection system when protection system fails to clear the fault instantly and there is a time delay of zone two involved. T_F is a much longer time period compared to the other two and can cause instability and potential cascading failures. Therefore it is not normally desired for protection systems to be in state F.The expected clearing time for the protection system would be:

$$\in_i = P_i(S).T_S + P_i(F).T_F + P_i(SD).T_{SD} \quad (87)$$

Where $P_i(S)$, $P_i(F)$, and $P_i(SD)$ are probabilities of the protection system residing in corresponding states for a fault in zone A_i . We assume that the substation shown in Figure 83 is equipped with pilot protection scheme (described in Chapter 3) for protection of the incoming/outgoing lines. Therefore, we use the results of the calculation performed in Chapter 3 to find probabilities of the protection system residing in each of the above states. In order to be able to compare the effects of adding redundancy to specific parts of the pilot

protection system, as well as using different media for communication, the following configurations have been considered and studied for each pilot scheme:

- Single relay/ Single Microwave (MW) channel
- Single relay/ Redundant channel (MW+ relay to relay on phone line)
- Single relay/ Single channel (dedicated fiber optic)
- Single relay/ Single channel (multiplexed fiber optic)
- Redundant relay/ Single channel (MW)
- Redundant Relay/ Independent channels (MW+ relay to relay on phone line)

Figure 84 shows the increase in failure rate of transformer T_3 without and with various type FCL's in 50 years (which is average life time of a power transformer [105]) in the presence of various arrangements of the PUTT protection scheme. Model parameters for a power transformer have been selected to fit the failure data over a 50 year lifetime of power transformers [105] .

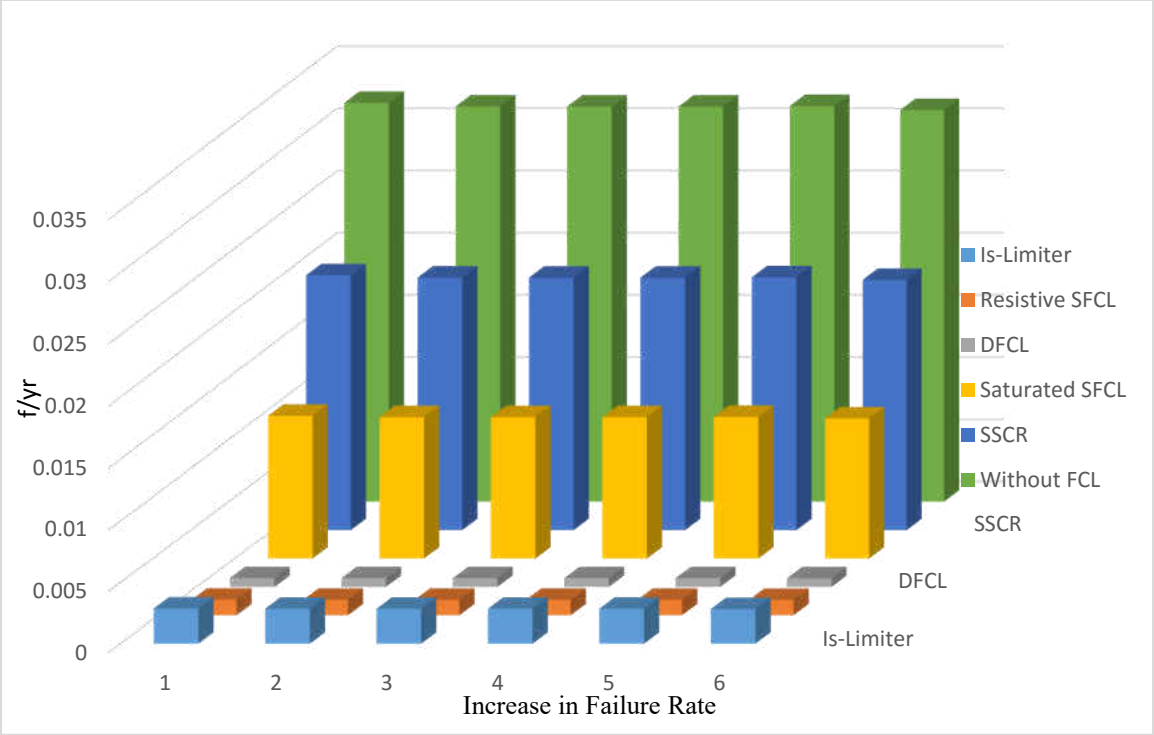

Figure 84. Increase in failure rate in presence of several FCL's for PUTT Scheme arrangements:

1: Single Relay/Single Channel (MW)
2: Redundant Relay/Single Channel (MW)
3: Single Relay/Redundant Channel (MW+Phone)
4: Single Relay/Single Channel (Dedicated Fiber Optic)
5: Single Relay/Single Channel (Multiplexed Fiber)
6: Redundant Relay/ Independent Channels (MW+Phone)

As seen in this figure, without FCL, there will be a huge increase in failure rate of the transformer. As matter of fact, without the FCL in the arrangement, the failure rate of the transformer will reach an unacceptable level within a small fraction of this time.

To see the difference in various arrangements of the PUTT scheme better, Figure 85 shows the increase in failure rates of transformer T_3 for various arrangements and without the FCL.

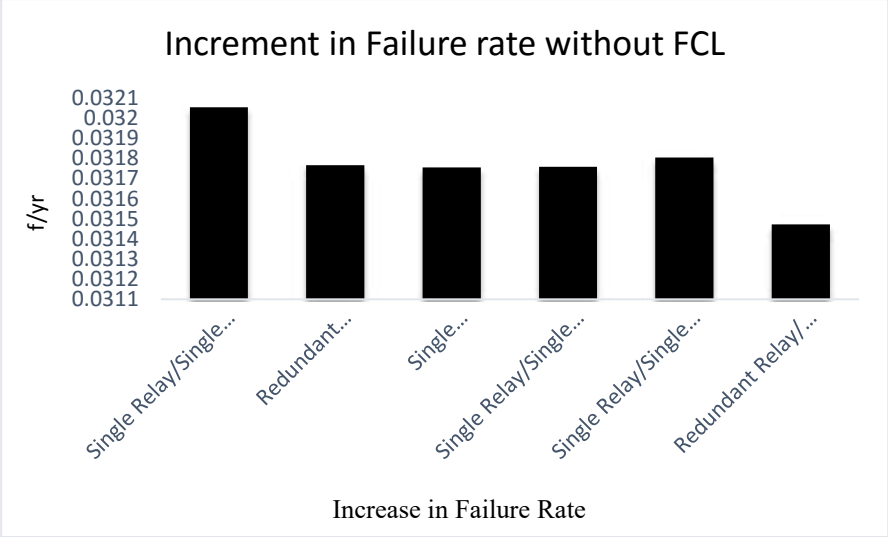

Figure 85. Increase in failure rate without FCL for various PUTT Scheme arrangements.

Figure 86 shows the same data for case of resistive SFCL.

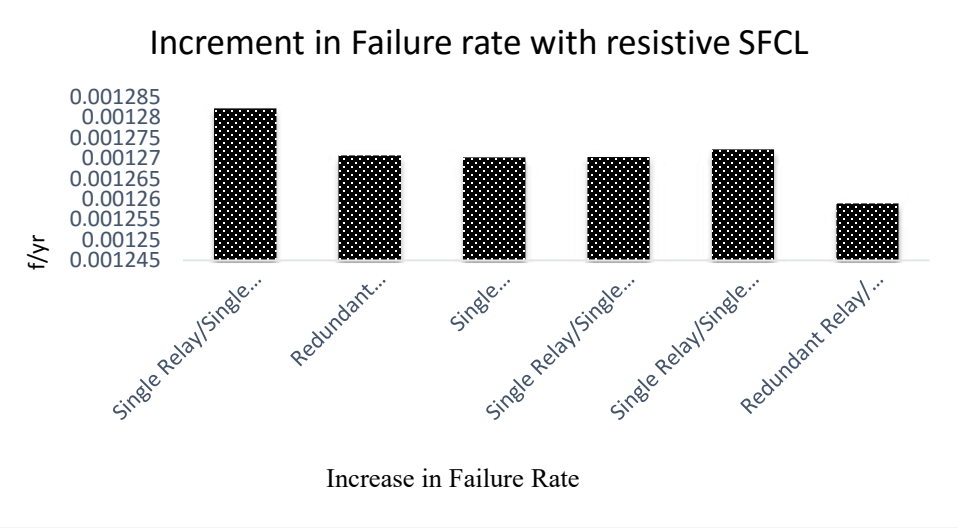

Figure 86. Increase in failure rate in presence of resistive SFCL for various PUTT Scheme arrangements.

Figure 87 shows the increment in failure rate for various types of FCL's and the single relay/single channel PUTT scheme.

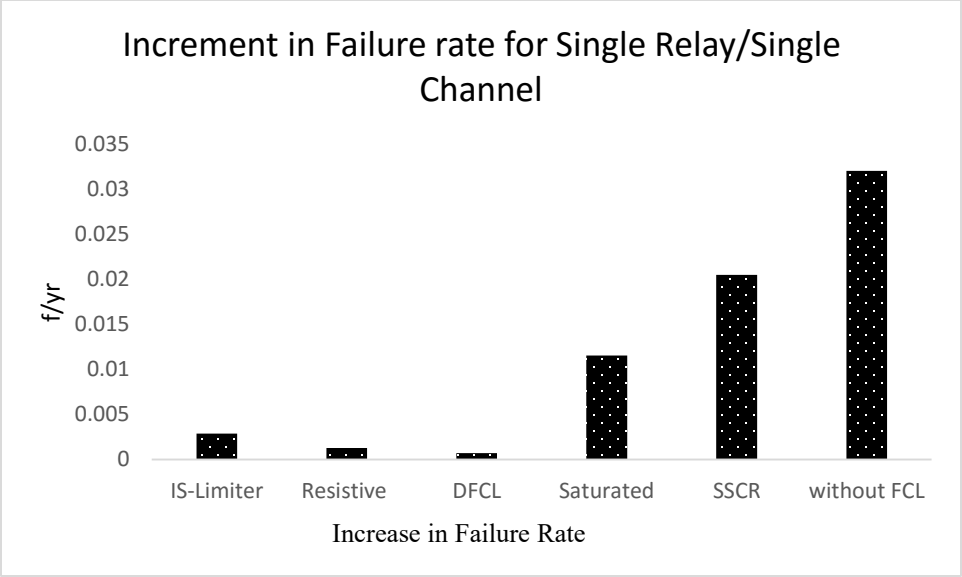

Figure 87. Increase in failure rate in presence of various type SFCL's for PUTT single relay/single channel arrangements..

Figure 88 shows change in the average failure rate of transformer T_3 during a one year period, without FCL and in the presence of various types of FCL's. As seen in this figure, as FCL is being employed and the fault current limiting ratio increases, the role of protection system and the fault clearance time type on increased failure rate becomes less and less of an issue. This is clearly seen in the figure by comparing the slope of the line from top to bottom for the case of without FCL with various FCL cases. This suggests another added value for using FCL's in the power network, in that it will eliminate the need for accurate selection and setting of the protection system by making the entire system less sensitive to the selection and setting process of the protection scheme.

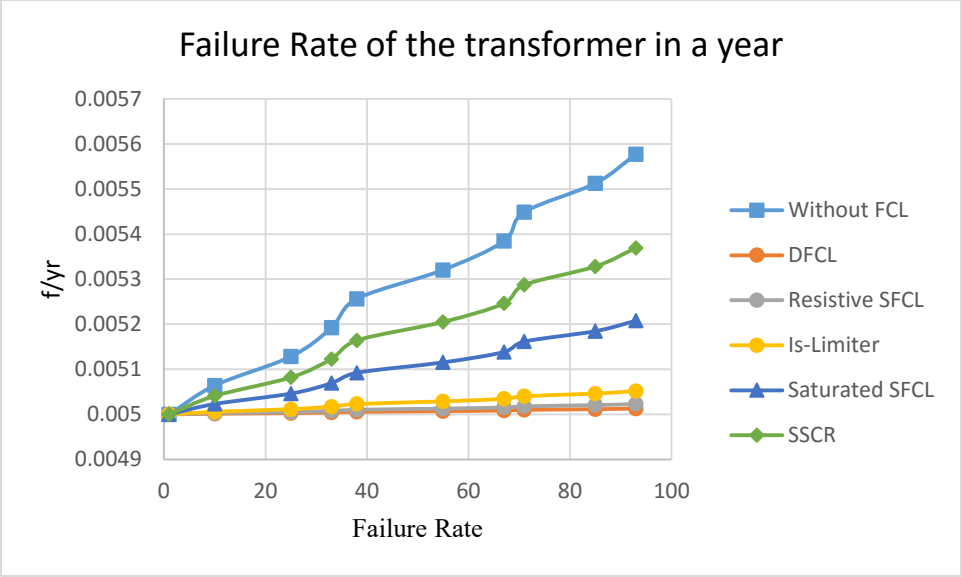

Figure 88. Profile of failure rate of the transformer in one year without FCL and with different types of FCL.

Figure 89 illustrates the increase in failure rate of the transformer, with different types of FCL's and various arrangements of the DCB scheme.

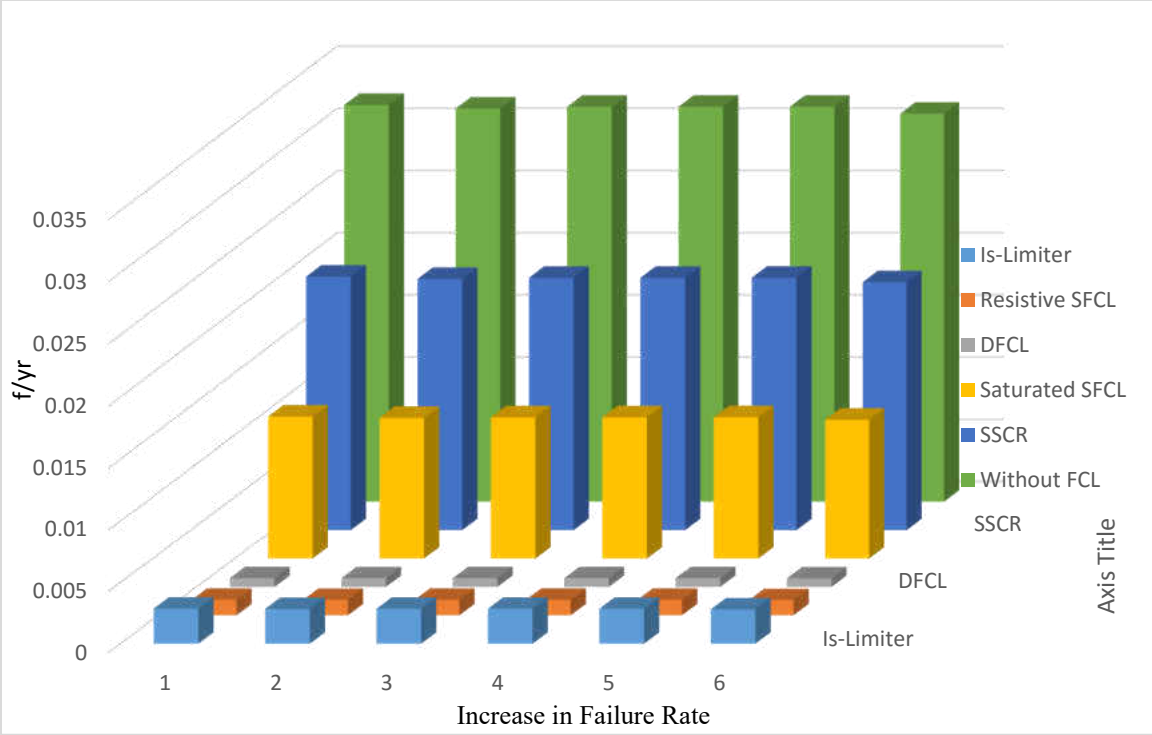

Figure 89. Increase in failure rate in presence of several FCL's for DCB Scheme arrangements:

1: Single Relay/Single Channel (MW)
2: Redundant Relay/Single Channel (MW)
3: Single Relay/Redundant Channel (MW+Phone)
4: Single Relay/Single Channel (Dedicated Fiber Optic)
5: Single Relay/Single Channel (Multiplexed Fiber)
6: Redundant Relay/ Independent Channels (MW+Phone)

Figures 90 and 91 show the increase in failure rate without FCL and with the resistive SFCL for various arrangements of the DCB scheme.

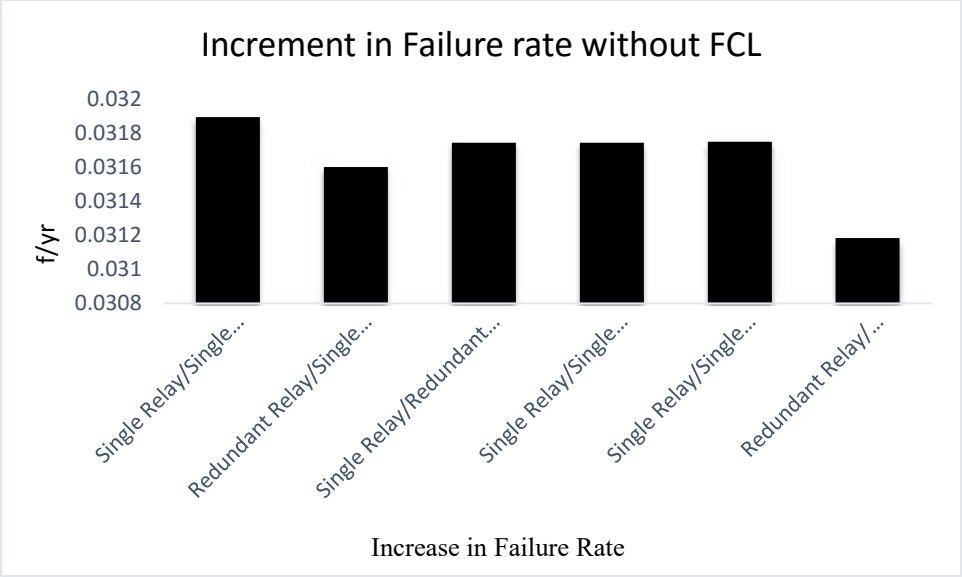

Figure 90. Increase in failure rate without FCL for various DCB Scheme arrangements.

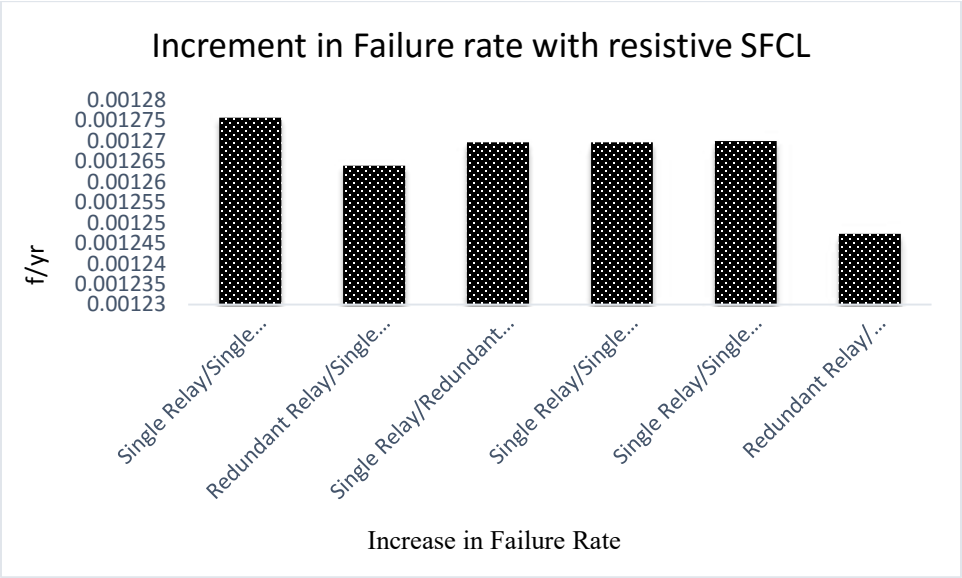

Figure 91. Increase in failure rate with resistive SFCL for various DCB Scheme arrangements.

Figure 92 compares the increment in failure rate for the single relay/single channel arrangement of the DCB scheme, without FCL and in case of various types of FCL's.

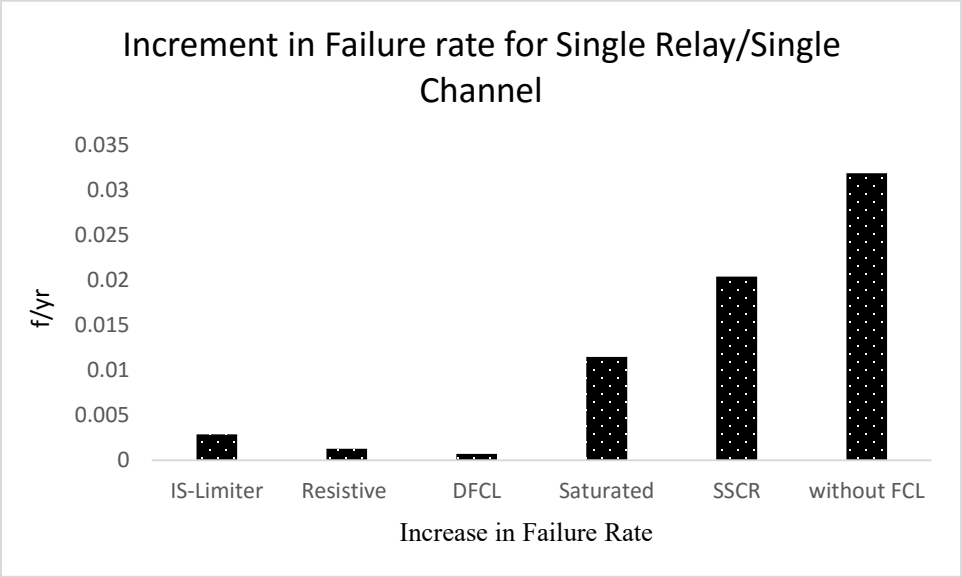

Figure 92. Increase in failure rate in presence of various type SFCL's for DCB single relay/single channel arrangements.

From above figures, it is seen that for the DCB scheme there is generally a greater increase in the failure rate values, but as before the role of FCL types and limitation ratio on limiting the failure rate is incredible.

Figure 93 shows the sensitivity of failure rate for various combinations of the DCB system arrangements and three types of FCL's. This figure, again, confirms the positive impact of FCL in reducing the sensitivity of failure rate to the protection scheme selection and settings.

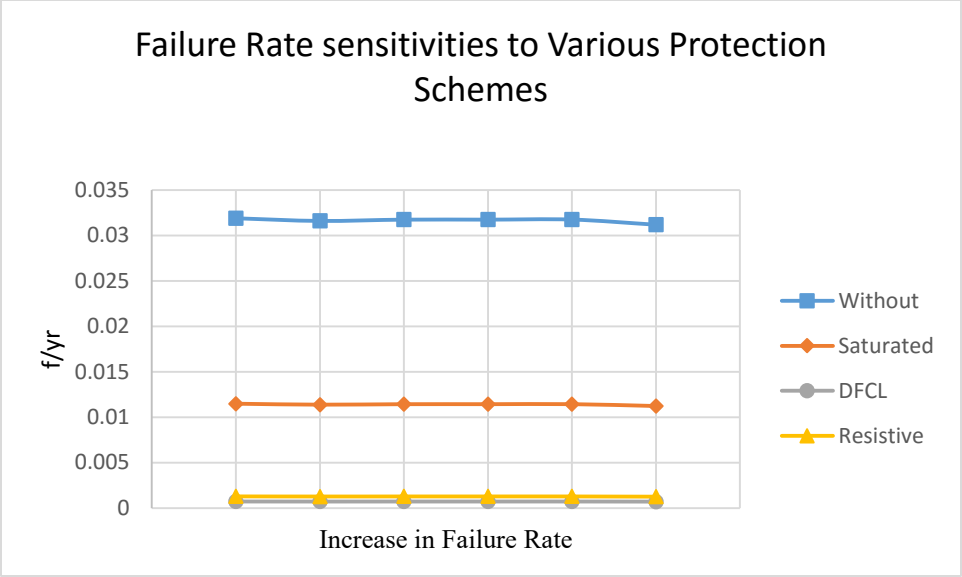

Figure 93. Increase in failure rate for three type SFCL's and various arrangements of the DCB scheme:

1: Single Relay/Single Channel (MW)
2: Redundant Relay/Single Channel (MW)
3: Single Relay/Redundant Channel (MW+Phone)
4: Single Relay/Single Channel (Dedicated Fiber Optic)
5: Single Relay/Single Channel (Multiplexed Fiber)
6: Redundant Relay/ Independent Channels (MW+Phone)

Finally, Figure 94 shows the growth in the total failure rate of the transformer T_3 for various

FCL types and single relay/single channel arrangement of the DCB scheme.

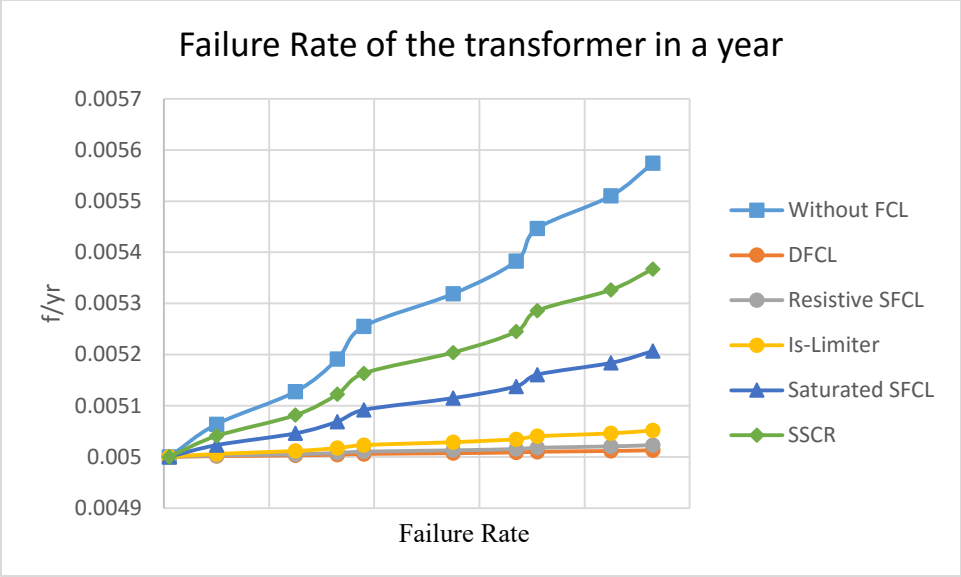

Figure 94. Profile of failure rate of the transformer in one year without FCL and with different types of FCL.

Figures 95 to 99 show the failure rate profiles for the DCUB scheme. These figures again demonstrate the positive impact of FCL devices in limiting the failure rate values and also in reducing the sensitivity of power system to the protection system performance.

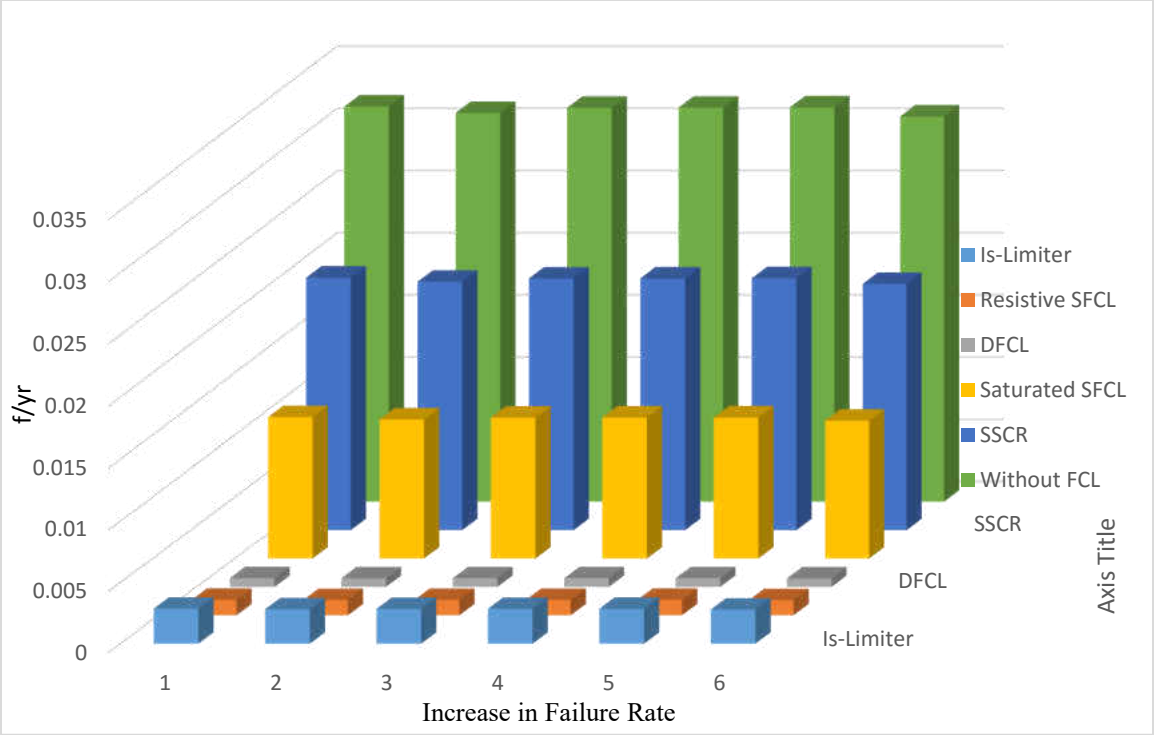

Figure 95. Increase in failure rate in presence of several FCL's for DCUB Scheme arrangements:

1: Single Relay/Single Channel (MW)
2: Redundant Relay/Single Channel (MW)
3: Single Relay/Redundant Channel (MW+Phone)
4: Single Relay/Single Channel (Dedicated Fiber Optic)
5: Single Relay/Single Channel (Multiplexed Fiber)
6: Redundant Relay/ Independent Channels (MW+Phone)

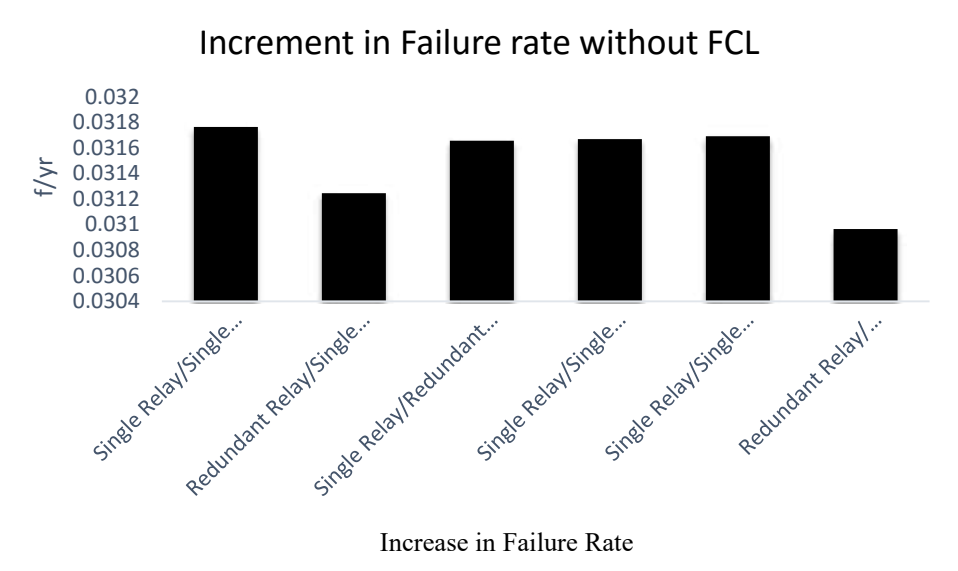

Figure 96. Increase in failure rate without FCL for various DCUB Scheme arrangements.

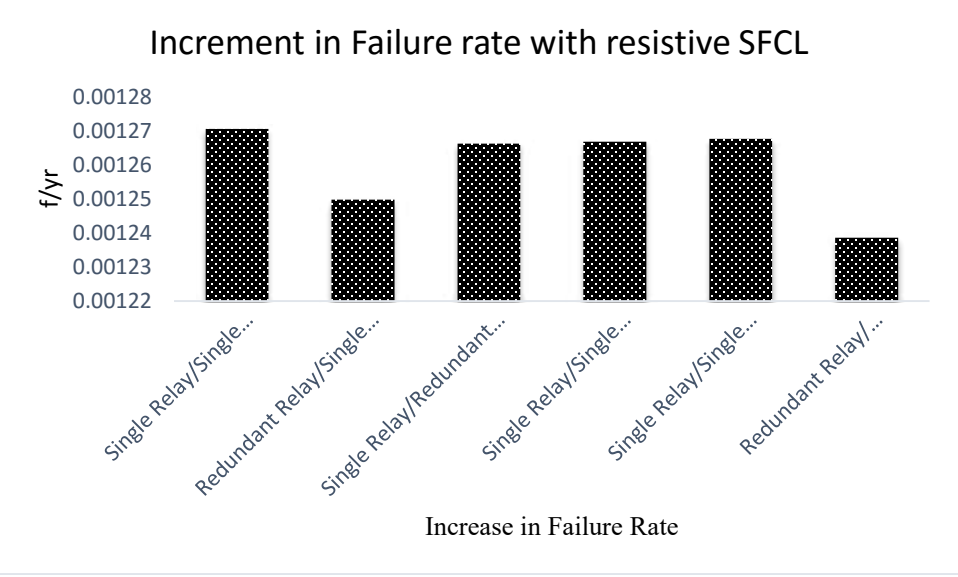

Figure 97. Increase in failure rate with resistive SFCL for various DCUB Scheme arrangements.

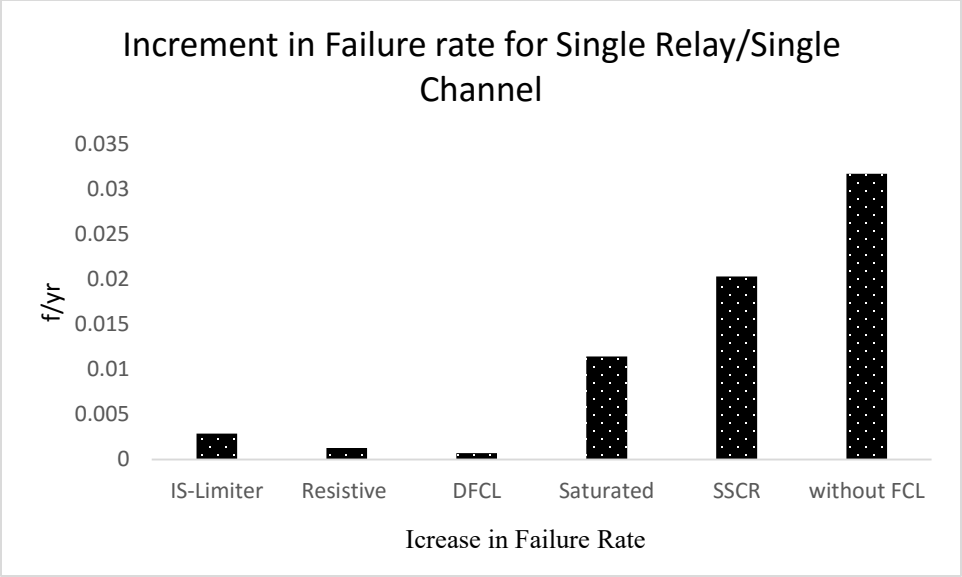

Figure 98. Increase in failure rate in presence of various type SFCL's for DCUB single relay/single channel arrangements.

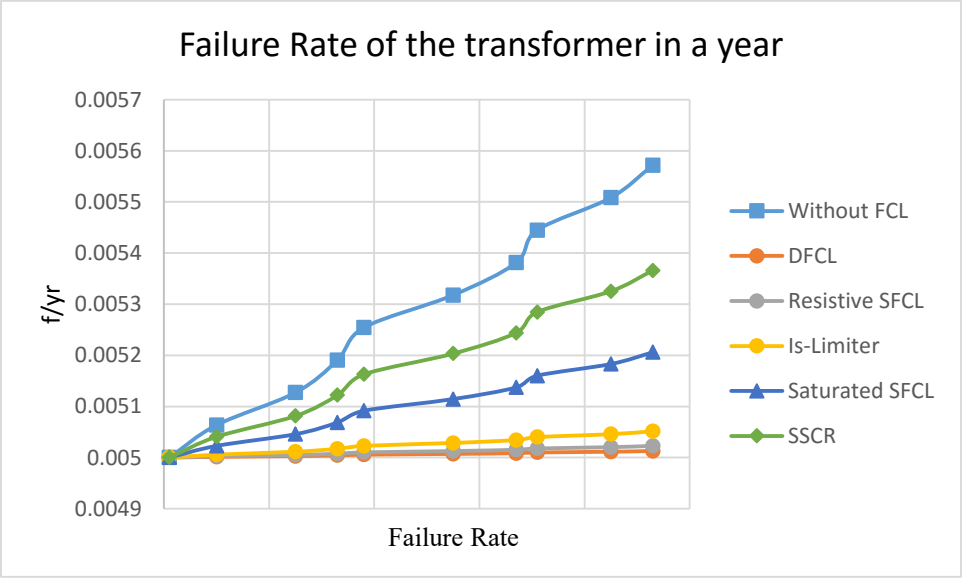

Figure 99. Profile of failure rate of the transformer in one year without FCL and with different types of FCL.

CHAPTER VII
IMPACT OF DEMAND REPONSE PROGRAMS ON ASSET

Overloads in the forms of over-consumption, especially during peak hours, happen frequently in power systems and will pose an extra burden on the power system equipment. Demand response (DR) programs temporarily shifts customer energy load during peak demand hours to off-peak periods, thus alleviating the load burden on the power grid during high demand times. Reducing the peak energy demand not only allows more electricity to be produced by cheaper base load generation but also saves the cost of building additional power plants to meet the critical peak demand. Utility DR programs will also extend the useful lifetime of power system assets by preventing them from carrying extra loads and currents. In this chapter, in order to study the effects of DR programs on utility asset management, at first DR programs are modelled and their impact on load pattern are studied. Then, using the developed model in previous chapters, the impact of DR programs, in terms of reducing the overload levels, on utility asset management plans is studied.

Introduction

The ongoing increases in the consumer demand profiles is stressing the aged electrical network as governed by the increase in the System Average Interruption Duration Index (SAIDI) and System Average Interruption Frequency Index (SAIFI). The increase in the values of these indices is a result of the growing power complications like blackouts, voltage sags and overloads which considerably lower the power quality and reliability. In order to keep up with the increasing power demand, there is a need to supply electricity more efficiently and reliably. Reducing losses through the generation, transmission and

distribution networks and increasing the transmission capacity will certainly increase the throughput of the current power system, minimizes or eliminates the requirement to build new power plants and will give way to better and cleaner means to generate & transmit electrical power. Reference [106] shows that creating more efficient end-use and reducing consumption will cut generation capital investment by 28% to 35%.

Demand Side Management (DSM), also known as Energy Demand Management or Load Management, entails utility actions that influence the patterns of use of energy consumed by end users, such as actions targeting reduction of demand during peak periods or when energy-supply systems are constrained. The relatively low utilization of generation and networks means that there is a significant scope for DSM in contributing to increasing the efficiency of the system investment. Several potential applications of DSM are [107]:

-Reducing the generation margin

-Improving transmission grid investment and operation efficiency

-Improving distribution network investment

-Managing demand–supply balance in systems with intermittent renewables

The term DSM encompasses several energy demand modification activities such as [108]:

Energy Efficiency

Energy Conservation: involves using less energy

Demand response (DR): not necessarily reduction in usage but more likely shifting usage to off-peak hours (and also Load building [109]).

Demand Response

Demand response is defined as: Changes in electric usage by end-use customers from their normal consumption patterns in response to changes in the price of electricity over time, or to incentive payments designed to induce lower electricity use at time of high wholesale market prices or when system reliability is jeopardized [110]. In brief, DR is the change in electricity consumption triggered by some utility actions in order to gain specific results.

Some benefits of DR programs include reduction of power overloads, bill savings for customers, lower electricity wholesale market prices and reliability improvements in electrical network ([111] , [112] , [107] , [113] and [109]). Utilities are using various techniques to determine if consumers follow more intelligent energy consumption patterns.

The Federal Energy Regulatory Commission (FERC) report entitled “Assessment of DR and Advanced Metering” has found that only five percent of customers are on some form of DR programs [114]. This is mainly due to the lack of proper models in this area that could enable customers and utilities to unveil the strong potentials of these programs.

Experience indicates that DR programs are more effective when system wise indices and parameters are involved and if no contradictory results appear. This is the case of DR initiatives with the only aim of securing the system stability, which promotes load shifting to periods of time when electricity tariffs are lower. However due to the lack of reliability

targets and incentives, average energy consumption on yearly basis may increase due to inefficient usage promoted by low rates during off-peak hours, that would in turn deteriorate system reliability indices and margins [21].

There is a lack of an accurate model in the DR area that allows utilities to observe the impact of various DR programs on system indices. Some literatures have made good attempts in classifying DR programs and modeling each type, but they have assumed a constant elasticity that can be inaccurate in predicting customer behaviors in reality [20].

In this chapter a new DR model is developed used that is completely consistent with the demand-price curve and does not have the inaccuracies of the constant-elasticity model. Using the new DR model, a control panel is developed that enables utilities to monitor and simulate various DR programs in their service areas and view the results on the screen. It also allows changing load combinations on various load buses and at different time of the year to simulate the realistic situation of the system. Results would then allow for a proper planning and utilization of available DR resources in a system based on system reliability needs.

Having the system load profile in the presence of various DR programs, new levels of system overloads can be calculated and used in the proposed mathematical model to forecast the reliability improvements of DR programs.

Demand Response Programs

Demand response programs are divided into two basic categories namely Time-Based Rate Programs (TBRPs), and Incentive Based Programs (IBPs) [115]. Figure 100 shows this classification.

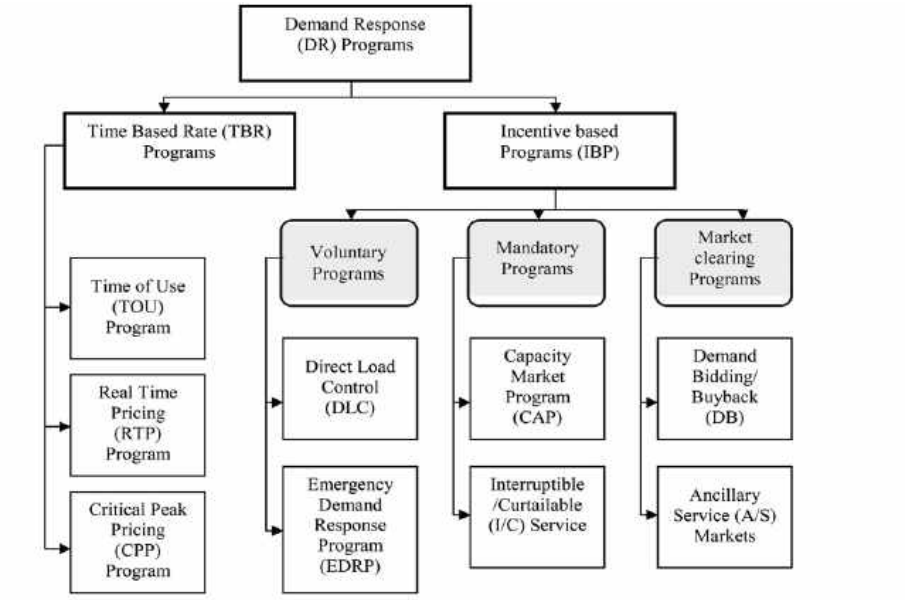

Figure 100. Classification of DR programs.

In time-based rate programs, i.e., Time of Use (TOU), Real Time Pricing (RTP), and Critical Peak Pricing (CPP) programs, the electricity price changes for different periods according to the electricity supply cost. TOU rates establish two or more daily periods that reflect hours when the system load is higher (peak) or lower (off-peak), and charge a higher rate during peak hours. RTP rates vary continuously during the day reflecting the wholesale

price of electricity. CPP is an overlay on either TOU or flat pricing. CPP uses real-time prices at times of extreme system peaks.

Incentive-based programs include Direct Load Control (DLC), Emergency Demand Response Program (EDRP), Capacity Market Program (CAP), Interruptible/Curtailable (I/C) service, Demand Bidding (DB), and Ancillary Service (A/S) program. These programs can be classified into three main subgroups namely; voluntary, mandatory and market clearing programs.

DLC and EDRP are voluntary programs which mean that if customers do not curtail consumption, they are not penalized but they might lose some of the credits that they could gain by fully participating in the program. DLC refers to a program in which a utility or system operator remotely shuts down or cycles a customer's electrical equipment on short notice to address a system or local reliability issue. EDRP provides incentive payments to customers for reducing their loads during reliability triggered events, but curtailment is voluntary.

I/C and CAP are mandatory programs and participating customers are subject to penalties if they do not curtail consumption when directed. Customers on I/C service rates receive a rate discount or bill credit in exchange for agreeing to reduce load during system contingencies. If customers do not curtail, they can be penalized. In CAP, customers commit to provide pre-specified load reductions during system contingencies, and are subject to penalties if they do not curtail consumption when directed.

DB and A/S are market clearing programs, where large customers are encouraged to offer or to provide load reductions at a price at which they are willing to be curtailed, or to identify how much load they would be willing to curtail at posted prices. DB program encourages large customers to offer load reductions at a price at which they are willing to be curtailed, or to identify how much load they would be willing to curtail at posted prices. A/S program allows customers to bid load curtailments in ISO markets as operating reserves. If their bids are accepted, they are paid the market price for committing to be on standby. If their load curtailments are needed, they are called by ISO, and may be paid the spot market electricity price. More detailed explanations of various DR programs can be found in [115].

Available DR Models

References [116] and [117] have studied the impact of several DSM (demand side management) programs such as: peak clipping, load shifting and load addition on load curve and reliability indices. The studied DSM programs encounter an addition or subtraction of specific percentages of annual peak load to the base load. While this representation of DSM is helpful for giving an estimation of the impact of DSM on power system indices, it doesn't give a realistic picture of the DSM programs because these programs are usually known in terms of pricing and incentives rather than power percentages. Moreover, these programs normally do not result in the addition or subtraction of an exact power value to the load curve.

At this point, it is helpful to review the important concept of price elasticity of demand in the Demand Response terminology before presenting the new DR model.

Price Elasticity of Electrical Demand

Price elasticity of electrical demand is defined as the ratio of relative change in demand to relative change in price [118].

$$E = \frac{\frac{\Delta d}{d_0}}{\frac{\Delta p}{p_0}} \tag{88}$$

Where E is the price elasticity, Δd and Up are change in consumption and change in electricity price, respectively and d_0 and p_0 are base consumtion and base electricity price, respectively.

According to Eq.(88), the so called "cross-elasticity" of the ith period versus jth period can be defined as:

$$E_{i,j} = \frac{p_0(j)}{d_0(i)} \cdot \frac{\partial d(i)}{\partial p(j)} \tag{89}$$

Now if $\Delta d(i)\ \ i=1,....24$ is the change in demand in the i_{th} hour and $\Delta p(i)\ \ i=1,....24$ is the change in price in the i_{th} hour and $E_{i,j}$ is cross elasticity values, for the complete price-demand impacts we may write:

$$\begin{pmatrix} \Delta d(1) \\ \Delta d(2) \\ . \\ . \\ \Delta d(24) \end{pmatrix} = \begin{pmatrix} E_{1,1} & E_{1,2} & . & . & E_{1,24} \\ E_{2,1} & E_{2,2} & . & . & E_{2,24} \\ . & & . & . & E_{3,24} \\ . & & & . & . \\ E_{24,1} & E_{24,2} & . & . & E_{24,24} \end{pmatrix} = \begin{pmatrix} \Delta p(1) \\ \Delta p(2) \\ . \\ . \\ \Delta p(24) \end{pmatrix} \tag{90}$$

where

$$d(i) = f_i(p(1), p(2),..., p(24))\ \ i=1,....24 \tag{91}$$

and

$$E_{i,j} = \frac{\partial f_i}{\partial p(j)} \tag{92}$$

Models Using Elasticity of Demand

A model has been presented and studied in [119] for TOU and EDRP programs that is close to what happens in reality. However, this model doesn't consider the diversity of customers. For example residential customers may have different reactions and preferences to prices and incentives. For a comprehensive study of DR, the intended model should consider the diversity and preferences of costumers and should respond differently when the combination percentage of costumers in an area changes.

References [20] and [120] have provided a good classification and modeling of various types of DR, but they have assumed a constant elasticity; i.e., linear f_i functions. This might be helpful in simplifying the problem and giving general results but is not acceptable for accurate studies. Another problem with the linear demand-price model is that when the price approaches zero, it reaches a steady value and does not grow unlimitedly. Whilst in reality, if the price of a commodity drops to zero, its demand will grow in a free market. [121] has modified the constant-elasticity assumption by considering an elasticity that is constant but that also changes depending on the spot price being considered. This approach needs elasticity values to be recalculated for every change in the price and still has the deficiency of considering a linear demand function in the first place.

New DR Model

[122] has assumed another shape for the demand function, f_i, a trans-log function which is more consistent with the real demand curve. This model doesn't assume a simple linear form for the f_i function like before, and is widely considered in the economical modelling of electricity demand ([123], [124], [125], [126]). The model also considers other parameters such as customer's income and the price of natural gas in the formulation of demand-price function. Equation (93) describes this model:

$$lnD = \alpha_0 + \alpha_1 lnY + \alpha_2 lnEP + \alpha_3 lnGP \quad (93)$$

where:

ln

D is the electricity consumption

Y is the customer income

EP is the electricity price

GP is the price of a substitute good, that in this case is natural gas [127], [128], [129].

The above model is more consistent with demand-price behavior-especially in areas where price goes towards zero- than the constant-elasticity model reported in the literature [20].

In this chapter this model has been adopted as a base in modeling the DR programs. In using Equation (93) for this chapter, all parameters other than electricity price could be assumed equal to their predetermined values, and hence demand would change only by change in the electricity price. Values of the parameters used in this model are given in the literature ([123], [124], [125], [127]) for various countries including the US.

Modeling Demand Response including Penalties and Incentives

Suppose that the customer changes his demand from $d_0(i)$ (initial value) to $d(i)$ (where i could be the i_{th} hour or i_{th} period depending on the DR program type), based on the value which is considered for the incentive and the penalty mentioned in the contract. The change in demand is:

$$\Delta d(i) = d(i) - d_0(i) \tag{94}$$

If $\$ A(i)$ is paid as incentive to the customer for each kWh load reduction, the total incentive for participating in the program will be as follows:

$$P(\Delta d(i)) = A(i).[d_0(i) - d(i)] \tag{95}$$

If the costumer doesn't curtail or reduce its consumption as to the contract, it will be faced with a penalty. If the agreed upon level of the contract is $IC(i)$ and the penalty is $\$ pen(i)$, then the total penalty, $PEN(\Delta d(i))$ can be calculated as:

$$PEN(\Delta d(i)) = pen(i).\{IC(i) - [d_0(i) - d(i)]\} \tag{96}$$

It is obvious that for DR programs without penalty, the value of the penalty function would be set to zero.

Let's assume that $B(d(i))$ is the customer income of using $d(i)$ kWh electrical energy in the considered period. The function that is most often used for this purpose is the quadratic benefit function [130]:

$$B(d(i)) = B_0(i) + \rho_0(i).[d(i) - d_0(i)].\left\{1 + \frac{d(i) - d_0(i)}{2E_{i,i}.d_0(i)}\right\} \tag{97}$$

Where ρ is the electricity price and the subscription "0" denotes values before applying the DR program. The total benefit, S, of the customer in this interval would be :

$$S = B(d(i)) - d(i).\rho(i) + P(\Delta d(i)) - PEN(\Delta d(i)) \tag{98}$$

It is assumed that customer tends to optimize its benefit. By differentiating the above equation and setting it to zero, the costumer's consumption will be as following:

$$d(i) = d_0(i).\left\{1 + E_{i,i}.\frac{[\rho(i) - \rho_0(i) + A(i) + pen(i)]}{\rho_0(i)}\right\} \tag{99}$$

The above Equation gives the demand value in any interval, based on the features of a given DR program, such as price, incentives and penalty values.

In Equation (99), it can be seen that if the electricity price does not change and the incentive and the penalty are zero, then $d(i)$ will remain the same as the initial value of $d_0(i)$.

By extending the above concept to calculating the consumption in an interval when the price changes in other intervals, using the cross elasticity values one can write:

$$d(i) = d_0(i).\left\{1 + E(i,i).\frac{[\rho(i) - \rho_0(i) + A(i) + pen(i)]}{\rho_0(i)} + \sum_{\substack{j=1 \\ j\neq i}}^{24} E(i,j).\frac{[\rho(j) - \rho_0(j) + A(j) + pen(j)]}{\rho_0(j)}\right\} \tag{100}$$

Representation of the load at each load bus.

The IEEE-Reliability Test System (IEEE-RTS) has been used extensively to develop and illustrate composite system evaluations [131]. The load model information provided can be used to calculate total system hourly loads for one complete year on a per unit basis, expressed in a chronological fashion so that daily, weekly and seasonal patterns can be developed. The system load is described by specifying the weekly peak loads in percent of the annual peak load, the daily peak load in percent of the weekly peak load and the hourly

peak load in percent of the daily peak load. A problem with this approach is that it doesn't consider that individual buses follow different load curves depending on the mix of customers at that bus. A more comprehensive load model would recognize that individual load buses have different load curves with respect to combination of customer classes at that load bus.

The Standard Industrial Classification (SIC) has been used to identify seven types of customer sectors [132]**.**These sectors are as follows:

- Large users,
- Industrial,
- Commercial,
- Agricultural,
- Residential,
- Government & Institutions,
- Office & Buildings

The assumed load profiles of these seven customer sectors for a typical day are shown in Figures 101 through 103 [133] .

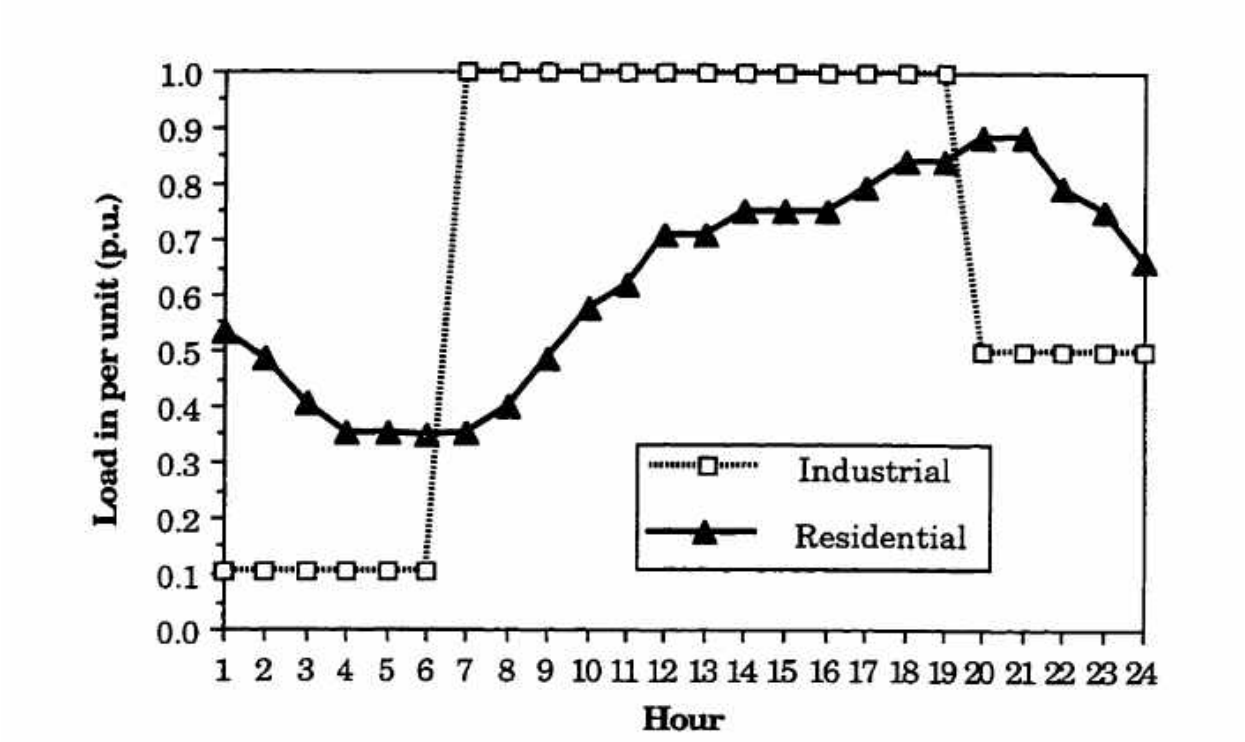

Figure 101. Load profile for the Residential and Industrial Sectors..

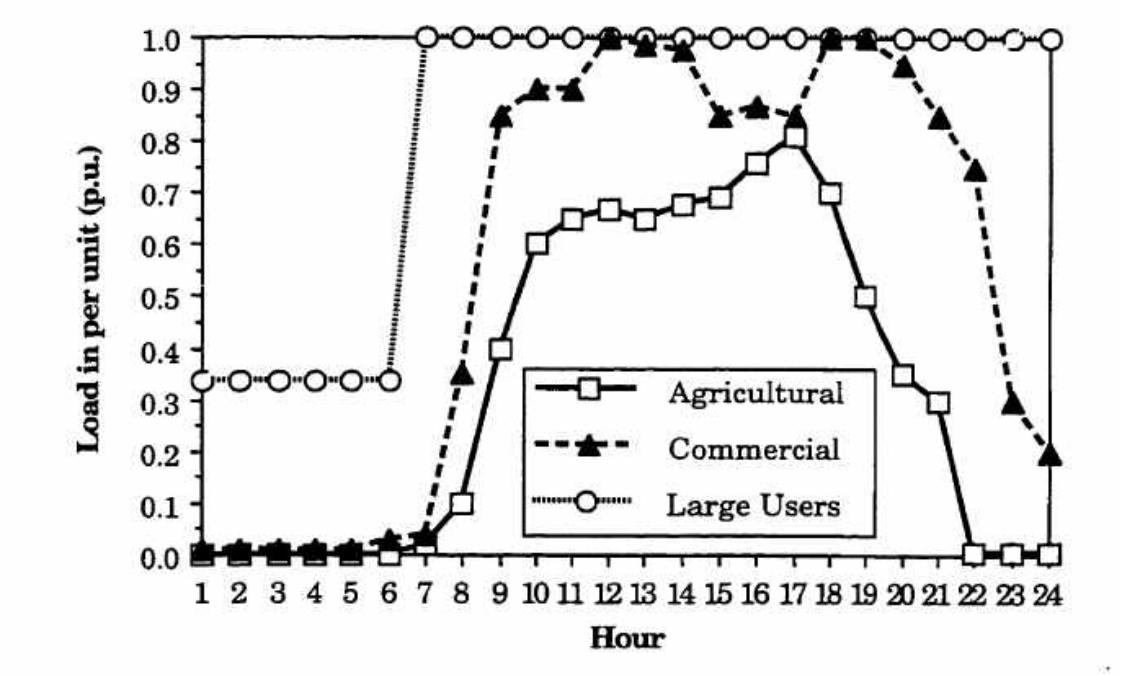

Figure 102. Load profile for the Commercial, Large Users and Agricultural Sectors.

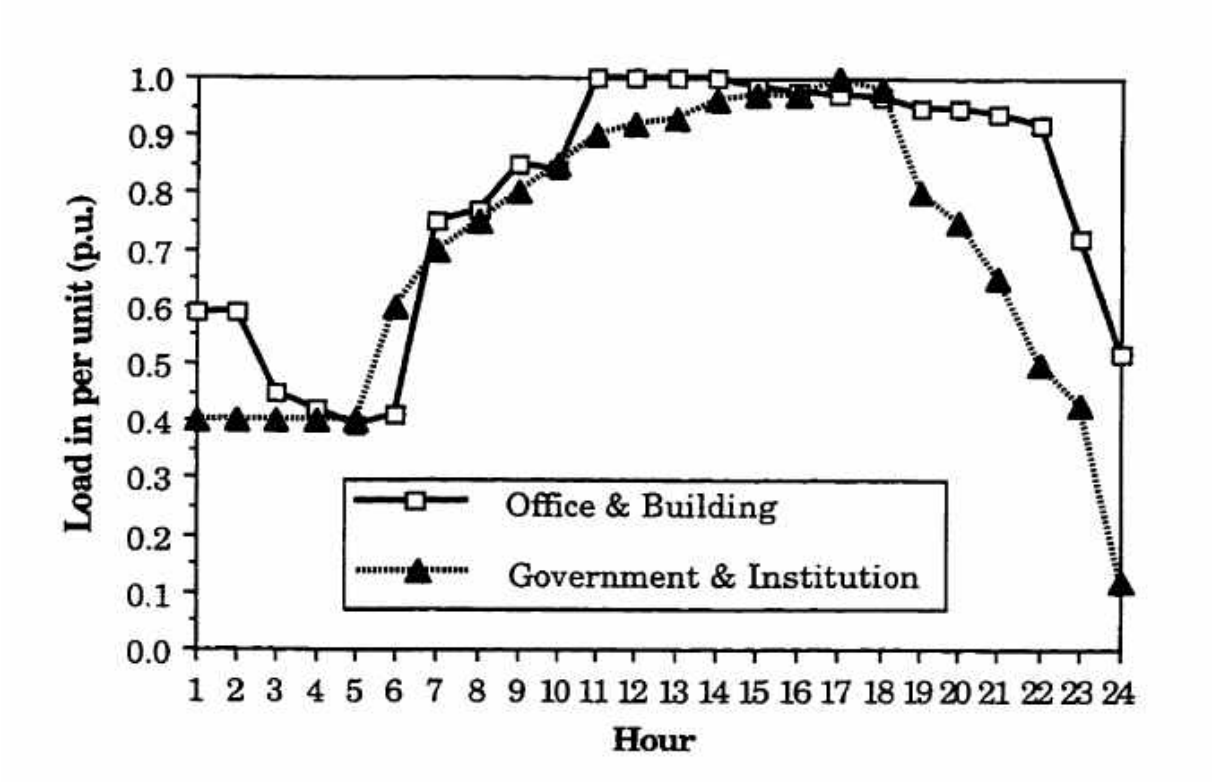

Figure 103. Load profile for the Government & Institution and Office & Building Sectors..

Reference [130] shows a method to calculate and illustrate chronological load curves of a given bus depending on its combination of these seven sectors. In this method, load curve of each sector is determined and combined to give the overall bus load curve. If L_{ji} is the proportion of the sector peak load contributed by sector i during hour j, to the load at bus k, the load at bus k, for hour j is given by Equation (101).

Load at Bus k for hour j=$\sum_{i=1}^{All\ sectors\ in\ Bus\ k}(L_{ji} \times Sector\ j'speak\ load\ at\ Bus\ k)$ (101)

L_{ji} is also referred to as the allocation factor. Tables 12 to 14 in Appendix of this document gives the allocation factor of each sector depending on weak of the year, day of the week, and time of the day.

DR Control Panel

To implement and test the developed model, the RBTS test system has been selected because of its simplicity and its selection of parameters and values that can represent various possible scenarios in a power system [134] , [135].

A single line diagram of the RBTS test system which shows the assigned load bus customer compositions is shown in Figure 91. It can be seen from this figure that there are some residential and commercial sector customers at every load bus. As an example, Bus 2 has industrial, commercial, residential, and government and institutional users allotted to it. The bus data and generator data of this system are given in Appendix of this document.

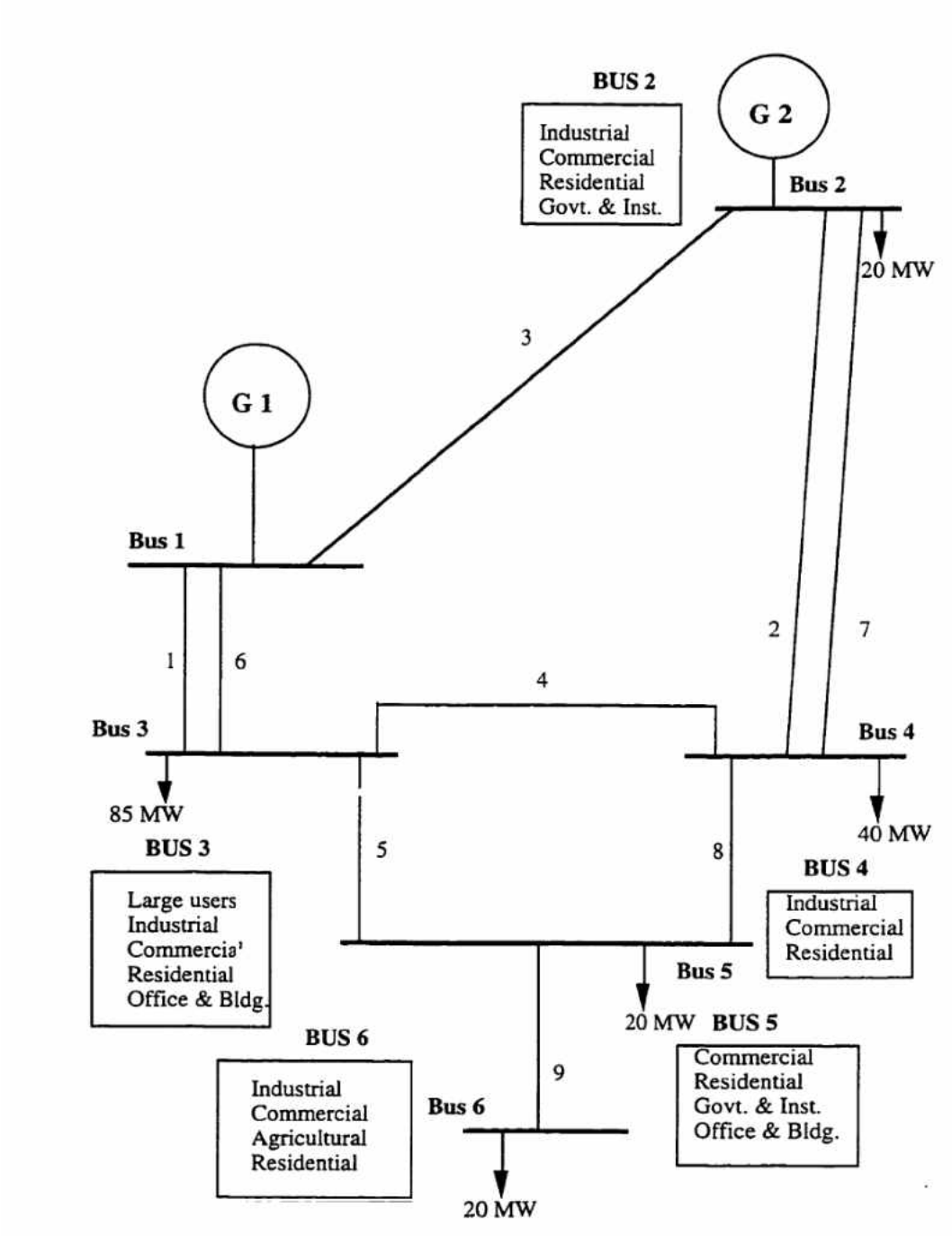

Figure 104. Single line diagram of the RBTS with customer compositions.

Using the approach outlined in previous section, load profiles have been developed for the buses of the RBTS for all hours of the day, all days of the week and all weeks of the year. The profiles are also calculated for every possible combination of the 7 major sectors of a load: residential, commercial, office and buildings, governmental and institutions, industrial, agricultural and large users. Table 12 shows the RBTS bus combinations (MW) for each of the load sectors [130] .

Table 12. RBTS Bus Load Combinations (MW)

User Sector	Bus2	Bus3	Bus4	Bus5	Bus6
Large Users	---	55.5	--	--	--
Industrial	3.5	3.05	16.3	--	3.05
Commercial	3.75	4.7	4.7	3.7	1.7
Agricultural	--	--	--	--	7.4
Residential	7.25	19.90	19	8.9	7.85
Government and Institutions	5.55	--	--	5.55	--
Office and Building	--	1.85	--	1.85	--

DR programs are modeled using Equation (100) and the elasticity model of Equation (90). These models were integrated into the developed control panel shown in Figure 105. This panel would allow the utilities to forecast consumption based on the time of the year and load combination of each bus and see the results of implementing their various DR programs.

Figure 105. DR control panel showing loads on RBTS buses.

Table 13 shows various scenarios used to obtain the study results. In this table values of incentives and penalties are stated in cents/kWh. The load curve is divided into three different periods, namely low load period (00:00 am–9:00 am), off-peak period (9:00 am–7:00 pm) and peak period (7:00 pm–12:00 pm).

Table 13. Scenarios Used for Comparison

No.	Scenario	Color
1	Initial Load	Blue
2	Incentive 5 , penalty 5	Red
3	Incentive 5 , penalty 7	Cyan
4	Incentive 10 , penalty 5	Green

Figures 106 to 109 show the results of using DR programs on different load buses of the system under various scenarios.

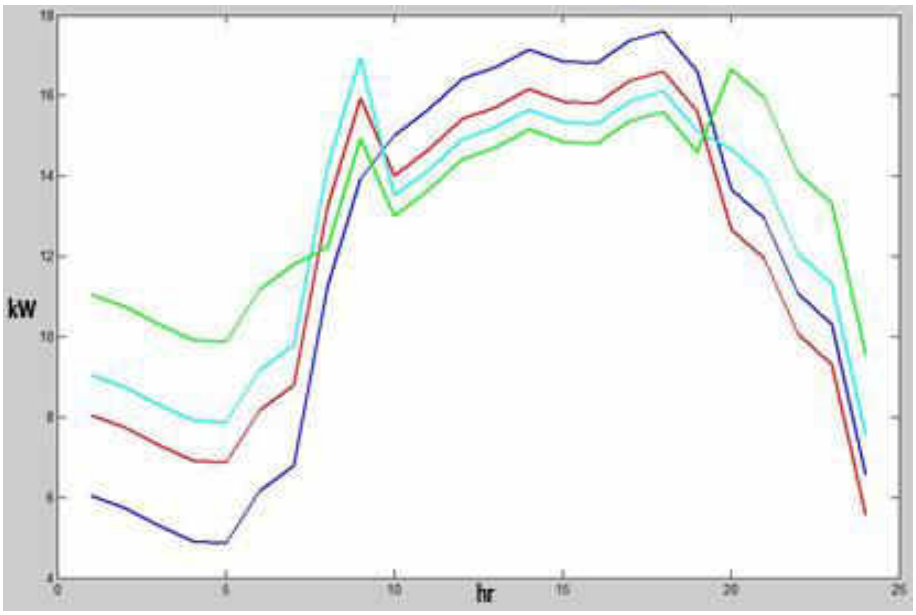

Figure 106. Load profile on Bus 2. Colors codes as defined in Table 13.

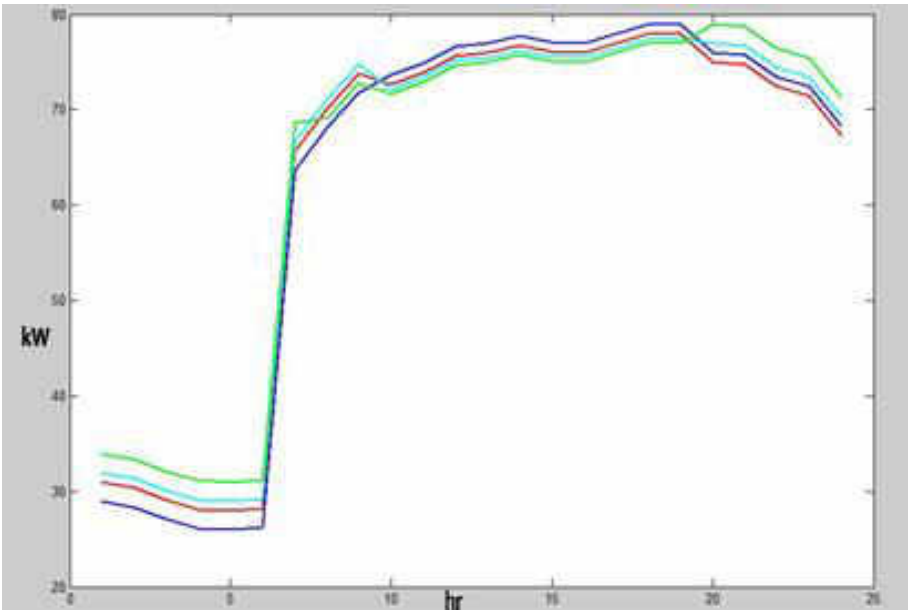

Figure 107. Load profile on Bus 3. Colors codes as defined in Table 13.

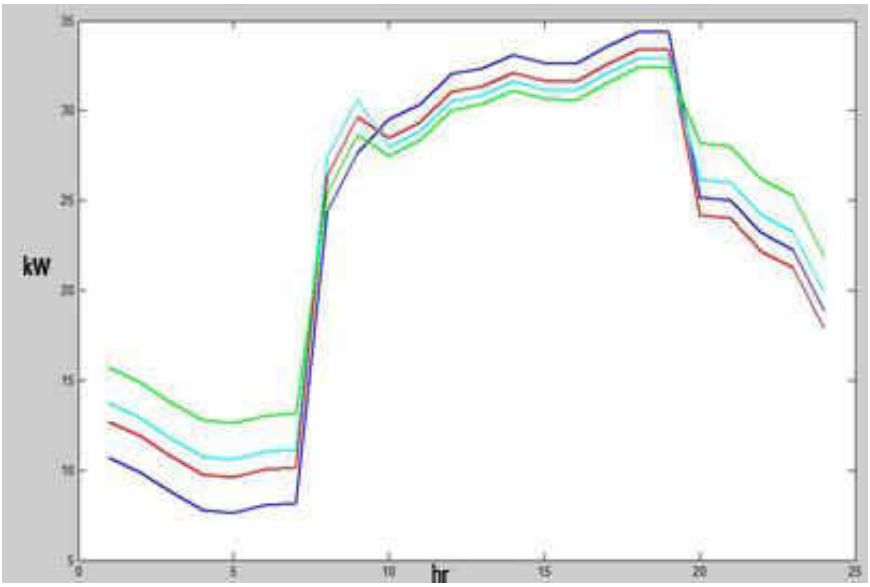

Figure 108. Load profile on Bus 4. Colors codes as defined in Table 13.

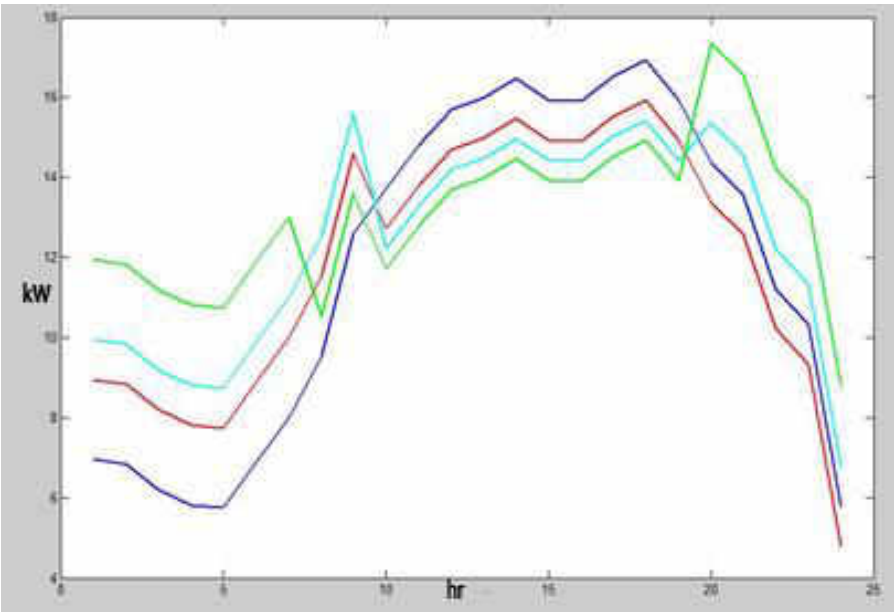

Figure 109. Load profile on Bus 5. Colors codes as defined in Table 13

It is seen in the figures that buses 2 and 5 which are more of residential nature are very sensitive to incentive and penalty values. Improper selection of these values might result in new peaks being created during the off-peak hours. Large loads (Bus 3), however, show a more robust pattern and more advanced programs and studies should be in place to effectively impress their patterns of consumption in a short run. This would highlight the important role that customer types play in determining their response to the DR programs and implies the need for models that tend to consider customer types when evaluating the demand response characteristics.

Reliability Impacts of DR Programs

Using generated plots for each DR program, overloads in each bus were calculated. For calculating the overload current from the consumption data given, electrical and statistical

data given in Appendix of this document were used. It is assumed that overload percentage on any single equipment at each bus is proportional to the total overload percentage on that bus [136]. Based on the values of overload currents and associated time durations, failure rate increases can be calculated for each case. Figure 110 below shows the failure rate increase over time period of 50 years for various DR programs applied to the test system.

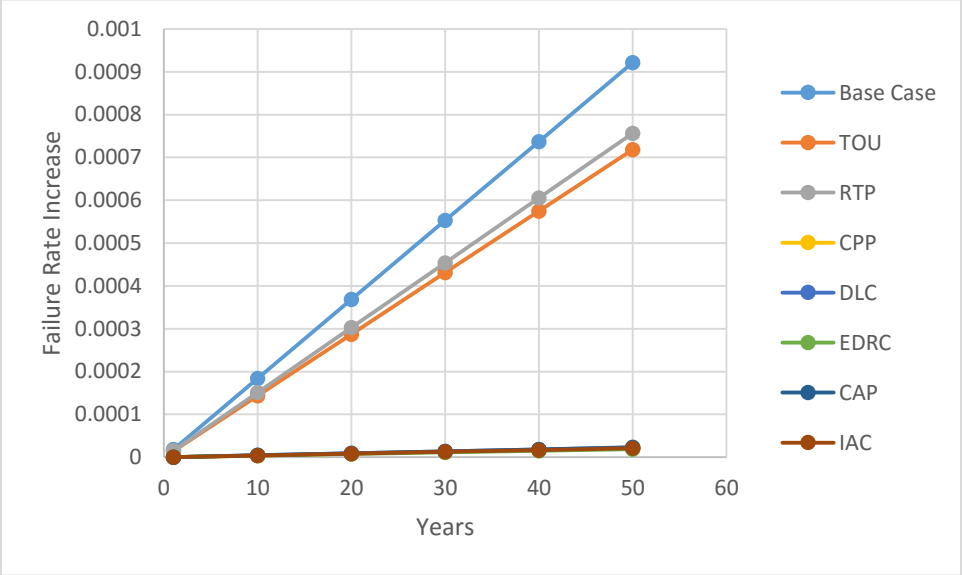

Figure 110. Failure rate increase of transformer T_3 over time period of 50 years for various DR programs applied to the test system..

CHAPTER VIII
CONCLUSIONS AND SUGGESTED FUTURE WORK

In this dissertation a new model was proposed and developed to study the impact of overcurrent levels in power system reliability. This model will enable us to consider the impact of various types of fault current limiting devices (FCL's) from an angle that hasn't been seen or discussed before. Using the proposed model, impact of various types of FCL's and protection systems on failure rates were studied and compared. Current limiting devices are mainly used to reduce short circuit stresses on components and the proposed model allows to quantify this impact. These types of studies would assist utilities in their long term plantings and asset management programs. Overload currents and utility programs for reducing their impact, known as Demand Response (DR) programs, were also modeled using this approach. Since overloads have less a sever role in causing power system outages, their reliability impacts have been neglected in conventional outage-based models reported in the literatures.

The author believes that continuation of line of study presented in this dissertation would lead to new era of reliability evaluation of power systems using electrical parameters. Novel reliability methods that use electrical parameters of the system, as opposed to the merely statistical approaches, not only will give quicker and more accurate results, but will enable analysis and decision making routines that commensurate with available electrical parameters and measures of the electrical network. Some of the possibilities to continue this work further are include but not limited to:

1- Find parameters of the failure rate model presented in this dissertation from stress-strength and accelerated lifetime tests on any given equipment. The obtained parameters can then be used to accurately model and schedule preventive maintenance for that equipment.
2- Incorporate the electrical models of failure rates in various aspects of reliability evaluations and compare the results with those from traditional models.
3- Perform security and dependability analysis for more types of protection systems and compare their effects on failure rates based on their fault clearance times.
4- Find maintenance intervals for power system components based on magnitude and duration of fault currents in that area. Fault current magnitudes and durations can be found from historical data obtained from fault recorders in substations, or calculated from short circuit analysis. Dependability/security analysis is also required to find fault clearance times by the protection systems.
5- Use the model developed for failure rate in this dissertation to model other reliability indices for a component such as MTTR, MTTF, unavailability, etc.
6- Study other methods of fault current reduction presented in chapter two and model them using the developed approach. Pros and Cons of each method can be calculated and compared and most efficient method introduced for each application.
7- In this dissertation, effects of fault currents as the dominant cause of components failure, were modelled on reliability. Models can be developed to consider and include other electrical parameters such as over-voltages. Although historically

over-voltages are having a less important role in component deterioration -especially in modern power systems with high standard on system grounding-, they are still posing threats to insulations and material strengths causing undesired effects that could result in damages.

REFERENCES

[1] S. Behzadirafi and H. Salehfar, "Preventive Maintenance Scheduling Based on Short Circuit and Overload Currents," *IEEE Transactions on Smart Grid,* vol. Vol.6, no. 4, pp. 1740-1747, July 2015.

[2] R. Smeets, L. Te Paske and A. Lathouwers, "Significant Failure Rate Observed at Short Circuit Testing of Large Power Transformers," in *IEEE PES Transmission and Distribution Conference and Exposition*, Sep. 2003.

[3] R. Billinton and R. Allan, Reliability Evaluation of Engineering Systems: Concepts and Techniques", Plenum Press, 1994., Plenum Press, 1994.

[4] H. Schmitt, "Fault current limiters report on the activities of CIGRE," in *Power Eng. Soc. Gen. Meeting*, Montreal, QC, Canada, 2006.

[5] I. Vajda, S. Semperger, T. Porjesz, A. Szalay, V. Meerovich, V. Sokolovsky and W. Gawalek, "Three phase inductive HTS fault current limiter for the protection of a 12 kVA synchronous generator," *IEEE Transactions on Applied Superconductivity,* vol. 11, no. 1, p. 2515–2518, Jun. 2001.

[6] Y. Shirai, A. Mochida, T. Morimoto, M. Shiotsu, T. Oide, M. Chiba and T. Nitta, "Repetitive operation of three-phase superconducting fault current limiter in a

model power system," *IEEE Transactions on Applied Superconductivity,* vol. 15, no. 2, pp. 2110-2113, June 2005.

[7] T. Sato, M. Yamaguchi, T. Terashima, S. Fukui, J. Ogawa, H. Shimizu and T. Sato, "Study on the Effect of Fault Current Limiter in Power System With Dispersed Generators," *IEEE Transactions on Applied Superconductivity,* vol. 17, no. 2, pp. 2331-2334, June 2007.

[8] Y. Shirai, K. Furushiba, Y. Shouno, M. Shiotsu and T. Nitta, "Improvement of power system stability by use of superconducting fault current limiter with ZnO device and resistor in parallel," *IEEE Transactions on Applied Superconductivity,* vol. 18, no. 2, pp. 680-683, June 2008.

[9] S.-Y. Kim and J.-O. Kim, "Reliability Evaluation of Distribution Network With DG Considering the Reliability of Protective Devices Affected by SFCL," *IEEE Transactions on Applied Superconductivity, ,* vol. 21, no. 5, pp. 3561-3569 , Oct. 2011.

[10] S.-Y. Kim, W.-W. Kim and J.-O. Kim, "Evaluation of Distribution Reliability with Superconducting Fault Current Limiter," in *10th International Conference on Environment and Electrical Engineering*, May 2011.

[11] V. V. Vadlamudi, O. Gjerde and G. Kjolle, "Impact of Protection System Reliability on Power System Reliability: : A new minimal cutset approach," *IEEE PES Transmission and Distribution Conference and Exposition PES T and D,* 10 November 2014.

[12] C. Singh and A. Patton, "Models and concepts for power system reliability evaluation including protection-system failures," *International Journal of Electrical Power and Energy Systems,* vol. 2, no. 24, pp. 161-168 , 1980.

[13] K. Jiang and C. Singh, "New Models and Concepts for Power System Reliability Evaluation Including Protection System Failures," *IEEE Transactions on Power Systems,* vol. 26, no. 4, pp. 1845-1855, Nov. 2011.

[14] R. Billinton and R. N. Allan, Reliability Evaluation of Power Systems, Springer, 1996.

[15] I. Rahmati and M. Fotuhi-Firuzabad, "Reliability evaluation of HV substations in the presence of Fault Current Limiter," in *IEEE Bucharest PowerTech*, June 2009.

[16] X. Yu and C. Singh, "Power system reliability analysis considering protection failures," *IEEE Power Engineering Society Summer Meeting,* vol. 2, pp. 963-968, 2002.

[17] M. Shahidehpour, R. Allan and P. Anderson, "Effect of protection systems on bulk power reliability evaluation," *IEEE Transactions on Power Systems,* vol. 9, no. 1, 1994.

[18] S.-Y. Kim, I.-S. Bae and J.-O. Kim, "An Optimal Location for Superconducting Fault Current Limiter Considering Distribution Reliability," in *IEEE PES General Meeting*, July 2010.

[19] A. Brandão, "A model for substation reliability analysis including overload effects," *International Journal of Electrical Power and Energy Systems ,* vol. 9, no. 4, pp. 194-205, 1987.

[20] H. Aalami, M. Parsa Moghaddam and G. Yousefi, "Modeling and prioritizing demand response programs in power markets," *Electric Power Systems Research,* vol. 80, p. 426–435, 2010.

[21] C. King and D. Delurey, " Efficiency and demand response, Twins, Siblings, or Cousins?," *Pablic Utilities Fortnightly,* Mar. 2005.

[22] S. Behzadirafi and H. Salehfar, "Using Superconducting Fault Current Limiters to Enhance Reliability of Power Transmission System," in *IEEE PES General Meeting*, Minneapolis , 2008.

[23] L. Kovalsky, "Applications of Superconducting Fault Current Limiters in Electric Power Transmission Systems," *IEEE Transactions on Applied Superconductivity,* vol. 15, no. 2, June 2005.

[24] L. Kovalsky, X. Yuan, K. Tekletsadik, A. Keri, J. Bock and F. Breuer, "Applications of SupApplications of Superconducting Fault Current Limiters in Electric Power Transmission Systems," *IEEE TRANSACTIONS ON APPLIED SUPERCONDUCTIVITY,* vol. 15, no. 2, pp. 2130-2133, JUNE 2005.

[25] X. Wu, J. Mutale, N. Jenkins and G. Strbac, "An investigation of Network Splitting for Fault Level Reduction," The Manchester Centre for Electrical Energy (MCEE), UMIST, January 2003.

[26] D. Sarkar, D. Roy, A. Choudhury and S. Yamada, "Performance analysis of saturated iron core superconducting fault current limiter using Jiles–Atherton hysteresis model," *Journal of Magnetism and Magnetic Materials,* vol. 390, pp. 100-106, September 2015.

[27] M. A. H. Sadi and M. H. Ali, "Transient stability enhancement by bridge type fault current limiter considering coordination with optimal reclosing of circuit breakers," *Electric Power Systems Research,* vol. 124, p. 160(13), 2015.

[28] H.-C. Jo and S.-K. Joo, "Superconducting Fault Current Limiter Placement for Power System Protection Using the Minimax Regret Criterion," *IEEE Transactions on Applied Superconductivity,* vol. 25, no. 3, 1 June 2015.

[29] F. Zheng, C. Deng, L. Chen, S. Li, Y. Liu and Y. Liao, "Transient performance improvement of microgrid by a resistive superconducting fault current limiter," *IEEE Transactions on Applied Superconductivity,* vol. 25, no. 3, 1 June 2015.

[30] B. Li, F. Guo, J. Wang and C. Li, "Electromagnetic transient analysis of the saturated iron-core superconductor fault current limiter," *IEEE Transactions on Applied Superconductivity,* vol. 25, no. 3, 1 June 2015.

[31] S. Behzadirafi and M. H. Varahram, "A Novel Approach to Modeling the Superconductive Shielded Core Reactor (SSCR)," in *IFACPPS Power Plants and Power Systems Control*, September 2003.

[32] M. Ichikawan and M. Okazaki, "A Magnetic Shielding Type Superconducting Fault Current Limiter Using a Bi2212 Thick Film Cylinder," *IEEE Transactions on Applied Superconductivity,* vol. 5, no. 2, June 1995.

[33] J. Cave, D. Willen, R. Nadi and Y. Brissette, "Development of Inductive Fault Current Limiters Up to 100kVA Class Using Bulk HTS Materials," *IEEE Transactions on Applied Superconductivity,* vol. 9, no. 2, June 1999.

[34] M. M. Aly and E. A. Mohamed, "Comparison between Resistive and Inductive Superconducting Fault Current Limiters for Fault Current Limiting," in *2012 Seventh International Conference on Computer Engineering & Systems*, Nov. 2012.

[35] S. Behzadirafi, H. Salehfar and H. Varahram, "Limiting Fault Currents in Wind Power Plants Using Superconductive Shielded Core Reactors," in *IEEE PES General Meeting*, 2008.

[36] S. Behzadirafi, M. Fotuhi-Firuzabad and T. Sidhu, "Reliability Enhancement in Switching Substations Using Fault Current Limiters," in *2006 International Conference on Probabilistic Methods Applied to Power Systems*, June 2006.

[37] X. N. Bin Shu, Z. Y. Li, Q. H. Kai Zhang, B. Q. Xin Sun, B. Q. Wei Li, B. Q. Liu, B. Q. Lou and B. Yu Liu, "Behaviors and Application Prospects of Superconducting Fault Current Limiters in Power Grids," *IEEE Transactions on Applied Superconductivity,* vol. 24, no. 5, pp. 1-4, Oct. 2014.

[38] J. Cerulli, "Requirements for a Superconducting Fault Current Limiter in the Utility Bus-Tie Location," in *IEEE proceedings* , 1998.

[39] G. Cakal, F. G. Bagriyanik and M. Bagriyanik, "The Effect of Fault Current Limiters on Distribution Systems with Wind Turbine Generators,"

INTERNATIONAL JOURNAL of RENEWABLE ENERGY RESEARCH , vol. 3, no. 1, 2013.

[40] M. E. Elshiekh, D. E. A. Mansour and A. M. Azmy, "Improving Fault Ride-Through Capability of DFIG-Based Wind Turbine Using Superconducting Fault Current Limiter," *IEEE Transactions on Applied Superconductivity,* vol. 23, no. 3, 2013.

[41] H.-I. Du, "Evaluation on Current-Limiting Performance With the Fault Type of the 3-Phase Resistive Type SFCLs," *IEEE Transactions on Applied Superconductivity,* vol. 23, no. 3, 2013.

[42] K.-H. Hartung and V. Schmidt, "Limitation of Short Circuit Current by an I - Limiter," in *Electrical Power Quality and Utilization*, Lodz, Poland, September 15-17, 2009.

[43] E. Dreimann, V. Grafe and K. Hartung, *Schutzeinrichtungen zur Begrenzung von Kurzschlussströmen,* vol. 115, no. 9, pp. 492-494, 1994.

[44] K. H. Hartung, "Is-limiter, the Solution for High Short- Circuit Current Applications," ABB Calor Emag, 2002.

[45] H. Seyedi and B. Tabei, "Appropriate Placement of Fault Current Limiting Reactors in Different HV Substation Arrangements," in *Circuits and Systems*, 2012.

[46] S. Yadav, G. Choudhary and R. Mandal, "Review on Fault Current Limiters," *International Journal of Engineering Research & Technology (IJERT),* vol. 3, no. 4, pp. 1595-1603, April - 2014.

[47] A. Abramovitz and K. M. Smedley, "Survey of Solid-State Fault Current Limiters," *IEEE Transactions on Power Electronics,* vol. 27, no. 6, June 2012.

[48] P. R. Deo and T. P. Shah, "Innovative electromagnetic dynamic fault current limiter operating at ambient temperature for smart grids," in *IEEE Innovative Smart Grid Technologies*, Gaithersburg, MD, January 2010.

[49] P. R. Deo and T. P. Shah, "Ambient-Temperature Fault Current Limiter for Electric Ship Power Systems," in *IEEE Electric Ship Technologies Symposium*, Alexandria, VA., April 2011.

[50] J. N. Nielsen and J. J. Ostergaard, "Applications of HTS fault current limiters in the Danish utility network," in *16th International Conference and Exhibition on Electricity Distribution*, 2001.

[51] H. Kado and M. Ichikawa, "Performance of a High-Tc Superconductive Fault Current Limiter- Design of a 6.6 kv Magnetic Shielding Type Superconductive Fault Current Limiter," *IEEE Transactions on Applied Superconductivity,* vol. 7, no. 2, 1997.

[52] "Fault Current Limiters - Protect Today's Electrical Grid for Tomorrow's Growth," Zenergy Power Inc..

[53] "Superconductivity for Electric Systems , Matrix Fault Current Limiter Project," Annual DOE Peer Review, 2006 .

[54] X. Yuan, K. Tekletsadik, L. Kovalsky, J. Bock, F. Breuer and S. Elschner, "Proof-of-Concept Prototype Test Results of a Superconducting Fault Current Limiter for Transmission-Level Applications," *IEEE Transactions on Applied Superconductivity,* vol. 15, no. 2, June 2005.

[55] N. E. Reimann, R. R. Cherkaoui, B. Dutoit, D. Djukic and G. Grasso, "“imulation of the transient response of a high-Tc superconducting current limiter inserted in an electrical distribution system," *IEEE Transaction on Applied Superconductivity, Vol. 7, pp: , ,* vol. 7, pp. 836-839, June 1997.

[56] V. Meerovich, V. Sokolovsky, G. Jung and S. Goren, "Inductive superconducting current limiter: state of art and prospects," in *Applied Superconductivity*, 1995.

[57] Y. Zhang and R. A. Dougal, "State of the Art of Fault Current Limiters and Their Applications in Smart Grid," *2012 IEEE Power and Energy Society General Meeting,* pp. 1-6, July 2012.

[58] B.-I. Jung, H.-S. Choi, Y.-S. Cho and D.-C. Chung, "Current Limitation and Power Burden of a Flux-Coupling Type SFCL in the Three-Phase Power System According to Turn's Ratio and Fault Type," *IEEE Transactions on Applied Superconductivity,* vol. 21, no. 3, pp. 1225-1228, June 2011.

[59] J. Kim, S. Lim and J. Kim, "Analysis on fault current limiting and bus-voltage sag suppressing operations of SFCLs using magnetic coupling of two coils according to their application locations in a power distribution system," *Physica C: Superconductivity and its applications,* vol. 471, no. 21, pp. 1358-1363, 2011.

[60] S. Messalti and S. Belkhiat, "Comparative Study of Resistive and Inductive Superconducting Fault Current Limiters SFCL for Power System Transient Stability Improvement," *Journal of Superconductivity and Novel Magnetism,* vol. 26, no. 10, pp. 3009-3015, 2013.

[61] G. Didier, C. Bonnard, T. Lubin and J. Lévêque, "Comparison between inductive and resistive SFCL in terms of current limitation and power system transient stability," *Electric Power Systems Research,* vol. 125, pp. 150-158, August 2015.

[62] A. Morandi, "Comparison of the performances of three different types of fault current limiter in the distribution network," *Journal of Physics: Conference Series,* vol. 43, no. 1, pp. 909-912, 2006.

[63] M. M. Lanes, H. A. C. Braga and P. G. Barbosa, "Limitador de Corrente de Curto-Circuito Baseado em Circuito Ressonante Controlado por Dispositivos Semicondutores de Potência," *IEEE LATIN AMERICA TRANSACTIONS,* vol. 5, no. 5, SEPTEMBER 2007.

[64] A. Morandi, "State of the art of superconducting fault current limiters and their application to the electric power system," *Physica C,* vol. 484, p. 242–247, 2013.

[65] A. Agheli, H. A. Abyaneh, R. M. Chabanloo and H. H. Dezaki, "Reducing the impact of DG in distribution networks protection using fault current limiters," in *2010 4th International Power Engineering and Optimization Conference*, June 2010.

[66] S. Kazemi and M. Lehtonen, "Impact of smart subtransmission level fault current mitigation solutions on service reliability," *Electric Power System Research,* vol. 96, pp. 9-15, 2013.

[67] Working Group on Distribution Protection, IEEE Power System Relaying Committee Report, "Distribution Line Protection Practices, Industry Survey Results," IEEE Transactions on Power Delivery, January 1995.

[68] P. G. Slade, "The Utility Requirements for a Distribution Fault Current Limiter," *IEEE Transactions on Power Delivery,* vol. 7, no. 2, pp. 507-514, April 1992.

[69] P. A. Anderson, Power System Protection, IEEE Press, 1999.

[70] M. Panteli, P. Crossley and J. Fitch, "Quantifying the Reliability Level of System Integrity Protection Schemes," in *IET Generation Transmission & Distribution*, 2014.

[71] R. Billinton, M. Fotuhi-Firuzabad and T. S. Sidhu, "Determination of the Optimum Routine Test and Self-Checking Intervals in Protective Relaying Using a Reliability Model," *IEEE Power Engineering Review,* vol. 22, no. 7, 2002.

[72] R. C. d. Santos and E. C. Senger, "Transmission lines distance protection using artificial neural networks," *International Journal of Electrical Power and Energy Systems,* vol. 33, no. 3, pp. 721-730 , 2011.

[73] Y. G. Paithankar and S. R. Bhide, Fundamentals of Power System Protection, PHI Learning, 2013.

[74] G. A. T&D, Protective Relay Application Guide, GEC ALSTOM T&D, 1987.

[75] E. O. Schweitzer III and J. J. Kumm, "Statistical Comparison and Evaluation of Pilot Protection Schemes," in *12th Annual CEPSI Exhibition*, November 2–6, 1998.

[76] E. O. Schweitzer, B. Fleming, T. J. Lee and P. M. Anderson, "Reliability Analysis of Transmission Protection Using Fault Tree Methods," in *24th annual Western Protective Relay Conference*, 1997.

[77] X. Yuan, K. Tekletsadik, L. Kovalsky, J. Bock, F. Breuer and S. Elschner, "Proof-of-Concept Prototype Test Results of," *IEEE TRANSACTIONS ON APPLIED SUPERCONDUCTIVITY,* vol. 15, no. 2, JUNE 2005.

[78] "Matrix Fault Current Limiter Project," Annual DOE Peer Review, 2006.

[79] "Transmission Grid MFCL Prototype Developed," *Transmission and Distribution,* April 2005.

[80] R. Billinton and R. N. Allan, Reliability Evaluation of Engineering Systems: Concepts and Techniques, Springer, June 30, 1992.

[81] L. Ye and L. Z. Lin, "Study of Superconducting Fault Current Limiters for System Integration of Wind," *IEEE Transactions on Applied Superconductivity,* vol. 20, no. 3, pp. 1229-1233, 2010.

[82] G. Tang and M. R. Iravani, "Application of a Fault Current Limiter To Minimize Distributed Generation Impact on Coordinated Relay Protection," in *International Conference on Power Systems Transients (IPST'05)*, Montreal CA, June 2005.

[83] S. A. A. Shahriari, M. Abaspour, A. Yazdian and M. R. Haghifam, "Minimizing the Impact of Distributed Generation on Distribution Protection System by Solid State Fault Current Limiter," in *2010 IEEE PES Transmission and Distribution Conference and Exposition:Smart Solutions for a Changing World*, New Orleans, April 2010.

[84] M. H. Varahram and S. Behzadirafi, "A Novel Approach to Modelling the Superconductive Sshielded Core Reactor," in *Power Plants and Power Systems Control 2003*, 2003.

[85] Fitzgerald and Kingsley, Electric Machinery, McGraw-Hill , 2013.

[86] H. Shim, S.-Y. Kim, I.-S. Bae and J.-O. Kim, "The Reliability-Based Model for Superconducting Fault Current Limiter," in *IEEE Transmission and Distribution Asia* , 2009.

[87] S.-Y. Kim, J.-O. Kim, I.-S. Bae and J.-M. Cha, "Distribution Reliability Evaluation Affected by Superconducting Fault Current Limiter," in *IEEE/PES Transmission and Distribution Conference and Exposition: Latin America*, 2010 .

[88] S.-Y. Kim, I.-S. Bae and J.-O. Kim, "An Optimal Location for Superconducting Fault Current Limiter Considering Distribution Reliability," in *EEE PES General Meeting*, July 2010.

[89] M. Fotuhi-Firuzabad, F. Aminifar and I. Rahmati, "Reliability study of HV substations equipped with the fault current limiter," *IEEE Transactions on Power Delivery,* vol. 27, no. 2, pp. 610-617, April 2012.

[90] Q. Binh Dam and A. P. Sakis Meliopoulos, "Reliability Implications of Increased Fault Currents and Breaker Failures," in *iREP Symposium- Bulk Power System Dynamics and Control* , Charleston, SC, USA, August 19-24, 2007.

[91] L. M. Shooman, Probabilistic Reliability: An Engineering Approach, New York: McGraw-Hill, 1968.

[92] D. Roy and G. V. Rao, Elements of Structural Dynamics: A New Perspective, Wiley, 2012.

[93] L. Garver, "Adjusting maintenance schedules to levelize risk," *IEEE Transactions on Power Apparatus and Systems,* Vols. PAS-91, no. 5, p. 2057–2063, Sep./Oct. 1991.

[94] P. Hilber, V. Miranda, M. Matos and L. Bertling, "Multiobjective Optimization Applied to Maintenance Policy for Electrical Networks," *IEEE Transactions on Power Systems,* vol. 22, no. 4, pp. 1675-1682, 2007.

[95] M. Rausch and L. Haitao, "Joint Production and Spare Part Inventory Control Strategy Driven by Condition Based Maintenance," *IEEE Transactions on Reliability,* vol. 59, no. 3, pp. 507-516, 2010.

[96] D. Karamousantas, K. G. Technol. Educ. Inst. of Kalamata, G. Chatzarakis, D. Oikonomou and L. Ekonomou, "Effective insulator maintenance scheduling using artificial neural networks," *Generation, Transmission & Distribution, IET ,* vol. 4, no. 4, pp. 479 - 484.

[97] K. Dahal and J. McDonald, "A review of generator maintenance scheduling using artificial intelligence techniques," in *Proceedings of 32nd Universities Power Engineering Conference*, Manchester, U.K, 1997.

[98] C. Tsatsoulis and M. Van Dyne, "Integrating artificial intelligence techniques to generate ground station schedules," in *IEEE Aerospace Conference*, 2014.

[99] e. a. Yong Fu, "Coordination of Midterm Outage Scheduling With Short-Term Security-Constrained Unit Commitment," *IEEE Transactions on Power Systems,* vol. 24, no. 4, November 2009.

[100] R. Briš, "Exact reliability quantification of highly reliable systems with maintenance," *Reliability Engineering & System Safety,* vol. 95, no. 12, p. 1286–1292, 2009.

[101] L. E. E., "Introduction to Reliability Engineering,," Wiley, Nov 15 1995.

[102] E. C. E., An Introduction to Reliability and Maintainability Engineering, McGraw Hill, 1997.

[103] R. Briš, "Exact reliability quantification of highly reliable systems with maintenance," in *Safety, Reliability and Risk Analysis: Theory, Methods and Applications*, London, 2009.

[104] H. Saadat, Power System Analysis, PSA Publishing, June 16, 2010.

[105] D. Zhou, C. Li and Z. Wang, "Power Transformer Lifetime Modeling," in *Proceedings of the IEEE 2012 Prognostics and System Health Management Conference*, May 2012.

[106] C. W. Gellings, "Observations on Investments in Smart Grid Technologies," EPRI, March 6, 2009..

[107] G. Strbac, "Demand side management: Benefits and challenges," *Energy Policy,* vol. 36, 2008.

[108] F. Boshell and O. Veloza, "Review of developed demand side management programs including different concepts and their results," in *IEEE/PES Transmission and Distribution Conference and Exposition Latin America*, 2008. .

[109] S. Nadel, "Utility Demand-Side Management Experience and Potential- A Critical Review," *Annual Review of Energy and the Environment,* vol. 17, pp. 507-535 , November 1992.

[110] "DOE website: http://www.energy.gov," DOE. [Online].

[111] U. D. o. Energy, "The Smart Grid: An Introduction".

[112] U. D. o. Energy, "Benefits of Demand Response in Electricity Markets and Recommendations for Achieving Them," February 2006.

[113] F. Boshell and O. Veloza, "Review of developed demand side management programs including different concepts and their results," in *IEEE/PES Transmission and Distribution Conference and Exposition: Latin America*, 2008.

[114] B. J. Kirby, "Demand Response for Power System Reliability: Frequently Asked Questions," December 2006.

[115] FERC, "Assessment of Demand Response and Advanced Metering," FERC, August, 2006.

[116] S. Adzanu, "Reliability Assessment of Non-Utility Generation and Demand-Side Management in Composite Power Systems," PhD Thesis, University of Saskatchewan, , Saskatoon, 1998.

[117] H. Dange, "Bulk Electric System Reliability Evaluation Incorporating Wind Power and Demand Side Management," PhD Thesis, Saskatoon, February 2010.

[118] D. S. Kirschen, G. Strbac, P. Cumperayot and D. d. P. Mendes, "Factoring the Elasticity of Demand in Electricity Prices," *IEEE TRANSACTIONS ON POWER SYSTEMS,* vol. 15, May 2000.

[119] P. Khajavi, H. Monsef and H. Abniki, "Load Profile Reformation through Demand Response Programs," in *Modern Electric Power Systems*, Wroclaw, Poland, 2010.

[120] H. Aalami, M. Parsa Moghaddam and G. Yousefi, "Demand response modeling considering Interruptible/Curtailable loads and capacity market programs," *Applied Energy,* vol. 87, p. 243–250, 2010.

[121] M. Parsa Moghaddam, A. Abdollahi and M. Rashidinejad, "Flexible demand response programs modeling in competitive electricity markets," *Applied Energy,* vol. 88, p. 3257–3269, 2011.

[122] P. K. Narayana, R. Smythb and A. Prasadc, "Electricity consumption in G7 countries: A panel cointegration analysis," *Energy Policy,* p. 4485–4494, 2007.

[123] D. R. Kamerschen, P. G. Klein and D. V. Porter, "Market Structure in the US Electricity Industry: A Long Term Perspective," *Energy Economics,* pp. 731-751, 2005.

[124] R. Inglesi-Lotz, "The Evolution of Price Elasticity Demand in South Africa: A Kalman Filter Application," *Energy Policy,* 2011.

[125] J. I. Silk and F. L. Joutz, "Short and Long-Run Elasticity in US Residential Electricity Demand: A Co-Integration Approach," *Energy Economics,* vol. 19, pp. 493-513, 1997.

[126] I. Matsukawa, "Household Response to Optional Peak Load Pricing of Electricity," *Journal of Regulatory Economics,* vol. 20, pp. 249-267, 2001.

[127] P. Narayan and R. Smyth, "The Residential Demand for Electricity in Australia: An Application of the Bounds Testing Approach to Co-integration," *Energy Policy,* vol. 33, pp. 457-464, 2005.

[128] H. Neeland, "The Residential Demand for Electricity in the United States," *Economic Analysis & Policy,* 2009. .

[129] M. Beenstock, E. Goldin and D. Nabot, "The Demand for Electricity in Israel," *Energy Economics,* vol. Vol. 21, p. 168–183, 1999.

[130] S. Adzanu, *RELIABILITY ASSESSMENT OF NON-UTILITY GENERATION AND DEMAND-SIDE MANAGEMENT IN COMPOSITE POWER SYSTEMS,* Saskatoon,, 1998.

[131] IEEE, "IEEE Reliability Test System," *IEEE Transactions on Power Apparatus and Systems,* 1979.

[132] R. Ghajar, "Evaluation of the Marginal Outage Costs in Electric," Ph.D. Thesis, June 1993.

[133] S. Adzanu, "RELIABILITY ASSESSMENT OF NON-UTILITY GENERATION AND DEMAND-SIDE MANAGEMENT IN COMPOSITE POWER SYSTEMS," PhD Thesis, Saskatoon, 1998.

[134] R. Billinton, S. Kumar, K. Chowdhury, K. Chu, K. Debnath and L. Goel, "A Reliability Test System for Educational Purposes- Basic Data. ,. ,, pp. 1238-1244.," *IEEE Transaction on Power Systems,* August 1989.

[135] R. Billinton, S. Kumar and N. Chowdhury, "A Reliability Test System For Educational Purposes-Basic Results," *IEEE Transactions on Power Systems,* pp. 319-325, February 1990.

[136] S. Behzadirafi and H. Salehfar, "A utility control panel for demand response planning," in *North American Power Symposium (NAPS)*, Manhattan, KS, 2013.

[137] I. C. Report, ""IEEE Reliability Test System"," *IEEE Transactions on Power Apparatus and Systems,* 1979.

[138] E. P. R. Institute, "Strategic Program: Power Electronics," *EPRI Research ,* July 2011.

[139] "Solid State Current Limiter – Product Datasheet," Silicon Power Corporation, August 2008.

[140] B. Jack, S. Marcelo, C. Joe and H. A. Mantooth, "Initial Development of a Solid-State Fault Current Limiter for Naval Power Systems Protection," in *IEEE Electric Ship Technologies Symposium (ESTS)*, Baltimore, MD, April 2009.

[141] J. Zarnikaua, G. Landrethb, I. Hallettb and S. Kumbhakarc, "Industrial customer response to wholesale prices in the restructured Texas electricity market," *Energy, Vol.32(9),* vol. 32, no. 9, pp. 1715-1723 , 2007.

[142] R. Billinton, M. Fotuhi and T. Sidhu, "Determination of the Optimum Routine Test and Self-Checking Intervals in Protective Relaying Using a Reliability Model," *IEEE POWER ENGINEERING REVIEW,* vol. 22, no. 7, JULY 2002.

APPENDICES

Table1. Eliminated failure modes for Single Sectionalized bus arrangement

Arrangement	Proposed Configuration	Failure modes that are eliminated	Operation taken to clear the fault
single sectionalized bus arrangement	SFCL + LID @ 1a, 2a, 4a, 6b	1A *	LID No. "1a" opens
		4A	LID No. "4a" opens
		2A+4S	LID No. "2a" opens
		6A+4S	LID No. "6b" opens
		2A	LID No. "2a" opens

* Active Failure in component No.1: Short circuit in breaker No. 1
** Active failure in component No.13 and total failure in component No.1: Short circuit in component No. 13 and any failure (short circuit or open circuit) in components No.1.
"S" is "stuck breaker" and denotes the event that a breaker doesn't open when required.

Table2. Eliminated failure modes for Breaker and a Half

Breaker and a half	SFCL + Lid @ 7a, 7b, 9a, 9b, 13a, 13b,	3A+13S	LID No. "3b" opens
		9A+8S	LID No. "9a" opens
		13A+3S	LID No. "13a" opens
		13A+1 **	LID No. "13a" opens
		13A+6	LID No. "13a" opens
		5A+13S+1	LID No. "13b" opens
		5A+13S+6	LID No. "13b" opens
		7A+4S+1	LID No. "7b" opens
		7A+4S+6	LID No. "13a" opens
		7A+9S+1	LIDs No.s "7a" & "7b" open
		7A+9S+6	LIDs No.s "7a" & "7b" open
		10A+13S+1	LID No. "13a" opens
		12A+7S+1	LIDs No.s "7a" & "9b" open

Table3. Eliminated failure modes for Breaker and a Half

main and transfer bus system	SFCL1 + Lid @ 10a, 10b	10A	LIDs No.s "10a" & "10b" open
		4A+10S	LID No. "10b" opens
	SFCL2 + Lid @ 11a, 11b	11A	LIDs No.s "11a" & "11b" open
		1A+11S	LID No. "11b" opens
		4A+11S	LID No. "11b" opens
	SFCL1 +SFCL2 Lid @ 9a, 10a, 10b, 11a, 11b	Above cases + 9A	LID No. "9a" opens

Table 4. Failure modes of main and transfer bus system

Failure Event	λ (f/yr)	r (hours)	U (hours/yr)	
8	0.01	1	0.01	
5+6	2.28311E-08	0.5	1.14155E-08	
7+10	2.73973E-07	6	1.64384E-06	
7+11	2.73973E-07	6	1.64384E-06	
7+12	1.82648E-07	3	5.47945E-07	
13	0.01	4	0.04	
14	0.01	4	0.04	
3A	0.005	1	0.005	
5A	0.005	1	0.005	
6A	0.005	1	0.005	
7A	0.005	1	0.005	
9A	0.005	1	0.005	
10A	0.005	1	0.005	
11A	0.005	1	0.005	
4A+7	7.42009E-08	3	2.22603E-07	
1A+6	1.14155E-08	0.8	9.13242E-09	
2A+5	1.14155E-08	0.5	5.70776E-09	
1A+7	7.42009E-08	0.92307692	6.84932E-08	

1A+11S	0.0005	1	0.0005	
2A+6S	0.0005	1	0.0005	
4A+9S	0.0005	1	0.0005	
4A+11S	0.0005	1	0.0005	
4A+10S	0.0005	1	0.0005	
TOTAL	0.0675008	1.88893	0.127504153	
Total with FCL1	0.0580009	2.03452	0.118004153	
Total with FCL2	0.0575008	2.04352	0.117504153	
Total with FCL1 & FCL2	0.0515008	2.16509	0.111504153	
FCl1				
FCL2				

Table 5. Failure Modes of Single Sectionalized Bus Arrangement

quipment	Failure Rate (f/yr)			Repair Time (hrs)	Switching Time(hrs)	Pc
	Open Circuit	Short Circuit	Total			
Power Transformer	0.015	0.02	0.035	55	1	
Circuit Breaker	0.005	0.005	0.01	12	1	0.1
Disconnector Switch	0.005	0.005	0.01	4	1	
Bus Bar	0.005	0.005	0.01	4	1	

Failure Event	λ (f/yr)	r (hours)	U (hours/yr)
5	0.01	12	0.12
3	0.01	4	0.04
1+2	2.73973E-07	6	1.64384E-06
1+4	2.73973E-07	6	1.64384E-06
1A	0.005	1	0.005

4A	0.005	1	0.005
6A+1	7.42009E-08	0.923076923	6.84932E-08
2A+4S	0.0005	1	0.0005
6A+4S	0.0005	1	0.0005
Total	0.031000622	5.516126591	0.171003356
Total with FCL	0.020000622	7.999918952	0.160003356
Δ I	0.011	Δ I	0.011

Table 6:Failure Modes of Breaker and a Half System

Equipment	**Failure Rate (f/yr)**			**Repair Time (hrs)**	**Switching Time(hrs)**	**Pc**
	Open Circuit	**Short Circuit**	**Total**			
Power Transformer	0.015	0.02	0.035	55	1	0.1
Circuit Breaker	0.005	0.005	0.01	12	1	
Disconnector Switch	0.005	0.005	0.01	4	1	
Bus Bar	0.005	0.005	0.01	4	1	

Failure Event	**λ (f/yr)**	**r (hours)**	**U (hours/yr)**	
11	0.01	4	0.04	Load Point of Interest: L1
8+6	2.73973E-07	6	1.64384E-06	
10+6	1.82648E-07	3	5.47945E-07	
1+2	9.13242E-08	2	1.82648E-07	
6+9	2.73973E-07	6		
6+7	2.73973E-07	6		
6A	0.005	1	0.005	

6A+2	2.85388E-08	0.8	2.28311E-08
6A+6aS	0.0005	1	0.0005
8A	0.005	1	0.005
1A+8	9.13242E-08	3	2.73973E-07
1A+10	4.56621E-08	2	9.13242E-08
1A+9	9.13242E-08	3	2.73973E-07
1A+7	9.13242E-08	3	2.73973E-07
2A+6	9.13242E-08	3	2.73973E-07
3A+2	2.85388E-08	0.8	2.28311E-08
3A+8	7.42009E-08	0.923076923	6.84932E-08
3A+10	2.85388E-08	0.8	2.28311E-08
3A+7	7.42009E-08	0.923076923	6.84932E-08
3A+9	7.42009E-08	0.923076923	6.84932E-08
4A+1	2.85388E-08	0.8	2.28311E-08
4A+6	7.42009E-08	0.923076923	6.84932E-08
7A+1	2.85388E-08	0.8	2.28311E-08
12A+6	9.13242E-08	3	2.73973E-07
1A+6S	0.0005	1	0.0005
3A+6S	0.0005	1	0.0005
3A+4S	0.0005	1	0.0005

4A+3S	0.0005	1	0.0005
9A+8S	0.0005	1	0.0005
10A+8S	0.0005	1	0.0005
Total	0.023502038	2.276578078	0.053504224
Total with FCL1	0.018502066	2.621558372	0.048504247
Δ I	0.004999971		0.004999977
Total with FCL2	0.022502038	2.333309743	0.052504224
Δ I	0.001		0.001
Total with FCL1&2	0.017502066	2.714207912	0.047504247
Δ I	0.005999971		0.005999977
	Eliminated due to FCL1		
	When FCL1 is installed		
	Eliminated due to FCL2		

Table 7: Electrical data of Sporn Substation

Transformer T_3	Short Circuit Capacity	Customer Plant	Loads	Unit #5
400 MVA, 345 Y kV/138 Δ kV	6200 MVA	50 MW	350 MW, Load factor 96%	Up to 450 MW

Table 8. Modes of operation for Sporn Substation

Mode	Description	Transformer T_3 status	Current through FCL	Details
1	Normal Operation:	Normal carrying light load with assistance from T_4 and Unit #5	400 Arms	Unit #5 Generator in service, T_3 and T_4 each carry light load
2	Unit #5 Generator out of service	Share load with T_4	1250 Arms	T_3 and T_4 share load
3	Unit #5 Generator is down and either T3 or T4 fails	Remaining transformer will provide all load	Up to 2300Arms (if T4 fails)	
4	Fault between FCL and T_3	Close fault in Secondary of Transformer	26kArms	E/E3 Breakers open and lock-out
5	Fault in 138kV system	Fault in Secondary of Transformer	13.8kArams	Re-close scheme employed –up to 4 re-close with possibility of stuck breaker

Table 9: Electrical Data of the IEEE Reliability Test System: Generators

Unit Number	Bus Number	Rating (MW)	Failures per year	Repair time (Hrs)
1	22	50.00	4.42	20.00
2	22	50.00	4.42	20.00
3	22	50.00	4.42	20.00
4	22	50.00	4.42	20.00
5	22	50.00	4.42	20.00
6	22	50.00	4.42	20.00
7	15	12.00	2.98	60.00
8	15	12.00	2.98	60.00
9	15	12.00	2.98	60.00
10	15	12.00	2.98	60.00
11	15	12.00	2.98	60.00
12	15	155.00	9.13	40.00
13	7	100.00	7.30	50.00
14	7	100.00	7.30	50.00
15	7	100.00	7.30	50.00
16	13	197.00	9.22	50.00
17	13	197.00	9.22	50.00
18	13	197.00	9.22	50.00
19	1	20.00	19.47	50.00
20	1	20.00	19.47	50.00
21	1	76.00	4.47	40.00
22	1	76.00	4.47	40.00
23	2	20.00	19.47	50.00
24	2	20.00	19.47	50.00
25	2	76.00	4.47	40.00
26	2	76.00	4.47	40.00
27	23	155.00	9.13	40.00
28	23	155.00	9.13	40.00
29	23	350.00	7.62	100.00
30	18	400.00	7.96	150.00
31	21	400.00	7.96	150.00
32	16	155.00	9.13	40.00

Table 10: Electrical Data of the IEEE Reliability Test System: Buses

Bus No.	Active Load (p.u)	Reactive Load (p.u)	P_g (p.u.)	Q_{max} (p.u.)	Q_{min} (p.u.)	V_0 (p.u.)	V_{max} (p.u.)	V_{min} (p.u.)
1	1.080	0.220	1.720	1.20	-0.75	1.00	1.05	0.95
2	0.970	0.200	1.720	1.20	-0.75	1.00	1.05	0.95
3	1.800	0.370	0.000	0.00	0.00	1.00	1.05	0.95
4	0.740	0.150	0.000	0.00	0.00	1.00	1.05	0.95
5	0.710	0.140	0.000	0.00	0.00	1.00	1.05	0.95
6	1.360	0.280	0.000	0.00	0.00	1.00	1.05	0.95
7	1.250	0.250	3.000	2.70	0.00	1.00	1.05	0.95
8	1.710	0.350	0.000	0.00	0.00	1.00	1.05	0.95
9	1.750	0.360	0.000	0.00	0.00	1.00	1.05	0.95
10	1.950	0.400	0.000	0.00	0.00	1.00	1.05	0.95
11	0.000	0.000	0.000	0.00	0.00	1.00	1.05	0.95
12	0.000	0.000	0.000	0.00	0.00	1.00	1.05	0.95
13	2.650	0.540	5.500	3.60	0.00	1.00	1.05	0.95
14	1.940	0.390	0.000	3.00	-0.75	1.00	1.05	0.95
15	3.170	0.640	2.100	1.65	-0.75	1.00	1.05	0.95
16	1.000	0.200	1.450	1.20	-0.75	1.00	1.05	0.95
17	0.000	0.000	0.000	0.00	0.00	1.00	1.05	0.95
18	3.330	0.680	4.000	3.00	-0.75	1.00	1.05	0.95
19	1.810	0.370	0.000	0.00	0.00	1.00	1.05	0.95
20	1.280	0.260	0.000	0.00	0.00	1.00	1.05	0.95
21	0.000	0.000	3.500	3.00	-0.75	1.00	1.05	0.95
22	0.000	0.000	2.500	1.45	-0.90	1.00	1.05	0.95
23	0.000	0.000	6.600	4.50	-1.75	1.00	1.05	0.95
24	0.000	0.000	0.000	0.00	0.00	1.00	1.05	0.95

Table 11: Electrical Data of the IEEE Reliability Test System: Lines

Line No.	Bus No. (From)	Bus No. (To)	R	X	Current Rating (p.u)	Failures per year	Repair Time (Hrs)
1	1	2	0.0260	0.0139	1.93	0.240	16.0
2	1	3	0.0546	0.2112	2.08	0.510	10.0
3	1	5	0.0218	0.0845	2.08	0.330	10.0
4	2	4	0.0328	0.1267	2.08	0.390	10.0
5	2	6	0.0497	0.1920	2.08	0.390	10.0
6	3	9	0.0308	0.1190	2.08	0.480	10.0
7	3	24	0.0023	0.0839	5.10	0.020	768.0
8	4	9	0.0268	0.1037	2.08	0.360	10.0
9	5	10	0.0228	0.0883	2.08	0.340	10.0
10	6	10	0.0139	0.0605	1.93	0.330	35.0
11	7	8	0.0159	0.0614	2.08	0.300	10.0
12	8	9	0.0427	0.1651	2.08	0.440	10.0
13	8	10	0.0427	0.1651	2.08	0.440	10.0
14	9	11	0.0023	0.0839	6.00	0.020	768.0
15	9	12	0.0023	0.0839	6.00	0.020	768.0
16	10	11	0.0023	0.0839	6.00	0.020	768.0
17	10	12	0.0023	0.0839	6.00	0.020	768.0
18	11	13	0.0061	0.0476	6.00	0.020	768.0
19	11	14	0.0054	0.0418	6.00	0.390	11.0
20	12	13	0.0061	0.0476	6.00	0.400	11.0
21	12	23	0.0124	0.0966	6.00	0.520	11.0
22	13	23	0.0111	0.0865	6.00	0.490	11.0
23	14	16	0.0050	0.0389	6.00	0.380	11.0
24	15	16	0.0022	0.0173	6.00	0.330	11.0
25	15	21	0.0063	0.0490	6.00	0.410	11.0
26	15	21	0.0063	0.0490	6.00	0.410	11.0
27	15	24	0.0067	0.0519	6.00	0.410	11.0
28	16	17	0.0033	0.0259	6.00	0.350	11.0
29	16	19	0.0030	0.0231	6.00	0.340	11.0
30	17	18	0.0018	0.0144	6.00	0.320	11.0
31	17	22	0.0135	0.1053	6.00	0.540	11.0
32	18	21	0.0033	0.0259	6.00	0.350	11.0
33	18	21	0.0033	0.0259	6.00	0.350	11.0
34	19	20	0.0051	0.0396	6.00	0.380	11.0
35	19	20	0.0051	0.0396	6.00	0.380	11.0
36	20	23	0.0028	0.0216	6.00	0.340	11.0
37	20	23	0.0028	0.0216	6.00	0.340	11.0
38	21	22	0.0087	0.0678	6.00	0.450	11.0

Table 12. Hourly percentage of the sector peak load for all sectors

Hour #	Large Users	Govt. & Inst.	Peak Office & Bldg.	Avg. Office & Bldg.	Avg. Agri.	Peak Agri.
1	0.337	0.400	0.590	0.270	0.001	0.010
2	0.337	0.400	0.590	0.410	0.001	0.010
3	0.337	0.400	0.450	0.350	0.001	0.010
4	0.337	0.400	0.420	0.400	0.001	0.010
5	0.337	0.400	0.390	0.400	0.001	0.010
6	0.337	0.600	0.410	0.300	0.001	0.010
7	1.000	0.700	0.750	0.550	0.020	0.100
8	1.000	0.750	0.770	0.650	0.100	0.200
9	1.000	0.800	0.850	0.850	0.400	0.600
10	1.000	0.850	0.840	0.800	0.600	0.700
11	1.000	0.900	1.000	1.000	0.650	0.750
12	1.000	0.920	1.000	1.000	0.670	0.800
13	1.000	0.930	1.000	0.985	0.650	0.770
14	1.000	0.960	1.000	0.975	0.680	0.850
15	1.000	0.970	0.985	0.850	0.690	1.000
16	1.000	0.970	0.975	0.865	0.760	0.970
17	1.000	1.000	0.970	0.850	0.810	0.950
18	1.000	0.980	0.965	0.900	0.700	0.920
19	1.000	0.800	0.950	0.900	0.500	0.900
20	1.000	0.750	0.950	0.680	0.350	0.750
21	1.000	0.650	0.940	0.640	0.300	0.550
22	1.000	0.500	0.920	0.420	0.005	0.100
23	1.000	0.430	0.720	0.400	0.004	0.020
24	1.000	0.120	0.520	0.025	0.003	0.010

Table 13: Daily percentage of the sector peak load

Day	Residential	Government & Inst.	Office & Bldg.
Monday	0.96	1.00	1.00
Tuesday	1.00	1.00	1.00
Wednesday	0.98	1.00	1.00
Thursday	0.96	1.00	1.00
Friday	0.97	1.00	1.00
Saturday	0.83	0.40	0.50
Sunday	0.81	0.30	0.40

Table 14: Daily percentage of the sector peak load

Day	Industrial	Large User	Agricultural	Commercial
Monday	1.00	1.00	1.00	1.00
Tuesday	1.00	1.00	1.00	1.00
Wednesday	1.00	1.00	1.00	1.00
Thursday	1.00	1.00	1.00	1.00
Friday	1.00	1.00	1.00	1.00
Saturday	1.00	1.00	1.00	1.00
Sunday	1.00	1.00	1.00	1.00